ABSTRACT

Title of Document: MECHANISTIC INVESTIGATIONS OF STOICHIOMETRIC AND CATALYTIC Pt-MEDIATED OXIDATIVE FUNCTIONALIZATION AT A PROXIMAL BORON CENTER

Shrinwantu Pal, Doctor of Philosophy, 2013

Directed By: Prof. Andrei N. Vedernikov
Departmentof Chemistry and Biochemistry
University of Maryland, College Park

The focus of the work detailed in this dissertation is the investigation of mechanism and catalytic applications of Pt complexes supported by novel anionic di(2-pyridyl)borate ligands.

It was found that oxidation of $^{Me,Me}BPy_2$-supported Pt^{II} complexes bearing no hydrocarbyl complexes directly generated dimethyl ether in quantitative yields, with one methyl originating from the ^{Me}B fragment. We also found that increasing formal charge on the metal center renders related complexes reluctant to undergo oxidation. Based on a proposed mechanism involving a transient Pt^{IV}-Me complex, we set out to develop a series of modified $^{R,R}BPy_2$ ligands to prevent such oxidatively induced hydrocarbyl transfer.

We found that the strategy of replacing one hydrocarbyl (Me) group in the dmdpb ligand by methoxo (OMe) was not sufficient in completely preventing degradation of the borate center. However, derived mono- and di-hydrocarbyl Pt^{II} complexes could still be easily oxidized under aerobic conditions. Interestingly, oxidation products corresponding to both B-to-Pt^{IV} methyl migration and ligand retention were observed. We focused our attention to a unique $^{1,5\text{-cyclooctanediyl}}BPy_2$ ligand, which, we presumed, would prevent hydrocarbyl migration due to the rigid structure imposed by the bicyclic framework. The derived $Pt^{IV}Me_3$ complex was found to exhibit 'enhanced' BC-H agostic stabilization of the penta-coordinate Pt^{IV} center. Oxidation of derived Pt^{II} complexes results in hydride migration from the B-C*H* fragment onto the Pt^{IV} center, led to the formation of a series of $^{(MeO),(MeO)}BPy_2$ supported Pt complexes, and unanticipated C-C and C=C coupling at the borate center.

The $^{(MeO),(MeO)}BPy_2$ ligand proved to be the first example of anionic facially chelating borate ligand capable of resisting oxidative degradation. The derived $Pt^{IV}(Ph)_2(OH)$ can be used for catalytic aerobic oxidation of $NaBH(OMe)_3$ and $NaBH_4$, with TOFs of 178/h and 216/h respectively. This may be of particular interest from the perspective of a direct-borohydride-fuel-cell (DBFC). We also found that the $Pt^{IV}(Ph)_2(OH)$ complex could be used as a catalyst to oxidize isopropanol to acetone under aerobic conditions with a TON of 3.8 after 56h at 80 °C. A mechanism involving *selective* hydride migration from a B-bound isopropoxy fragment to the Pt^{IV} center was proposed.

MECHANISTIC INVESTIGATIONS OF STOICHIOMETRIC AND CATALYTIC Pt-MEDIATED OXIDATIVE FUNCTIONALIZATION AT A PROXIMAL BORON CENTER

By

Shrinwantu Pal

Dissertation submitted to the Faculty of the Graduate School of the
University of Maryland, College Park, in partial fulfillment
of the requirements for the degree of
Doctor of Philosophy
2013

Advisory Committee:
Professor Andrei N. Vedernikov, Chair
Professor Philip DeShong
Professor Bryan W. Eichhorn
Professor Lawrence R. Sita
Professor Kyu Yong Choi

Dedication

This thesis is dedicated to the teachers who took the time to have me learn.

Acknowledgements

I take this opportunity to thank all the wonderful people who, in my becoming of what I am now, have all had equally important parts to play. Firstly I would like to thank my advisor, Prof. Vedernikov, without whose patience, and guidance, experimental chemistry would not be as enjoyable. I am happy to have gained an additional skill-set, and even happier to have been involved in mechanistic organo-transition metal chemistry. I also want to thank Prof. Vedernikov for enduring countless mistakes, and random exclamations regarding 'fantastic' reaction products, which, many a time, were simply sourced at 'unbalanced equations'. Academically speaking, I want to thank Prof. Vedernikov for sharing with me results of his DFT calculations. I want to thank the National Science Foundation (CHE-0614798, CHE-1112019) for the financial support of this work. I would like to thank Profs. DeShong, Sita and Eichhorn not just for agreeing to serve on my thesis committee, but also for making the courses in the first few semesters a basis for the chemical knowledge I applied towards my graduate research. I would also like to thank Profs. Doyle and Isaacs, for having their doors open for me. I would like to thank the magicians in the chemistry Dept., Dr. Yiu Fai Lam and Dr. Peter Zavalij: without their support in NMR and XRD, my complexes would be truly undecipherable.

I would like to thank my parents, both of whom are chemists. It is neither fate, nor genetic inclination that I studied chemistry, but simply because mathematics and physics were too complicated for me. I thank my mother for countless hours of discussions involving absurd mechanisms and my father for making me memorize the entire periodic table, well, sans the lanthanides and actinides, that is.

I want to thank Max, Abu, Brendan and Neeraja for great times during the 'course-work days'. To my lab-mates, Eugene, Julia, Will, Pratheep, Daoyong, Anna, Dave, Eli and David, a big thank you for going out of your ways to make lab a fun place to work. I want to thank the undergraduate students who worked with me: Josh, Stephanie and Zoe for helping me in ligand synthesis, because with the extra pair of hands, running lithium reactions are so much easier.

Finally, I would like to thank my friends outside of chemistry, Geetanjali, Anmol, Joyreeta, Rajibul, Souvik, Anirban, Sudipta-da, Shantanu and Sandip for making an environment reminiscent of home, that, because of them, I am sure I missed less. Thank you for always being there. I believe too many friends never spoil the evening, but the names of those too many can never be penned down here, for it is very surprising to find a thesis where the page count for the acknowledgement section overrides that for the subject matter. I would thus end this never-ending list here, and beg forgiveness from those people whose names I unavoidably could not write here, and from those about whom two lines would never be enough.

Table of Contents

List of Schemes

List of Figures

List of Tables

List of Abbreviations

C-H	bonded carbon-hydrogen
inorganic	bearing no formal metal-carbon bond
Me	methyl
Bpym	2,2'-bypyrimidine
TMEDA	tetramethylethylenediamine
DFT	Density functional theory
dpdmb	di(2-pyridyl)dimethylborate
dpms	di(2-pyridyl)methanesulfonate
nacnac	n-acetyl-n-acetonate
^{t}butyl	tert-butyl
^{n}Bu	n-butyl
THF	tetrahydrofuran
TBE	tert-butylethylene
TFE	trifluoroethylene
DMSO	dimethyl sufloxide
MeOH	methanol
^{1}H-NMR	hydrogen-1 nuclear magnetic resonance
^{13}C-NMR	carbon-13 nuclear magnetic resonance
J	^{1}H-^{1}H coupling
$J_{Pt\text{-}H}$	^{195}Pt -^{1}H coupling
$J_{Pt\text{-}C}$	^{195}Pt -^{13}C coupling
MS	mass-spectrometry
ESI-MS	Electron-spray ionization MS
DART-MS	direct analysis in real-time MS
mL	milliliter
µL	microliter
mol	mole
µmol	micromole
mmol	millimole
g	gram
mg	milligram

General Comments

All manipulations were carried out under purified argon using standard Schlenk and Glove-box techniques. All reagents for which syntheses is not given are commercially available from Aldrich, Acros or Pressure Chemicals and were used as received without further purification. PTFE-syringe filters were purchased from VWR and used as obtained. $Pt_2Me_4(SMe_2)_2$ and $PtPh_2(SMe_2)_2$ were prepared as described previously [1]. ^1H (500.132 MHz) and ^{13}C NMR (125.770 MHz) spectra were recorded on a Bruker Avance 500 spectrometer. ^1H NMR (400.132 MHz) spectra were recorded on a Bruker Avance 400 spectrometer. Chemical shifts are reported in ppm and referenced to residual protio-solvent resonance peaks. Coupling constants (represented as *J*=) indicate the ^1H-^1H coupling unless noted otherwise. ^1H NMR peaks corresponding to pyridine fragments in unsymmetrical complexes are assigned (as py or py'). However in many cases distinction between them could not be made, except in cases where Pt-coupling constants were influenced strongly by difference in the *trans*-influence of ligands. In such cases, appropriate assignments are noted. Elemental analyses were performed by Columbia Analytical Services, Inc. ESI-MS were recorded on a JEOL AccuTOF-CS instrument using direct-injection technique, preventing exposure to O_2 and /or adventitious acid, unless stated explicitly. ESI-MS were compared with mass envelopes for B and/or Pt –containing compounds and most intense peaks are reported. Formulas for some solvent (THF) - containing sodium salts that we used to calculate their percent composition were deduced based on the amount of solvent we observed in the ^1H NMR spectra of the same batch of the compounds. Sodium di(2-pyridyl)(methoxy)(methyl)borate and derived complexes reported in Chapter-III did not match elemental analyses, presumably due to the presence of sodium trifluoroacetate contamination. X-ray structures were solved by Dr. Peter Zavalij and are displayed as ORTEP drawings with 30% probability ellipsoids. DFT calculations were performed by Prof. Andrei Vedernikov using Priroda/Jaguar program with PBE96 exchange correlation and appropriate solvent PCM-model [2]. DART ESI-MS analysis was performed by Dr. Yiu Li.

Chapter 1: Development of anionic borate ligands for oxidative C-H functionalization

1.1 Importance and Scope of C-H activation reactions

C-H activation, defined by Periana [3] as "a facile C-H cleavage reaction with an 'MX' species that proceeds by coordination of an alkane to the inner sphere of 'M'… leading to an M-C intermediate", can be categorized according to reaction stoichiometries. Stahl's distinction [4] between C-H oxidative addition, σ-bond metathesis, electrophilic substitution, 1,2 addition to an M=X bond and homolytic (metallo-radical) activation does not necessarily imply a 'mechanistic connotation'. For an intended C-H activation and subsequent functionalization, homolytic pathways are less desirable as the C-H bonds in intended products are usually weaker than in the parent compounds, and leads to the 'classical selectivity' of $3° > 2° > 1° > H_3C\text{-}H$ [5].

C-H bond activation is the key step towards functionalization [6]. For alkanes, featuring C-H bonds with energies of ~100 kcal/mole, a C-H activation step is quite difficult [7]. Via functionalization, hydrocarbons can be used as feed-stock for a plethora of organic compounds [8] while no longer being confined as merely fuel, the latter resulting in complete oxidation to CO_2 [9].

Hence, transition-metal mediated non-homolytic, i.e. heterolytic C-H activation and functionalization is a desirable alternative [10]. Although, from a mechanistic standpoint, transition metal mediated heterolytic activation can be classified according to Scheme 1.1, it is sometimes very difficult to draw a fine line between

them. The different modes however, have one mechanistic similarity; they "appear to proceed through a σ-bond complexed intermediate" [5]. This leads to a metal-hydrocarbyl complex Periana refers to as 'M-C', which can then be submitted to subsequent transformations.

Scheme 1.1: Mechanisms of heterolytic C-H activation

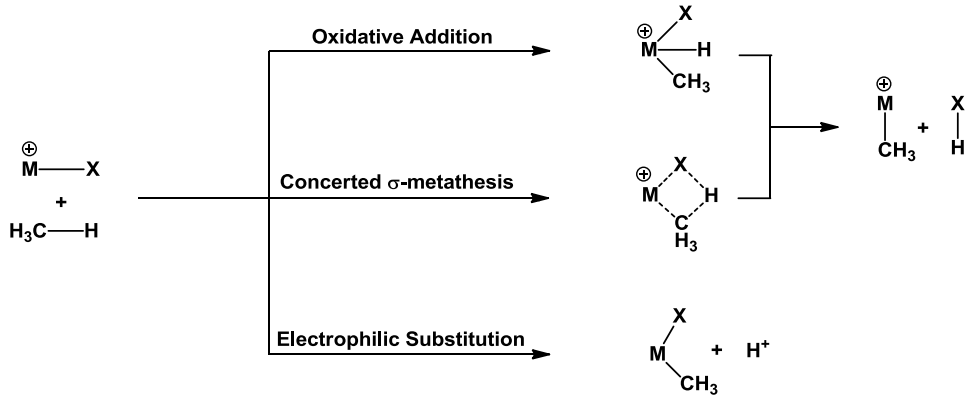

1.2 Pt^{II} -mediated C-H activation and subsequent functionalization

Typically, for second and third-row 18e transition metal complexes to activate C-H bonds, a coordination vacancy must be generated by the loss of a ligand L' from **1.1**, as shown in Scheme 1.2. For most widely investigated systems [11], the ligand L' remains unbonded from the final oxidative addition product, **1.2**. Square planar $16e^-$ Pt^{II} complexes, **1.3**, however, show a substantial thermodynamic favorability, as the final product, an octahedral $18e^-$ Pt^{IV} complex, **1.4**, will have either L' or a new ligand bound to the Pt^{IV}-center. Protic solvents such as alcohols or water can be sufficiently basic to afford deprotonation of the Pt^{IV} complex, **1.4**, to produce a Pt^{II}-complex, **1.5**. In cases where the intermediacy of **1.4** cannot be established, the overall outcome is the substitution of L' in **1.3** by 'R' in **1.5**, i.e. electrophilic substitution of hydrogen in the R-H with Pt^{II}.

Scheme 1.2: C-H activation by 18 e⁻ and 16 e⁻ complexes

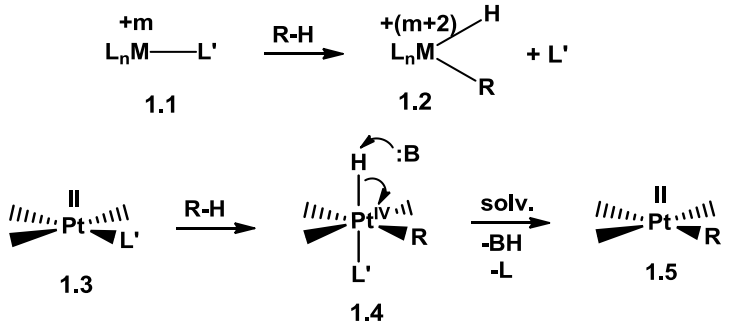

Pt complexes have shown immense promise in C-H bond activation and functionalization chemistry, mainly because of their selectivity and capability to work in mild conditions [12]. Often, the C-H activation process is reversible, which leads to the consideration of Pt-complexes as homogenous H/D exchange catalysts. In 1967 Garnett and Hodges found that K_2PtCl_4 dissolved in D_2O/CD_3COOD could promoted H/D exchange in benzene and benzene derivatives [13], however, reactions with cyclohexane were reported to be slow. Concurrently Hay reported oxidative coupling of acetylenes [14]. Shilov et al demonstrated a system involving $K_2Pt^{II}Cl_4$ and $H_2Pt^{IV}Cl_6$ capable of functionalizing C-H bonds of methane into C-OH or C-Cl [15].

The Shilov cycle, depicted in Scheme 1.3, involves the rate-limiting binding of an alkane to an 'inorganic' Pt^{II}-complex **1.6**, to form a transient Pt^{II}-σ(C-H) intermediate, **1.7**, which oxidatively adds the C-H bond to form a hydrocarbyl-hydrido-Pt^{IV} species, **1.8**. The Pt^{IV}-bound hydride is easily deprotonated by solvent (water or methanol) to form the Pt^{II}-hydrocarbyl complex, **1.9**. In the presence of stoichiometric amounts of $[PtCl_6]^{2-}$ as oxidant, **1.9** is oxidized to the monohydrocarbyl-Pt^{IV} complex, **1.10**, which then undergoes reductive elimination via nucleophilic substitution of the Pt^{IV}-CH_3 fragment leading to regeneration of the 'inorganic' Pt^{II}-precursor, **1.6**.

Scheme 1.3: The Shilov cycle

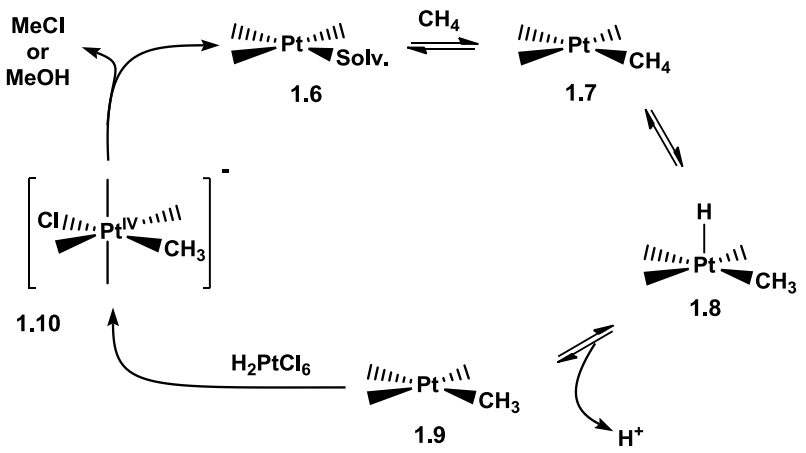

The scope of the Shilov system is not limited to methane alone, and the C-H bonds of higher alkanes also react, exhibiting a selectivity of the order: CH_4 > 1° > 2° >> 3° [15]. This non-classical selectivity is in complete contrast to that observed for radical reactions, and hence lucrative. On the other hand, the use of the very expensive $H_2Pt^{IV}Cl_6$ in stoichiometric amounts is a great drawback of the Shilov system. Another drawback that limits the Shilov system is the catalyst instability and Pt-black formation believed to originate from the disproportionation of $Pt^{II}Cl_4^{2-}$ []. A number of groups, including Shilov himself, have investigated the possibility of the use of other oxidizing agents, viz. SO_3, H_2O_2, O_2/heteropolyacids, Cl_2, O_2/Cu^{II} [16]. The (bipyrimidine)$PtCl_2/H_2SO_4$ system, developed by Periana et al, commonly called the Catalytica system deserves special mention [17]. In this system, following methane activation, the (bpym)Pt^{II}(Me)(Cl) is oxidized by SO_3 in oleum, while the latter is reduced to SO_2. The monomethyl-Pt^{IV} complex then reductively eliminates CH_3-OSO_3H. Although the reaction is severely inhibited by water or methanol, and any concentrations of H_2SO_4 below 90% results in unattractive rates, till date, this is the best known example of catalytic homogenous methane functionalization. It achieves

C-H activation, oxidation, and functionalization without significant over oxidation of CH_4 into CO_2 [9] or formation of halogenated derivatives of methane, with a yield of 70%, a selectivity of 90%, and TONs of 300. The main drawbacks that limit practical applications are however, the use of fuming sulfuric acid as an oxidizing agent under harsh conditions (~200 °C) and the difficulty of separating CH_3-OSO_3H from oleum. Thus, the most imminent and compelling alternative is the use of O_2 [18]. To this regard, there has been but only slight success in the oxidation of Pt^{II}-hydrocarbyl complexes by O_2. In 2001, A. Sen et al showed catalytic oxidation of terminal methyl groups in ethylsulfonates by O_2 and Na_2PtCl_6 with the use of mediators (co-catalysts) such as $CuCl_2$ [19]. In the same year, Sames et al oxidized amino acids with SiO_2 supported $[Pt(Mebipym)Cl_2][H_4PV_2Mo_{10}O_{40}]$ complexes [20]. Not only are mediator-enabled oxidations low in the TONs achieved, selectivity remains poor. Success in the regard has been modest, and no commercially applicable system exists till date.

1.3 Oxidation of Dihydrocarbyl-Pt^{II} complexes with O_2

Developing an aerobic catalytic cycle capable of oxidizing alkanes is a challenge due to factors outlined below. Firstly, the use of O_2 as a terminal oxidant also requires the use of protic solvents [21] which are more coordinating than alkane C-H bonds. Thus, the competition between initial rate-limiting σ(C-H) bond coordination is dominated by coordination of the solvent. On the other hand, the C-H bonds in the resulting alcohol are more reactive than the parent alkane C-H bonds [22], and over-oxidation is highly likely. Ligand environment around the Pt^{II}-center, thus may be crucial in fine-tuning aforementioned parameters.

In the late 90s, Vedernikov et al screened via *ab initio* and DFT methodologies a number of d^8 Pt complexes capable of activating C-H bonds in methane [23], and concurrent with experimental evidence found some pyridyl N-N ligands to be ligands of choice. Recalling that the initial binding of CH_4 to the Pt^{II} center is rate limiting, the de-ligation of the coordinated 'solv' (Scheme 1.3), is crucial in generating a site for C-H activation [24]. In 1998-2002, Bercaw and Labinger reinvestigated Puddephatt's report of 1984 [25] and found that even trace amounts of O_2 could be used to oxidize (TMEDA)$Pt^{II}Me_2$ and (bpy)$Pt^{II}Me_2$ to form the corresponding oxidized $Pt^{IV}Me_2$(OH)(OMe) complexes [26]. Molecular oxygen has later been shown to insert into Pt^{II}-Me bonds [27] to generate isolable Pt^{II}-OOMe species. Importantly, these examples feature facile oxidation of electron-rich $Pt^{II}Me_2$ complexes, which when oxidized, lead to $Pt^{IV}Me_2$ complexes that are reluctant to C-X eliminate. Less electron-rich diphenyl and monomethyl analogues could not be oxidized. The key intermediate in the Shilov cycle, on the other hand, is a Pt^{II}-Me complex, which is expected to be less electron rich and hence expected to be more difficult to oxidize.

1.4 Ligand development towards C-H activation and aerobic oxidation

Alongside concurrent developments illustrating easy access of octahedral Pt^{IV} complexes via anionic tripodal ligands such as tris(pyrazolyl)borate demonstrated by Brrokhart [28] and Templeton [29], Vedernikov et al demonstrated for the first time in 2006 [30], facile aerobic oxidation of monohydrocarbyl-Pt^{II} (as well as

dihydrocarbyl-Pt^{II}) complexes supported by facially chelating anionic ligands such as di(2-pyridyl)methane sulfonate (dpms), as shown in Scheme 1.4.

Scheme 1.4 Proposed mechanism of O_2 activation by (dpms)Pt^{II}-alkyl complexes

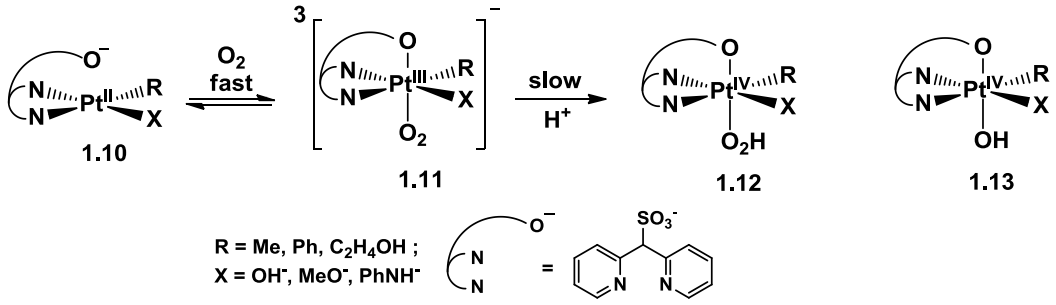

The activation of O_2 by the Pt^{II}-complex, **1.10** was proposed to involve a triplet-Pt^{III}-superoxo intermediate, **1.11**. Protonation at the terminal O-atom followed by proton-coupled electron transfer forms a hydroperoxo intermediate, **1.12**, which then undergoes O-O cleavage to generate Pt^{IV} intermediates such as **1.13**, capable of R-X reductive elimination.

In addition to easy access to Pt^{IV}-complexes via aerobic oxidation enabled by facile switching of κ2/κ3 coordination modes, the use of facially chelating anionic ligands have far-reaching outcomes. Under the presumption that anionic $[LPt^{II}(R)(X)]^-$ complexes are lipophilic enough to afford dilute solutions in hydrocarbons, related $LPt^{IV}(R)(X)(H)$ complexes (generated via protonation at the Pt^{II}-center) or $LPt^{II}(R)(XH)$ (generated via ligand protonation) are both neutral and might be even more soluble in non-polar or hydrocarbon solvents. This is particularly important from a C-H activation standpoint as these complexes can allow access to a putative three-coordinate Pt^{II}-complex [11].

The dpms-scaffold features an 'explicit' SO_3^- polar head that renders related anionic complexes lipophobic, and limits solubility of the latter in hydrocarbon media [31].

Ligand development by Peters et al [32] and Tilley et al [33], involving bis(pyrazolyl)borate or indolide derived anionic $Pt^{II}Me_2$ complexes which could readily activate C-H bonds of benzene to form a $Pt^{II}Ph_2$ complex, confirmed that the putative three-coordinate Pt^{II} intermediate could be readily accessible. In both cases, sub-stoichiometric amounts of strong acids viz. $[HN(^{i}Pr_2)(Et)][BPh_4]$, was found to catalyze the 'double-C-H-activation' of benzene. Ideally, the use of milder acids in accessing this three-coordinate Pt^{II} complex is more lucrative. To this regard, the choice of a Lewis-acidic counter-ion such as Na^+ or K^+ makes the $[LPt^{II}Me_2]$ anionic complexes more basic due to enhanced acidity of added water or methanol in organic media via precipitation of NaOH or KOH. After initial screening, it was found by Khaskin and Vedernikov that a di(2-pyridyl)dimethylborato-Pt^{II} complex (Scheme 1.5) had a 13.4 kcal/mole Gibbs free energy of dissociation of the H_2O ligand, which, compared to that of 15.3 kcal/mole from the cis-$Pt^{II}(Cl)_2(OH_2)_2$ in the original Shilov system, is encouraging. Bearing an 'implicit' anionic B-center, derived (dpdmb)Pt^{II} complexes are expected to be more lipophilic as well [34].

Scheme 1.5: Calculated 'aqua' ligand dissociation energies

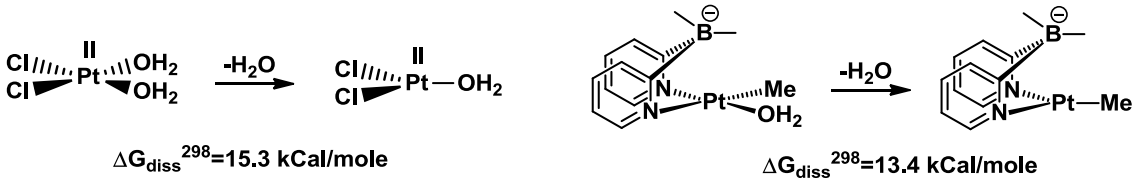

ΔG_{diss}^{298}=15.3 kCal/mole

ΔG_{diss}^{298}=13.4 kCal/mole

1.5 Reactivity of di(2-pyridyl)dimethylborato-Pt^{II} complexes

Scheme 1.6: Synthesis of di(2-pyridyl)dimethylborate and derived $Pt^{II}Me_2$ complex

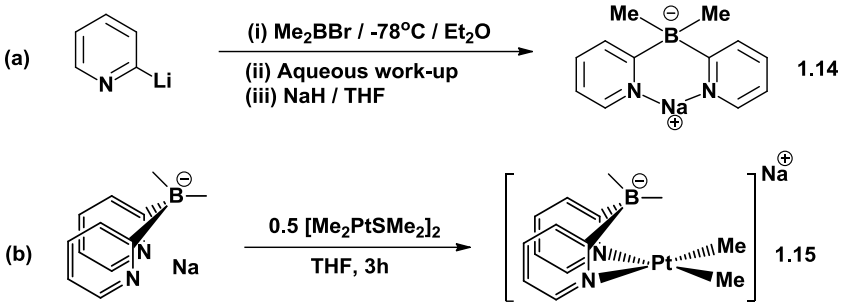

Khaskin [34], following upon Hodgkins and Powells' procedure [35], as shown in Scheme 1.6, added a solution of Dimethylbromoborane in ether to 2 equivalents of 2-pyridyl-lithium at -78 °C in ether with subsequent work-up to obtain moderate yields of the protonated and sodium ligand, H[**1.14**] Na[**1.14**], respectively. The dimethyl-Pt^{II} complex, **1.15**, was synthesized by standard protocol.

Khaskin found **1.15** to be extremely basic and reactive towards water [36]. As shown in Scheme 1.7(a), in the presence of benzene, it reacts with water to form the diphenyl-Pt^{II} complex, **1.16**. In the presence of an additional few equivalents of water, the monophenyl-Pt^{II} complex **1.17** is formed. Although **1.15** is not soluble in hydrocarbons, a suspension in huge excess of cyclohexane reacts with water to form the Pt^{II}-cyclohexene-hydride complex, **1.18**, as shown in Scheme 1.7(b).

Scheme 1.7: Reactivity of di(2-pyridyl)dimethylborato-$Pt^{II}Me_2$ complex towards protonolysis

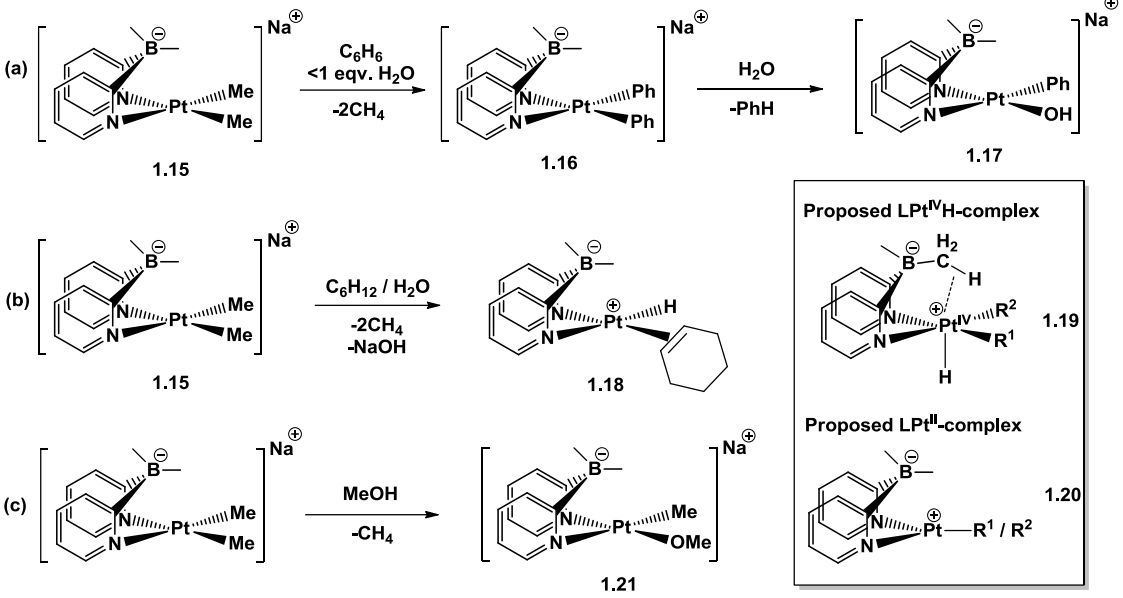

As mentioned before, the initial protonolysis of the $Pt^{II}Me$ fragment is believed to proceed via a $LPt^{IV}(R^1)(R^2)H$ complex, **1.19**, where R^1=R^2=Me along with the formation of NaOH. Unlike dpms or Tp analogues [37, 29], **1.19** (R^1=R^2=Me) eliminates methane with extreme facility, and the latter can be seen effervescing from the reactions immediately upon addition of a proton source. Following reductive elimination of methane and formation of the aforementioned putative three-coordinate $LPt^{II}Me$ complex, **1.20** (where R^1=Me), C-H activation of benzene or cyclohexane leads to the formation of **1.19**-analogue with R^1=Me, and R^2=Ph, or C_6H_{11}, respectively. One more reductive elimination step leads to the formation of methane and **1.20** (R^2=Ph or C_6H_{11}). When R^2=C_6H_{11}, β-H abstraction from the Pt-cyclohexyl fragment then leads to the formation of the olefin-hydride complex, **1.18**. In the case where no β-H is available, **1.20** (R^2=Ph) C-H activates yet another benzene molecule to yield **1.19** (R^1=R^2=Ph). The Pt^{IV}-H is abstracted by the NaOH formed in the initial step to yield **1.16**, and thus returns the proton to the solvent in a

catalytic fashion. This 'double-C-H-activation' mechanism is consistent with the requirement of catalytic amounts of acid, as reported by Peters [32] and Tilley [33], the only difference in this case being the use of water as a proton source. Usual protonolysis of the Pt^{II}-Ph fragment in **1.16** by water leads to formation of **1.17** and benzene. Similarly, the dimethyl complex, **1.15**, is also extremely reactive towards methanol, and within minutes of addition of methanol to **1.15**, the monomethyl-Pt^{II}-methoxy complex, **1.21** is formed (Scheme 1.7(c)).

The facility with which (dpdmb)-supported Pt^{II} complexes activates C-H bonds of benzene and cyclohexane was encouraging for two reasons: (i) the reactions were high-yielding and selective and (ii) the some of the products were tolerant of water. Interestingly, (dpdmb)$Pt^{II}Me_2$, **1.15** was found to be stable towards O_2 in THF solutions in the absence of a proton source. In the presence of a proton source, however, **1.15** quickly transformed into a Pt^{IV} complex. This means that coordination of O_2 to the Pt^{II} center is rapid and reversible, and that the coordinated O_2 can be trapped by hydroxylic solvents. This is consistent with previous reports from Goldberg [38] and Bercaw [39] who suggest that formal oxidation of the Pt^{II} center occurs after protonation of the coordinated O_2.

Scheme 1.8: Oxidation of di(2-pyridyl)dimethylborato-$Pt^{II}Me_n$ complexes (n = 1, 2)

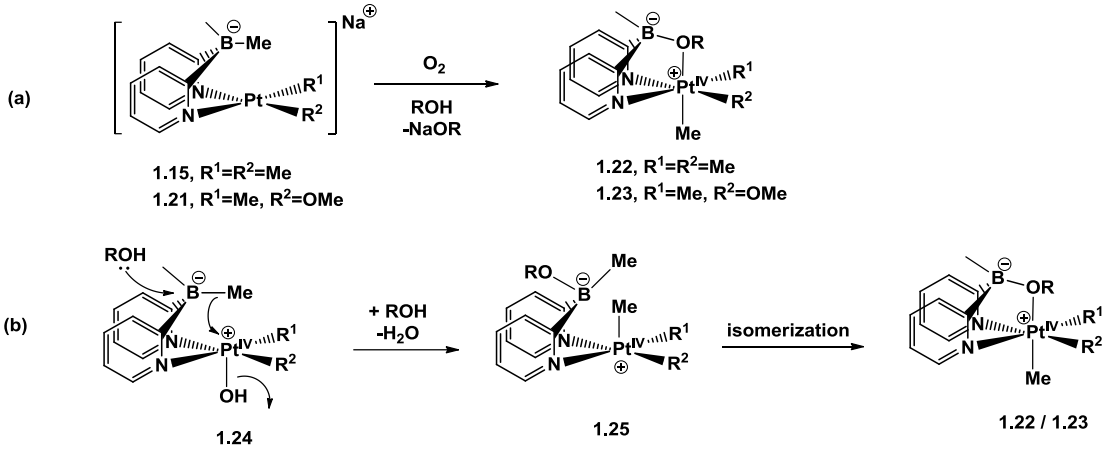

Oxidation of both dpdmb-supported monohydrocarbyl and dihydrocarbyl Pt^{II} complexes lead to methyl migration from the B to the Pt center, as shown in Scheme 1.8(a). Thus, oxidation of the monomethyl-Pt^{II} complex, **1.21** and dimethyl-Pt^{II} complex, **1.15** led to the formation of **1.22** (R^1=Me, R^2=OMe) and **1.23** (R^1=R^2=Me) respectively. Under the assumption that the dimethyl-Pt^{II} complex, **1.15** was stable towards the choice of protic solvent, ROH, the product was unaffected by the latter [34]. When R^1=R^2=Ph, a mixture of symmetrical and unsymmetrical Pt^{IV} complexes was observed, and the ratios depended on the choice of solvent. The hydrocarbyl migration from B-to-Pt^{IV} was believed to involve a five-coordinate Pt^{IV}-hydroxo complex, **1.24**, which could then undergo back-side nucleophilic attack of ROH on the B-center, as shown in Scheme 1.8(b), to form **1.25**. The five coordinate Pt^{IV} complex, **1.25**, is expected to quickly isomerize to **1.22** or **1.23**, the product 'choosing' a bridging alkoxy fragment over an agostic C-H interaction to stabilize the Pt^{IV}-center in the final product . The migration of the hydrocarbyl fragment, was believed to be propelled by the formation of strong B-OR bonds leading to exceptionally stable final Pt^{IV} products. This is manifested in the fact that the

trimethyl complex, **1.26**, reacts with methanol, albeit slowly, to form **1.22** via loss of methane, as shown in Scheme 1.9. The origin of the 'Me' fragment in the lost methane was proven to be the Pt-Me, and not the B-Me fragment by reacting the C^{13}-labeled derivative, **1.26-C^{13}**, with methanol and observing C^{13}-labelled methane in the reaction mixture [40].

Scheme 1.9: Reaction of di(2-pyridyl)$Pt^{IV}Me_3$ with methanol: induced *methyl migration*

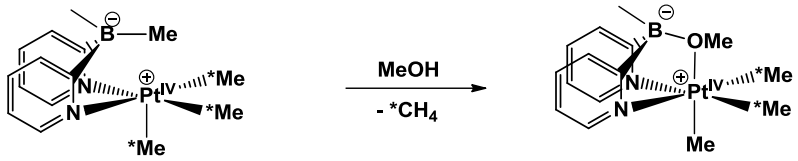

1.26 **1.22**

This phenomenon, termed oxidatively induced hydrocarbyl migration, lead to (i) a modification of the anionic borate center, and (ii) formation of a $Pt^{IV}Me_n$ complex, where $n \geq 2$. The resulting Pt^{IV} complexes had at least two hydrocarbyl groups on the Pt-center and were extremely stable and reluctant towards reductive elimination, even when heated up to 100 °C. Above such temperatures, amongst other undetermined thermal decomposition products, some C-C elimination product (viz. ethane) was observed, but C-O elimination products were never observed. This severely restricted the plausibility of the use of (dpdmb)-supported Pt^{II} systems towards Shilov-type applications, and further ligand development is necessary. Reports of such ligand developments will be forthcoming in the following chapters.

1.6 Lipophilic variants (dpdmb)-Pt^{II}(cyclohexene)(hydride) complexes: alkane transfer dehydrogenation

As opposed to oxidative functionalization, dehydrogenating alkanes to form olefins is another viable C-H functionalization strategy [41]. Once an alkane can be transformed to an olefin, a plethora of methods such as epoxidation [42], Grubbs-type metathesis [43], or even Wacker-type oxidation provide alternate routes [44]. Catalytic dehydrogenation in homogenous media was first reported by Crabtree [45], and in the 1990s, Group 9 transition metal catalysts have proven to be active in catalytic transfer dehydrogenation. Such reactions, examples of which are shown in Scheme 1.10, may employ a sacrificial hydrogen-acceptor, or may evolve hydrogen-gas in the case of acceptor-less reactions.

Scheme 1.10: Examples of alkane-dehydrogenation: with (a) and without (b) sacrificial hydrogen acceptors

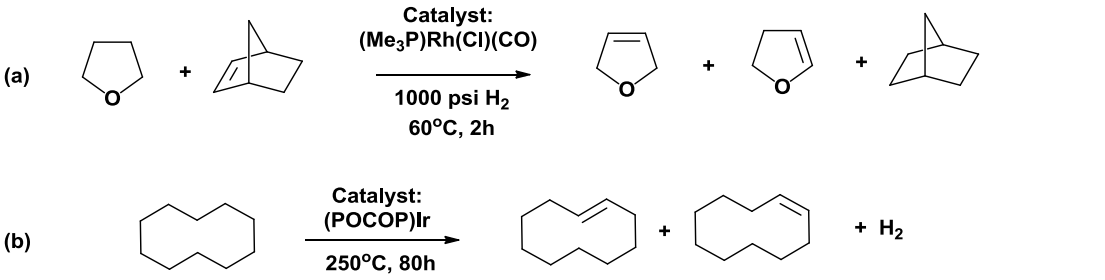

These systems are effective in terms of achieving large TONs, but require elevated temperatures. TBE is often used as the sacrificial hydrogen acceptor owing to the thermodynamic favorability of its hydrogenation, and thus milder conditions than that in acceptor-less dehydrogenations are found to work well [46]. Although acceptor-less dehydrogenations are lucrative from an atom-economical point of view, drawbacks, such as development of H_2 gas with the potential to shift the equilibrium backwards limit its application.

To this regard, Pt-complexes have been shown to stoichiometrically dehydrogenate alkanes. Examples include Goldberg's [47] ketiminate (nacnac)-supported and Templeton's [48] Tp-supported Pt^{II} complexes. Although these systems showed promise in stoichiometric reactions, non-innocence of the ketiminate ligands in the former, and low TONs of 1.1-1.3, alongside catalyst instability and Pt^0 formation in the latter, limit their use in catalytic fashion. It is noteworthy to mention here that Goldberg's ketiminate-supported Pt^{II}(cyclohexene)(H) complex was reported to be inert towards substitution of the cyclohexene fragment by TBE. The substitution of the alkene (corresponding to the alkane undergoing dehydrogenation) by the sacrificial alkene is crucial in realizing a catalytic cycle (c.f. Scheme 1.12).

Coming back to dpdmb-supported-Pt^{II} complexes, although the dimethyl complex, **1.15** was shown to cleanly dehydrogenate cyclohexane to form the olefin-hydride complex **1.18**, the yields of the reaction were poor, presumably due to limiting solubility of the starting material, **1.15**, as well as that of the involved intermediates, the related **1.19** and **1.20**. Thus, a lipophilic variant of **1.15** was sought after. It was presumed that with 4-*t*butyl substitutions on the pyridyl fragments in the dpdmb-ligand, a more lipophilic variant of the $Pt^{II}Me_2$ complex, **1.27**, shown in Scheme 1.11 could be obtained. Gratifyingly, **1.27** was appreciably soluble in cyclohexane, and upon addition of 3 equivalents of water produced **1.28**, quantitatively. Furthermore, ^{1}H-NMR signals corresponding to the olefinic protons of the bound Pt-cyclohexene fragment have chemical shifts (4.92 ppm, acetone-d_6) not too far from free cyclohexene (5.5 ppm, acetone-d_6) indicating that the extent of back-bonding from the Pt^{II}-center into the π^* orbitals of bound-cyclohexene was minimal. Consistent

with this indication, **1.28** underwent cyclohexene substitution even with a bulkier olefin such as TBE to form **1.29**, suggesting that the use of TBE as sacrificial hydrogen acceptor might be viable.

Scheme 1.11 Synthesis of ^{tbu}(dpdmb)-Pt^{II}(olefin)(hydride) complexes: substitution of olefins

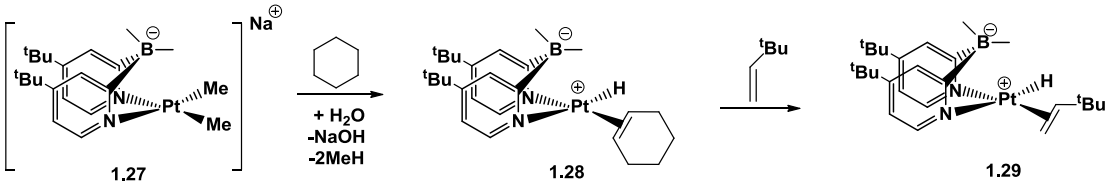

Indeed, **1.28** can be used as a transfer dehydrogenation catalyst [49]: a 5 mole % catalyst loading in a 3 mL cyclohexane solution with 20 equivalents of TBE added upon heating at 100 °C for 24h was found to produce 10-15 TONs of cyclohexene along with an equivalent decrease in TBE. Based on earlier reports, and to the best of our knowledge, the first proposed in-detail mechanism of transfer dehydrogenation with an Ir^{III}-pincer complex [50], a similar mechanism involving Pt^{II}(olefin)(hydride) complexes, shown in Scheme 1.12 was proposed. In the key-step, the active catalyst, **1.28**, i.e., the starting olefin-hydride complex, undergoes substitution of the bound olefin with the sacrificial olefin to form **1.29**. Reversible Pt-H insertion into the C=C bond of the bound-TBE generates 1.30. This reaction, in the case of TBE is expected to be extremely facile due to relief of steric-stress around the Pt-center. The putative 3-coordinate Pt^{II} center in **1.30** readily activates a C-H bond of cyclohexane, via a σ(C-H) complex, **1.31**, to form a dialkyl Pt^{IV}-hydride complex, **1.32**. In the event that the Pt-bound tertbutylethyl fragment reductively couples with the Pt-hydride, 1.33 is formed. Loss of tertbutylethane followed by *β*-hydride elimination of the Pt-bound cyclohexyl fragment in **1.34** regenerates the active catalyst.

Scheme 1.12 Catalytic transfer dehydrogenation of cyclohexane with TBE as sacrificial H acceptor

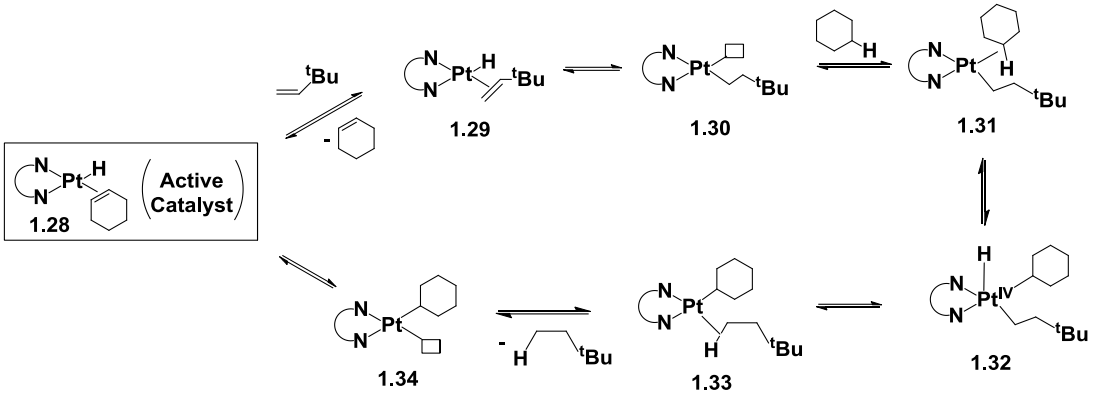

Based on the reversible nature of the steps in the proposed mechanism, it was presumed that a ^{n}alkenyl analogue of **1.28** could 'chain-walk' across the linear chain, similar to that reported by Bercaw and Labinger [51]. To this regard, Khaskin found [34] that **1.27** reacted with water in the presence of pentane within 20 minutes to form a multitude of products, with different Pt-H ^{1}H-NMR signals, corresponding to different cis/trans and region isomers of **1.35** (Scheme 1.13). If the reaction was stopped by quickly evacuating the reaction mixture, one major product was observed. Similar to Bercaw's report, this major isomer, viz. **1.35**, showed a AB-quartet in the olefinic region of the ^{1}H-NMR spectra indicating a terminal C-H activation product. Interestingly, a solution of freshly prepared **1.28** in Cyclohexane-d_{12} isomerized over 3 days, as evident by reappearance of the multitude of hydride signals in the ^{1}H-NMR spectrum.

Scheme 1.13: Olefin isomerization and 'chain-walking'

1.7 Remarks and proposed directions

The main drawback in using dialkyl and diaryl borates as ligands in the oxidation chemistry of supported $Pt^{II}Me_2$ and $Pt^{II}(Me)(OMe)$ complexes lies in the oxidatively induced migration of alkyl and aryl fragments from the borate to the platinum center. This leads to destruction of the borate ligand, resulting in replacement of one methyl group in the BMe_2 fragment by an alkoxy group, where the alkoxy originates from the alcohol the oxidation was performed in. Also, the resulting $LPt^{IV}Me_n$ ($n \geq 2$) complexes are very robust, and resistant to reductive elimination unless exposed to drastic conditions.

Based on our current knowledge of di(2-pyridyl)borate supported Pt^{II} complexes, we set out to synthesize di(2-pyridyl)borato-ligands with modified borate centers and explore reactions of derived-Pt^{II} complexes. Results of such attempts and mechanistic investigations of such transformations shall be forthcoming in the following chapters.

Chapter 2: Preparation and Oxidation of (dpdmb)Pt^{II} complexes bearing no hydrocarbyls on the Pt^{II} center: Tandem B-to-Pt^{IV} methyl migration and C-O elimination

2.1 Proposal

Based on Khaskin and Vedernikov's reports involving oxidatively induced B-to-Pt^{IV} hydrocarbyl migration [52], discussed in Chapter-I, we proposed that model '*inorganic*' (dpdmb)Pt^{II} complexes, such as **2.1** bearing no hydrocarbyls on the Pt^{II} center could be oxidized to produce a monomethyl-Pt^{IV} complex, **2.2**, via B-to-Pt^{IV} *methyl migration*. As such these complexes would allow investigation of reductive C-O or C-X elimination from the Pt^{IV} species. Furthermore, in the event of C-X reductive elimination, it might allow for successive transfer of the residual Me fragments from B to Pt, as shown in Scheme 2.1. This successive B-to-Pt^{IV} *methyl migration* can also lead to selective derivatization at the boron-center, i.e. allow preparation of di(2-pyridyl)(methoxy)(methyl)borato and di(2-pyridyl)dimethoxy borato Pt^{II} complexes, **2.3** and **2.5**, respectively.

Scheme 2.1: Hypothetical successive B(Me) functionalization via B-to-Pt^{IV} methyl migration

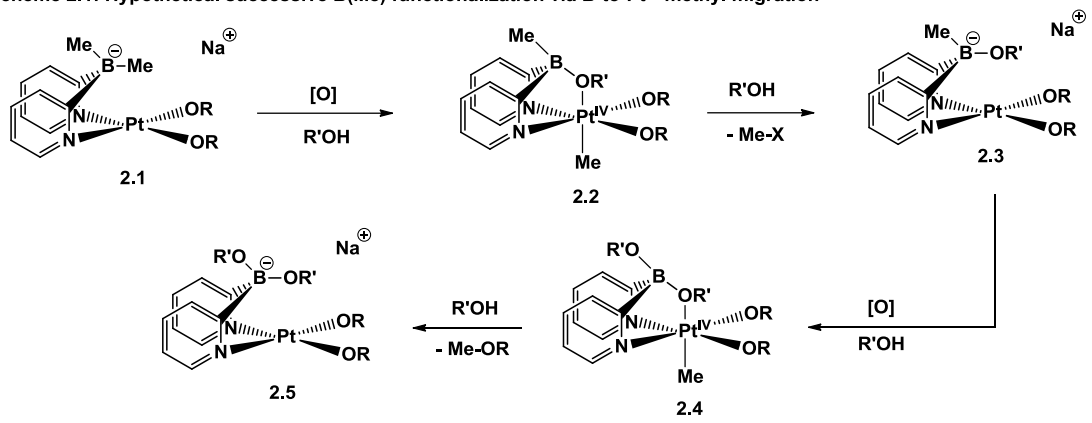

2.2 Implementation

Conceivably, the most straightforward synthetic route to generate the aforementioned 'inorganic' dpdmb-Pt^{II} complexes involves Na[(dpdmb)Pt^{II}(Me)(OMe)] complex, **1.21** since it could be easily prepared by the protonolysis of Na[(dpdmb)$Pt^{II}(Me)_2$] complex, **1.15** in methanol (c.f. Chapter-I). Thus, we presumed that either longer reaction times or stoichiometric amounts of a proton source would lead to a second protonolysis step, to form an 'inorganic' Pt-complex, **2.1**, as shown in Scheme 2.2(a). However, **1.21** in methanol, showed no signs of further protonolysis of the second Pt-bound methyl group for a period of up to 7 days. Although (dpdmb)Pt^{II}(Me)(OMe), **1.21** is expected to undergo methanolysis of the residual PtMe fragment by a mechanism similar to that discussed in Chapter-I (viz. initial protonation of the Pt^{II}-center, followed by elimination of methane and capture of the three-coordinate Pt^{II}-center by the methoxide ion, (c.f. Scheme 1.6, the presence of a electronegative O-atom on the Pt-OMe fragment in **1.21** makes protonation at the Pt^{II}-center competitively difficult, resulting in the equilibrium between **2.6** and **2.6'**, depicted in Scheme 2.2(b) biased towards the left.

Scheme 2.2: Subsequent protonolysis of $Pt^{II}Me$ fragments in $(dpdmb)Pt^{II}$ complexes

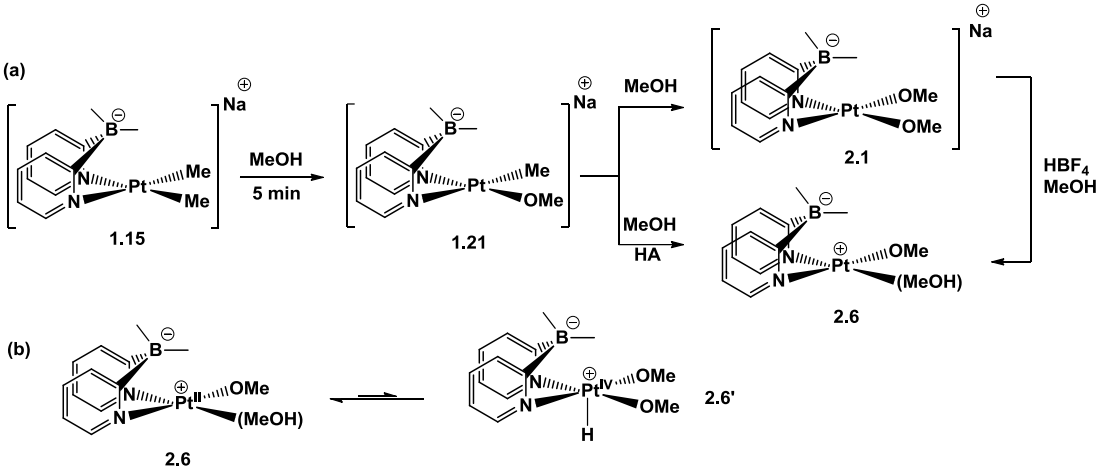

Thus, a stronger acid was called for. Although 1 equivalent of HBF_4 added to a solution of **1.21** in methanol quickly protonolyzed the PtMe fragment to produce **2.6** as shown in Scheme 2.2, the clear solution showed visible signs of decomposition over a period of 1h, i.e. formation of Pt-black. ESI^+-MS of an aliquot recorded immediately after addition of HBF_4 showed a peak at 456.1 corresponding to **2.6**H^+. Attempts to isolate **2.6** by removal of solvent failed owing to the decomposition which, we presumed, happens due to *β*-hydride elimination of the coordinated methanol ligand [53] in **2.6**, similar to that discussed in Scheme 2.7. A sample of $(dpdmb)PtMe_2$ **1.15**, was dissolved in CD_3OD in a NMR-tube. A ^{1}H-NMR spectra recorded after 5 minutes of dissolution confirmed to the presence of $(dpdmb)Pt^{II}(CD_3)(OCD_3)$, **1.21-*d*$_6$**. After this time, 1 equivalent of HBF_4 was added to the solution. The reaction was carefully monitored by ^{1}H-NMR. Although after 1h Pt-black could be seen in the NMR-tube, the immediate product of *β*-hydride elimination, formaldehyde, was not seen in the NMR spectra. Instead, a peak at 4.16 ppm, assigned to the acetal $CH_2(OCD_3)(OD)$ was observed. The spectrum was compared to that of an authentic sample of paraformaldehyde in CD_3OD acidified

with HBF_4 and found to be a match. Protonolysis reactions of **1.21** in CD_3OD with 1 equivalent of HBF_4 at low temperatures with subsequent low-T NMR monitoring were not successful in observing any transient Pt^{IV}-H or $Pt^{II}(CH_4)$ species.

Synthesis of dpdmb-supported Pt^{II} chloro or dichloro complexes, **2.7** and **2.8**, respectively, were also considered as shown in Scheme 2.3. The routes described in scheme 2.3 were attempted based on literature precedence [54] of the synthesis of Pt^{II}-complexes featuring di(2-pyridyl) ligands, in which, an aqueous solution of potassium tetrachloroplatinate(II) was added to an equivalent amount of the ligand dissolved in water by adding appropriate amounts of acid [55]. Although such complexation reactions were virtually quantitative, all our attempts to synthesize **2.7**, via this route, depicted in Scheme 2.3(a), proved to be unsuccessful. The difference in reactivities of dpdmb vs. neutral dipyridyl ligands can be ascribed to the difference in their basicities. The dpdmb ligand is expected to be more basic than neutral dipyridyl ligands. Allowing for longer reaction times produces no change in overall yield of the reaction. We hypothesized that the need of acid to involve K_2PtCl_4 and ligand homogenously in aqueous media could be avoided by allowing reaction of lipophilized derivatives of both the dpdmb ligand as well as the tetracholoroplatinate salt [56], as shown in Scheme 2.3 (b). Although the ligand in this form is expected to be more coordinating in this form, **2.8** could not be obtained.

Scheme 2.3: Attempted syntheses of (dpdmb)Pt^{II}-chloro complexes

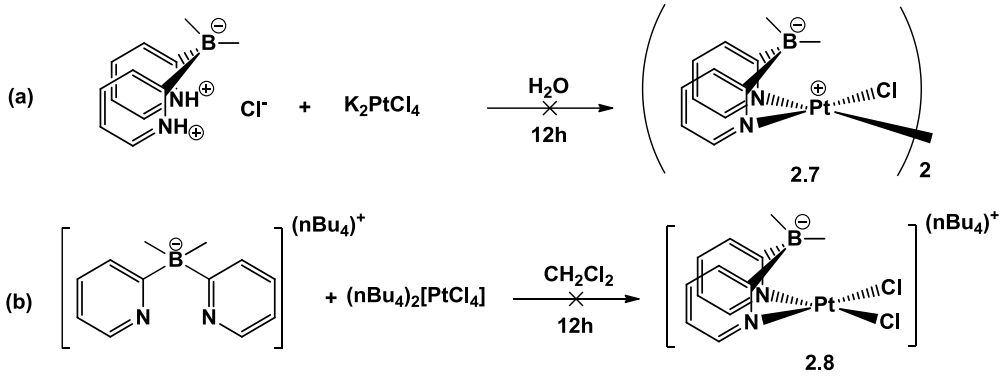

Henceforth, we discarded a bottom-up approach to synthesizing dpdmb-supported 'inorganic' Pt^{II}-complexes and started investigating variations in ancillary ligands that would allow protonolysis of the second PtMe fragment, similar to what was illustrated in Scheme 2.2(a). We considered dimethylsulfide as an ancillary ligand in lieu of methanol, based on established inertness [57] and low basicity [58] of the coordinated dimethylsulfide moiety. To our advantage, complex **2.9** can be easily synthesized in analytically pure form in virtually quantitative yields, as shown in Scheme 2.4. Furthermore, with a weakly basic ancillary ligand, the equilibrium such as that shown in Scheme 2.2(b) is expected to be biased more to the right, which might allow direct protonation of the Pt^{II}-center.

2.3 Results and Discussion

2.3.1 Synthesis of (dpdmb)Pt^{II}(Me)(SMe_2) complex

Scheme 2.4: Synthesis of (dpdmb)Pt^{II}(Me)(SMe_2) complex

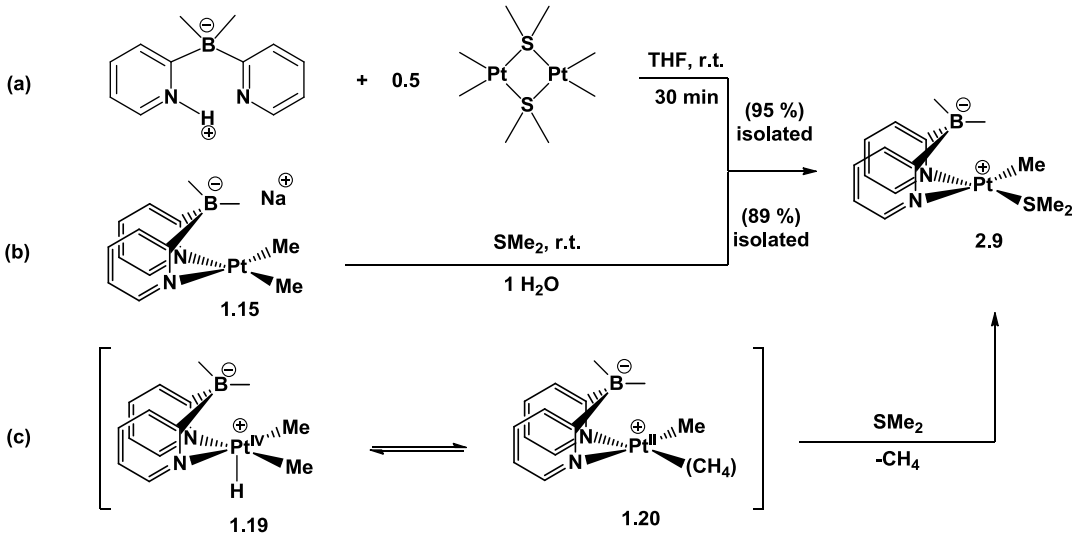

Complex **2.9** can be synthesized in excellent yields by two routes, as shown in Scheme 2.4, by either (a) reacting equivalent amounts of dpdmb-H with $[Me_2Pt(\mu\text{-}SMe_2)]_2$ or (b) by reacting of Na(dpdmb)$Pt^{II}Me_2$, **1.15** with water in the presence of dimethylsulfide. We presume that both reactions in Schemes 2.4(a) and 2.4(b) involve protonation of the Pt^{II} center in **1.15** by either H-dpdmb or water to form the transient Pt^{IV} hydride **1.19**, which then reductively eliminates methane to form the methane complex **1.20**, as was also discussed in Chapter-I. Substitution of the coordinated methane with Me_2S leads to free methane and the target complex **2.6**. The overall reaction is very fast owing to (i) previously established high basicity of electron rich **1.15** complexes, (ii) the kinetic instability of both rapidly equilibrating **1.19** and **1.20** and (iii) thermodynamic driving force of forming a strong Pt^{II}-SMe_2 bond, via known affinity of neutral sulfur ligands for the Pt^{II} center [59]. ^1H and ^{13}C NMR spectra of

2.9 in acetonitrile-d_3 are consistent with the presence of a C_1 symmetric species in these solutions. ^{1}H NMR spectra of **2.9** exhibit eight multiplets of equal intensity in the aromatic region, indicating the presence of two non-equivalent pyridyl rings, and two signals of nonequivalent boron-bound methyl groups integrating as 3H each suggesting the presence of a relatively rigid dipyridylborate fragment. In addition, two singlets of sulfur-bound methyl groups with the platinum-195 satellites confirm the presence of the Pt-coordinated dimethylsulfide ligand. ESI$^+$-MS of **2.9** dissolved in methanol containing an acid additive indicates the presence of the cation **2.9**·H$^+$ with m/z = 470.14 (calculated for $C_{15}H_{23}BN_2PtS$, 470.13).

Figure 2.1: ^{1}H-NMR spectrum of (dpdmb)Pt^{II}(Me)(SMe$_2$), **2.9** in CD_3CN (22 °C, 500.132 MHz). Note the non-equivalence of the signals corresponding to the BMe groups at 0.22 and 0.65 ppm.

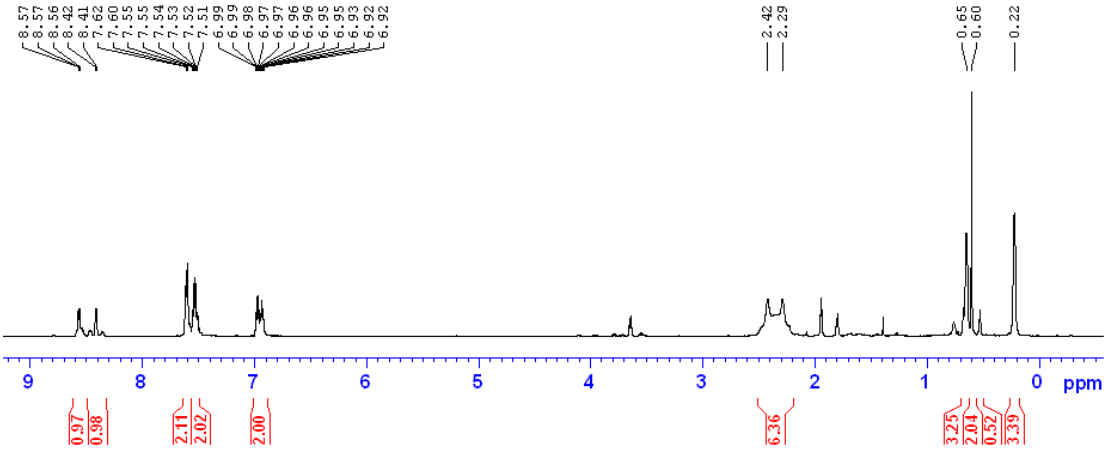

2.3.2 Preparation of cationic (dpdmb)$Pt^{II}(SMe_2)$-solvento complexes by protonolysis of the $Pt^{II}Me$ fragment

Scheme 2.5: Protonolysis of the $Pt^{II}Me$ fragment in (dpdmb)$Pt^{II}(Me)(SMe_2)$ complex

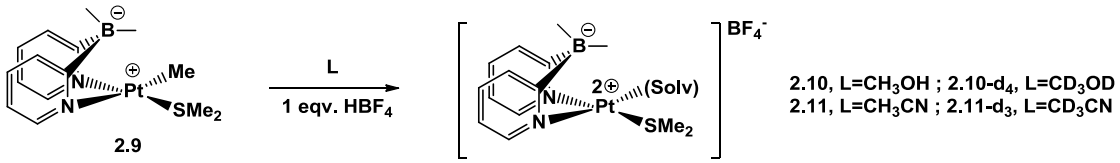

The strategy of using neutral sulfido complex **2.9** as a starting material to protonolyze the $Pt^{II}Me$ fragment proved to be promising. The $Pt^{II}Me$ fragment in **2.9** is much less basic than that in the anionic **1.15**. While the former cannot be protonolyzed by weak acids such as acetic and propionic acid, the latter, as established previously by Khaskin [34], undergoes protonolysis in methanol almost immediately. Reaction of complex **2.9** suspended in CD_3OD or CD_3CN in NMR tubes and equivalent amount of 50% aqueous HBF_4 leads to immediate evolution of methane gas and formation of the target complexes **2.10-*d*$_4$** or **2.11-*d*$_3$**, respectively, as shown in Scheme 2.5. NMR monitoring revealed that the formation of either complex was extremely facile and quantitative and no detectable intermediates were observed. Similar protonolysis reactions of neutral monohydrocarbyl-Pt^{II} complexes have been demonstrated in literature [60]. The ^1H and ^{13}C NMR spectra of **2.10-*d*$_4$** in CD_3OD show the presence of a fluxional C_1 symmetric species lacking the $Pt^{II}Me$ fragment.

Figure 2.2: ^{1}H-NMR spectrum of (dpdmb)Pt^{II}(SMe$_2$)(CD$_3$OD), **2.10-*d*$_4$** in CD$_3$OD (22 °C, 500.132 MHz) Note the equivalence of the signals corresponding to the BMe and SMe groups at 0.17 ppm and 2.45 ppm, respectively, and the absence of a Pt-Me resonance (~0-1ppm)

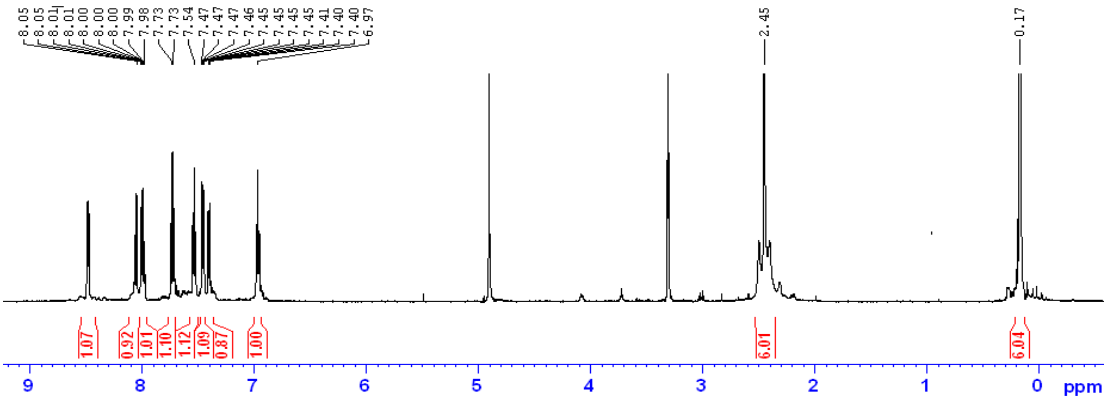

Additionally, an increase in the Pt-H coupling of the ortho-H of the pyridine from 22Hz in **2.9** to 46 Hz in **2.10-*d*$_4$** indicates the substitution of a strong trans-influencing group such as CH$_3$, by a weak trans-influencing group such as CD$_3$OD. Two methyl groups attached to the sulfur atom of the Pt-bound SMe$_2$ ligand in **2.10-*d*$_4$** produce a single broad peak integrating as 6H at 2.45 ppm ($^{3}J_{Pt\text{-}H}$=47 Hz) suggesting that, unlike in **2.9**, there is a fast exchange of the two methyl groups of the SMe$_2$ ligand. Similarly, two methyl groups attached to the boron atom of the dpdmb ligand produce one broad signal at 0.17 ppm integrating as 6H.

Scheme 2.6: Mechanism of exchange of the B-Me fragments in [(dpdmb)Pt^{II}(SMe$_2$)(CD$_3$OD)]BF$_4$

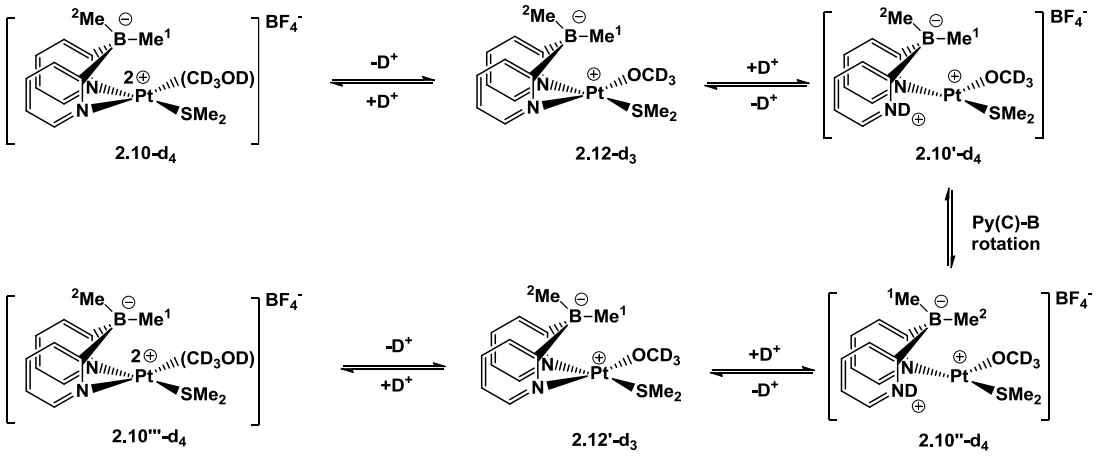

We performed VT-NMR studies to find the temperatures at which exchange of the methyl groups of the SMe_2 and BMe_2 fragments could be halted. At -15 °C the methyl group signals of the SMe_2 fragment de-coalesce whereas the signals of the BMe_2 fragment de-coalesce at –30 °C. Various mechanisms accounting for the fluxional behavior may be proposed, such as 'rotation' of dpdmb and Pt(OMe)(SMe_2) fragments relative to each other leading to the methyl group exchange in the SMe_2 fragment as well as a reversible dissociation of one of the Pt-N bonds with subsequent protonation of the dissociated pyridine nitrogen atom. As shown in Scheme 2.6, deprotonation of cationic **2.10-*d*$_4$** to form neutral (dpdmb)Pt^{II}(OCD_3)(SMe_2), **2.12-*d*$_3$**, might facilitate the Pt-N bond dissociation whereas protonation of the dissociated nitrogen may allow for a relatively long life of the protonated intermediate, **2.10'-*d*$_4$**, sufficient for rotation of the dpdmb ligand about the remaining Pt-N bond by 180^o to form **2.10''-*d*$_4$**. Subsequent deprotonation and re-coordination of the free pyridine residue produces the neutral (dpdmb)Pt^{II}(OCD_3)(SMe_2) complex, **2.12'-*d*$_3$**. The result of this reaction sequence is an apparent BC_2N_2Pt ring inversion and the methyl group exchange in the BMe_2 fragment, viz. the conversion of **2.10-*d*$_4$** to **2.10'''-*d*$_4$**. A

solution of **2.10-*d*$_4$** in CD_3OD diluted with methanol showed masses corresponding to both **[2.7-*d*$_4$]**$^+$ and **[2.7-*d*$_3$·H]**$^+$ in the ESI-MS indicating facile proton exchange, in accord with reversible deprotonation.

Attempts were made to isolate the corresponding non-deuterated complexes: while **2.11** could be isolated by removal of CH_3CN from the reaction vessel, complex **2.10** could not be isolated without observing substantial decomposition. Although more stable than **2.6** which decomposed within 1h, **2.10-*d*$_4$** in CD_3OD or **2.10** in CH_3OH are both unstable in solution at room temperature over long periods of time. In less than 12 h a dark precipitate formed consistent with an intractable mess observed in the ^{1}H-NMR spectra recorded after this time period. Even faster decomposition was observed when attempted to isolate it by removal of solvent. Presumably, the neutral methanol ligand is weakly bound to the Pt^{II}-center in **2.10** and prolonged exposure to vacuum generates a highly unstable three-coordinate Pt^{II} species, **2.13**, as shown in Scheme 2.7.

Scheme 2.7: Decomposition of cationic (dpdmb)$Pt^{II}(SMe_2)$(MeOH) complex

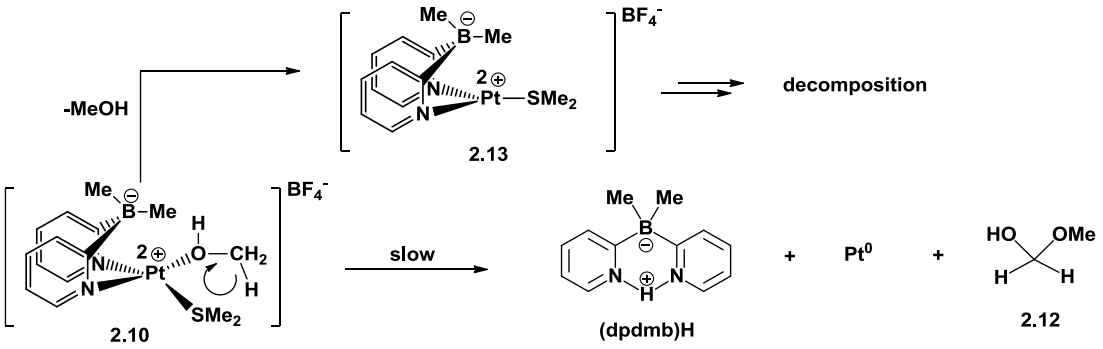

The slow decomposition of **2.10** in solution most likely involves β-hydride elimination of methanol ligand leading to formation of an unstable Pt^{II} hydride along with formaldehyde-derived acetal, as shown in Scheme 2.7. Accordingly, a sample of **2.10-*d*$_1$** prepared by reacting **2.9** in CH_3OD was let to sit for 12h at room temperature

after which precipitate of Pt-black was clearly visible. According to the ^{1}H-NMR spectra, products of decomposition of **2.10-*d*$_1$** in CH_3OD solutions contain a singlet at 4.16 ppm assigned to the methylene group of methoxy methanol CH_3OCH_2OD [61]. This signal was compared to that of an authentic sample of the latter compound prepared by dissolving paraformaldehyde in the same solvent. ESI^{+}-MS of the CH_3OD sample showed a peak at 199.1 corresponding to doubly-protonated ligand, H_2-dpdmb, consistent with the aforementioned mechanism. This decomposition route might be similar to that observed for **2.6** discussed before.

The acetonitrile analogues **2.11 and 2.11-*d*$_3$** are more stable both in solutions and in solid state but still shows signs of decomposition in the course of few days and hence could not be isolated in an analytically pure form. As compared to **2.10-*d*$_4$**, the acetonitrile complex, **2.11-*d*$_3$** is not so fluxional in solution at room temperature. The ^{1}H NMR spectrum of **2.11-*d*$_3$** in CD_3CN shows two broad singlets of two sulfur-bound methyl groups with the platinum-195 satellites and two broad singlets of two boron-bound methyl groups.

Figure 2.3: ^{1}H-NMR spectrum of [(dpdmb)Pt^{II}(SMe_2)(CD_3CN)]BF_4^-, **2.11-*d*$_3$** in CD_3CN (22 °C, 500.132 MHz). Note the inequivalent BMe resonances at 0.24 and 0.81 ppm, and the inequivalent SMe resonances at 2.36 and 2.66 ppm.

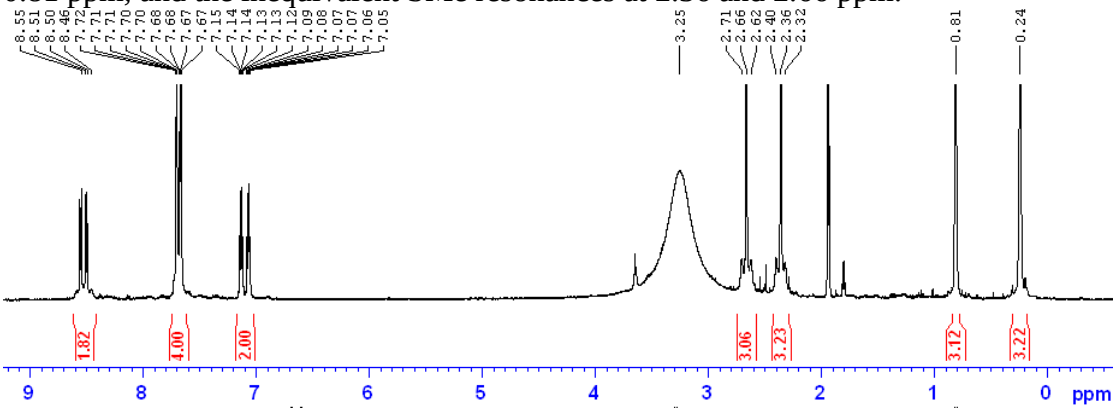

The fluxionality of complex **2.10-*d*$_4$** as opposed to complex **2.11-*d*$_3$** may be attributed to the ability of the former to exchange the Pt-bound (CD_3OD) with solvent. Acetonitrile on the other hand is expected to be very tightly bound to the Pt^{II}-center. Experimentally, the non-deuterated variant, **2.11** showed no signs of exchange with CD_3CN when dissolved in it for a period of up to 2 days. ESI-MS of a sample of **2.10-*d*$_4$** in CD_3OD diluted with excess CH_3OH showed peaks corresponding to both **2.10-*d*$_4$** (m/z=490.1) and **2.10** (m/z=486.1) indicating that exchange of the Pt-bound CD_3OD with CH_3OH was facile.

2.3.3 Oxidation of di(2-pyridyl)dimethylborato-Pt^{II}(Me)(SMe_2) complex with H_2O_2

Scheme 2.8: Oxidation of (dpdmb)Pt^{II}(Me)(SMe_2) complex with H_2O_2

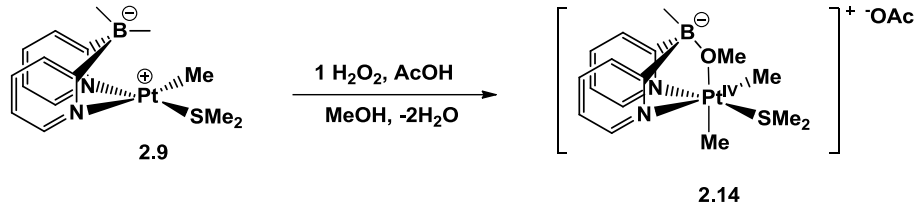

In contrast to $[(dpdmb)Pt^{II}Me(OMe)]^-$, **1.21**, complex **2.9** does not react with oxygen. Similar change in reactivity towards O_2 is observed for monomethyl Pt^{II} complexes supported by di(2-pyridyl)methanesulfonate ligand (dpms) [62]. In particular, for $(dpms)Pt^{II}Me(L)$, an ionizable ligand such as methanol replaced with non-ionizable neutral ligand such as DMSO renders the Pt^{II}-complex inert towards oxygen. Nevertheless, oxidation of **2.9** to form a cationic Pt^{IV} derivative **2.14** is facile when a stronger oxidant, H_2O_2, is used in combination with a few equivalents of acetic acid in methanol, as shown in Scheme 2.8. The ^1H NMR spectrum of the product of

oxidation dissolved in acetone-d_6 shows the presence of a C_1-symmetric species with two singlets of two non-equivalent Pt-bound methyl groups at 1.33 ppm ($^2J_{Pt\text{-}H}$=66 Hz) and 1.83 ppm ($^2J_{Pt\text{-}H}$=74 Hz), integrating as 3H each. Only one signal of the boron-bound methyl group at 0.53 ppm integrating as 3H can be found, indicating complete *methyl migration*. The singlet at 3.33 ppm ($J_{Pt\text{-}H}$ = 12.4 Hz) integrating as 3H could be assigned to the B-(μ-OC*H*$_3$)-Pt fragment of the Pt-coordinated (methoxy)(methyl)di(2-pyridyl)borate (MeO-mdpb) (c.f. p-28 for ^{1}H-NMR and appendix p-127 for ^{13}C-NMR spectra).

Figure 2.4: ^{1}H-NMR spectrum of [(Me)BPy$_2$(μ-OMe)Pt^{IV}(SMe$_2$)(Me$_2$)]OAc, **2.14** in acetone-d_6 (22 °C, 500.132 MHz). Note the residual B-Me resonance at 0.51 ppm integrating to 3 hydrogens. Also note two Pt-Me resonances at 1.36 and 1.84 ppm, consistent with a C_1 symmetric structure. The region corresponding to the pyridine ortho hydrogens has been expanded: clear distinction of the effect of trans PtMe and trans PtSMe$_2$ fragments on the Pt-coupling to the pyridine ortho hydrogens are visible.

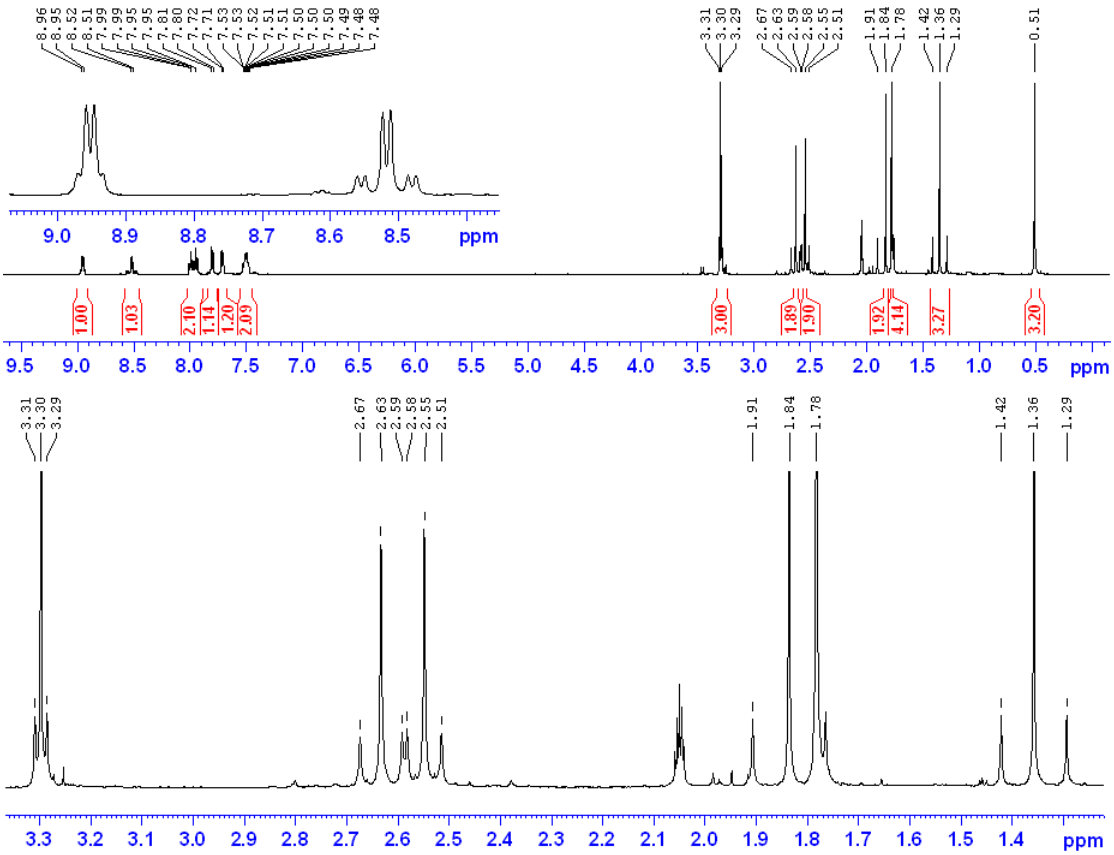

As in the case of the aerobic oxidation of anionic species (dpdmb)Pt^{II} complexes described previously [34], (methoxy)(methyl)di(2-pyridyl)borate ligand results from oxidatively induced B-to-Pt methyl group migration assisted by nucleophilic attack of methanol at the boron atom. Two singlets of the sulfur-bound methyl groups are observed in the NMR spectrum of **2.14** as well, each corresponding to 3H and having the platinum-195 satellites so confirming retention of the SMe_2 ligand in the platinum coordination sphere. The identity of **2.14** was also confirmed by ESI^+-MS, and purity was ascertained by elemental analysis. **2.14** bears resemblance to a Ru^{II} complex bearing a $(Me)(OH)BPy_2$ ligand synthesized by Williams et al. [63] via agostic demethylation of the original dimethylborato ligand, **1.14**. The oxidation of **2.9** is the first example of oxidation of a di(2-pyrdiyl)dimethylborato-Pt^{II}-complex with H_2O_2 and provides proof of concept that oxidation with H_2O_2 also results in B-to-Pt^{IV} Me-migration.

It was previously established by Vedernikov et al. that the trihydrocarbyl and dihydrocarbyl Pt^{IV} complexes supported by (methoxy)(methyl)di(2-pyridyl)borate ligand, such as **1.22** and **1.23**, are inert towards C-C and C-O reductive elimination at temperatures up to 120^oC [34]. Therefore, it was interesting to check if the analogous electron-poorer cationic dimethyl Pt^{IV} complex **2.14** exhibit different reactivity and can reductively eliminate products with new C-C or C-O bonds. It has been demonstrated in literature that reductive elimination from octahedral Pt^{IV} or Pd^{IV} centers is possible via a five-coordinate intermediates [64]. Thus, in order to explore the possibility of C-C or C-O reductive elimination from **2.14**, the complex must be converted to a five-coordinate system. While the bridging B-μ(methoxy) ligand does

not exchange in CD_3OD even when heated at 80°C, as evidenced by clearly visible Pt-satellites in the ^{1}H-NMR spectra, addition of 1 eqv. of 50% aqueous HBF_4 caused immediate disappearance of the corresponding ^{1}H-NMR signal.

Figure 2.5: ^{1}H-NMR Spectrum of [(Me)(CD_3O)B$Py_2Pt^{IV}(Me_2)(SMe_2)$]OAc, **2.14-*d*$_3$** in CD_3OD after addition of HBF_4 and heating at 80 °C for 24h. Note absence of the bridging B-μ(methoxy).

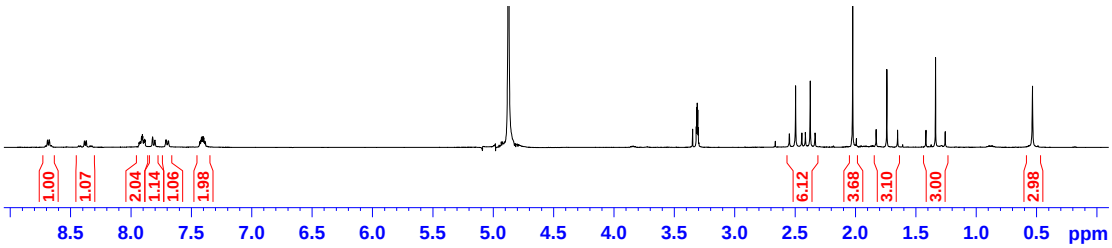

In this acidified CD_3OD solution, **2.14** showed no signs of decomposition at 20 °C, according to ^{1}H-NMR spectroscopy. Heating the mixture at 100°C for 2 days caused no changes. Heating the solution further at 120 °C led to its darkening, decomposition and formation of black solid. In all cases, neither methanol, dimethyl ether nor ethane were detected by ^{1}H-NMR. According to these observations, cationic dimethyl complex **2.14** does not undergo either C-C or C-O reductive elimination up to 100 °C. Hence, the presence of a positive charge is not sufficient to make $Pt^{IV}Me_2$ complex electrophilic enough to undergo attack by solvent (e.g. MeOH) to afford reductive elimination.

2.3.4 Oxidation of di(2-pyridyl)dimethylborato-$Pt^{II}(CD_3OD)(SMe_2)^+$ complex with H_2O_2

We next explored the oxidation of the cationic complexes **2.10-*d*$_4$** (generated in-situ) and **2.11** in CD_3OD. A solution of **2.10-*d*$_4$** in CD_3OD is stable under bubbling O_2 for at least 2h but reacts rapidly with H_2O_2. The oxidation is cleaner when performed at

lower temperatures using slight excess H_2O_2. When performed at 0°C the reaction leads to virtually quantitative and immediate formation of methyldi(2-pyridyl)borane (mdpb) complex **2.15-*d*$_3$** in 71% yield, as shown in Scheme 2.9, along with 1 equivalent of CD_3OCH_3, **2.17-*d*$_3$**, detectable by ^{1}H-NMR.

Scheme 2.9: Oxidation of (dpdmb)Pt^{II}(CD$_3$OD)(SMe$_2$)$^+$ complex with H_2O_2

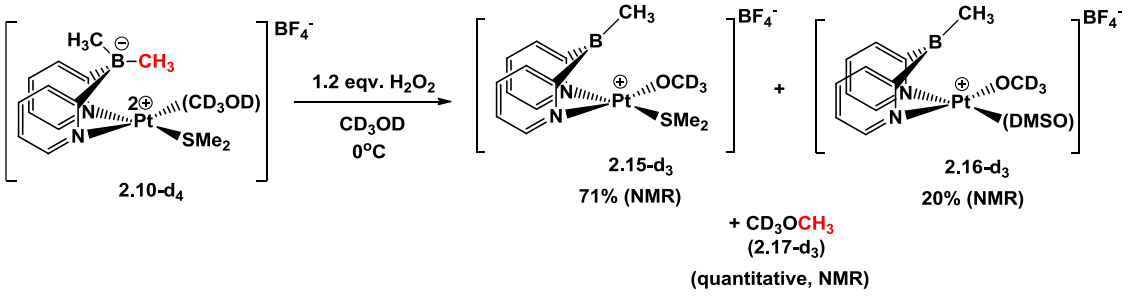

The presence of excess H_2O_2 leads also to the oxidation of the ancillary SMe_2 ligand and formation of the dimethylsulfoxide analogue, **2.16-*d*$_3$**, in 20% yield. While a short-lived Pt^{IV}-peroxo intermediate is believed to form upon reaction of H_2O_2 with **2.10-*d*$_4$**, we presumed that the oxidation of the ancillary SMe_2 fragment was directly by the oxidant and not by the peroxo-intermediate as demonstrated by Goldberg et al. [65]. **2.17-*d*$_3$** was characterized in the reaction mixture using the ^{1}H-NMR spectroscopy and ESI$^+$-MS. The results were compared to that of an authentic sample of CD_3OCH_3 independently prepared by reacting NaOMe with CD_3I in methanol. Complex **2.15-*d*$_3$**, as formed in-situ, was dirty, and could not be isolated as a solid due to rapid darkening upon removal of CD_3OD, a behavior similar to that of **2.10-*d*$_4$**. The evacuation of CD_3OD was stopped at this point, and a ^{1}H-NMR spectrum was recorded. The ^{1}H-NMR spectrum of **2.15-*d*$_3$** is typical for a C_1 symmetric dipyridylborate species. The coordinated SMe_2 produces two broad singlets of equal

intensity 3H at 2.64 ppm and 2.89 ppm, both with the platinum-195 satellites and almost identical Pt-H coupling constants of 39 Hz.

Figure 2.6: ^{1}H-NMR spectrum of [(Me)BPy$_2$Pt^{II}(SMe$_2$)(OCD$_3$)]BF$_4$, **2.15-*d*$_3$** in CD$_3$OD (22 °C, 400.131 MHz) (contains trace amounts of decomposition products). Note the residual B-Me resonance at 0.26 ppm and the resoances corresponding to the non-equivalent SMe fragments at 2.64 and 2.89 ppm.

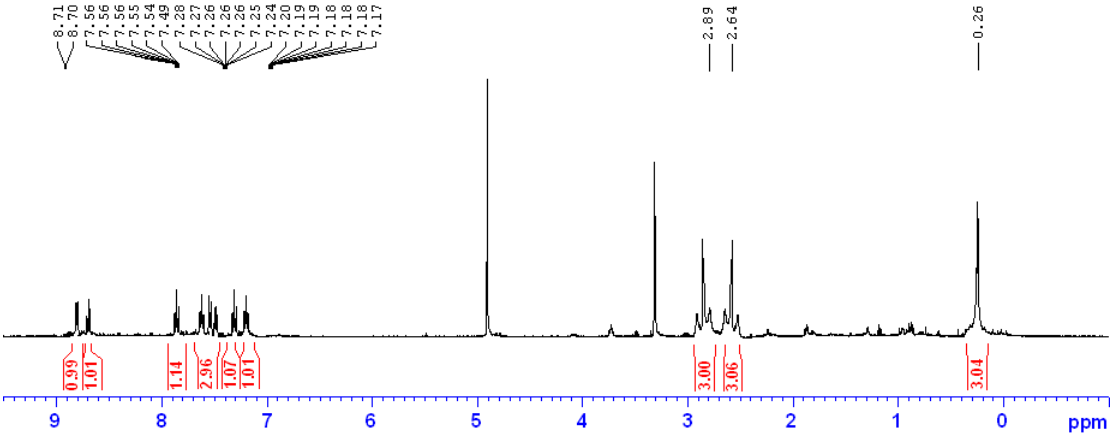

Only one signal originating from the boron-bound methyl group at 0.26 ppm integrating as 3H could be found suggesting that the second methyl group of the original B(CH$_3$)$_2$ fragment was lost in the course of the reaction. Analysis of the organic reaction product, CD$_3$OCH$_3$, indicates the direction of this loss. Finally, ESI$^+$-MS characterization of the CD$_3$OD solution indicates the presence of the cation **2.15-*d*$_3$** with m/z = 473.13 (calculated for C$_{14}$H$_{17}$BD$_3$N$_2$O^{195}PtS, 473.12). It is noteworthy at this point to mention that unlike **2.10-*d*$_4$**, **2.11** could not be oxidized in CD$_3$OD even with up to 5 equivalents of H$_2$O$_2$.

2.3.5 Mechanism of oxidation of di(2-pyridyl)dimethylborato-Pt^{II}(L)(SMe$_2$)$^+$ complexes, L=CD$_3$OD, CH$_3$CN with H$_2$O$_2$

While discussing the role of the Pt center in the formation of dimethyl ether, it is important to note that in the absence of coordinated platinum, the dpdmb ligand used

in the form of H(dpdmb) does not react with H_2O_2, which was proven in a separate experiment under conditions identical to those employed for oxidation of **2.10-*d*$_4$**. The mechanism of oxidation of **2.9** and that of **2.10-*d*$_4$** in CD_3OD solutions presumably progress via methyl migration to the Pt^{IV} center. While for **2.9** it leads to a stable dimethyl-Pt^{IV} complex, **2.14**, for **2.10-*d*$_4$** it leads to **2.15-*d*$_3$** and CD_3OCH_3, **2.17-*d*$_3$**.

Scheme 2.10: Mechanism of tandem B-to-Pt^{IV} *methyl migration* and C-O elimination

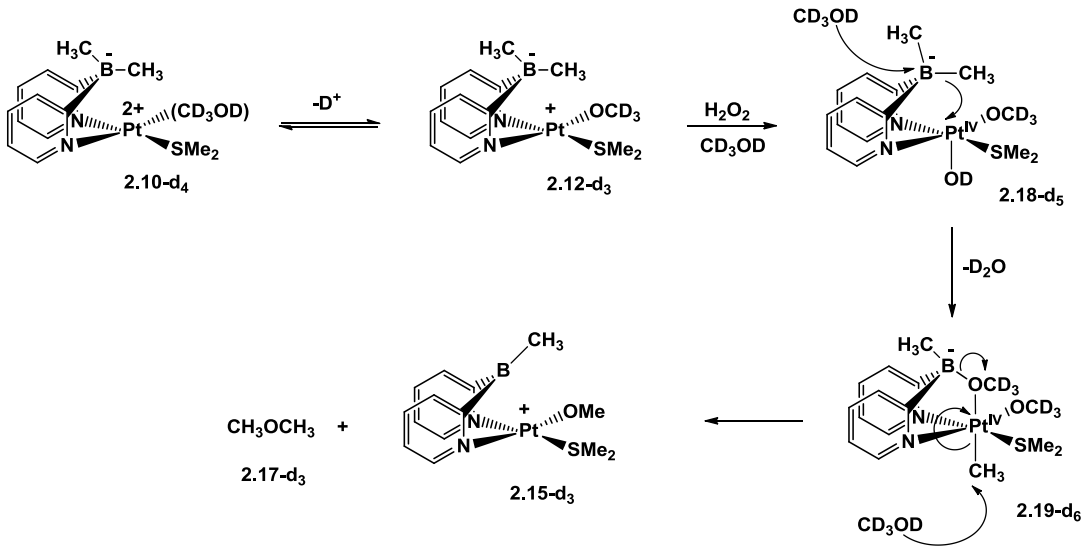

The reaction sequence shown includes an electrophilic attack of H_2O_2 at the Pt^{II} center leading to the cationic Pt^{IV} intermediate **2.18-*d*$_5$**. The attack most likely involves a zwitterionic complex **2.12-*d*$_3$** with the Pt^{II} center bearing a formal charge +1, lower than a formal charger of +2 in **2.10-*d*$_4$**. In turn, complex **2.12-*d*$_3$** results from dissociation of acidic proton of the coordinated methanol ligand in **2.10-*d*$_4$**. The same formal charge +1 at the Pt^{II} atom is found in complex **2.9**, hence explaining its facile and clean oxidation with H_2O_2. Interestingly, complex **2.11** does not react with H_2O_2 under comparable reaction conditions which may be due to the presence of a too electron-poor Pt atom bearing +2 formal charge. The facile deprotonation of the

$Pt^{II}(CD_3OD)$ fragment in **2.10-*d*$_4$** may also be invoked to explain why unlike the former, **2.11** is reluctant to undergo oxidation by H_2O_2, under similar conditions.

The cationic Pt^{IV} center in the transient **2.18-*d*$_5$** is involved in the B-to-Pt methyl group transfer leading to another cationic monomethyl Pt^{IV} intermediate **2.19-*d*$_6$**. We propose that the B-to-Pt methyl group transfer step involving **2.18-*d*$_5$** is similar to that operational in the aerobic oxidation of anionic (dpdmb)Pt^{II} complexes, **1.15** and **1.21**. The cationic Pt^{IV} transient **2.19-*d*$_6$** has only one methyl group at the metal and, therefore, is more electron-poor than the cationic dimethyl Pt^{IV} complex **2.14**. We propose that complex **2.19-*d*$_6$** is electrophilic enough to accept fast nucleophilic attack of CD_3OD at the *C*-atom of the Pt^{IV}-Me fragment, leading to the formation of **2.15-*d*$_3$** and CD_3OCH_3, **2.17-*d*$_3$**.

In order to detect plausible intermediates in oxidation of **2.10-*d*$_4$** with H_2O_2, the reaction was performed at lower temperatures. The oxidation did not occur at appreciable rate below -30 °C even with 20 equivalents of H_2O_2 used. When performed at -15 °C, the disappearance of the starting material was accompanied with formation of CD_3OCH_3 with no detectable intermediate complexes. Hence, we suggest that the reductive elimination step involving presumed transient **2.19-*d*$_6$** is much faster than conversion of **2.18-*d*$_5$** to **2.19-*d*$_6$** at -15 °C. A possible way to change the ratio of these two reaction rates was to perform the oxidation of the neutral complex **2.12-*d*$_3$** generated from cationic **2.10-*d*$_4$** in the presence of sodium methoxide. The larger fraction of **2.12-*d*$_3$** present in such solution would lead to a faster oxidation rate. However, no reaction intermediates were detected by means of ^{1}H NMR spectroscopy in reaction mixtures containing **2.10-*d*$_4$** and 1 equivalent of

NaOMe though the rate of disappearance of **2.10-*d*$_4$** and formation of dimethylether-d_3 at -15 °C increased 1.4 fold compared to the case when no base additives were present. A possible explanation is that complex **2.10-*d*$_4$** dissociates to produce **2.12-*d*$_3$** in a significant extent already in neat CD_3OD, and as the latter undergoes oxidation, it is replenished rapidly be further deprotonation of **2.10-*d*$_4$**.

2.4 Conclusions

Although attempts to synthesize anionic 'inorganic' complexes supported by the dpdmb ligand failed, the observation of the facile C-O bond formation in the course of oxidation of complexes bearing no hydrocarbyls on the Pt^{II} center with H_2O_2 allows us to propose that model di(2-pyridyl)borate Pt^{IV} complexes may be involved at the C-O bond forming step of a potential catalytic cycle allowing for aerobic functionalization of C-H bond donors. We find that even towards a strong oxidant like H_2O_2, formal charge on the Pt-center plays a crucial role in the oxidation of complexes. Based on direct comparison to the aerobic oxidation of anionic dpdmb-supported monohydrocarbyl and dihydrocarbyl Pt^{II} complexes, we propose that similar mechanism of '*oxidatively induced hydrocarbyl migration*' may be in operation for oxidation of the cationic complexes with H_2O_2 discussed herein.

2.5 Experimental Section

2.5.1 Attempted synthesis of (dpdmb)$Pt^{II}(OMe)_2$, 2.1 (a) and (dpdmb)$Pt^{II}(OCD_3)(CD_3OD)$, 2.6-d_7 (b):

(a) 25 mg (54.2 µmol) of Na(dpdmb)Pt^{II}(Me)(OMe), **1.21**, was dissolved in 1 mL of methanol in a vial equipped with a stir bar in the glove-box, and to it was added 6.8 µL (1 eqv.) aq. 50% HBF_4. Slight evolution of gas could be seen, followed by progressive formation of dark-brown solution and particulates within 10 minutes. At this point an ESI^+-MS of an aliquot was recorded, and a signal at m/z=199.1, corresponding to (dpdmb)H_2^+ was seen. The sample decomposed completely within 1h. In another experiment, faster decomposition was observed when the sample was exposed to high-vacuum within 2 minutes after addition of HBF_4.

(b) Henceforth we decided to monitor the reaction by ^{1}H-NMR spectroscopy. 15 mg (33.7 µmol) of **1.15** was dissolved in CD_3OD and a ^{1}H-NMR spectra was recorded. According to the NMR, clean formation of **1.21-*d_6*** had occurred [34]. At this point, 4.2 µL (1 eqv.) of HBF_4 was added and a ^{1}H-NMR spectra was quickly recorded. Although significant decomposition could be visible, one set of aromatic signals presumed to belong to **2.6-*d_7*** were identified. After 10 minutes, more than 30 peaks in the aromatic region were visible along with the formation of *Pt-mirror* on the walls of NMR-tube. Integrations were not reliable due to line-broadening and overlap of multitude of peaks.

2.6-*d_7* (tentative assignment): ^{1}H NMR (22 °C, 400 MHz, CD_3OD, ppm), δ: 0.18 (BMe), 6.97, 7.11, 7.78, 8.01 ($J_{Pt\text{-}H}$=~31 Hz).

2.5.2 Attempted synthesis of [(dpdmb)$Pt^{II}(Cl)]_2$, 2.7 (a), and nBu_4[(dpdmb)$Pt^{II}Cl_2$], 2.8 (b):

(a) 50 mg (252.4 µmol) of dpdmb-H and 10.4 mg (1 eqv.) of K_2PtCl_4 was added to a reaction vial containing 1 mL of H_2O. To this suspension was added 42 µL of aq. HCl, and immediate dissolution of all components was observed to form an orange colored solution. The reaction mixture was stirred, periodically monitoring for color change. After 24h when no color change or formation of precipitate was observed, the solution was stripped to dryness to obtain an amorphous powder. The powder seemed to consist of two separate entities, one soluble in CD_2Cl_2, and the other soluble in D_2O. While the former confirmed to free ligand by ^{1}H-NMR spectroscopy, corresponding to no Pt-H coupling of the ortho pyridine hydrogens, the latter was almost ^{1}H-NMR-silent. No complexation had occurred.

(b) 10 mg of nBu_4N[dpdmb] (22.7 µmol) [34] was combined with 19 mg (1 eqv) of $(nBu_4N)_2[PtCl_4]$ in 0.7 mL of CD_2Cl_2 in an NMR tube. Immediate dissolution of all components was seen. No reaction, as evident from the absence of Pt-H coupling of the ortho pyridine hydrogens, was observed even after 24 h.

2.5.3 Synthesis of (dpdmb)Pt^{II}(Me)(SMe_2), 2.9:

(a) Protonated dimethyldipyridylborate ligand, H(dpdmb) (138 mg, 696 µmol) was dissolved in 20 mL of THF in a vial. This solution was added dropwise with vigorous stirring over a 2 minute period to a 100 mL Schlenk flask containing 200mg

$Pt_2Me_4(\mu\text{-}SMe_2)_2$ (348 µmol). Gas evolution was seen, and after 15 minutes of addition, the solution turned light-brown. After a total of 30 minutes the Schlenk flask was evacuated and kept under vacuum overnight to yield a tan colored powder. The solid was washed with hexanes and recrystallized from methanol to yield 309 mg of a pure product, a yellow colored powder, **2.9** in 95% yield.

(b) Complex **2.9** was independently synthesized from Na[(dpdmb)$PtMe_2$], **1.15**, as follows: 50 mg of Na[(dpdmb)$PtMe_2$] complex (112.3 µmol) was dissolved in 3 mL of dimethyl sulfide placed in a vial equipped with a stirring bar. To this solution was added 4.0 µL H_2O (2 equivalents) with vigorous stirring. Gas evolution and some yellow particulates were seen immediately. After 5 minutes, the contents were filtered through Celite and the residues were washed with 1 mL of THF. The solvent was removed from the combined filtrate and washings. The residue was dried under high vacuum to give a tan colored solid. The solid was washed with 3 mL of 1:1 v/v ether-hexane mixture to give 46.9 mg of **2.9**, 89% yield. Complex **2.9** is an air-stable solid, showing no signs of thermal decomposition at temperatures up to 80 °C under argon atmosphere. Complex **2.9** is resistant toward the protonolysis of the Pt-Me fragment by methanol and water but reacts with acetic acid slowly over 24h. Complex **2.9** is sparingly soluble in methanol and ether, moderately soluble in benzene, and highly soluble in acetone, THF, and acetonitrile. c.f. appendix p-125 for ^{13}C-NMR spectrum.

^{1}H NMR (22 °C, 500 MHz, CD_3CN, ppm), δ: 0.22 (br, s, 3H, B-Me), 0.59 (s, $^2J_{Pt\text{-}H}$=72 Hz, 3H, Pt-Me), 0.64 (br s, 3H, B-Me), 2.28 (br s, $^3J_{Pt\text{-}H}$=54 Hz, 3H, SMe), 2.42 (br s, $^3J_{Pt\text{-}H}$=54 Hz, 3H, SMe), 6.93 (dt, *J*=6.7, 1.9 Hz, 1H), 6.97 (dt, *J*=6.9, 1.9 Hz, 1H), 7.53 (dq, *J*=7.2, 1.8 Hz, 1H), 7.61 (vd, *J*=7.6 Hz, 1H), 8.41 (d, $J_{H\text{-}H}$=8.41, $J_{Pt\text{-}H}$=52 Hz, 1H), 8.56 (d, $J_{H\text{-}H}$=5.7, $J_{Pt\text{-}H}$=29 Hz, 1H).

^{13}C NMR (22 °C, 500 MHz, CD_3CN, ppm), δ: -15.2 (s, $^1J_{Pt\text{-}C}$=733 Hz), 11.9 (br, BMe), 15.9 (br, BMe), 20.8 (br, SMe), 24.4 (br, SMe), 121.2, 121.5, 129.1, 129.4, 135.8, 135.9, 150.5 (*o*-py carbon *trans*- to Pt-Me, Pt-195 coupling not seen), 151.5 (*o*-py carbon, $J_{Pt\text{-}C}$=43 Hz), 187-193 (br, py-2-C(B))

ESI of a methanolic solution of **2.9** with 10% aqueous acetic acid, **2.9**·H^+, $C_{15}H_{24}BN_2PtS$: 470.14, Calculated: 470.13.

Elemental analysis: calculated for $C_{15}H_{23}BN_2PtS$, C, H, N: 38.5, 4.94, 5.96. Found C, H, N 39.0, 4.99, 5.65.

2.5.4 Preparation of [(dpdmb)$Pt^{II}(SMe_2)(MeOH)](BF_4)$ complex, 2.10-*d*$_4$:

15 mg (31.96 µmol) of **2.9** was suspended in 0.5 mL of CD_3OD in an NMR tube and 4 µL (32 µmol) of 50% aqueous HBF_4 was added. Immediate evolution of gas was observed. The methanolic solution decomposes slowly over a period of 12 h. Attempted isolation of **2(BF_4)** in a solid state leads to even faster decomposition.

^{1}H NMR (22 °C, 500 MHz, CD_3OD, ppm), δ: 0.17 (br s, 6H, BMe_2), 2.45 (br s, $^3J_{Pt\text{-}H}$=47 Hz, 6H, SMe_2), 6.9 (dt, *J*=6.8, 2 Hz, 1H), 7.45 (vd, *J*=6.2 Hz, 1H), 7.46 (vd, *J*=7.5 Hz, 1H), 7.5 (dt, *J*=7.0, 1.4 Hz, 1H), 7.7 (dt, *J*=7.6, 1.5 Hz, 1H), 7.9 (dt, *J*=7.9, 1.5 Hz, 1H), 8.01 (d, *J*=8.1, $J_{Pt\text{-}H}$=34 Hz, 1H), 8.4 (d, *J*=6.2, $J_{Pt\text{-}H}$=60 Hz, 1H).

^{13}C NMR (22 °C, 500 MHz, CD_3OD, ppm), δ: 23.43 (SMe_2), 122.8, 123.1, 129.6, 138.2, 139.8, 142.9, 143.1, 149.4. B-Me fragment and *ipso*-C of the pyridine ring were not seen due to boron splitting.

ESI^+ of a CD_3OD solution of **2.10-*d*$_4$**, $C_{15}H_{20}D_4OBN_2PtS$: 490.18. Calculated: 490.16.

2.5.5 Decomposition of 2.10-d_4 in CH_3OD leading to formaldehyde and methoxymethanol:

10 mg (21.31 µmol) of **2.9** was dissolved in CH_3OD in an NMR tube, 2.7 µL (21.6 µmol) of 50% aqueous HBF_4 was added and the tube was sealed. Immediate evolution of gas was seen. An NMR spectrum recorded by suppressing the methyl group signal of the CH_3OD solvent confirmed the quantitative and clean formation of **2.10-*d*$_4$**. The solution was left standing overnight after which a black particulate was seen. In the NMR spectrum, two new sets of signals were clearly identifiable. One set of signals was assigned to the protonated dpdmb ligand, H(dpdmb). The second set included one singlet at 4.61 ppm. The spectrum was compared to that of a solution of paraformaldehyde in CH_3OD acidified with small amount of HBF_4. The peak at 4.61 ppm matched in both cases.

2.5.6 Synthesis of [(dpdmb)$Pt^{II}(SMe_2)(NCMe)](BF_4)$ complex, 2.11:

50 mg (106.54 µmol) of **2.9** was dissolved in 4 ml of acetonitrile in a reaction vial equipped with a stirring bar and 19 µL (108 µmol) of 50% aqueous HBF_4 was added with vigorous stirring. Immediate evolution of gas was observed. After 10 minutes the solution was stripped to dryness and a white solid was obtained. The solid was washed with a 1:1 v/v ether - hexane mixture, followed by further drying to yield 52 mg of a highly-hygroscopic micro-crystalline white solid **2.11** in quantitative yield. Complex **2.11** is insoluble in ether and methanol, but soluble in THF, acetone and acetonitrile. c.f. appendix p-126 for ^{13}C-NMR spectrum.

^{1}H NMR (22 °C, 500 MHz, acetone-d_6, ppm), δ: 0.26 (br s, 3H, B-Me), 0.83 (br s, 3H, B-Me), 2.53 (br s, $^3J_{Pt\text{-}H}$=33 Hz, 3H, SMe), 2.85 (br s, 3H, NCMe), 2.88 (br s, $^3J_{Pt\text{-}H}$=33 Hz, 3H, SMe), 7.15 (dt, *J*=6.8, 2.1 Hz, 1H), 7.20 (dt, *J*=6.6, 2.0 Hz, 1H), 7.66-7.77 (m, 4H), 8.71 (d, *J*=6.2 Hz, 1H), 8.78 (d, *J*=5.8 Hz, $J_{Pt\text{-}H}$=30 Hz, 1H).

^{13}C NMR (22 °C, 500 MHz, acetone-d_6, ppm), δ: 4.1 (NC*C*H3), 10.9 (br, BMe), 15.64 (br, BMe), 22.4 (SMe), 24.5 (SMe), 122.5, 122.8, 129.9, 130.0, 138.3, 151.5, 152.7. *ipso*-carbon of the pyridine ring were not seen due to boron splitting.

ESI(+)-MS of a THF solution of **2.11**: 495.14, Calculated: 495.14.

The solid complex shows signs of decomposition in the course of few days when stored at 20 ºC under an argon atmosphere. Hence, satisfactory elemental analysis could not be obtained. Elemental analysis: calculated for $C_{16}H_{23}B_2F_4N_3PtS$, C, H, N: 33.01, 3.98, 7.22. Found C, H, N 33.60, 3.59, 6.50

2.5.7 In-situ preparation of [(dpdmb)$Pt^{II}(SMe_2)(NCCD_3](BF_4)$, 2.11-$d_3$ in CD_3CN:

The protonolysis of 10m mg of **2.9** in CD_3CN in an NMR tube was performed in a manner identical to that above with equivalent amount of aq. HBF4. Note the signal corresponding to water in the NMR spectrum.

^{1}H NMR (22 °C, 500 MHz, CD_3CN, ppm), δ: 0.24 (br, s, 3H, BMe), 0.81 (br, s, 3H, BMe), 2.35 (s+Pt-satellites, 3H, *J*=~40 Hz, PtSMe), 2.66 (s+Pt-satellites, 3H, *J*=~41 Hz, PtSMe), 3.25 (br, H_2O from aq. HBF_4), 7.06 (m, 1H, py-5-CH), 7.13 (m, 1H, py'-5-CH), 7.62-7.75 (overlapping m+m, 4H, py-3-CH, py'-3-CH, py-4-CH, py'-4-CH),

8.5 (d+Pt-satellites, 1H, J=6.4, J_{Pt-H}=~23 Hz, py-6-CH), 8.55 (d+Pt-satellites, J=5.9, J_{Pt-H}=~18 Hz, py'-6-CH).
ESI(+)-MS of a THF solution of **2.11-*d*$_3$**: 498.16, Calculated: 498.14

2.5.8 Oxidation of (dpdmb)Pt^{II}Me(SMe$_2$), 2.9, to form [(MeO-mdpb)Pt^{IV}Me$_2$(SMe$_2$)]OAc, 2.14

51 mg (108.6 µmol) of **2.9** was dissolved in 4 mL of methanol in a Schlenk flask equipped with a stirring bar. The solution was acidified with 6.2 µL (1 equiv.) of acetic acid. To this solution, with rapid stirring was added 11.2 µL (1 equiv.) of aq. 30% H_2O_2. Stirring was continued for 5 minutes and some fine yellow particulates were observed. After this time, the solution was filtered through a cotton plug and the filtrate was stripped to dryness to obtain a yellow solid. The solid was recrystallized from benzene to produce **2.14**, 55.3 mg, 91% yield. c.f. appendix p-127 for ^{13}C-NMR spectrum.
^{1}H NMR (22 °C, 500 MHz, acetone-d_6, ppm), δ: 0.51 (br s, B-Me, 3H), 1.36 (s, $^2J_{Pt-H}$=66 Hz, Pt-Me, 3H), 1.78 (s, OAc, overlapping with a Pt-satellite, 3H), 1.84 (s, $^2J_{Pt-H}$=74 Hz, Pt-Me, 3H), 2.55 (s, $^3J_{Pt-H}$=35 Hz, SC*H*$_3$, 3H), 2.63 (s, $^3J_{Pt-H}$=42 Hz, SC*H*$_3$, 3H), 3.30 (s, $^3J_{Pt-H}$=12 Hz, B-µ-OC*H*$_3$-Pt, 3H), 7.48-7.53 (m, 2H), 7.7 (vd, J=7.9 Hz, 1H), 7.8 (vd, J=8.4 Hz, 1H), 7.94 (vt, J=7.9 Hz, 1H), 7.99 (vt, J=8.4 Hz, 1H), 8.51 (d, J=5.9, J_{Pt-H}=19 Hz, 1H), 8.95 (d, J=5.9, J_{Pt-H}=20 Hz, 1H).
^{1}H NMR (22 °C, 400 MHz, CD_3OD, ppm), δ: 0.53 (br s, B-Me, 3H), 1.34 (s, $^2J_{Pt-H}$=64 Hz, Pt-Me, 3H), 1.74 (s, $^2J_{Pt-H}$=71 Hz, Pt-Me, 3H), 1.92 (s, OAc, 3H), 2.37 (s, $^3J_{Pt-H}$=32 Hz, SC*H*$_3$, 3H), 2.50 (s, $^3J_{Pt-H}$=42 Hz, SC*H*$_3$, 3H), 7.38-7.43 (m, 2H), 7.7 (vd, J=7.9 Hz, 1H), 7.81 (vd, J=7.7 Hz, 1H), 7.88-7.93 (m, 2H), 8.38 (d, J=6.0, J_{Pt-H}=38 Hz, 1H), 8.68 (d, J=5.9, J_{Pt-H}=15 Hz, 1H).
^{13}C NMR (22 °C, 500 MHz, acetone-d_6, ppm), δ: -0.4 ($^2J_{Pt-C}$=307 Hz, PtMe), -0.2 ($^2J_{Pt-C}$=285 Hz), 1.34 (br, BMe), 19.9 ($^2J_{Pt-C}$=9 Hz, SMe), 21.2 ($^2J_{Pt-C}$=13 Hz, SMe), 24.5 (OCO*C*H$_3$), 53.9 (br, B-µ-O*C*H$_3$-Pt, Pt-satellites not resolved), 124.5 (J_{Pt-C}=16 Hz), 125.5 (J_{Pt-C}=40 Hz), 128.8, 129.9 (J_{Pt-C}=26), 139.3, 139.8, 147.3 (J_{Pt-C}=35 Hz), 147.5, 174.2 (OCO*C*H$_3$).
ESI$^+$-MS of a methanolic solution of **2.14**: 500.18. Calculated for $C_{16}H_{26}BN_2OPtS$: 500.15.
Elemental analysis: calculated for $C_{18}H_{29}BN_2O_3PtS$, C, H, N: 38.65, 5.23, 5.01. Found C, H, N: 39.00, 4.93, 5.08.

2.5.9 Oxidation of [(dpdmb)Pt^{II}(SMe$_2$)(CD$_3$OD)]BF$_4$ complex, 2.10-*d*$_4$, to form [(mdpb)Pt^{II}(SMe$_2$)(OCD$_3$)]BF$_4$, 2.15-*d*$_3$, [(mdpb)Pt^{II}(OSMe$_2$)(OCD$_3$)]BF$_4$, 2.16-*d*$_3$ and dimethyl ether-*d*$_3$, 2.17-*d*$_3$:

An NMR tube containing 21.3µmol of **2.10-*d*$_4$** (synthesized in CD_3OD) was cooled to 0 °C in an ice-bath. 2.4 µL of aq. 30% H_2O_2 was added, Teflon sealed and shaken for homogeneity. An NMR experiment revealed the formation of 1 equivalent of d_3-dimethylether and the formation of **2.15-*d*$_3$**. To quantify the amount of d_3-dimethylether observed, the above reaction was repeated with 1,4-dioxane as an internal standard, and following addition of 1.2 equivalents H_2O_2, d_3-dimethylether (1 equivalent) was observed.
2.15-*d*$_3$:

^{1}H NMR (22 °C, 500 MHz, CD_3OD, ppm), δ: 0.26 (br s, BMe, 3H), 2.64 (br s, $^3J_{Pt-H}$=40 Hz, 3H, SMe), 2.89 (br s, $^3J_{Pt-H}$=39 Hz, 3H, SMe), 7.18 (dt, *J*=6.5, 2.0 Hz, 1H), 7.26 (dt, *J*=6.7, 1.9 Hz, 1H), 7.48-7.60 (m, 3H), 7.89 (vt, *J*=7.0 Hz, 1H), 8.71 (d, *J*=6.2 Hz, 1H), 8.78 (d, *J*=5.4 Hz, J_{Pt-H}=29 Hz, 1H).
ESI(+)-MS of an aliquot of the NMR solution above gave m/z = 473.13 (calculated for $C_{14}H_{17}OBD_3N_2PtS$, **2.15-*d*$_3$**$^+$: 473.12), 50.12 (calculated for CD_3OCH_3-H^+) as the major peaks. Complex **2.16-*d*$_3$**$^+$ was observed at m/z = 489.12 (calculated for $C_{14}H_{17}O_2BD_3N_2PtS$, **2.16-*d*$_3$**$^+$, 489.12).

2.5.10 Attempted ^{1}H NMR detection of the presumed reactive intermediate, 2.19-*d*$_6$.

21.3 µmol of fresh **2.10-*d*$_4$** in CD_3OD, prepared from 10 mg (21.3 µmol) of **2.9** by protonolysis with equivalent amounts of 50% aqueous HBF_4 was taken in a sealable NMR tube and cooled to -90 °C. To it was added 1 µL dichloromethane as internal standard, and added 2.2 µL of 30% H_2O_2 (1.0 equivalent), through a long needle, very slowly in order to avoid local heating. The NMR tube was quickly lowered into the NMR spectrometer where the probe was precooled to -60 °C. No changes to the starting material were observed. The sample was warmed up slowly in 10 °C intervals with careful monitoring. Formation of dimethyl ether-*d*$_3$ was first observed at -15 °C, however the rate of accumulation of dimethyl ether-*d*$_3$ was very slow. After 90 min at -15 °C formation of 0.34 equivalents of dimethyl ether-*d*$_3$ was observed. No detectable accumulation of intermediate complexes was noticed. The above experiment was repeated with 10 equivalents of H_2O_2 with a starting temperature of -20 °C. In this case also, no intermediate were detected, although increase in the rate of formation of dimethyl ether-*d*$_3$ was observed.
Attempts were also made to observe Pt(IV)-Me intermediate, **2.19-*d*$_6$**, by performing the oxidation reaction with added sodium methoxide. To 21.3 µmol of **2.10-*d*$_4$**, prepared as above in a sealable NMR tube, was added 1.2 mg (1 equivalent) 95% sodium methoxide and shaken for homogeneity. 1 µL of 1,4-dioxane as internal standard was added. The NMR tube was cooled to -90 °C; 10 equivalents of H_2O_2 was added, sealed, shaken and inserted into the precooled NMR probe. No dimethyl ether-*d*$_3$ was observed below -15 °C, as above. The progress of the reaction was monitored at -15 °C, in ten minute intervals up to 90 min. At the end of that time period a total of 0.66 equivalents of dimethyl ether-*d*$_3$ were obtained. The average rate of formation of dimethyl ether-*d*$_3$ was found to be 1.4 faster in the latter experiment.

2.5.11 Attempted oxidation of H(dpdmb) with H_2O_2 :

12.0 mg (60.6 µmol) of H(dpdmb) was dissolved in 0.5 mL CD_3OD, 7.57 µL aq. 50% HBF_4 (1 equivalent) was added and an ^{1}H NMR spectrum was acquired. Further, 6.2 - 62 µL (1-10 equivalents) of aq. 30% H_2O_2 was added to the solution. No change in the NMR spectra was seen after 1h, establishing the inertness of the ligand towards oxidative degradation.

2.5.12 Attempted oxidation of of [(dpdmb)Pt^{II}(SMe_2)(NCMe)]BF_4, 3(BF_4), in CD_3CN:

[(dpdmb)$Pt^{II}(SMe_2)(NCCD_3)$]BF_4, **2.11-*d*$_3$** was generated by dissolving 15 mg (31.96 μmol) of **2.9** in 0.5 mL of CD_3CN in a NMR Young tube followed by addition of 4.0 μL of aq. 50% HBF_4 (1 equiv.). According to NMR spectroscopy, **2.11-*d*$_3$** formed quantitatively. To this solution was added 1 equiv. of H_2O_2. The complex was found to be resistant towards oxidation by H_2O_2, tested with up to 20 equiv. of the oxidant.

2.5.13 Attempted reductive elimination from 2.14 in CD_3OD:

16.2 mg (32.4 μmol) of **2.14** was dissolved in 0.5 mL of CD_3OD in a NMR Young tube and acidified with 4 μL of aq. 50% HBF_4 (1 equiv.). The acidified solution was analyzed by ^1H NMR spectroscopy. The spectrum still conformed to **2.14** with minor chemical shift changes of the peaks. No new products generated by protonolysis were observed. Further, the NMR Young tube was exposed to elevated temperatures with careful monitoring by NMR spectroscopy. Initially, the NMR tube was left in an oil bath pre-set at 80 °C for several days and no changes were observed. Similar results were found when the temperature was raised to 100 °C and kept at this temperature for 2 days. ESI-MS of an aliquot from the NMR solution conformed to **2.14-*d*$_3$** with a m/z =503.1, corresponding to exchange of the B(μ-OCH_3-Pt^{IV}) fragment with CD_3OD. When temperature was raised to 120 °C, quick darkening of the solution was observed along with some black particulates.

Figure 2.7: Expanded region of 3.1-3.5 ppm (c.f. section **2.5.10**) showing evolution of CD_3OCH_3 with time. From bottom to top: -40 °C, -30 °C, -20 °C, -15 °C, -12 °C (0 min, 10 min, 20 min, 30 min, 40 min, 60 min, 90 min), -10 °C (0 min, 10 min, 30 min). No Pt^{IV}-Me intermediate was observed

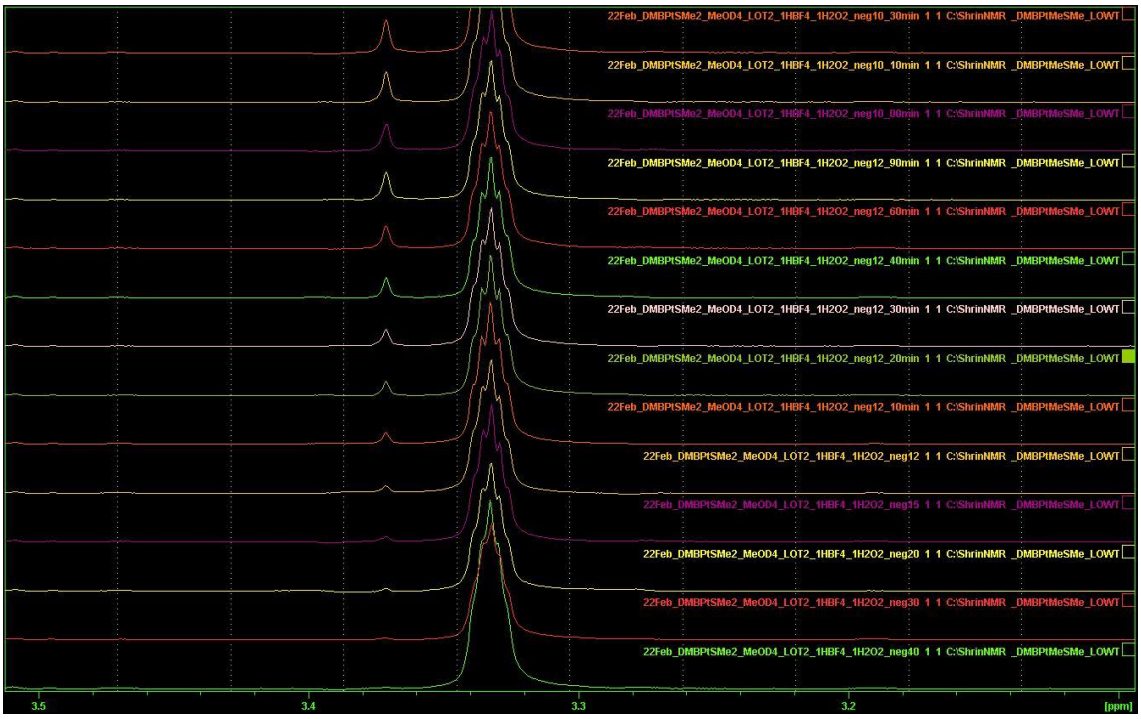

Chapter 3: Aerobic Oxidation of di(2-pyridyl)(methoxy)(methyl)borato -Pt^{II} complexes: Competition of *O*-coordination and methyl migration

3.1 Proposal

Based on the observation of the C-O elimination products upon oxidation of a model dimethyldi(2-pyridyl)borato-Pt^{II} complexes, as discussed in Chapter-II, we set out to modify the borate center to potentially avoid oxidatively induced B-to-Pt^{IV} *methyl migration*. Although the cationic complexes discussed in Chapter-II could only be oxidized by a stronger oxidant such as H_2O_2, we presumed that both mono- and dihydrocarbyl anionic Pt^{II} complexes derived from a resistant ligand could potentially be involved in O_2 activation. It was proposed earlier, based on DFT analysis [2], that the major driving force for B-to-Pt^{IV} hydrocarbyl migration observed upon oxidation of complexes such as **1.15** is the formation of strong B-OR bonds, where ROH corresponds to the protic solvent the oxidation is performed in. We proposed that by substituting the B-bound methyl fragments in the dpdmb ligand, **1.14**, by alkoxy groups, the ligand would become more resistant towards such *methyl migration*. Envisioned ligands with one (**3.1**) or both (**3.2**) alkyl-for-alkoxy substitutions, depicted in Scheme 3.1, may serve this purpose. To the best of our knowledge, there were no literature precedents for either free-ligands, although Williams et al. reported in-situ formation of complex **3.3**, featuring a Ru^{II}-bound **3.1** (R=Me) [63].

Scheme 3.1 New di(2-pyridyl) borate ligands featuring B-alkoxy substitutions

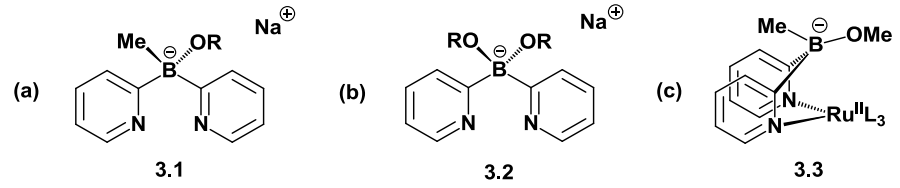

3.2 Implementation

Scheme 3.2: Synthesis of sodium di(2-pyridyl)(methoxy)(methyl)borate

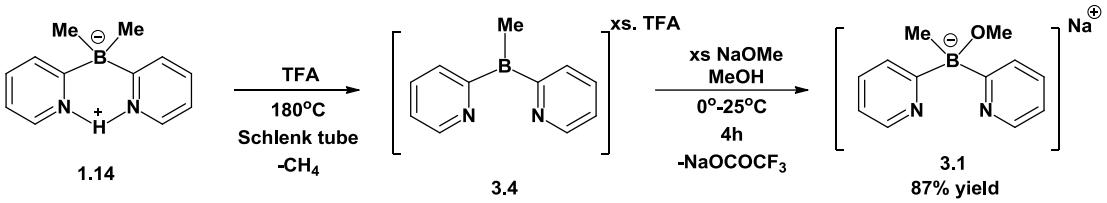

Synthesis of **3.1** was first attempted with H(dpdmb) **1.14** as the starting material via a top-down approach owing to the established ease of synthesis of the latter. **1.14** was found to be very stable towards various 'de-alkylating' agents such as Br_2, BBr_3 etc [66], although such reagents are known to cleave B-C bonds with facility. At temperatures above 100 °C with such reagents, ligand degradation was substantial, and no change in conversion whatsoever was observed for aqueous HBF_4. On the other hand, given the anionic boron center, we anticipated **1.14** to react with strong acids to protonate the B-Me fragment leading to B-C bond cleavage and elimination of methane. A sample of **1.14** in TFA-d at room-temperature showed trace amounts of CH_3D, identified by observing a small triplet at 0.18ppm in the ^{1}H-NMR after 7 days.

Figure 3.1: ^{1}H-NMR spectrum of $MeBPy_2$, **3.4**, in TFA-*d* (22 °C, 400.131 MHz) after heating at 180 °C for 24h. Note the triplet corresponding to CH_3D and the residual BCH_3 fragment integrating to 3H

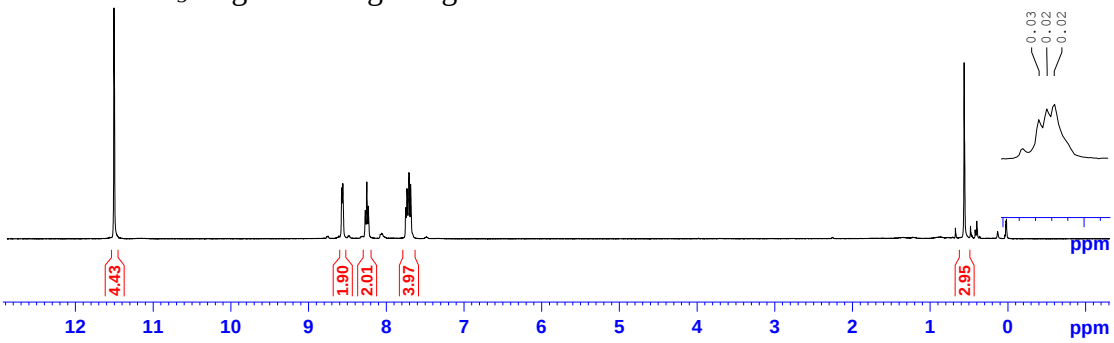

The rate of reaction was carefully monitored by ^{1}H-NMR by comparison of signals at 0.1 ppm and 0.5 ppm corresponding to the BMe_2 fragment in **1.14** and a new BMe fragment in **3.4**, respectively. A 24h reflux at 180 °C was found to be optimal in converting **1.14** to **3.4** without noticeable decomposition. **3.4** was could be isolated, however upon exposure to high-vacuum a gel-like material containing excess TFA was obtained. ESI^{+}-MS of the gel showed a signal at 183.1 consistent with the protio-adduct, **3.4**·H^{+}. Treatment with a methanolic solution containing excess sodium methoxide and extraction with THF afforded **3.1** in good yields. **3.1** was characterized by ^{1}H and ^{13}C-NMR (c.f. appendix pp. 128-129) and ESI-MS. **3.1** could not be obtained in analytically pure form, due to the presence of sodium trifluroacetate.

Synthesis of **3.2** was attempted via a bottom-up approach as **3.1** could not be cleanly 'de-methylated' a second time without observing substantial decomposition. Various ratios of 2-pyridyl-lithium and 2-pyridyl-magnesium chloride on boron precursors such as BBr_3, $B(OMe)_3$ and $B(O^{i}Pr)_3$ produced intractable mixtures of mono(2-pyridyl), di(2-pyridyl) and tri(2-pyridyl) borates and further attempts to purify mixtures were unsuccessful. Brown et al. reported similar reaction outcomes [67].

3.3 Results and Discussion

3.3.1 Synthesis of di(2-pyridyl)(methoxy)(methyl)borato-Pt^{II} complexes

Scheme 3.3: Synthesis of di(2-pyridyl)(methoxy)(methyl)borato-Pt^{II} complexes:

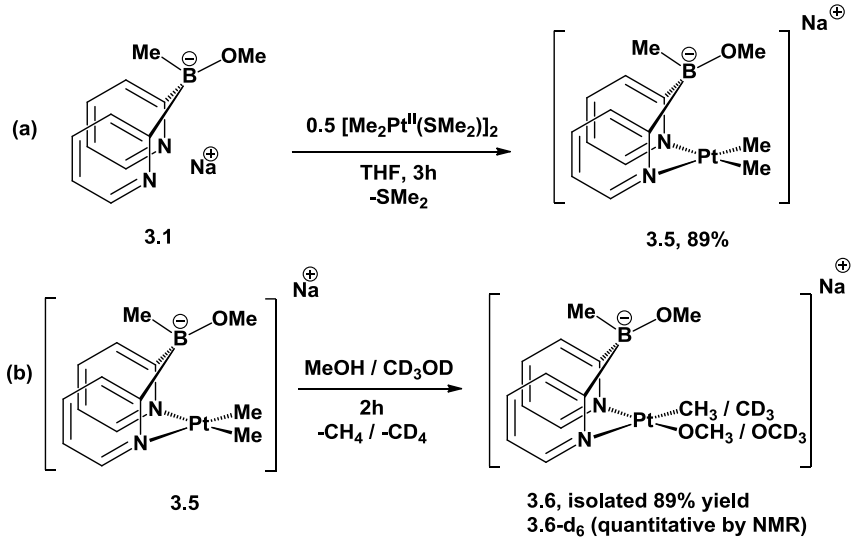

With our new ligand **3.1** at hand, the derived $Pt^{II}Me_2$ complex, **3.5**, was synthesized by standard protocol, as shown in Scheme 3.3(a). **3.5** was found to be stable at room-temperature in aprotic solvents in the absence of O_2. According to NMR, a solution of **3.5** in CD_3CN showed the presence of a C_s symmetric species with $J_{Pt\text{-}H}$ coupling of 81 Hz corresponding to the $PtMe_2$ fragment and broad singlets at 0.53 ppm and 3.32 ppm corresponding to the BMe and BOMe fragments, respectively. Although NMR spectra recorded in THF or CD_3CN were reasonably clean, **3.5** could not be isolated in analytically pure form due to decomposition, and was characterized in solution by ^1H and ^{13}C-NMR spectroscopy and ESI-MS (c.f. appendix p-130 for ^{13}C-NMR spectrum).

Figure 3.2: ^{1}H-NMR spectrum of (Me)(MeO)BPy$_2$Pt^{II}Me$_2$ complex, **3.5**, in CD_3CN (22 °C, 400.131 MHz)

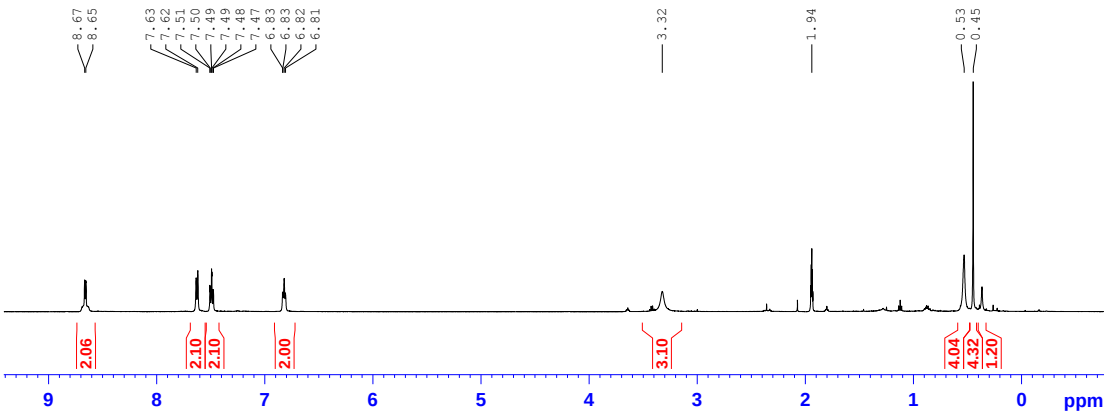

3.5 underwent complete H/D exchange of the Pt^{II}Me$_2$ fragment upon dissolution in CD_3OD within 10 minutes, without noticeable protonolysis of the Pt^{II}-Me fragment according to the ^{1}H-NMR spectra, which shows four multiplets of equal intensity corresponding to the pyridine hydrogens. The $J_{Pt\text{-}H}$ coupling of 28.8 Hz (400 MHz) of the ortho-pyridine hydrogen is typical of Pt^{II} complexes with Pt-bound trans methyl groups. Unlike **1.15**, **3.5** reacted extremely slowly with CD_3OD to form the monomethyl-Pt^{II} complex, **3.6-*d*$_6$**. No exchange of the B-OMe fragment was observed by ^{1}H-NMR in the course of the reaction. Hence, the new ligand, **3.1** makes the derived Pt^{II} complex, **3.5**, less basic and less electron-rich rendering the Pt^{II} center in **3.5** less susceptible to protonolysis of one of the PtMe fragments than in the (dpdmb)-analogue, **1.15**. After careful monitoring of the reaction, quantitative conversion of **3.5** to **3.6-*d*$_6$** was found to have occurred in 2h. ESI^{-}-MS showed a peak at 460.1, a mass 6 units higher than that calculated for **3.6**, consistent with the presence of Pt^{II}-bound CD_3 and OCD_3 fragments. **3.6-*d*$_6$** did not react further with CD_3OD and according to NMR, no decomposition in solution was evident up to 2 days at room-temperature. **3.6** was synthesized accordingly in methanol.

Figure 3.3: ^{1}H-NMR monitoring of reaction between **3.5** and CD_3OD (22 °C, 400.131 MHz) to form **3.5-*d*$_6$** (~5 min) and eventually, **3.6-*d*$_6$** (2h, quantitatively). Notice traces of **3.6-*d*$_6$**

(~5 minutes after dissolution)

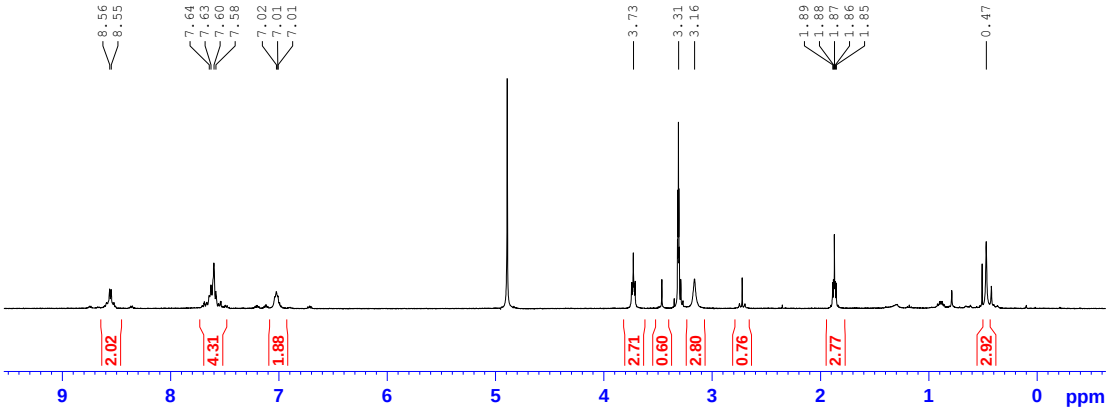

(2h after dissolution)

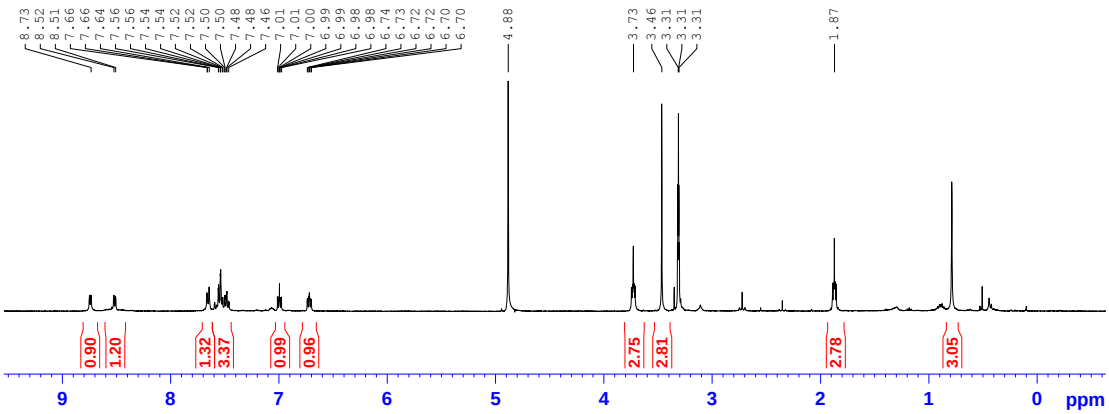

3.3.2 Synthesis of di(2-pyridyl)(methoxy)(methyl)borato-$Pt^{IV}Me_3$ complex

Scheme 3.4: Synthesis and reactivity of di(2-pyridyl)(methoxy)(methyl)borato-$Pt^{IV}Me_3$ complex, 3.7

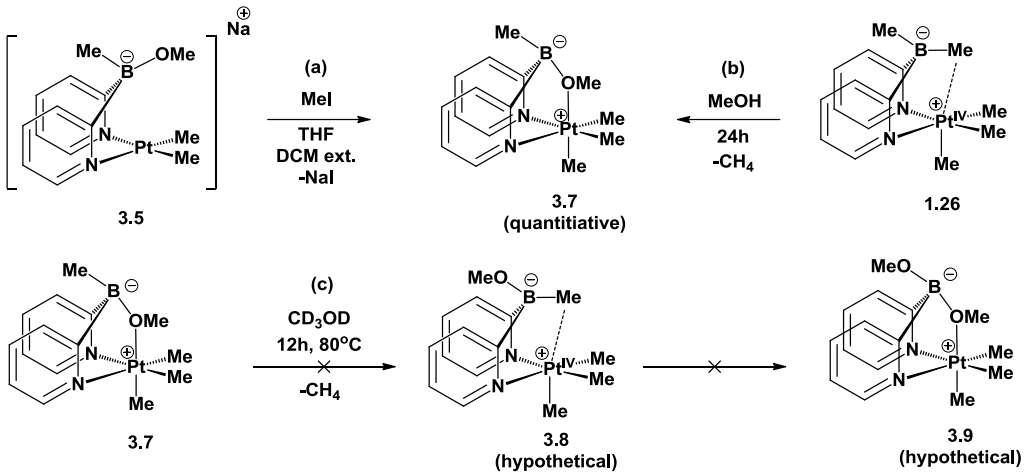

The dimethyl-Pt^{II} complex, **3.5** reacted with methyliodide to form the trimethyl-Pt^{IV} complex, **3.7**, as shown in Scheme 3.4(a). **3.7** is identical to the product obtained by Khaskin [34] by slow reaction of **1.26** with methanol (c.f. Scheme 1.8), as shown in Scheme 3.4(b). According to the ^{1}H-NMR spectra (c.f. appendix p-131), no C-H agostic interaction of the B-Me fragment with the Pt^{IV} center was present. The B-OMe fragment however, with a small $J_{Pt\text{-}H}$ coupling constant of 15 Hz ($CDCl_3$, 500 MHz) clearly indicative that the B-OMe fragment sufficed as the 6th axial ligand at the Pt^{IV} center, trans to a strongly trans-influencing axial Pt^{IV}-Me fragment. The higher preference of the B-OMe over an agostic C-H is expected due to better donicity of the lone pairs on the O-atom as opposed to C-H bonds of the B-Me fragment. The structure of **3.7**, shown in Figure 3.4, was established using X-ray diffraction of a single crystal grown from a dichloromethane solution by vapor diffusion with pentanes. In the X-ray structure, the bridging O-atom is tightly bound to both the B and Pt^{IV} centers, with distances of 1.55 and 2.21 Å, respectively.

Figure 3.4: X-ray structure of di(2-pyridyl)(methoxy)(methyl)borato-$Pt^{IV}Me_3$ complex, **3.7**

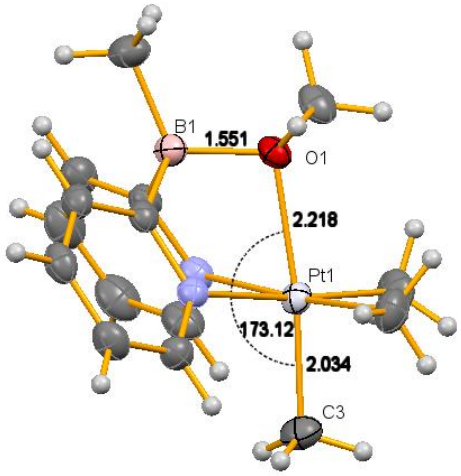

The bridging B-OMe fragment is basic enough to be protonated by acid. The ^{1}H-NMR of a THF-d_8 solution of **3.7** acidified with 2 equivalents of 50% HBF_4, shows a singlet at 3.35 ppm, corresponding to free CH_3OH produced as a result of protonation and loss of the bridging B-OMe fragment. However, unlike Goldberg's report on trimethyl-Pt^{IV} complexes [68], rapid exchange of axial and equatorial PtMe groups was not observed and was presumed to be slow on the NMR time scale, as evident from two sets of singlets at 0.77 ppm (6H, $J_{Pt\text{-}H}$=68.5 Hz, 400 MHz) and 1.02 ppm (3H, $J_{Pt\text{-}H}$=74.0 Hz, 400 MHz). To confirm this hypothesis, a ^{13}C-labelled derivative, **3.7*** was synthesized by reacting **3.5** with $^{13}CH_3I$.

Figure 3.5: ^{13}C-NMR spectrum of **3.7*** in CD_3OD (22 °C, 500.132 MHz) showing statistical 1:2 distribution of ^{13}C labelled $Pt^{IV}Me$ fragments (J_{Pt-C}=678 Hz, axial, J_{Pt-C}=764 equatorial)

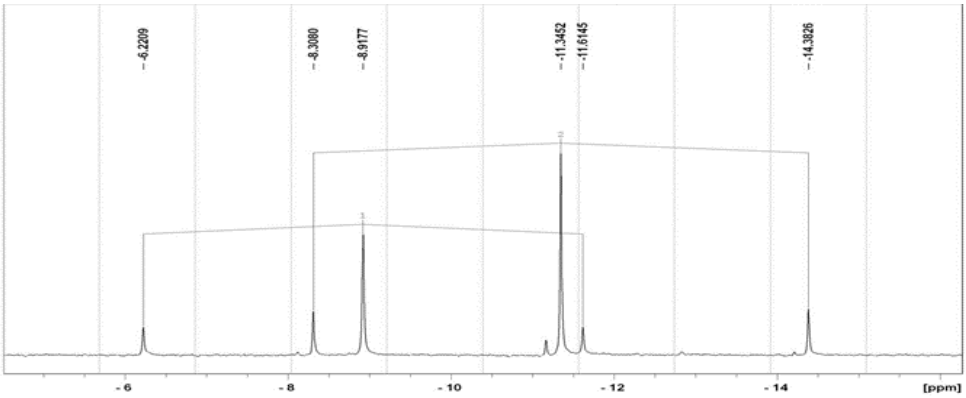

The ^{13}C-NMR spectra revealed complete $^{12}C/^{13}C$ scrambling, i.e. both axial and equatorial PtMe fragments had incorporated ^{13}C in the statistical 1:2 integral ratio. Extending the time-frame of Khaskin's observations [34], **3.7** is stable in CD_3OD solution for at least 10 days. No changes in the ^{1}H-NMR spectra of the CD_3OD solution of **3.7*** was observed upon heating at 80 °C for 12h.

3.3.3 Oxidation of di(2-pyridyl)(methoxy)(methyl)borato-$Pt^{II}Me_2$ complex

Owing to relatively slow reaction of **3.5** with methanol, compound **3.5** could be selectively oxidized in methanol unlike **1.15**, for which only much less acidic solvents such as isopropanol or ethanol could be used to avoid excessive protonolysis [34]. **3.5** was dissolved in methanol in the glove-box and quickly exposed to O_2 for 10 minutes. A ^{1}H-NMR spectrum recorded in $CDCl_3$ after stripping away methanol showed signals corresponding to two sets of compounds, in the ratio 3:1.

Scheme 3.5: Oxidation of di(2-pyridyl)(methoxy)(methyl)borato-$Pt^{II}Me_2$ complex, 3.5, in methanol: *methyl migration* and *ligand retention*

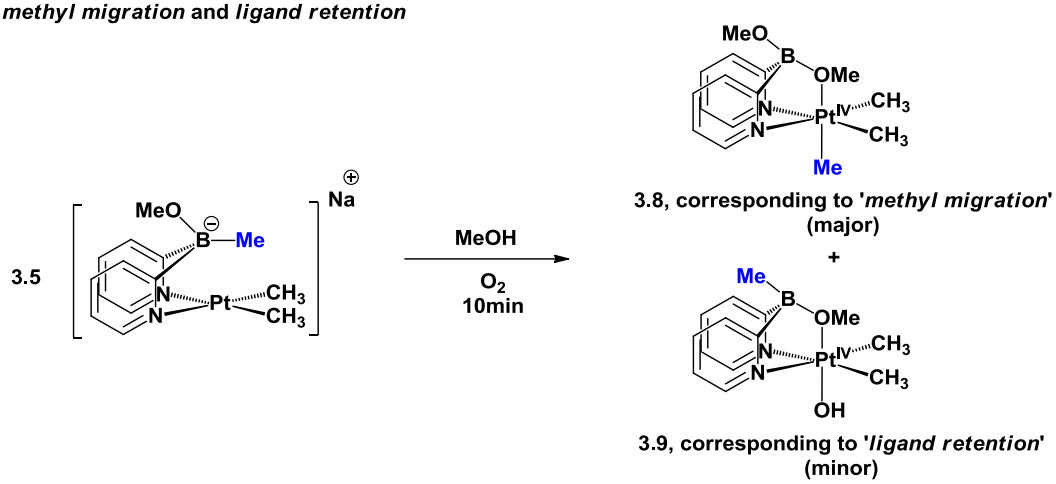

Interestingly, the major fraction of the corresponded to **3.8**, the product of methyl migration, as evident from a signal at 1.29 ppm with a $J_{Pt\text{-}H}$ coupling of 78.0 Hz, consistent with the presence of a B(μ-OMe) fragment *trans* to it. A singlet at 0.85 ppm, with $J_{Pt\text{-}H}$ coupling of 68 Hz, matching in intensity to that of the equatorial $Pt^{IV}Me_2$ fragment of the major product, **3.8**, was also visible. The presence of the bridging B(μ-OMe) fragment with a small $J_{Pt\text{-}H}$ coupling of 12.3 Hz is consistent with the presence of a trans Pt^{IV}-Me fragment. Four multiplets corresponding to resonances of the pyridine fragment matching in intensity to those of the major product, **3.8**, could also be located.

Figure 3.6: ^{1}H-NMR spectrum in $CDCl_3$ (22 °C, 400.131 MHz) corresponding to the mixture of products (**3.8** and **3.9**) produced upon oxidation of di(2-pyridyl)(methoxy)(methyl)borato-$Pt^{II}Me_2$ complex, **3.5**

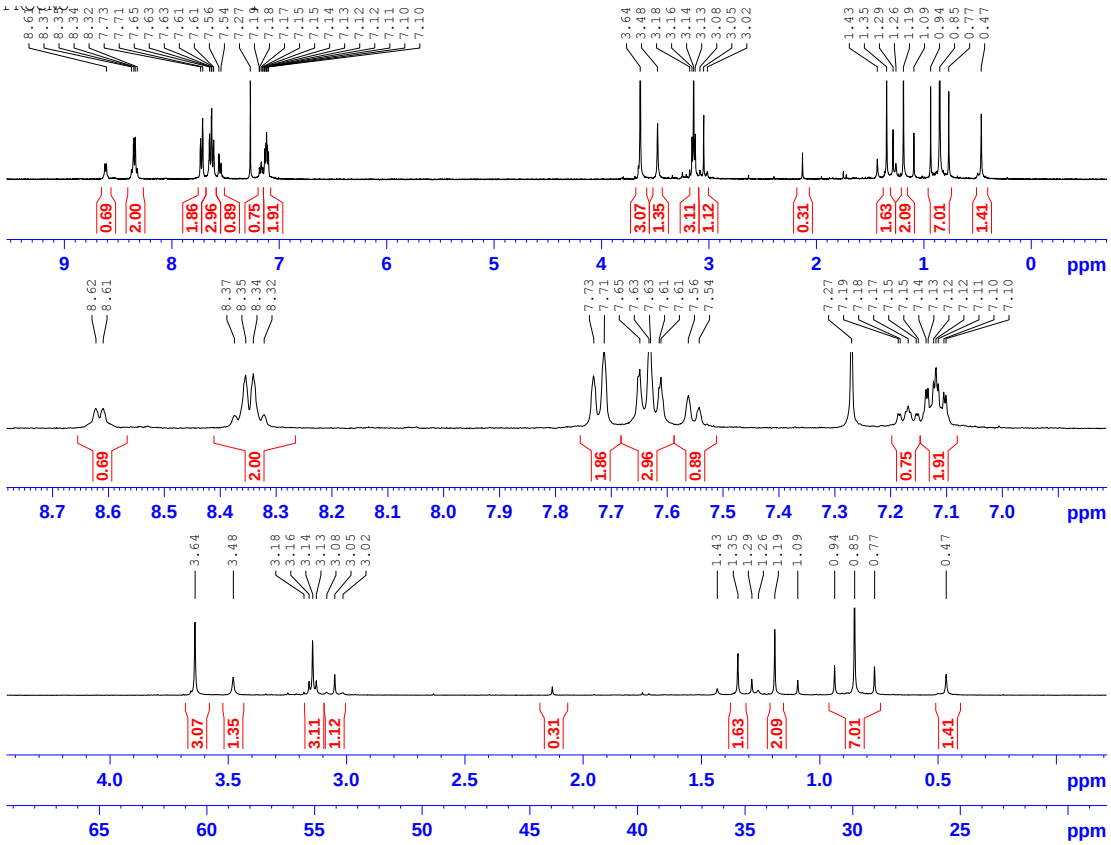

On the other hand, a singlet at 0.46 ppm with $J_{Pt\text{-}H}$ coupling of 70.2 Hz, matching in intensity to the minor product, **3.9**, is consistent with its assigned structure, i.e. the equatorial $Pt^{IV}Me_2$ fragment. As opposed to that in **3.8**, the bridging B(μ-OMe) fragment in **3.9** with a much larger $J_{Pt\text{-}H}$ coupling of 27.0 Hz, is consistent with the presence of a shorter Pt-OCH_3 bond due to weakly trans-influencing Pt^{IV}-OH (axial) fragment. A broad singlet at 0.46 ppm, corresponding to the residual BMe fragment, and four multiplets corresponding to resonances of the pyridine fragment matching in intensity to those of the minor product, **3.9**, could also be located. It is important to note here that although each of the Pt^{IV} products, viz. **3.8** and **3.9** are expected to be chiral due to the presence of a non-labile chiral bridging B(μ-OMe) fragment in

either, signals corresponding to non-equivalent pyridyl and methyl groups could not be resolved by NMR spectroscopy.

In order to investigate the origin of the methoxy groups in **3.8** and **3.9**, we performed oxidation of **3.5** in CD_3OD and closely looked at the ^{1}H-NMR spectra of the mixture after oxidation. According to the NMR spectra, and by comparison to the NMR spectra of **3.5-*d*$_6$** obtained immediately after dissolution in CD_3OD, none of the starting material remained. A noticeable degree (n) of H/D exchange of the $Pt^{II}Me_2$ fragment in **3.5**, with CD_3OD, proved to be extremely useful in identifying the origin of the PtMe signals in the products. Again, two sets of signals corresponding to a 3:1 product distribution ratio, as shown in Scheme 3.6, were visible in the ^{1}H-NMR spectrum.

Scheme 3.6: Oxidation of partially deuterated di(2-pyridyl)(methoxy)(methyl)borato-$Pt^{II}Me_2$, 3.5 complex in CD_3OD: origin of bridging B(μ-methoxy)Pt^{IV} fragments

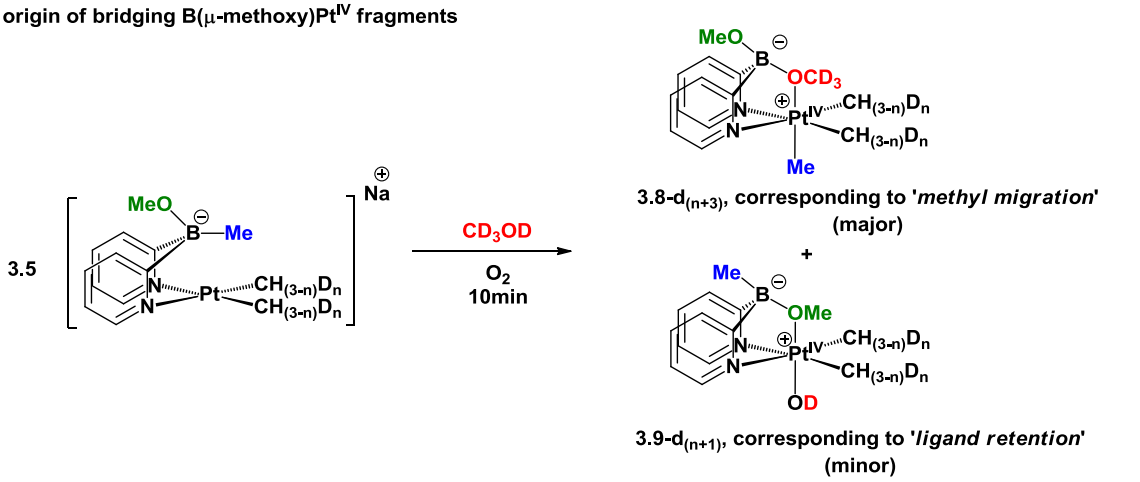

The spectral pattern did not change even after exposing the same CD_3OD solution to O_2 for an additional 1h, indicating that oxidation was already complete in the first ten minutes of exposure to O_2, ruling out the possibility that the BMe resonance seen in the NMR spectra might belong to starting material or its derivative(s). A clean singlet

at 1.19 ppm with a large $J_{Pt\text{-}H}$ of 78 Hz but no evident D-satellites, corresponded to the axial Pt^{IV}-Me fragment in **3.8-*d*$_{(n+3)}$**, where n represents the degree of deuteration prior to oxidation. No signal corresponding to the bridging B(μ-methoxy)Pt^{IV} matching in intensity to this major product was visible, indicating CD_3OD as its origin. A broad singlet at 3.6 ppm of intensity matching to the major product was concurrently assigned to the exo $BOCH_3$ fragment of **3.8-*d*$_{(n+3)}$**.

Figure 3.7: ^{1}H-NMR spectrum of **3.8-*d*$_{(n+3)}$** and **3.9-*d*$_{(n+1)}$** in CD_3OD (22 °C, 400.131 MHz) produced upon oxidation of partially deuterated di(2-pyridyl)(methoxy)(methyl)borato-$Pt^{II}(CD_{3-n}D_n)_2$ complex, **3.5-*d*$_n$** Note the signal at 2.99 ppm corresponding to the B-OCH_3 fragment of **3.9-*d*$_{(n+1)}$** and that at 1.20 ppm corresponding to the non-deuterated Pt-Me fragment of **3.8-*d*$_{(n+3)}$**

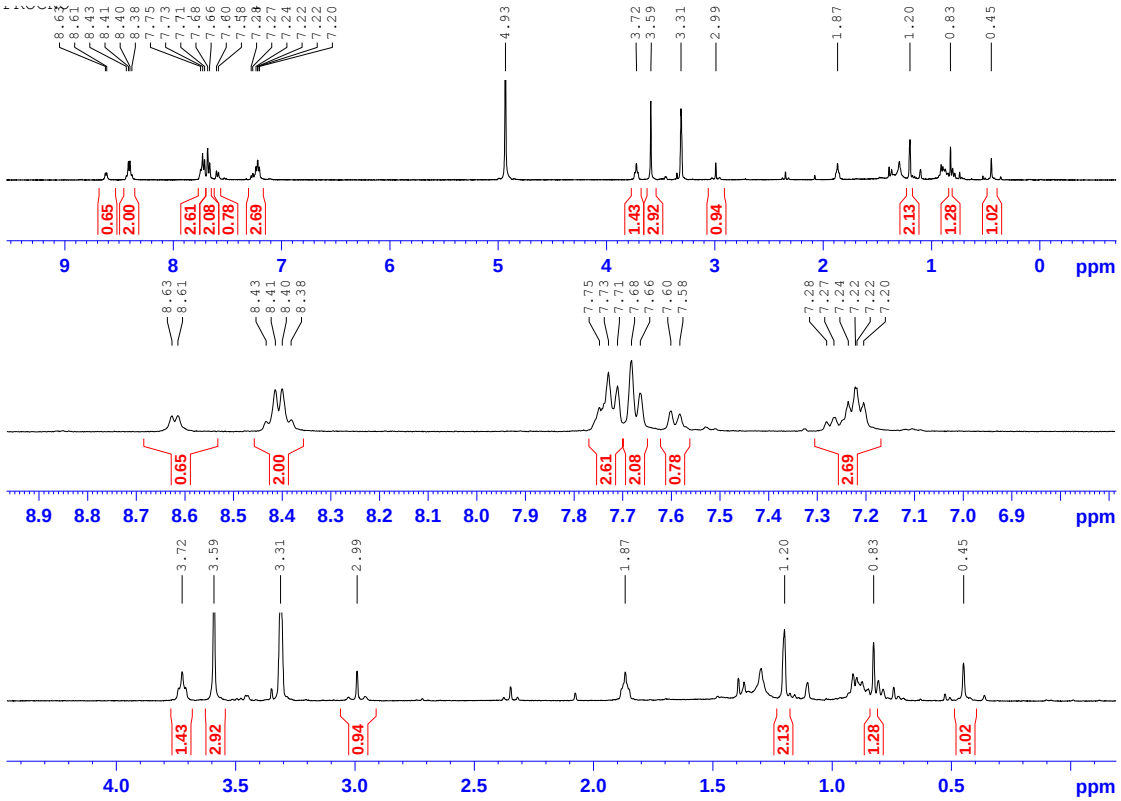

On the other hand, all resonances corresponding to the $Pt^{IV}Me_2$ fragment of the minor product, **3.9-*d*$_{(n+1)}$** showed D-satellites, consistent with its assigned structure. Furthermore, a singlet at 2.9 ppm, matching in intensity to that of the minor product

had corresponding $J_{Pt\text{-}H}$ coupling of 78 Hz, consistent with the presence of a trans Pt^{IV}-OD fragment, as would be expected for **3.9-*d*$_{(n+1)}$**.

Based on these labeling experiments, the bridging B(μ-methoxy)Pt^{IV} in the major product corresponding to *methyl migration* originates from solvent, whereas that for the minor product corresponding to *ligand retention* originates from the ligand.

We hypothesized that the result of the oxidation reaction reflects the composition of the starting material, **3.5**, as an equilibrium mixture of **3.5'** and **3.5''** in solution, with an exo-$BOCH_3$-endo-BCH_3 in **3.5'** and endo-$BOCH_3$-exo-BCH_3 in **3.5''**, as shown in Scheme 3.7. Each of these isomers undergoes oxidation to yield distinct products.

Scheme 3.7: Isomerization of di(2-pyridyl)(methoxy)(methyl)borato-Pt^{II} complexes

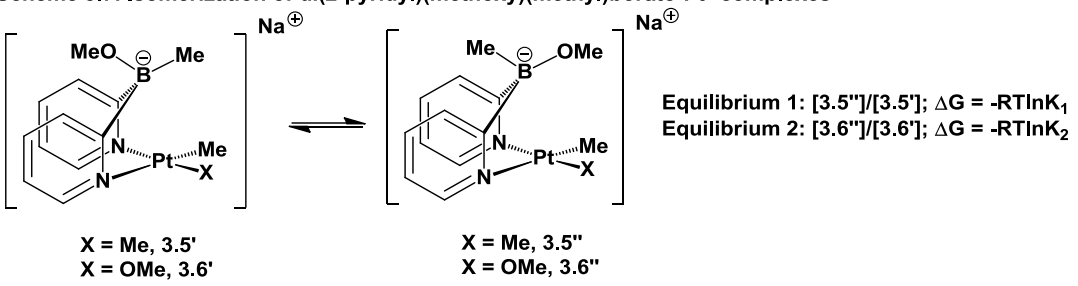

According to DFT calculations [2], the isomerization between the structures **3.5'** and **3.5''** and that between **3.6'** and **3.6''** corresponded to a Gibb's free energy change (MeOH solution, 298K) of 3.8 kcal/mole and 3.5 kcal/mole, respectively. The calculated [69] equilibrium constants (298 K) for the isomerization of **3.5'** and **3.5''** and that of **3.6''** and **3.6''** are $1.6x10^{-3}$ and $2.6x10^{-3}$, indicating significant predominance of the (endo-methyl, exo-methoxy) isomer (i.e. **3.5'** or **3.6'**) in solution. The ^{1}H-NMR spectrum of **3.5** in CD_3CN and CD_3OD shows only one set of sharp signals, consistent with either (i) fast equilibriation or (ii) predominance of one isomer in solution. On the other hand, oxidation leads to both products corresponding to *methyl migration* and *ligand retention*. Thus, if the rate of oxidation is slower than

the rate of isomerization, the ratio of the product corresponding to *methyl migration* and *ligand retention* is not governed by the equilibrium ratios of the starting material, but by the different rates of oxidation of the individual isomers.

3.3.4 Oxidation of di(2-pyridyl)(methoxy)(methyl)borato-PtII(Me)(OMe) complex

Scheme 3.8: Oxidation of di(2-pyridyl)(methoxy)(methyl)borato-Pt^{II}(Me)(OMe) complex, 3.6, in methanol: methyl migration and ligand retention

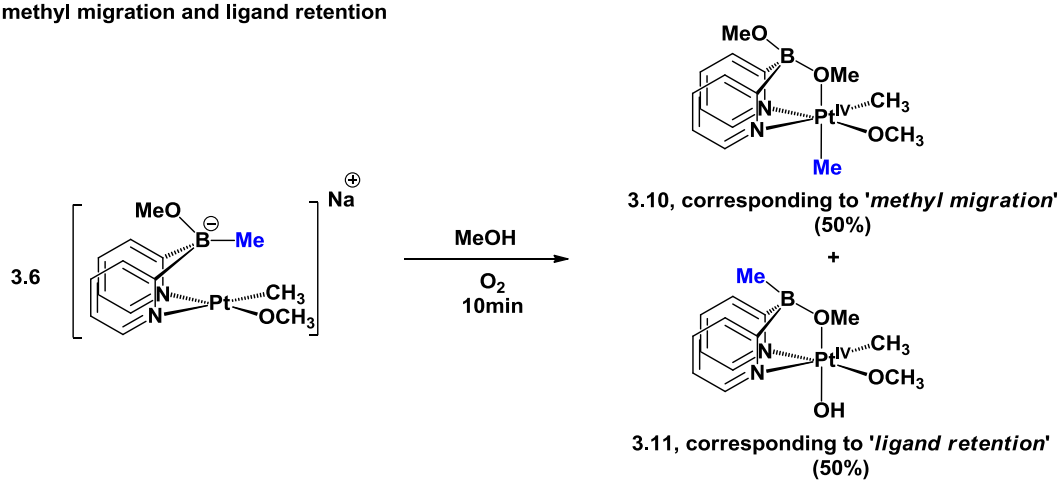

The oxidation of **3.6** was performed by dissolving **3.5** in methanol, waiting for 2h, as shown in Scheme 3.3(b), and then exposing the solution to O_2. A ^{1}H-NMR spectra recorded in $CDCl_3$ after stripping away methanol revealed two sets of products in 1:1 ratio. According to the NMR, some peaks could be definitively assigned. Singlets at 1.75 ppm with $J_{Pt\text{-}H}$ of 78 Hz and at 1.43 ppm with $J_{Pt\text{-}H}$ of 67.1 Hz were consistent with the axial and equatorial Pt^{IV}-Me fragments in **3.10**, respectively. On the other hand, singlets at 1.75 ppm with $J_{Pt\text{-}H}$ of 69.2 Hz and 0.49 ppm were consistent with the equatorial Pt^{IV}-Me fragment and residual BMe fragment in **3.10**, respectively. A lone-standing singlet at 3.11 ppm with $J_{Pt\text{-}H}$ of 18.5 Hz could also be assigned to the bridging B(μ-OMe)Pt^{IV} fragment of **3.11**. Although, the fortuitous product ratio of

1:1 made it very difficult to assign NMR signals corresponding to the pyridine hydrogens to the respective compounds, the identities of **3.10** and **3.11** were additionally confirmed by ESI-MS.

3.4 Conclusions

Based on the limitations imposed by a first-generation di(2-pyridyl)dimethylborate (dpdmb) ligand towards oxidative functionalization of Pt^{II}-hydrocarbyl fragments in derived complexes, a second-generation di(2-pyridyl)(methoxy)(methyl)borato borate ligand was conceived. A new, convenient and high-yielding synthetic route with dpdmb ligand as the starting material was developed. Derived $Pt^{II}Me_2$ complexes were found to behave similarly to (dpdmb)$Pt^{II}Me_2$ complexes with respect to Pt^{II}-Me protonolysis, albeit reacting a bit slower, which is presumably due to a less electron-rich ligand. However, the new ligand is sufficiently electron-rich in that it enables facile oxidation of even the derived Pt^{II}(Me)(OMe) complex. Products corresponding to both '*methyl migration*' and '*ligand retention'* were observed, consistent with the fast rate of oxidation of both rapidly equilibrating diastereomeric Pt^{II} complexes. Although replacement of one methyl in dpdmb for a methoxy does not completely prevent '*oxidatively induced methyl migration*', the structural dependence on product distribution is suggestive of future direction involving (i) a bulkier alkyl group (c.f. Chapter-IV for additional restrictions) or (ii) dimethoxy borate (c.f. Chapter-V for demonstration of redox reactions)

3.5 Experimental Section:

3.5.1 Preparation of MeBPy2. TFA, 3.4 by reaction with TFA-d:

15mg of **1.14** was dissolved in 0.6 mL TFA-d inside the glove-box in a Young tube, the tube sealed and a ^{1}H-NMR was recorded. The NMR tube was then immersed in an oil bath at 180 °C. The sample was monitored by ^{1}H-NMR over time. According to the NMR, after a period of 24h, complete protonolysis of one of the BMe_2 fragments had occurred to form **3.4**, along with the formation of CH_3D. No other products were observed.

Before reaction, 1.14 in TFA-d (22 °C, 400 MHz, TFA-d, ppm) δ: 0.12 (s, br, 6H, $B(CH_3)_2$), 7.47 (vt, 2H, *J*=7.3 Hz), 7.66 (d, 2H, *J*=8.6 Hz), 8.01 (vt, 2H, *J*=7.9 Hz)

After reaction, 3.4 in TFA-d (22 °C, 400 MHz, TFA-d, ppm) δ: 0.02 (t, J_{D-H}=2.0 Hz, CH_3D), 0.56 (s, br, 3H, BCH_3), 7.63-7.77 (m, 4H), 8.24 (vt, 2H, *J*=7.7 Hz), 8.56 (d, br, 2H).

3.5.2 Synthesis of sodium (Me)(MeO)BPy$_2$, 3.1

Based on the NMR reaction, protonolysis of 2g of **1.14** (10 mmol) was performed in 5 mL TFA in a Schlenk-tube under similar conditions. ESI^{+}-MS of an aliquot of the reaction mixture showed a peak at 183.1, corresponding to **3.4**, and none at 199.1 corresponding to **1.14**. The reaction mixture was exposed to high vacuum to yield a brown colored gel-like material. A 4mL methanolic suspension containing 4g NaOMe was slowly added to the Schlenk-tube at 0 °C with rapid stirring. Immediately upon addition, copious amounts of brown tar-like material formed. The Schlenk-tube was warmed to room-temperature, and stirring was continued for a period of 4h. After this time, only fine white precipitate could be seen suspended in a brown colored supernatant. The mixture was stripped to dryness under high-vacuum to obtain an amorphous brown solid. The solid was dispersed in 5mL THF, filtered through a PTFE filter, washed with an additional 1mL THF and concentrated. Recrystallization by adding hexanes afforded 2.0 g of **3.1** as a beige-colored powder, in 87% yield. **3.1**, although clean by ^{1}H-NMR and ^{13}C-NMR spectrosocopy could not be obtained as an analytically pure compound presumably due to the presence of sodium trifluoroacetate.

^{1}H NMR (22 °C, 500 MHz, DMSO-D_6, ppm) δ: 0.15 (s, 3H, BCH_3), 3.0 (s, 3H, $BOCH_3$), 6.78-6.80 (m 2H, py-5-CH), 7.25-7.31 (m, 4H, py-4-CH, py-3-CH), 8.33 (td, 2H, *J*=4.6, 1.3 Hz, py-6-CH)

^{13}C NMR (22 °C, 500 MHz, DMSO-D_6, ppm) δ: 50.34 (s, $BOCH_3$), 117.90, 125.90, 132.80, 147.81, B-bound Carbon atoms not seen due to B-coupling

ESI^{-}-MS of a methanolic solution, Found: 213.14, Calculated 213.12

3.5.3 Synthesis of sodium (methoxy)(methyl)di(2-pyridyl)borato-Pt^{II}Me$_2$ complex, 3.5:

250 mg (1.06 mmol) of **1.14** and 304 mg of $[Me_2Pt(\mu\text{-}SMe_2)]_2$ (1.06 mmol) were combined in a vial and 3 mL THF was added to it with rapid stirring. After a period of 3h, the light-brown solution formed was stripped to dryness to obtain an

amorphous solid. Recrystallization from THF with heptanes afforded 447 mg **3.5** as a beige solid in 92% yield. Complex **3.5** is highly unstable and could not be obtained in analytically pure form. The sample was, however, satisfactorily clean by NMR spectroscopy (c.f. ^{13}C-NMR spectra: appendix p-130).

^{1}H NMR (22 °C, 400 MHz, CD_3CN, ppm) δ: 0.44 (s+Pt-satellites, 6H, J_{Pt-H}=81 Hz, $PtMe_2$), 0.53 (br, 3H, BMe), 3.32(br, 3H, BOMe), 6.82 (t, 2H, *J*=6.3 Hz, py-5-CH), 7.49 (td, 2H, *J*=7.6, 1.7 Hz, py-4-CH), 7.62 (d, 2H, *J*=8.1 Hz, py-3-CH), 8.65 (d+Pt-satellites, 2H, J_{Pt-H}=25.2, *J*=5.5 Hz, py-6-CH)

^{13}C NMR (22 °C, 500 MHz, CD_3CN, ppm) δ: -18.42 (s+Pt-satellites, J_{Pt-C}=812.7 Hz, $PtMe_2$), 6.76-8.68 (br, BMe), 51.7 (s, BOMe), 121.15, 128.39, 133.35, 150.80, 183.0-187.5 (br, py-2C)

ESI$^-$-MS of a THF solution: 438.11, Calculated: 438.13

3.5.4 Preparation of sodium (methoxy)(methyl)di(2-pyridyl)borato-Pt^{II}(CD_3)(OCD_3) complex, 3.6-*d*$_6$:

15 mg of **3.5** was dissolved in CD_3OD in a Young tube and a ^{1}H-NMR was recorded. According to the NMR, methanolysis of one of the PtMe fragments was slow. The reaction was monitored over time and after a period of 2h, quantitative conversion of **3.5** to **3.6-*d*$_6$** was observed. Exchange of the B-OMe fragment with solvent was not observed in the course of the reaction.

(**3.5-*d*$_6$**, 10 minutes after dissolution in CD_3OD)

^{1}H NMR (22 °C, 400 MHz, CD_3OD, ppm) δ: 0.46 (br, s, 3H, BCH_3), 1.87 (m, 2.8H, THF), 3.16 (br, s, $BOCH_3$), 3.72 (m, 2.8H, THF), 7.0 (m, br, 2H, py-5-CH), 7.56-7.71 (m+m, 4H, py-3-CH, py-4-CH), 8.56 (d+Pt-satellites, 2H, *J*=5.4, J_{Pt-H}=28.8 Hz, py-6-CH).

(**3.6-*d*$_6$**, 2 hours after dissolution in CD_3OD)

^{1}H NMR (22 °C, 400 MHz, CD_3OD, ppm) δ: 0.78 (s, 3H, BMe), 1.87 (m, 2.8H, THF), 3.46 (s, 3H, BOMe), 3.72 (m, 2.8H, THF), 6.72 (dd, 1H, *J*=5.8, 2.0 Hz, py-5-CH), 6.99 (dd, 1H, *J*=5.4, 1.8 Hz, py'-5-CH), 7.44-7.57 (m, 3H, py-3-CH, py-4-CH, py'4-CH), 7.65 (d, 1H, py-3-CH), 8.51 (d+Pt-satellites, 1H, J_{Pt-H}=55 Hz, py-6-CH, trans to Pt-OCD_3), 8.74 (d+unresolved Pt-satellites, 1H, py'-6-CH, trans to Pt-CD_3)

3.5.5 Synthesis of sodium (methoxy)(methyl)di(2-pyridyl)borato-Pt^{II}(Me)(OMe) complex, 3.6:

Based on the NMR reaction, 100 mg of **3.5** (216 µmol) was dissolved in 2 mL methanol and left stirring for 2.5 h. At the end of this period the contents were striped to dryness and washed with ether to obtain 92.1 mg of **3.6**, in 89% yield. According to the NMR spectra, excess of methanol remained in the compound. Attempts to remove methanol over long periods of time resulted in darkening of the sample and the NMR spectra getting progressively dirtier.

^{1}H-NMR (22 °C, 400 MHz, acetone-*d*$_6$, ppm) δ: 0.53 (br, s, 3H, BMe), 0.83 (s+Pt-satellites, 3H, J_{Pt-H}=82.3 Hz, PtMe), 3.27 (could not be integrated due to overlap with methanol), 3.52 (s+Pt-satellites, 3H, J_{Pt-H}=53.3 Hz, PtOMe), 6.71 (vt, 1H, *J*=6.8 Hz,

py-5-CH), 6.97 (vt, 1H, *J*=7.1 Hz, py'-5-CH), 7.40-7.56 (m+m+m, 3H, py-4-CH, py'-4-CH, py-3-CH), 7.6 (d, 1H, *J*=7.1 Hz, py'-3-CH), 8.52 (d+Pt-satellites, 1H, *J*=6.5, J_{Pt-H}=53 Hz, py-6-CH, trans to PtOMe), 8.84 (d+unresolved Pt-satellites, 1H, *J*=4.7 Hz, py'-6-CH, trans to PtMe).

ESI^--MS of a methanolic solution basified with NaOMe: 454.12, Calculated: 454.13

3.5.6 Synthesis of (methoxy)(methyl)di(2-pyridyl)borato-$Pt^{IV}Me_3$ complex, 3.7

100 mg **3.5** was dissolved in 2mL THF and 25 µL MeI was added to it. After a period of 10 minutes, the contents of the vial were stripped to dryness to obtain a powder. The powder was re-dispersed in 3mL dichloromethane and the mixture was filtered through a PTFE filter, residues washed with an additional 1 mL of dichloromethane and the combined filtrates were dried under high-vacuum to obtain 100 mg of a 97 mg of **3.7** in quantitative yield. Crystals suitable for X-ray structure determination were grown by layering the dichloromethane solution with pentanes.

^{1}H-NMR (22 °C, 500 MHz, $CDCl_3$, ppm) δ: 0.47 (s, br, 3H, BMe), 0.81 (s+Pt-satellites, 6H, J_{Pt-H}=67.7 Hz, $PtMe_2$, equatorial), 1.16 (s+Pt-satellites, 3H, *J*=77 Hz, PtMe, axial), 3.13 (s+Pt-satellites, 3H, J_{Pt-H}=12.3 Hz, B(µ-OCH_3)Pt^{IV}), 7.06 (m, 2H, py-5-CH), 7.54 -7.61 (d+m, 4H, py-4-CH, py-3-CH), 8.33 (d+Pt-satellites, 2H, *J*=5.6, J_{Pt-H}=15.9 Hz, py-6-CH).
^{13}C NMR (22 °C, 500 MHz, $CDCl_3$, ppm) δ: -11.9 (s+Pt-satellites, J_{Pt-C}=763 Hz, PtMe, axial), -9.3 (s+Pt-satellites, J_{Pt-C}=676 Hz, $PtMe_2$, equatorial), 0.83-2.47 (br, BMe), 52.7 (s, B(µ-OCH_3)Pt^{IV}, no Pt-C coupling), 121.8 (s+Pt-satellites, J_{Pt-C}=18 Hz), 127.6, 135.7, 144.8 (s+Pt-satellites, J_{Pt-C}=20 Hz), 178-180 (py-2-C(B)).

3.5.7 Oxidation of 3.5 in methanol to produce 3.8 and 3.9 in the ratio 3:1

50 mg of **3.5** was dissolved in methanol in the glove-box and quickly taken out and exposed to O_2 for a period of 10 minutes. After this period, the solution was stripped to dryness to obtain 52 mg an amorphous powder. A ^{1}H-NMR of the mixture in produced the following peaks, resolved based on known ratio of **3.8** : **3.9**= 3:1. **3.8** and **3.9** have similar solubility in THF and chloroform, and could not be separated.
^{1}H-NMR of **3.8** (22 °C, 400 MHz, $CDCl_3$, ppm) δ: 0.85 (s+Pt-satellites, 6H, J_{Pt-H}=67.9 Hz, $PtMe_2$, equatorial), 1.19 (s+Pt-satellites, 3H, J_{Pt-H}=78 Hz, PtMe, axial), 3.14 (s+Pt-satellites, 3H, J_{Pt-H}=12.3 Hz, B(µ-OCH_3)Pt^{IV}), 3.07 (s, br, 3H, BOMe, exo), 7.11 (td, 2H, *J*=5.4, 1.8 Hz, py-5-CH), 7.63 (vt, 2H, *J*=7.7 Hz, py-4-CH, overlapping with py-4-CH of **3.9**), 7.72 (d, 2H, *J*=7.7 Hz, py-3-CH), 8.34 (d+Pt-satellites, 2H, *J*=5.6 Hz, J_{Pt-H}=16 Hz, py-6-CH)
^{1}H-NMR of **3.9** (22 °C, 400 MHz, $CDCl_3$, ppm) δ: 0.46 (s, br, 3H, BMe), 1.34 (s+Pt-satellites, 6H, J_{Pt-H}=70.2 Hz, $PtMe_2$, equatorial), 3.05 (s+Pt-satellites, 3H, J_{Pt-H}=27 Hz, B(µ-OCH_3)Pt^{IV}), 3.48 (s, br, 3H, BOMe, exo), 7.16 (vt, 2H, *J*=6.7 Hz, py-5-CH), 7.55 (d, 2H, *J*=7.7 Hz, py-3-CH), 7.63 (2H, overlapping with py-4-CH of **3.8**), 8.61 (d+unresolved Pt-satellites, 2H, *J*=5.9 Hz, py-6-CH).
ESI-MS of a methanolic solution containing **3.8** and **3.9**: 438.1 (**3.8**-OMe)$^+$, 456.1 (**3.9**H^+)

3.5.8 Oxidation of 3.5 in CD_3OD to form 3.8-$d_{(n+3)}$ and 3.9-$d_{(n+1)}$ in the ratio 3:1

15 mg of **3.5** was dissolved in CD_3OD in the glove-box in an NMR tube and quickly taken out and exposed to O_2 for 10 minutes. A ^{1}H-NMR was recorded after this time. The ^{1}H-NMR spectra was not resolved to correspond to individual products.

^{1}H NMR (22 °C, 400 MHz, CD_3OD, ppm) δ: 0.44 (s, br, **1H**, BCH_3), 0.82 (s+Pt-satellites+D-satellites, $Pt(CH_nD_{(3-n)})_2$, J_{Pt-H}=~66 Hz, could not be reliably integrated), 1.19 (s+Pt-satellites, no D-satellites, **3H**, J_{Pt-H}=~78 Hz), 2.99 (s+Pt-satellites, **1H**, J_{Pt-H}=28.6 Hz, B-μ-OCH_3-Pt), 3.6 (s, **3H**, $BOCH_3$), 7.2 (vt, **2H**), 7.26 (vt, **0.66H**), 7.6 (d, **0.66H**), 7.67 (d, **2H**), 7.70-7.77 (m, **2.66H**), 8.40 (d+Pt-satellites, **2H**, J=7.0, J_{Pt-H}=17 Hz), 8.62 (d+unresolved Pt-satellites, **0.66H**).

3.5.9 Oxidation of 3.6 in methanol:

25 mg of 3.5 was dissolved in methanol in a reaction and stirred inside the glove-box for a period of 2h. After this time, it was taken out and exposed to O_2 for 10 minutes. The solution was stripped to dryness and the mixture was analyzed by ^{1}H-NMR and ESI$^+$-MS. The ^{1}H-NMR spectra was not resolved to correspond to individual products. Only definite assignments are noted.

^{1}H-NMR of a mixture of **3.10** and **3.11** (22 °C, 400 MHz, $CDCl_3$, ppm) 0.48 (3H, BMe), 1.43 (s+Pt-satellites, 3H, J_{Pt-H}=68.4 Hz), 1.74 (s+Pt-satellites, 3H, J_{Pt-H}=77 Hz), 1.94 (s+Pt-satellites, 3H, J_{Pt-H}=68 Hz, PTMe axial, **3.10**), (overlapping s+Pt-satellites, 3.1, 3.16, 3.17, 3.24), 3.65 (s, br, 3H, BMe, exo, **3.11**), 7.02-7.16 (2H), 7.17-7.25 (2H), 7.47 (d, 1H), 7.56-7.71 (m, 6H), 7.76 (1H), 8.0 (d+Pt-satellites, 1H, J=5.9 Hz, J_{Pt-H}=33 Hz), 8.41(d+unresolved Pt-satellites, 1H), 8.53(d+unresolved Pt-satellites, 1H), 8.85(d+unresolved Pt-satellites, 1H).

ESI-MS of a methanolic solution containing **3.10** and **3.11**: 486.09 (**3.10**H$^+$), 472.09 (**3.11**H$^+$); Calculated: 486.1, 472.1

Figure 3.8: ESI-MS spectrum of solution containing **3.10** and **3.11:**

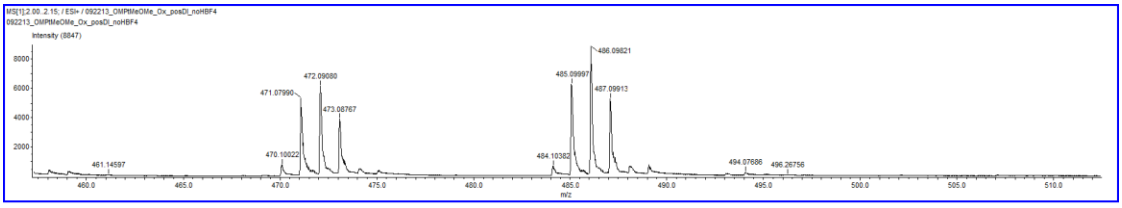

Chapter 4: Aerobic Oxidation of di(2-pyridyl)-1,5-cyclooctanediylborato-Pt^{II} complexes: C-C and C=C coupling at the Boron-center via multiple O_2 activation

4.1 Proposal

In our attempts towards developing di(2-pyridyl)borate ligands that would retain the anionic borate center upon oxidation of derived Pt^{II} complexes, we considered a bicyclic borate center. Inspired by Trofimenko's ligand, **4.1** [70], as shown in Scheme 4.1(a), we conceived a dipyridyl analogue, viz. di(2-pyridyl)-1,5-cyclooctanediylborate, **4.2**, as shown in (b). According to Trofimenko, the bis(pyrazolyl) analogues exhibit 'enhanced' agostic interaction (Scheme 4.1(c)), owing to the pseudoaxial bridgehead hydrogen forced into close proximity to the metal, **4.3** [70]. Furthermore, for a Co(III) center bound to two such ligands, the propensity of the ligand to 'donate' the C-H bond electron density can manifest in two axial agostic interactions [70].

We anticipated that such interaction would provide the necessary sixth axial ligation in an octahedral Pt^{IV}(OH) complex generated via O_2 activation (c.f. Scheme 1.3) while resisting B-to-Pt^{IV} hydrocarbyl migration due to the constraints imposed by the bicyclic (9-BBN) fragment. Other than a few substituted-pyrazolyl derivatives [71] of the original ligand (4.1), to the best of our knowledge, there are no reports of anionic borate ligands featuring the 9-BBN fragment.

Scheme 4.1 Bis(pyrazolyl) and new di(2-pyridyl) ligand featuring a 9-BBN fragment

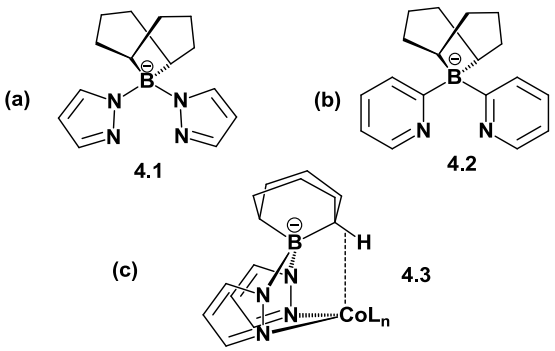

4.2 Implementation

Synthesis of **4.2** was first attempted in a manner similar to **1.14** [35]. Typically, 2 equivalents of 2-pyridyl-lithium is added at -78 °C to a dialkylboron-precursor in ether, and upon working up, good to moderate yields of the protonated ligand are obtained. A similar strategy involving B-methoxy-9-BBN was adopted, however **4.2** was not observed upon work-up. ESI-MS analysis revealed signals at M/z =200 and 157 corresponding to protonated-(2-pyridyl)-1,5-cyclooctanediylborane, **4.4**, and protonated-bipyridyl, respectively, as shown in Scheme 4.2(a). Disappointingly, addition of up to 10 equivalents of 2-pyridyl-lithium showed no changes in the ESI-MS spectra and no signals at M/z = 279, corresponding to diprotonated-**4.2** were seen. We presumed that the steric-bulk at the boron-center requires higher activation energy for the attack of the second pyridyl fragment, and higher temperatures might be required.

Scheme 4.2 Synthetic approach towards di(2-pyridyl)-1,5-cyclooctanediylborate

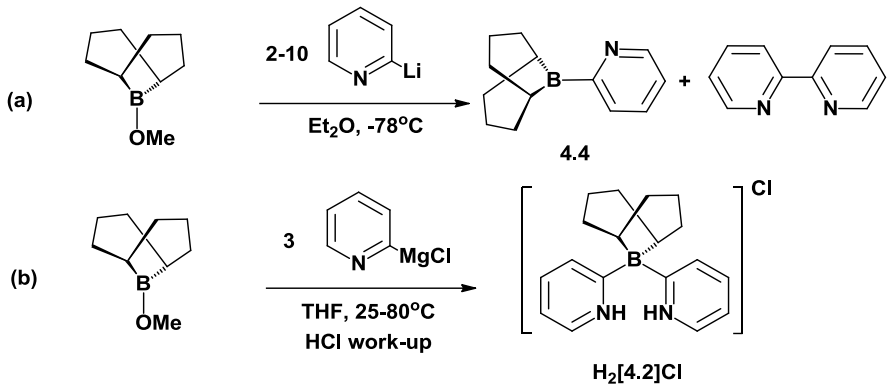

Based on the demonstration of the use of the more thermally stable 2-pyridyl-magnesium halides in the synthesis of boron compounds at room-temperatures by Cui et al [72], we pursued synthesis of 4.2 via a conveniently synthesized Grignard reagent, as shown in Scheme 4.2(b). Gratifyingly, analysis of an aliquot of the reaction mixture containing 3 equivalents of 2-pyridylmagnesium chloride after 24h at 25 °C, revealed, in addition to an intense peak at M/z 200, a small-peak at M/z 279 indicating the formation of di(2-pyridyl)-1,5-cyclooctanediylborate, **4.2**. To increase rates of reactions, a reaction mixture containing B-methoxy-9-BBN and 3 equivalents of 2-pyridylmagnesiumchloride in THF was ramped to 80 °C and the progress was monitored by ESI-MS, owing to the complicated nature of the ^{1}H-NMR spectra of aliquots. After 24h, the only observable signal was that of H_2[**4.2**]$^{+}$. Acid workup with HCl led to the formation of needle-like crystals of H_2[**4.2**]Cl. Single crystal X-ray diffraction in conjunction with ^{1}H-NMR and elemental analysis was used to definitively confirm the identity and purity of the ligand. An ORTEP representation for H_2[**4.2**]Cl is shown in Figure 4.1 along with relevant geometric parameters. Notice that the B-center displays a contracted $C^{exo}(11)\hat{B}C^{endo}(15)$ angle of 104°, consistent with a tight framework owing to the tethered B-alkyls of the 9-BBN

moiety. Na[**4.2**] was obtained by treatment of H_2[**4.2**]Cl with NaH. C.f. appendix pp 133-134 for ^{1}H-NMR and ^{13}C-NMR spectra.

Figure 4.1: X-ray structure of protio-di(2-pyridyl)-1,5-cyclooctanediylborate, HCl salt, **4.2**H_2Cl

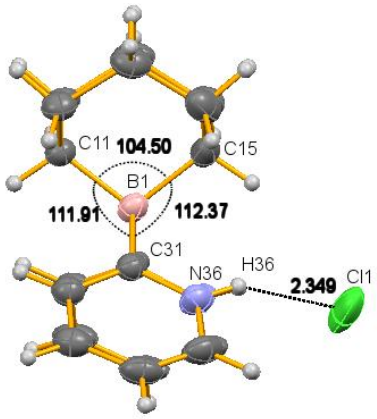

4.3 Results and Discussion

4.3.1 Synthesis of di(2-pyridyl)-1,5-cyclooctanediylborato-Pt^{II} complexes

With our new ligand at hand, derived dimethyl (**4.5**) and diphenyl (**4.6**) Pt^{II} complexes were synthesized from the sodium salt, Na[**4.2**], in excellent yields according to standard literature procedure, as shown in Scheme 4.3.

Scheme 4.3: Synthesis of di(2-pyridyl)-1,5-cyclooctanediylborato-Pt^{II} complexes

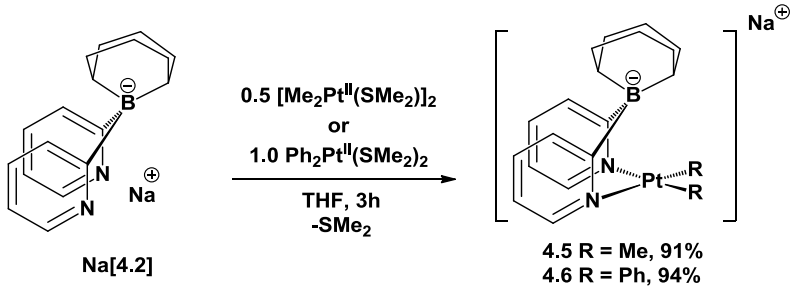

Figure 4.2: ^{1}H NMR spectrum of **4.5** in CD_3CN (22 °C, 500.132 MHz)

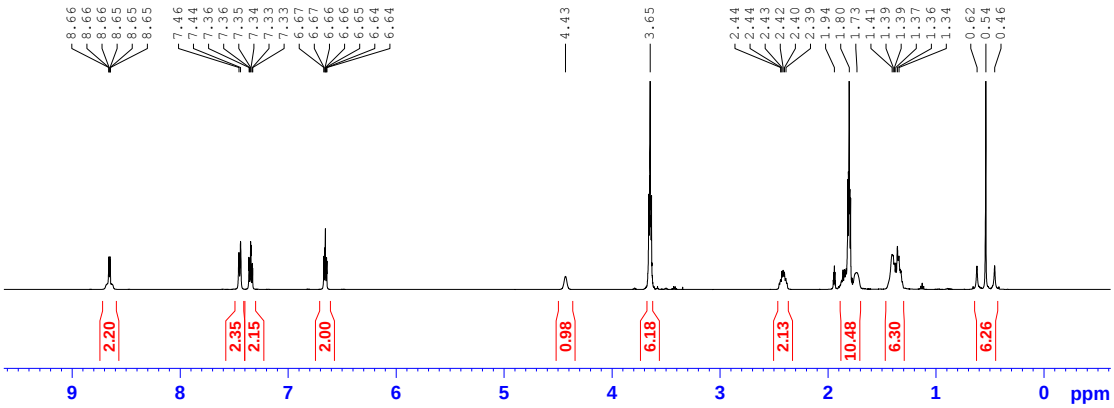

Both **4.5** and **4.6** are stable in aprotic solvents in the absence of O_2 for at least 24h at room-temperature. **4.5** reacts vigorously with water in the presence of an alkane such as cyclohexane to form the olefin hydride complex, **4.7**, and in the presence of a good donor such as dimethylsulfide to form **4.8**. This reactivity, shown in Scheme 4.4, is expected and similar to **1.15**

Scheme 4.4: Reactivity of sodium di(2-pyridyl)-1,5-cyclooctanediylborato-Pt^{II}Me$_2$ complex, 4.5

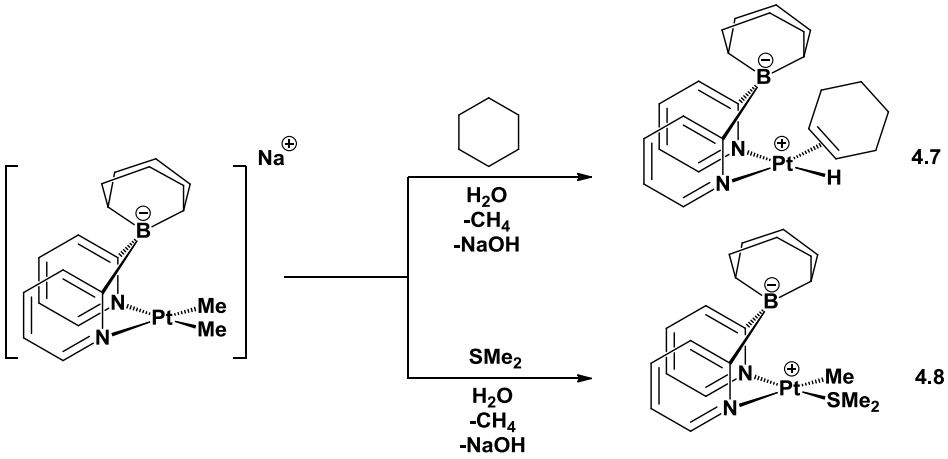

The ^{1}H and ^{13}C NMR spectra of **4.5** and **4.6** (c.f. appendix pp. 135-136) show the presence of a C_s symmetric species in solution, whereas that for **4.7** and **4.8**, a C_1 symmetric species (c.f. appendix pp. 137-140). Amidst the complex multiplets corresponding to the 9-BBN fragment in Pt^{II}-complexes **4.5**, **4.6**, **4.7** and **4.8**, one well

resolved signal integrating to 1 hydrogen, appears considerably downfield at ~4.5 ppm. This signal, assigned to the exo-BCH of the 9-BBN fragment, showed no significant NOE response in **4.5** and **4.8** to any pyridine-hydrogens which would have been expected for proximity. Distinction between the ^{1}H-NMR signals of the exo and endo bridgehead BCH signals were made by DEPT-45, 90 and 135 spectroscopy. We presume the downfield shift of the exo-BCH as opposed to the 'normal' chemical shift of the endo-BCH fragment (c.f. experimental section) is due to it being sandwiched between the two aromatic (pyridine) rings, enough for it to be shielded by aromatic ring currents, but not enough for it to show appreciable NOE response. X-ray structure of a representative stable Pt^{II} complex (**4.8**) featuring an intact 9-BBN fragment with clearly resolved exo-BCH ^{1}H-NMR signal is shown in Figure 4.3. It is important to note that the $C^{exo}\hat{B}Pt$ and $C^{endo}\hat{B}Pt$ angles in **4.8** are 175.7° and 72.4°.

Figure 4.3: X-ray structure of di(2-pyridyl)-1,5-cyclooctanediylborato-$Pt^{II}(SMe_2)(Me)$ complex, **4.8**

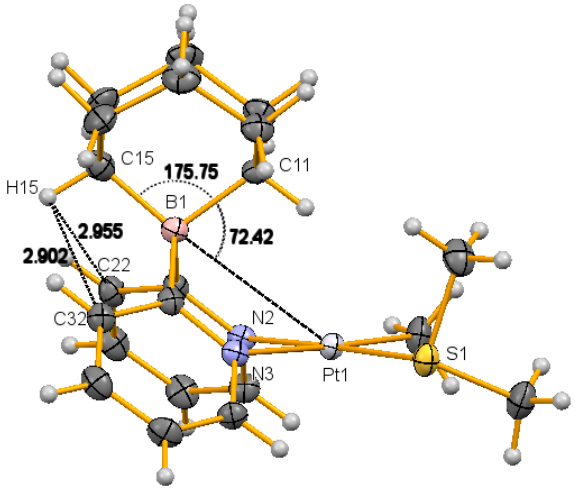

A stable trimethyl-Pt^{IV} complex, **4.9** was synthesized from the dimethyl-Pt^{II} complex, **4.5** by reaction with methyliodide. Complex **4.9** features a Pt^{IV}-CH agostic interaction, as shown in Figure 4.5. A direct proof of 'enhanced' agostic interaction

manifests in a short 1.99 Å (δ-C)H–Pt^{IV} distance. The 2.71 Å (B)C-Pt^{IV} contact is significantly longer, indicating unsymmetric η^1 (C-H)-donation to the Pt^{IV}-center. Interestingly, the 9-BBN fragment is tilted by ~10° towards the Pt^{IV}-center in **4.9** in order to accommodate the short(δ-C)H–Pt^{IV} contact, evident from the $C^{exo}\hat{B}Pt$ and $C^{endo}\hat{B}Pt$ angles of 165.8° and 62.4°, respectively. The signal corresponding to the agostic C-H fragment in the ^{1}H-NMR spectra of **4.9** , shown in Figure 4.4, has a considerable upfield shift (-3.36ppm, CD_2Cl_2) with higher J_{Pt-H} coupling of 207 Hz (500MHz, CD_2Cl_2) in comparison to that at -0.91 ppm with J_{Pt-H} coupling of 58.1 Hz (500 MHz, THF-d_8) for (dpdmb)$Pt^{IV}Me_3$, **1.26** [34]**.** The ^{1}H-NMR signal corresponding to the exo-BCH of the 9-BBN fragment in **4.9** shifts back to the 'aliphatic' region, integrating to 1H at 1.62 ppm in CD_2Cl_2 solution. Two sets, viz. axial and equatorial PtMe fragments of **4.9** could be clearly seen in the ^{13}C-NMR spectrum, shown in appendix, p-141.

Figure 4.4: ^{1}H NMR spectrum of **4.9** in CD_2Cl_2 (22 °C, 500.132 MHz)

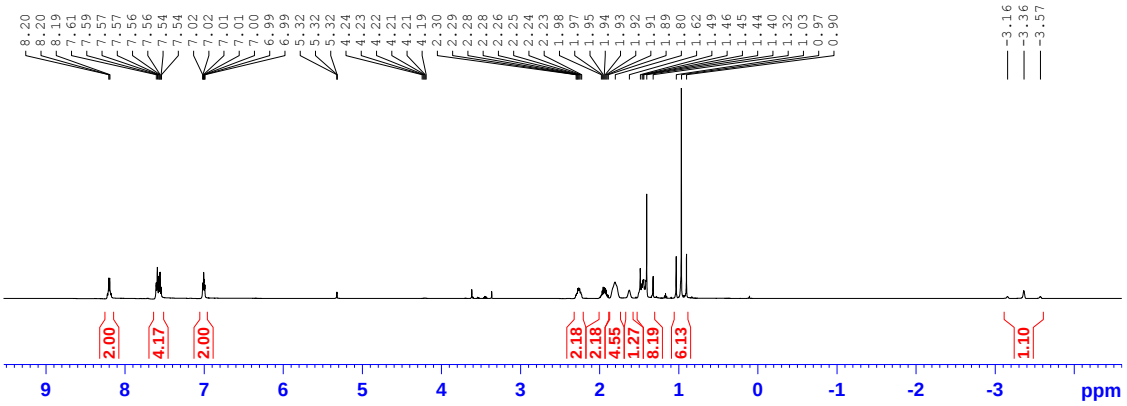

Figure 4.5: X-ray structure of di(2-pyridyl)-1,5-cyclooctanediylborato-$Pt^{IV}Me_3$ complex, **4.9**

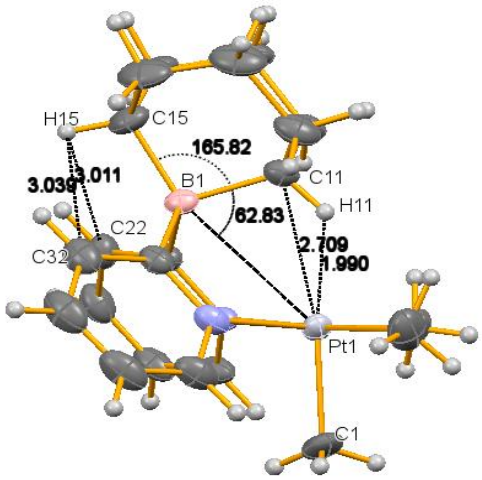

The closer proximity of the H atom to the Pt^{IV} center manifests itself in a more hydridic character. In contrast to **1.26**, which reacts with methanol at elevated temperatures to form **1.22** along with the elimination of methane [34], **4.9** was found to be resistant towards B-to-Pt^{IV} hydrocarbyl migration under similar conditions. Attempts to deprotonate the agostic C-H bond in **4.9** with a strong base such as NaOMe in MeOH was unsuccessful at elevated temperatures of up to 100 °C, as expected due to the constraints imposed by the 9-BBN fragment.

Scheme 4.5: Protonolysis of di(2-pyridyl)-1,5-cyclooctanediylborato-Pt^{II}-dihydrocarbyl complexes

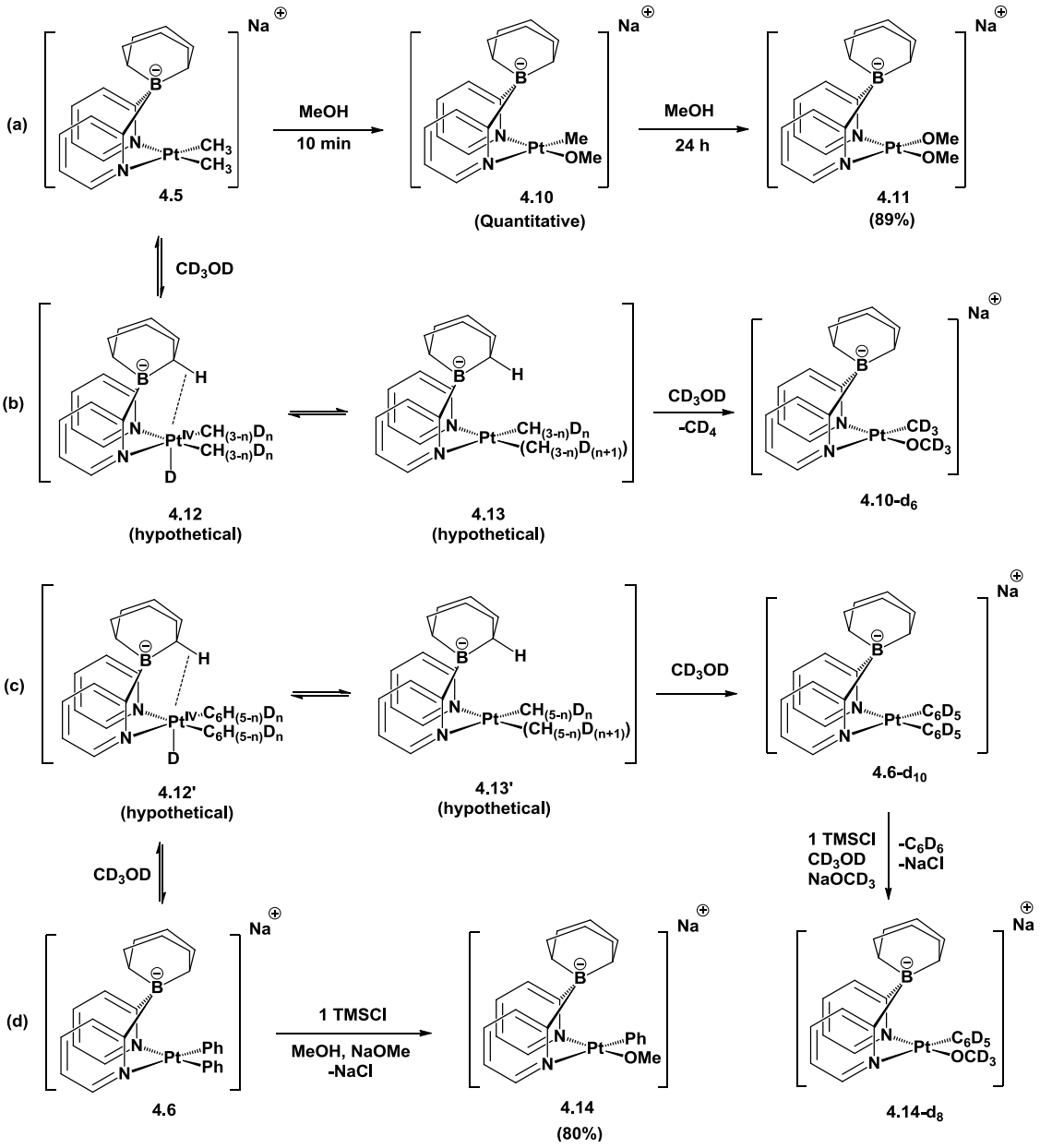

Similar to the (dpdmb)$PtMe_2$ complex, **1.15**, **4.5** reacted instantaneously with methanol along with visible evolution of methane (vide infra) to form, based on its ^{1}H-NMR spectra, the C_1 symmetric monomethyl complex, **4.10**, similar to (dpdmb)Pt(Me)(OMe), **1.21**, as shown in Scheme 4.5(a). On the other hand, the monomethyl Pt^{II} complex **4.9**, reacted slowly with methanol over a period of 24h to

form an 'inorganic' Pt^{II} complex, **4.11**, unlike **1.21** which did not undergo further methanolysis. This contrast is due to a more basic Pt^{II}-center in **4.9** due to the presence of a more electron donating borate ligand, i.e. **4.2**. The ^{1}H-NMR spectra recorded immediately after dissolution of **4.5** in CD_3OD corresponds to **4.10-*d*$_6$**, which was also confirmed by ESI^--MS. The absence of signals corresponding to either evolved CH_4 or a $Pt^{II}CH_3$ fragment in the ^{1}H-NMR spectra recorded immediately after dissolution of **4.5** in CD_3OD is consistent with rapid H/D exchange between CD_3OD and **4.5** that involves transient intermediates **4.12** and **4.13** before expulsion of CD_4 from the coordination sphere of Pt, as shown in Scheme 4.5(b). No deuteration of either B-CH fragments of the BBN moiety was observed even after 3 days establishing its inertness towards C-H activation by the proximal Pt-center.

Figure 4.6: ^{1}H NMR spectrum of **4.10-*d*$_6$** in CD_3OD (22 °C, 500.132 MHz)

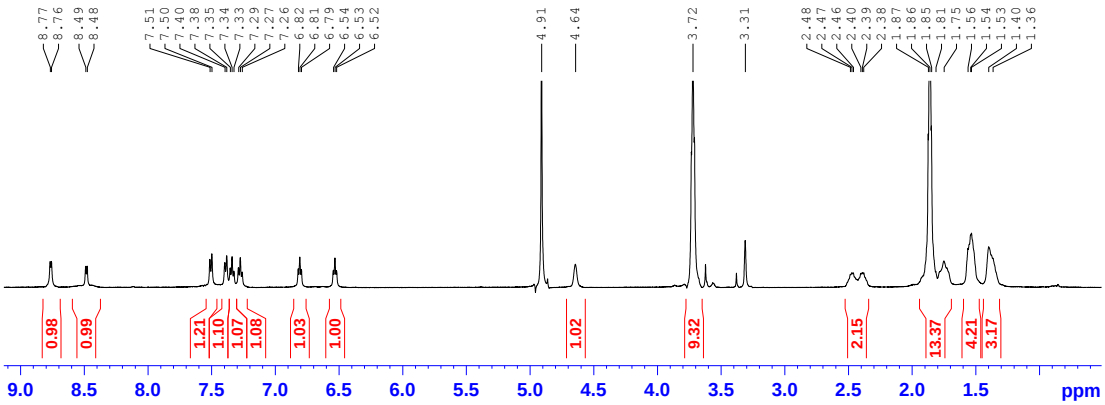

Although the diphenyl Pt^{II} complex, **4.6** is resistant towards methanolysis of the $Pt^{II}Ph$ fragment, a sample of **4.6** in CD_3OD underwent complete deuteration of the $Pt^{II}Ph_2$ fragment within 8h at 20 °C after dissolution (Figure 4.7), evident from the absence of the initially visible $Pt^{II}Ph_2$ ^{1}H-NMR signals. An aliquot of the NMR solution analyzed by ESI^--MS showed a signal with the mass increased by 10 mass units compared to **4.6**, confirming the presence of **4.6-*d*$_{10}$**. Interestingly, **4.6-*d*$_{10}$**

underwent complete H/D exchange in the reverse direction upon dissolution in CD_3OH in the course of 4h, confirmed by the reappearance of the $Pt^{II}Ph_2$ signals.

Figure 4.7: ^{1}H NMR spectrum of **4.6**/ **4.6-*d*$_{10}$** in CD_3OD (22 °C, 500.132 MHz)

(Immediately after dissolution)

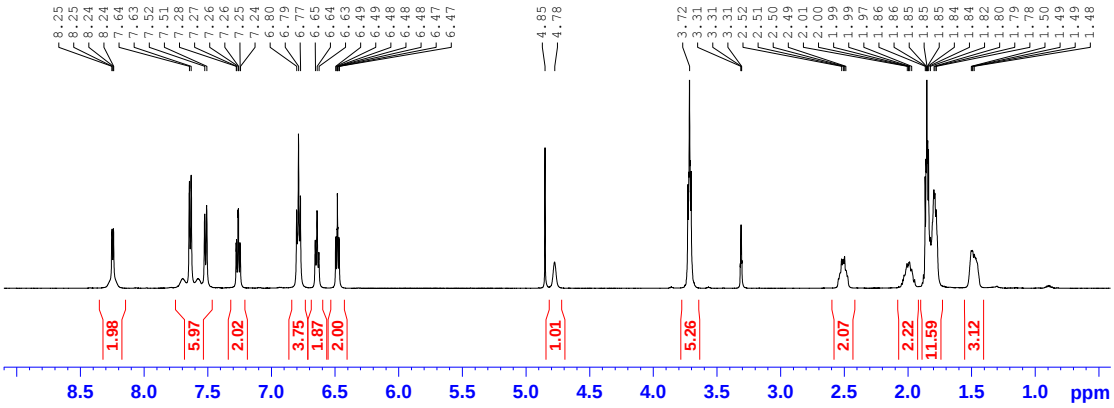

(8h after dissolution)

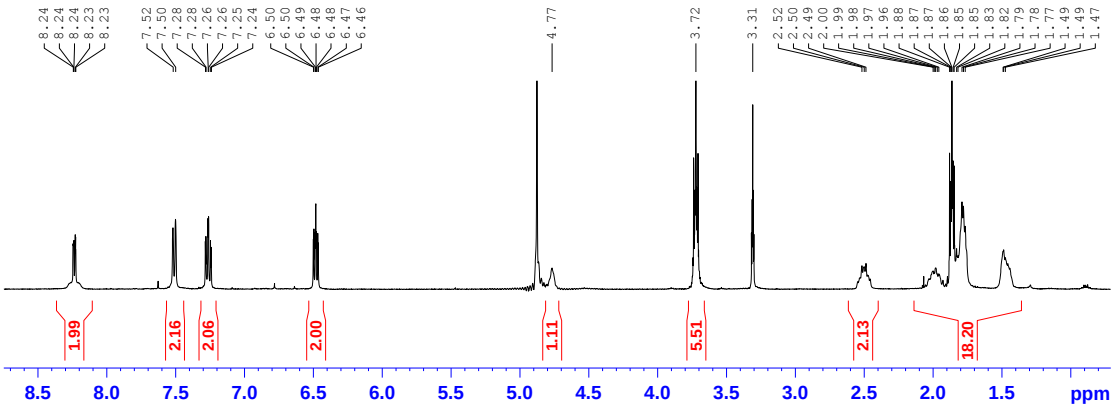

The difference in reactivity of **4.6** as opposed to that of **4.5** towards methanolysis can be attributed to the Pt^{II} center in **4.5** being more electron rich and more basic due to the presence of two electron donating Me fragments. Thus the initial protonation of the Pt^{II} center in **4.5** is expected to be shifted more toward the hydrido-$Pt^{IV}Me_2$ complex, **4.12**, as compared to a similar equilibrium between **4.6** and a derived hydrido-$Pt^{IV}Ph_2$ complex, **4.12'**. Once the consecutive equilibrium between the $Pt^{IV}Me_2$ complex, **4.12** and the Pt^{II}(methane) complex, **4.13**, is established, the

reaction proceeds irreversibly to **4.10** (or **4.10-d$_6$**) via rapid loss of gaseous methane. For the diphenyl analogue, **4.6**, however, the fraction of the hydrido-Pt^{IV}Ph$_2$ is much lower and the H/D exchange rate is much slower. Hence, in order to prepare a monophenyl Pt^{II} complex, viz. **4.14**, at a fast rate, an acid stronger than methanol was required. 1 equivalent of HCl generated in-situ by reacting TMSCl in methanol, followed by treatment with subsequent neutralization with NaOMe, afforded complex **4.14** in good yields (c.f. appendix pp. 143-144 for ^{1}H and ^{13}C-NMR spectra). The *d$_8$*-derivative, i.e. **4.14-*d$_8$*** can be similarly prepared by treatment of **4.6-*d$_{10}$*** with TMSCl in CD_3OD followed by treatment with $NaOCD_3$.

4.3.2 Oxidation of di(2-pyridyl)-1,5-cyclooctanediylborato-Pt^{II} complexes

Scheme 4.6: Oxidation of di(2-pyridyl)-1,5-cyclooctanediylborato-Pt^{II}-monohydrocarbyl complexes

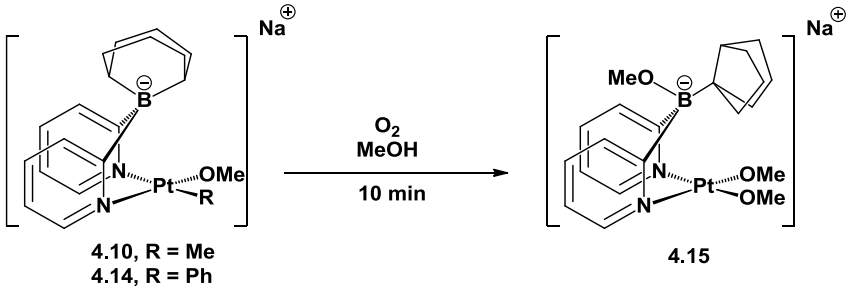

4.10, R = Me
4.14, R = Ph

4.15

Derived monohydrocarbyl complexes viz. **4.10** and **4.14** and dihydrocarbyl- Pt^{II} complexes viz. **4.5** and **4.6**, at hand, we set out to explore their reactivity towards aerobic oxidation. Solutions of **4.10** and **4.14** in CH_3OH were exposed to O_2 for a period of 10 minutes and upon drying a light-tan colored powder was obtained in either case. Signals corresponding to either Pt-Me or Pt-Ph fragments could not be located in the ^{1}H-NMR spectra of either reaction product in dmso-d$_6$. Interestingly, reaction products in either case was found to be an identical C*s* symmetric complex. When the oxidation of either **4.10** or **4.14** was performed in CD_3OD, in addition to an

identical set of aromatic signals in the ^{1}H-NMR spectra, singlets at 0.22 ppm assigned to CH_4 and 7.32 ppm assigned to C_6H_6 were observed in the respective cases.

Figure 4.8: ^{1}H NMR monitoring of *in-situ* oxidation of **4.10** in CD_3OD (22 °C, 400.131 MHz)

(Before oxidation)

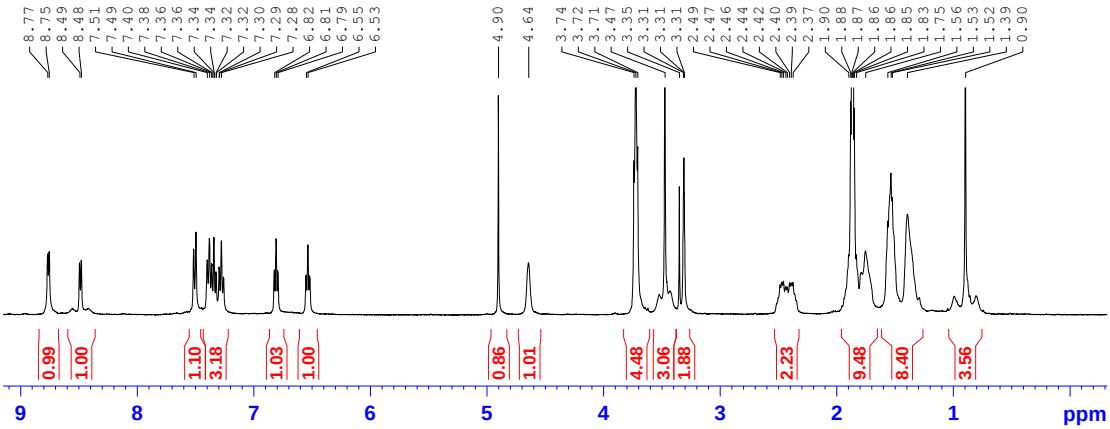

(After oxidation, showing methane at 0.18 ppm)

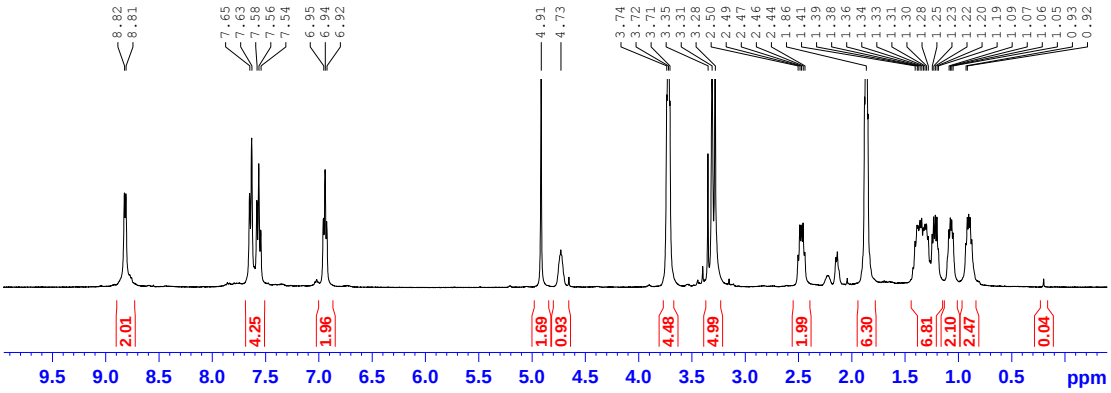

X-ray structure determination on crystals grown by saturating a THF solution of the product **4.15** with heptanes at -20 °C revealed unprecedented reorganization of the 9-BBN fragment in the starting material (viz. **4.10** and **4.14**) to a bicyclo[3.3.0]octyl fragment in the final product (Scheme 4.6, Figure 4.9). ESI$^-$-MS of the product obtained from the oxidation of **4.10** in CD_3OD revealed a M/z 6 units higher than that obtained from the oxidation in CH_3OH, consistent with the presence of two OCD_3

fragments and the structure assigned for the anionic Pt^{II} complex, **4.15**. The Pt^{II}-bound OCH_3 fragment in **4.10** did not undergo substitution in the course of the reaction. However, the Pt^{II}-OCH_3 fragment in **4.15** underwent slow exchange in CD_3OD to form **4.15-d$_9$** at elevated temperatures to form **4.15-d$_9$**. **4.15-d$_9$** did not afford further oxidation: a sample of **4.15-d$_9$** prepared in CD_3OD was exposed to O_2 and no changes were observed in the ^{1}H-NMR spectra even after a period of 2 days.

Figure 4.9: X-ray structure of di(2-pyridyl)-B-methoxy-B-[3.3.0]bicyclooctanylborato-$Pt^{II}(OMe)_2$, **4.15**

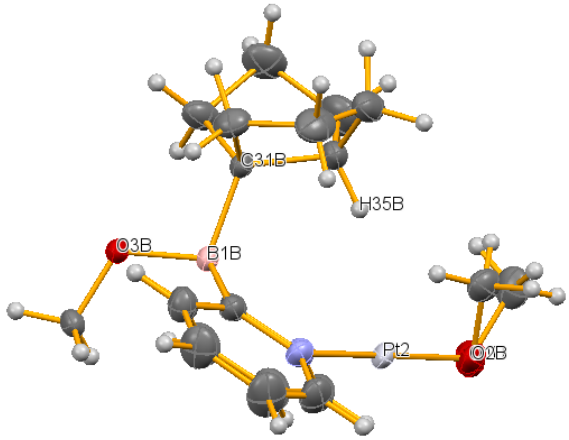

Similar 1-5 migration of the B-$^{2°C}$ alkyl of the 9-BBN fragment was observed by Brown et al [73] upon treating lithium tetra-alkylborate derivatives of 9-BBN with acetyl chloride to form l-bicyclo[3.3.0]nonanyl dialkylborane. Such rearrangements presumably led to *hydride migration* [74] from the bridgehead $B^{2°C}H$ fragment to an accepting electrophile such as an alkyl and aryl halides [75] or acylchlorides [76]. In our case, the *hydride*-accepting electrophile is a Pt^{IV}(OH) center generated via oxidation (vide infra).

Based on this unanticipated reaction involving oxidative C-C coupling at the boron-center [76], we next oxidized the dihydrocarbyl-Pt^{II} complexes, **4.5** and **4.6** in

CH_3OH. Owing to the stability of **4.6** in methanol, the oxidation of **4.6** in methanol was performed in straightforward manner. On the other hand, to avoid rapid methanolysis of one of the $Pt^{II}Me$ fragments (c.f. Scheme 4.5(a)) **4.5** was oxidized at -60 °C by adding a THF solution of **4.5** to a solution of O_2 in methanol pre-cooled to -60 °C. In both cases, upon removal of solvent, the ^{1}H-NMR spectra of the products, viz. **4.16** and **4.17** in $CDCl_3$ exhibited no signals in the aliphatic region matching to the initial 9-BBN or [3.3.0]bicyclooctyl fragment. As opposed to the oxidation of the monohydrocarbyl-Pt^{II} complexes, the $PtMe_2$ and $PtPh_2$ fragments were retained in the respective cases. To be able to characterize reaction products originating from the 1,5-cyclooctanediyl (9-BBN) fragment by ^{1}H-NMR spectroscopy, oxidation of **4.5** and **4.6** were performed in CD_3OD in a sealable NMR-tube. Upon close examination of the aliphatic region in the ^{1}H-NMR spectra, two new multiplets between 2.1-2.2 ppm integrating to 4H and 8H could be seen in either case, in addition to a new set of aromatic signals consistent with the presence of the C*s* symmetric species, **4.16** or **4.17** in solution. No methane or benzene was observed, respectively. X-ray diffraction was used to confirm the structure, shown in Figure 4.10, of the Pt-containing product of oxidation of **4.6**, i.e., **4.17**. **4.17** features two distinct B-bound methoxy groups: an exo group showing no coupling of the OCH_3 to the Pt^{IV} center in the ^{1}H-NMR spectra (c.f. appendix pp 146-147), and an endo group showing a $^3J_{Pt\text{-}H}$ of 22.5 Hz for the OCH_3 fragment corresponding to a short O-Pt^{IV} contact of 2.09 Å in the crystal-structure, shown in Figure 4.10. No exchange of the either $BOCH_3$ fragments in **4.17** was found to occur in CD_3OD for a period of up to 24h at room temperature. The identity of the organic compound, viz. 1,5-bicyclo[3.3.0]octene,

4.18, was confirmed by ^{1}H and ^{13}C-NMR spectroscopy and GC-MS of a C_6D_{12} extract of the reaction mixture and comparison to literature [77]. Based on analogy to the confirmed structure of **4.17**, together with ^{1}H and ^{13}C-NMR and ESI^{+}-MS, the structure of the oxidation product of **4.5**, viz. **4.16** was proposed. Furthermore, ESI^{+}-MS analysis of the products of oxidation of **4.5** performed in CD_3OD, revealed a mass of 479.1, as opposed to a mass of 472.1 when performed in methanol. An M/z 7 units higher is consistent with deuteration in $B(OCD_3)_2$ and Pt^{IV}-OD fragments (**4.16-*d*$_7$**) originating from CD_3OD only.

Scheme 4.7: Oxidation of di(2-pyridyl)-1,5-cyclooctanediylborato-Pt^{II}-dihydrocarbyl complexes

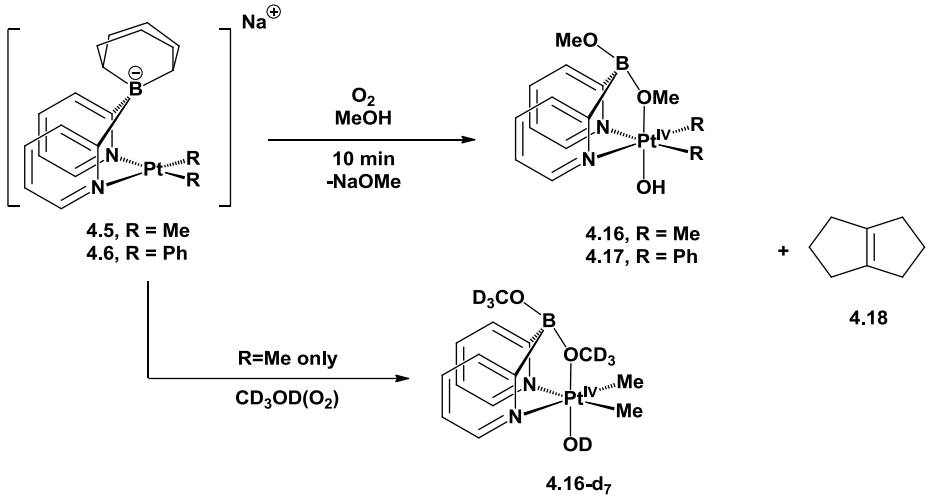

Figure 4.10: X-ray structure of di(2-pyridyl)-dimethoxyborato-Pt^{IV}-diphenyl-hydroxo complex, **4.17**

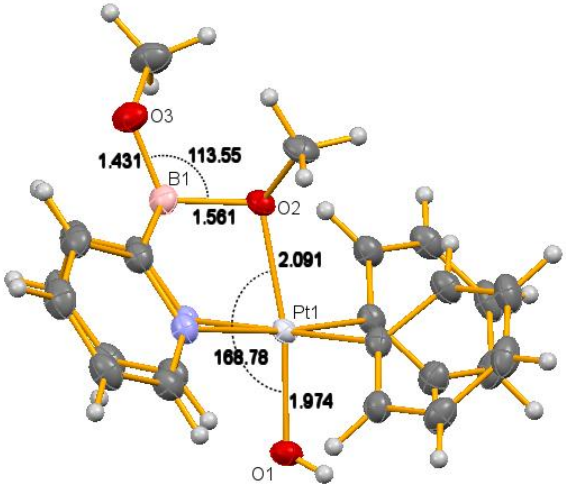

4.4 Mechanistic Investigations

Scheme 4.8: Possible pathways of the oxidatively induced (B)C-H bond cleavage, R = Me, Ph; X = R, OMe

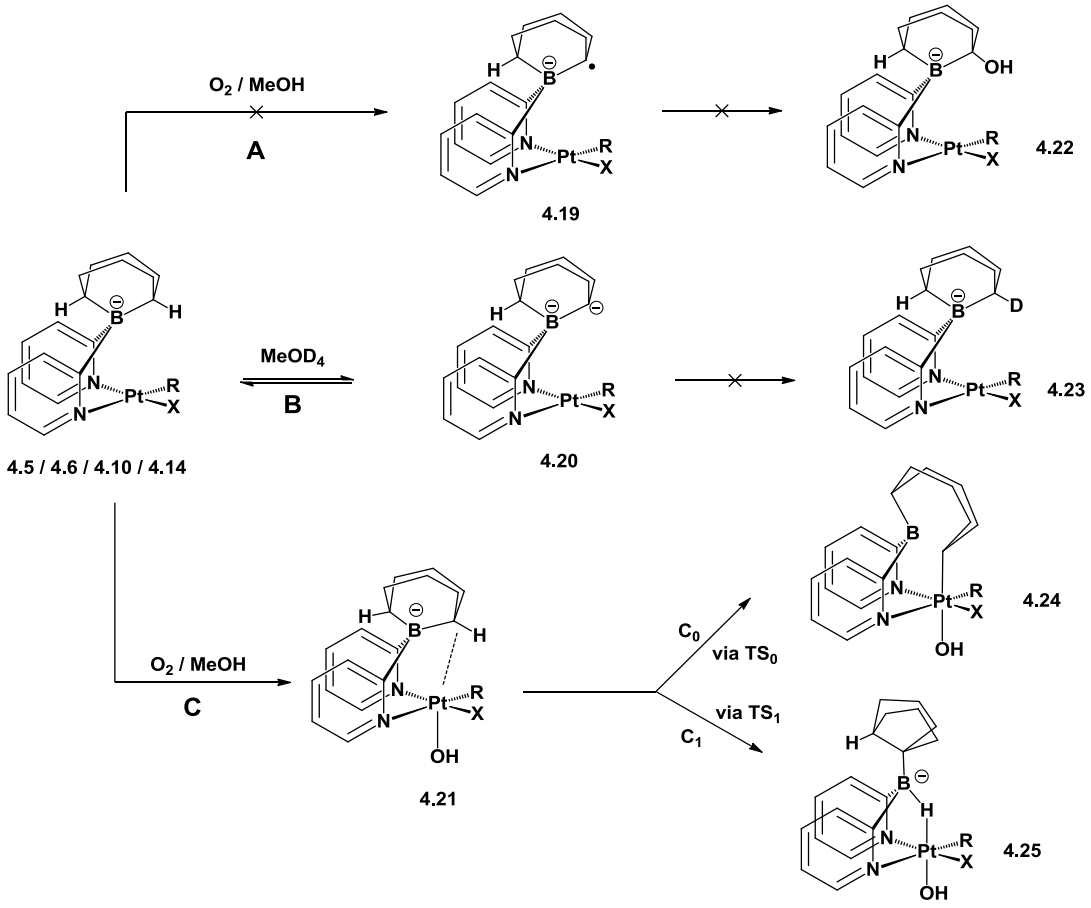

Although the oxidation of monohydrocarbyl-Pt^{II} (**4.10** and **4.14**) and dihydrocarbyl-Pt^{II} (**4.5** and **4.6**) complexes result in very different outcomes, leading to a reorganization of B-bound [3.3.1]bicyclooctyl fragment in the former, and complete loss of bicylooctyl fragment altogether in the latter, we anticipated a sequential mechanism involving a similar initial C-H bond cleavage / C-C bond formation for either case (Scheme 4.8). Three possibilities were considered: (A) formation and subsequent transformation a tertiary radical intermediate **4.19**, (B) formation and subsequent transformations of a carbanionic intermediate **4.20,** as well as (C)

formation of a CH-agostic Pt^{IV}-complex, **4.21**, featuring an axial hydroxo ligand. Pt^{IV}(OH) complexes are typically encountered in the oxidation of Pt^{II}-hydrocarbyl complexes with O_2 in hydroxylic solvents [78].

We performed oxidation of two representative complexes viz. **4.6** and **4.10** in the presence of 2 equivalents of TEMPO under otherwise similar conditions. The oxidation was equally facile as in the absence of TEMPO and no TEMPO-derived [79] new products were observed in the ^{1}H-NMR spectra as well as in the ESI-MS, thus arguing against a radical mechanism (A). Furthermore, no product of C-O bond formation, such as **4.22**, as expected in the oxidation of carbon-centered radical intermediates [80] were observed. To rule out a one-electron oxidation pathway, oxidation of **4.6** was also performed with H_2O_2. Products identical to those observed for the case when O_2 was used as terminal oxidant was observed (cf. sections 4.5 and 4.6).

No changes in the ^{1}H-NMR spectra of **4.10-*d*$_6$** or **4.6-*d*$_{10}$** prepared by dissolving **4.5** or **4.6** (respectively) in CD_3OD was observed even after a period of 24 h. No H/D exchange at either ligand bridgehead BC-H positions, leading to products such as **4.23** was observed in either case, arguing against initial C-H deprotonation, as shown in Scheme 4.8(B). Thus, the most plausible reaction pathway for the C-H cleavage / C-C coupling is that depicted in Scheme 4.8(C). Complex **4.21**, bearing an agostic BC-H-Pt^{IV} bond, can undergo B-C bond cleavage and C-Pt^{IV} bond formation, dubbed 'hydrocarbyl migration' (pathway C_0), to form **4.24** or undergo concerted C-C coupling and '*hydride migration*' to form **4.25,** (pathway C_1). The DFT-calculated [2] Gibbs activation energies of the transition state TS_0 corresponding to the conversion

of **4.21** to **4.24** and TS_1, corresponding to the conversion of **4.21** to **4.25**, were found to be 17.5 kcal/mole and 9.1 kcal/mole, respectively (vide infra). The much higher activation energy of *hydrocarbyl migration* is in accord with the stability of the model trimethyl-Pt^{IV}-complex, **4.9** in methanol at elevated temperatures, as mentioned before. **4.21** (when R=X=Me) differs from **4.9** in that the ligand trans to the agostic CH fragment is a 'OH' ligand in the former, as opposed to a 'Me' in the latter. The presumed high reactivity of **4.21** towards *hydride migration* as opposed to that **4.9** can be explained by a much weaker trans-influence of the axial OH ligand, which allows to bring the H atom in proximity to the Pt^{IV} center, strongly encouraging *hydride migration*. This is observed in the DFT optimized structures [2] of **4.9** and **4.21**, shown in Figure 4.11: the calculated distances between the agostic H and the Pt^{IV} center are 1.94 Å and 1.76 Å, respectively. It is worthy to note at this point that the same H-Pt^{IV} distance observed in the X-ray structure of **4.9** (1.99 Å) is very close to that projected by DFT calculations (1.94 Å).

Figure 4.11: DFT optimized structures of di(2-pyridyl)-1,5-cycloctanediylborate supported $Pt^{IV}Me_3$, **4.9** (left) and $Pt^{IV}(Me_2)(OH)$, **4.21** (right) complexes

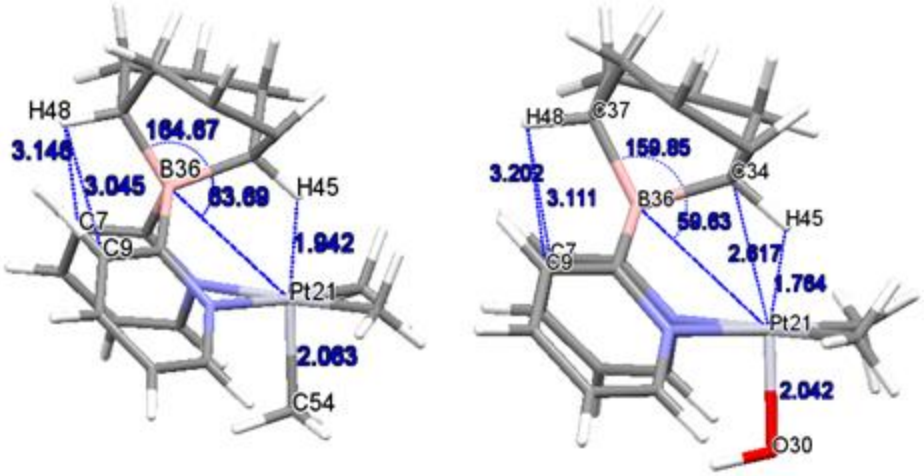

The proposed B-H-Pt bridged intermediate, **4.25** can undergo an attack by a methoxide ion, as shown in Scheme 4.9, to produce a Pt^{IV}-hydride complex, **4.26**, presumed to be an intermediate featuring di(2-pyridyl)-B-methoxo-B-[3.3.0]bicyclooctylborate-supported monohydrocarbyl-Pt^{II} (R=Me, Ph, X=OMe) and dihydrocarbyl-Pt^{II} (R=X=Me, Ph) complexes. The difference in outcomes of the oxidation reactions stems from the possibility of **4.26** to react via pathway (i) when R=X=Me or Ph or via pathway (ii) when R=Me or Ph and X=OMe, as shown in Scheme 4.9.

Scheme 4.9: Comparison of mechanism of oxidatively induced (B)C-H cleavage, 1st H- migration and C-C coupling for both monohydrocarbyl- and dihydrocarbyl-Pt^{II} complexes

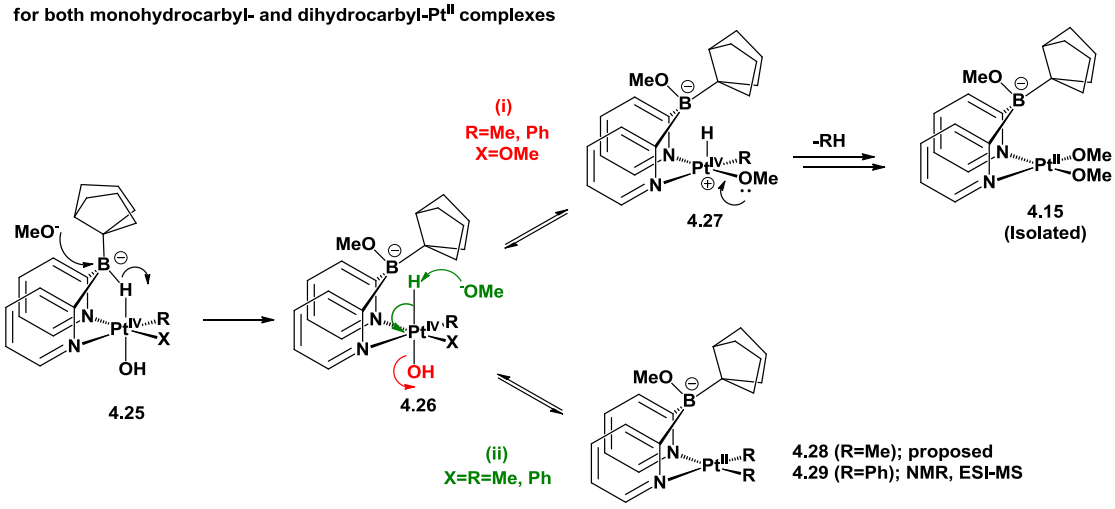

We presume that the complex **4.26** is the point of divergence in the observed reactivities of monohydrocarbyl and dihydrocarbyl Pt^{IV} complexes:

(i) When X=OMe, **4.26** can afford loss of the OH^- fragment from the Pt^{IV} center, thus establishing pathway (i) to form **4.27**. The cationic Pt^{IV} center in **4.27** may additionally be stabilized by the methoxide *O* lone-pairs. **4.27** reacts in a fashion typical of 5-coordinate Pt^{IV}(R)(H) complexes [81] via reductive elimination of methane (when R=CH_3) or benzene (when R=C_6H_5) to form **4.15**. The absence of any

hydrocarbyl groups makes the Pt^{II} center in **4.15** electron poor, thereby rendering it unable to oxidize further even when exposed to O_2 for extended periods of time.

(ii) When R=Me, Ph and X=OMe, loss of the OH^- from the Pt^{IV} center is less likely in the absence of lone-pair aided stabilization discussed in case (i). External attack of a MeO^- onto the Pt^{IV}-H fragment in **4.26**, followed expulsion of OH^- leads to the reduced Pt^{II} complex, **4.28** (R=Me) or **4.29** (R=Ph).

To prove the origin of the H-atom in the R-H coupling products, samples of **4.10-*d*$_6$** and **4.14-*d*$_8$** were prepared in CD_3OD and oxidized in-situ in a closed NMR-tube, to ensure that all volatiles remained in the NMR-tube. Upon oxidation, a septet at 0.16 ppm assigned to CD_3H (Figure 4.12) and a singlet at 7.33 ppm assigned to C_6D_5H were observed, respectively, along with quantitative (by NMR) formation of **4.15-*d*$_9$** in both cases. Since all Pt-bound hydrocarbyl and methoxy groups were deuterated in the starting material, and the oxidation was performed in CD_3OD, the only origin of the H-atom could have been the bridgehead BC-H group of the 1,5-bicyclooctyl (9-BBN) fragment. Furthermore, since no other isotopologues of $CD_nH_{(4-n)}$ (where n>1) were observed in the reaction mixture after oxidation of the non-deuterated **4.10** in CD_3OD, the H-migration was presumed to have occurred in an intramolecular fashion, thus reinforcing our mechanistic statement that **4.25**, **4.26** and **4.27** are all transient intermediates.

Figure 4.12: ^{1}H NMR of **4.15-*d*$_9$** in CD_3OD (22 °C, 400.131 MHz) produced upon oxidation of **4.10-*d*$_6$** showing formation of CD_3H

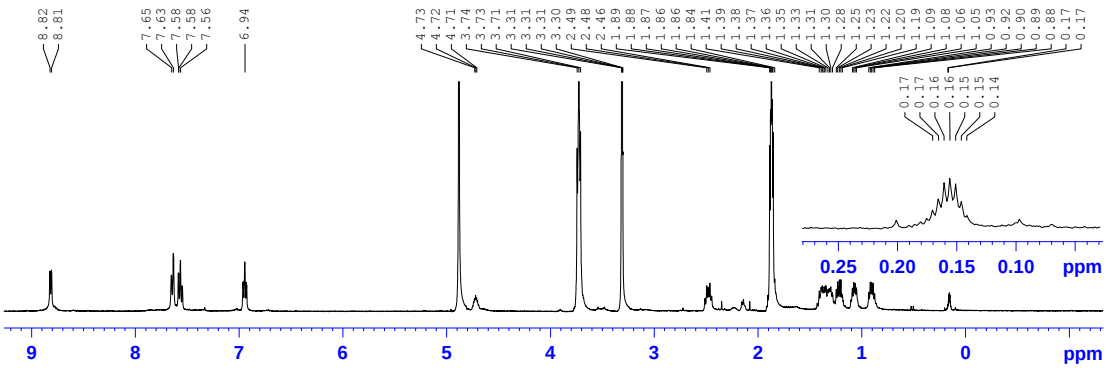

Although the 'inorganic' [3.3.0]bicycloctylborato complex **4.15** does not afford further oxidation, the intermediates **4.28** and **4.29**, bearing two hydrocarbyl groups on the Pt^{II}-center afford further oxidation to generate the final dimethoxyborate-Pt^{IV} complexes, **4.16** (when R=Me) and **4.17** (when R=Ph) along with bicyclooctene (**4.18**) via another O_2-activation / Hydride-abstraction / C-C coupling sequence as shown in Scheme 4.10(a).

Scheme 4.10: Mechanism of the oxidatively induced (BC)C-H cleavage, 2nd H$^-$ migration and C=C coupling

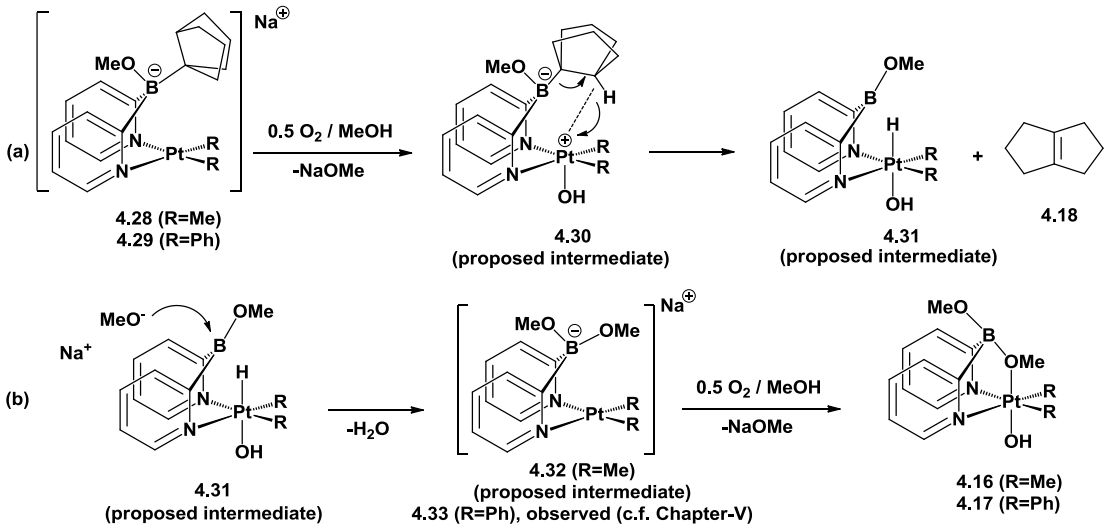

The sequence is similar to that explained earlier in Scheme 4.9. In the case of **4.28** and **4.29**, the aerobic oxidation produces a C-H agostic Pt^{IV}-hydroxo intermediate

4.30, which, similar to **4.21**, undergoes a facile hydride migration from the agostic C-H bond to the Pt^{IV} center, accompanied with the unprecedented intramolecular C=C coupling. This reaction produces the bicycloolefin **4.18** and a neutral dihydrocarbyl-Pt^{II} complex, **4.31**. As shown in Scheme 4.10(b), the borate center can then undergo an attack by the methoxide ion produced in the first step of oxidation (Scheme 4.8(a)), and reductively eliminates H_2O to from an anionic dihydrocarbyl-Pt^{II} complex, **4.32** (R=Me) or **4.33** (R=Ph). Surprisingly, the end product of oxidation, viz. **4.16** (where R=Me) or **4.17** (where R=Ph), respectively) is formed by oxidation of **4.32** or **4.33**, respectively, via yet another O_2 activation step.

To support the step-wise manner of oxidation in the proposed mechanism involving two sequences of O_2-activation / Hydride migration / C-C coupling, a known amount of **4.6** was oxidized in CD_3OD first with 0.5 mol of O_2 in a closed NMR-tube. Upon shaking and recording a ^{1}H-NMR, no starting material was found to have remained in solution. Based on THF as internal standard, a new compound, with an aliphatic signals matching in pattern to that of **4.15** was observed in 94% yield (Figure 4.13), along with the formation of 6.5% of bicyclooctene, **4.18**, and 6.5% of **4.17-*d*$_7$**. The product was confirmed to be **4.29-*d*$_3$** by observing a mass of 659.2 in the ESI^--MS spectra of an aliquot of the NMR reaction mixture. Upon further exposure to O_2, quantitative NMR-yields of **4.16-d$_7$** and **4.18** were obtained, thus proving the intermediacy of **4.29** in the oxidation of **4.6** to **4.17**. The oxidation of **4.5** under limited supply of O_2 was not performed as the oxidation is expected to generate a dimethyl-Pt^{II} complex, **4.28**, which would then lead to protonolysis products, both of which are expected to oxidize to different products.

Figure 4.13: ^{1}H NMR monitoring of stepwise oxidation of **4.6** (c.f. NMR 4.4) in CD_3OD (22 °C, 400.131 MHz) under controlled amounts of O_2, leading to **4.29-*d*$_3$** and finally **4.17-*d*$_7$** (and **4.18**)
After admitting 0.5 eqv. O_2, showing formation of **4.29-*d*$_3$** and trace amounts of **4.18** and **4.17-*d*$_7$**

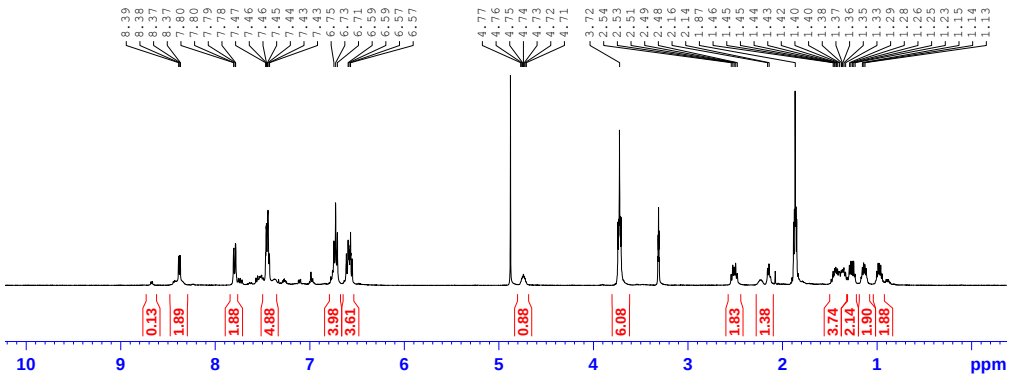

Completion of oxidation showing complete conversion to **4.18** and **4.17-*d*$_7$**

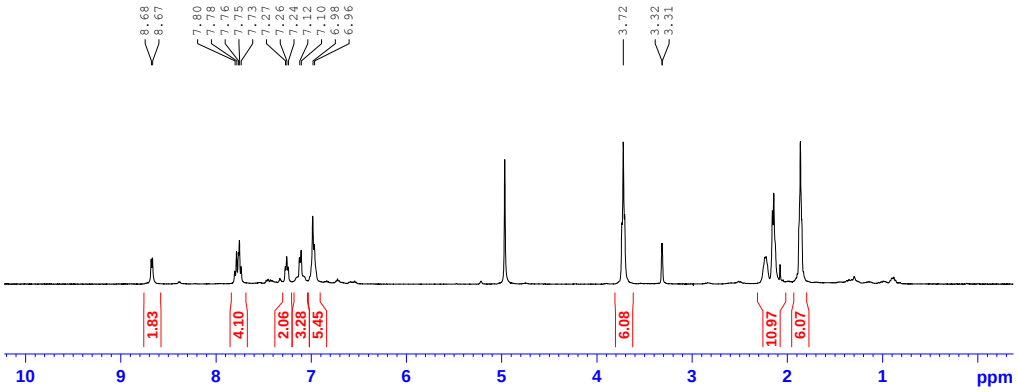

4.5 Forced oxidation of O_2-inert Pt^{II}-complexes with H_2O_2

Although the 'inorganic' Pt^{II}-complex **4.15** was reluctant to oxidize under O_2, it reacted cleanly with 2 equivalents of H_2O_2 in methanol, leading to a similar outcome: formation of the dimethoxy-Pt^{IV} complex **4.34**, in 89% yield, as shown in Scheme 4.11(a). Oxidation of **4.15-*d*$_9$** in CD_3OD similarly with THF as internal standard led to the formation of bicyclooctene, **4.18**, and **4.34-*d*$_{13}$** in quantitative NMR-yields. The identity of **4.34-*d*$_{13}$** was additionally proven by ESI^+-MS. A crude sample of **4.11** in

methanol also went underwent oxidation to form **4.34**, identified by NMR. Yields were not determined owing to the unavailability of pure **4.11**. Reasonably clean ^{1}H-NMR and ^{13}C-NMR spectra were obtained (c.f. appendix pp 148-149). Crystals suitable for X-ray structure determination were grown by vapor diffusion of pentanes into a dichloromethane solution. **4.34** features a dimethoxy- borate center, with the endo-methoxy group bridging B and the Pt^{IV}-center, as shown in Figure 4.14. The two reactions, represented in Scheme 4.11, leading to the same product, **4.34**, is consistent with the previously discussed mechanism involving sequential BC-H cleavage / Hydride migration and C-C bond formation, since **4.15** can be envisioned as an intermediate in the oxidation of **4.11** to **4.34**.

Scheme 4.11: Complete oxidation of 'inorganic' Pt^{II} complexes with H_2O_2

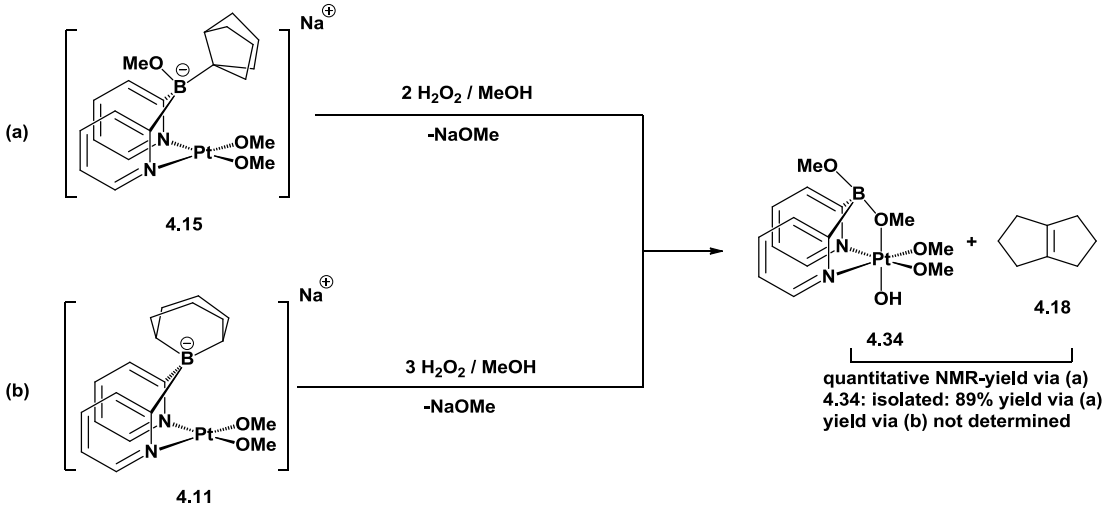

Figure 4.14: X-ray structure of di(2-pyridyl)-dimethoxyborato-Pt^{IV}-dimethoxo-hydroxo complex, **4.34**

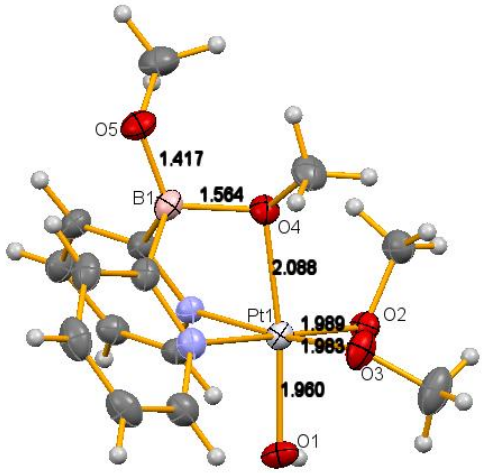

4.6 Oxidation of $LPt^{II}Ph_2$, 4.6 complex in CD_3OD with H_2O_2

To compare the reactivity of di(2-pyridyl)-1,5-cyclooctanediylborato-Pt^{II} complexes with O_2 and H_2O_2, we decided to compare the outcome of the oxidation of the supported $LPt^{II}Ph_2$ complex, **4.6** with H_2O_2 to that with O_2. Owing to the unappreciable solubility of the expected product, viz. **4.17** in CD_3OD, a 1:1 v/v mixture of CD_3OD: THF-d_8 was used. Upon addition of 4 equivalents of H_2O_2, according to NMR, formation of **4.17-d_7** and **4.18** in 90% and 84 % yields respectively, was observed.

Figure 4.15: ^1H NMR monitoring of oxidation of **4.6** in CD_3OD: THF-d_8 with H_2O_2 (22 °C, 400.131 MHz)
(Before oxidation, note integral intensity of internal standard)

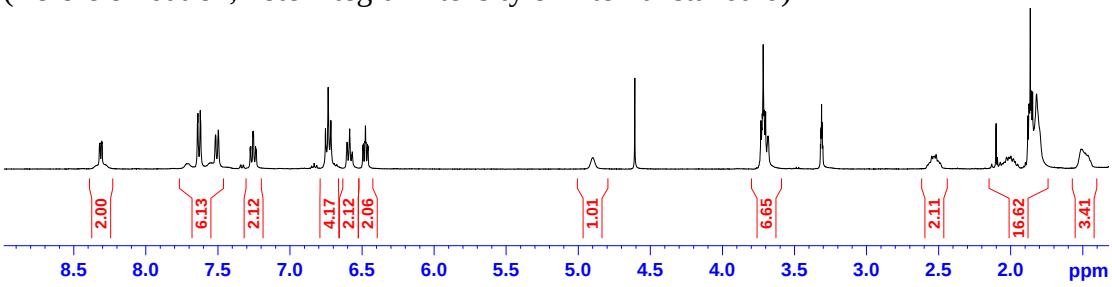

(after oxidation, showing quantitative formation of **4.17-*d*$_7$** and **4.18**

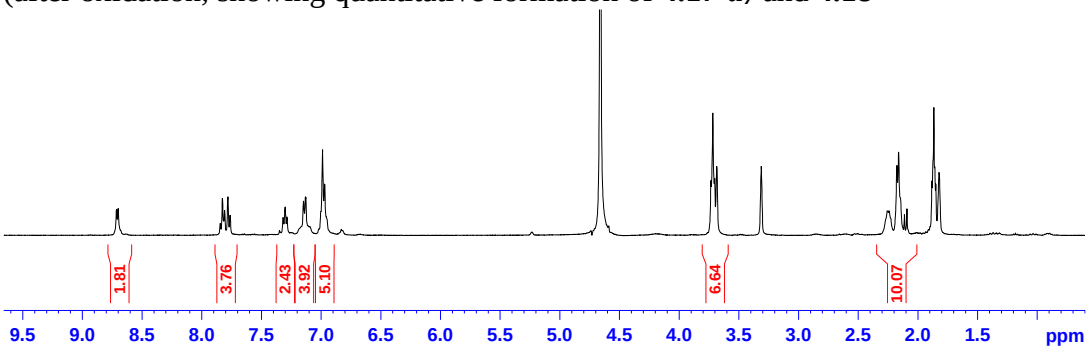

4.7 Conclusion

To the best of our knowledge, di(2-pyridyl)-1,5-cyclooctanediylborate supported Pt^{II} complexes represent the first system to demonstrate oxidative C-C and C=C bond formation at the boron center with O_2 as the terminal oxidant. Derived dimethyl-Pt^{II}-complexes behave similar to (dpdmb)Pt^{II} complexes with respect to C-H activation and Pt^{II}-Me protonolysis. Although we were unable to generate the desired monohydrocarbyl $LPt^{IV}(R)(OH)$ complexes due to unusual ligand reactivity in this study, we investigated the mechanism involved for such transformations and have characterized possible intermediates. In addition to the restrictions imposed by having methyl or phenyl groups on the B-center, as demonstrated by Khaskin and Vedernikov [40], we have unveiled yet another restriction on the choice of the alkyl fragment in a sought-after di(2-pyridyl)-B-alkyl-B-alkoxy borate: the alkyl group cannot have *β*-H available for agostic bonding. The '*enhanced*' C-H--Pt^{IV} agostic interaction, influenced by the choice of axial trans-ligands on the Pt^{IV} center, furthers our understanding of the reactivity of C-H bonds near a proximal Pt^{IV} center. Finally, and gratifyingly, complete oxidation of related dihydrocarbyl-Pt^{II} complexes affords a

route to di(2-pyridyl)dimethoxo borato-Pt^{IV} complexes, which, as forthcoming in the following chapter (V), proves to be a system demonstrating an '*inert*' anionic borate center leading to facile redox reactions of derived Pt complexes.

4.8 Experimental Section

4.8.1 Synthesis of hydrogen-di(2-pyridyl)-1,5-cyclooctanediylborate(L), LH·HCl, 4.2

2-pyridylmagnesium chloride was synthesized similar to Cui et al [72]. An air-free 250 mL round-bottom Schlenk flask was equipped with a stir-bar. To it 50 mL of dry THF and 4.3 mL of 2-bromopyridine (0.045 mole) were added. To this solution 22.5 mL of 2M isopropylmagnesium chloride (0.045 mole) was added dropwise with stirring, at room temperature. Immediately upon addition, the solution turned yellow. Stirring was continued for a period of 12h, over which, the solution gradually changed color from yellow to orange to wine-red. 18 mL of a 1M solution of 9-methoxy-9-borabicyclo[3.3.1]nonane in hexanes (0.018 mole) was added dropwise to it. The color immediately changed to light brown, followed by formation of copious amounts of precipitate within 10 minutes. The mixture was left to stir for 12h, followed by a 1-hour temperature increase to 80 °C. During this period all precipitate dissolved, forming a greenish-brown solution. The mixture was stirred for a period of 24h at 80 °C. The solution was then cooled down to room temperature and carefully transferred to a beaker containing 450 mL of ice water. Immediately upon contact with water, a tan precipitate developed with a yellow-brown supernatant solution. After 30 minutes of stirring the mixture was filtered through a medium fritted funnel. An excess of water is required to minimize loss of ligand dissolved in THF. The residue produced upon drying is a cream colored amorphous solid. The residue was washed with 100 mL of water followed by 100 mL of hexanes to aid in removal of organic byproducts. The filtrates were analyzed by ESI-MS and confirmed to contain a mixture of 2-bromopyridine, pyridine, and *B*-(2-pyridyl)-9-borabicyclo[3.3.1]nonane. The off-white residue was air-dried overnight to yield 11.2 g of an off-white solid. The solid is poorly soluble in THF, acetone and acetonitrile and but soluble in all of the above in the in the presence of 1 equivalent of acid. 3.0 g of the residue was suspended in 200 mL of dichloromethane and 25 mL of 10 M aqueous hydrochloric acid was added to it. The biphasic system was left to stir for a period of 5 hours. A yellow organic layer and a yellow aqueous layer formed. The organic layer was collected and the aqueous layer was extracted twice with 50 mL of dichloromethane. The organic layers were combined, dried with anhydrous sodium sulfate, and stripped to dryness to yield 3.0 g of the target compound as a hydrogen chloride salt [**4.2**]H·HCl in virtually quantitative yield. Crystals suitable for XRD structure determination were obtained by dissolving 400 mg of [**4.2**]H·HCl in dichloromethane and vapor diffusion of pentane at 40 °C.

^{1}H NMR (22 °C, 500 MHz, DMSO-D_6, ppm) δ: 1.21-1.24 (br, m, 2H, *J*=6.4 Hz), 1.47-1.7 (br, 2m, 8H), 1.70-1.85 (m, 2H), 1.90-2.0 (br, 2H, B-CH), 3.5 (residual H_2O), 5.75 (residual CH_2Cl_2), 7.57 (t, 2H, *J*=6.8 Hz, py-5-CH), 8.01 (d, 2H, *J*=8.0 Hz, py-3-CH), 8.19 (t, 2H, *J*=7.4 Hz, py-4-CH), 8.53 (t, 2H, *J*=6.2 Hz, py-6-CH), 14.33 (br, s, 2H, NH)
^{13}C NMR (22 °C, 500 MHz, DMSO-D_6, ppm) δ: 19.9 (br, B-C), 24.1, 31.0, 54.9(residual CH_2Cl_2), 122.36, 131.0, 140.5, 142.6, 180.2 (br, BC)
ESI^+ MS of a solution of **1** in MeOH acidified with HBF_4: 279.19, Calculated 279.20.

4.8.2 Synthesis of L, sodium salt, Na[4.2]

3.0 g of **4.2·HCl** was dissolved in 20 mL of THF in a large vial inside a glove box. To this vial 1.0 g sodium hydride was carefully added with vigorous stirring. Vigorous evolution of hydrogen gas was observed. The color of the solution became light brown. Stirring was continued for another 8h. After this period, the solution was filtered through Celite, the residues washed with an additional 5 mL of THF in two portions. The combined filtrate was stripped to dryness and washed with hexanes to obtain 1.08 g of Na[**4.2**] in quantitative yield. The solvent of crystallization could not be removed even upon exposure of the product to high-vacuum for extended periods of time. Na[**4.2**] is extremely moisture sensitive, but stable in the presence of oxygen.
^{1}H-NMR (22 °C, 500 MHz, Acetone-D_6, ppm) δ: 1.27 (br, q, 2H, *J*=6.0 Hz), 1.49 (br, 2H), 1.55-1.69 (br, m, 4H), 1.84-2.0 (m, 6H), 3.63 (THF), 6.60 (td, 2H, *J*=6.0, 1.4 Hz, py-5-CH), 7.21 (td, 2H, *J*=7.4, 1.9 Hz, py-4-CH), 7.44 (d, 2H, *J*=8.0 Hz, py-3-CH), 8.26 (d, 2H, *J*=4.7 Hz, py-6-CH)
^{13}C-NMR (22 °C, 500 MHz, DMSO-D_6, ppm) δ: 24.2(br, q, B-CH), 25.1 (THF), 26.0 (CH_2), 32.4 (CH_2), 116.0, 126.7, 131.6, 147.8, 192.1-193.1 (q, BC).
ESI^- MS of a solution of Na[**4.2**] in MeOH basified with $NaOCH_3$: 277.18, Calculated 277.19.
Elemental Analysis (C, H, N): Calculated ($C_{26}H_{38}BN_2NaO_2$): 70.27, 8.62, 6.30, Found: 69.82, 7.67, 7.63

4.8.3 Attempted reaction of Na[4.2] with O_2

A 15mg sample of Na**[4.2]** dissolved in a (0.4 mL CD_3OD : 0.2 mL THF-D_8) solution showed no change after a 4-day exposure to O_2.

4.8.4 Synthesis of $LPt^{II}Me_2$ complex, 4.5

1.0 g (2.25 mmol) of Na[**4.2**] was dissolved in 10 mL THF in a reaction vial equipped with a stir bar. To the solution was added 0.646 g (1.125 mmol) of $Pt_2Me_4(\mu\text{-}SMe_2)_2$ with rapid stirring. The solution became light yellow in ten minutes. Stirring was continued for 5h with intermittent exposure to vacuum to facilitate removal of Me_2S. After this period, the solution was stripped to dryness to obtain a tan powder. The sample was recrystallized from a THF solution by precipitation with hexanes to yield 1.520 g of a tan colored powder, in 91% yield. **4.5** is unstable and decomposes at room temperature even if kept under Ar over long periods of time (10 days), and therefore must be stored in cold conditions. No decomposition was observed by NMR after 2 months when kept at -20 °C in a vial sealed under Argon.

^{1}H NMR (22 °C, 500 MHz, CD_3CN, ppm): 0.53 (s+Pt-satellites, J_{Pt-H}=82.4 Hz, 6H, $PtMe_2$), 1.29-1.46 (complex multiplet, br, 6H, BCH (1H), CH_2 (5H)), 1.68-1.90 (m, 10H, THF(6H), CH_2 (4H)), 2.41 (m+m, 2H, CH_2), 3.64 (m, 6H, THF), 4.43 (br, 1H, BCH), 6.65 (vt, *J*=5.5, 1.7 Hz, 2H, py-5-CH), 7.34 (td, *J*=7.5, 1.7 Hz, 2H, py-4-CH), 7.45 (d, *J*=7.7 Hz, 2H, py-3-CH), 8.65 (d+Pt-satellites, J_{Pt-H}=26.4, *J*=5.9 Hz, 2H, py-6-CH).
^{13}C NMR (22 °C, 500 MHz, CD_3CN, ppm): -19.95 (s+Pt-satellites, J_{Pt-C}=830.8 Hz, $PtMe_2$) 21.3 (br), 23.8, 26.1, 30.6, 120.7, 127.2, 138.4, 143.5 ($^{2}J_{Pt-C}$=38Hz).
ESI$^-$ MS of a THF solution of **4.5**: 502.20, Calculated 502.20.
Elemental Analysis (C, H, N): Calculated ($C_{20}H_{28}BN_2NaPt\cdot1.5THF$): 49.30, 6.36, 4.42 Found: 49.32, 6.41, 3.65

4.8.5 Synthesis of $LPt^{II}Ph_2$ complex, 4.6

1.0 g (2.25 mmol) of Na[**4.2**] was dissolved in 10 mL THF in a reaction vial equipped with a stir bar. To the solution was added 1.06 g (2.25 mmol) of $PtPh_2(SMe_2)_2$ with rapid stirring. The solution became yellow in ten minutes. Stirring was continued for 5h with intermittent exposure to vacuum to facilitate removal of Me_2S. After this period, the solution was stripped to dryness to obtain a light-tan colored powder. The sample was recrystallized from THF-hexanes mixture to yield 1.68 g of a cream colored powder, analytically pure **4.6**, in 94% yield. Complex **4.6** is stable both in solution in THF-d_8, CD_3CN, and acetone-d_6 at room temperature if kept under Ar over long periods of time (2-3 days), and as a solid when stored under inert conditions.
^{1}H NMR (22 °C, 500 MHz, CD_3CN, ppm) δ: 144-1.54 (br, multiplet, 3H, B(CH)+B(C*H*)(CH_2), 1.70-1.88 (m, 11.7H, THF=5.6H, CH_2=6H), 1.96-2.06 (m, 2H, B(CH)(CH_2)), 2.43-2.55 (m+m, 2H, B(CH)(CH_2)), 3.58 (THF, 5.6H), 5.15 (br, 1H, B(CH)), 6.52 (vt, *J*=5.5, 1.6 Hz, 2H, py-5-CH), 6.62 (tt, *J*=7.2, 1.5 Hz, 2H, Ph-p-CH), 6.78 (unresolved t, *J*=7.5 Hz, 4H, Ph-m-CH), 7.31 (td, *J*=7.6, 1.8 Hz, 2H, py-4-CH), 7.53 (d, *J*=7.9 Hz, 2H, py-3-CH), 7.57 (d+Pt-satellites, J_{Pt-H}=67, *J*=7.9 Hz, 4H, Ph-o-CH), 8.29 (d+Pt-satellites, J_{Pt-H}=27, *J*=5.9 Hz, 2H, py-6-CH).
^{13}C NMR (22 °C, 500 MHz, CD_3CN, ppm) δ: 23.0-24.75 (br, m, B-*C*H), 26.36 (s, THF), 26.42 (s, BCH(*C*H_2)), 33.72 (s, BCH(*C*H_2)), 34.82 (s, BCH(*C*H_2)), 68.42 (s, THF), 119.09 (s+Pt-satellites, J_{Pt-C}=28.4 Hz), 128.45 (s+unresolved-Pt-satellites), 126.74 (s+Pt-satellites, J_{Pt-C}=76.7 Hz), 130.17 (s+unresolved-Pt-satellites), 133.38 (s), 140.71 (s+Pt-satellites, J_{Pt-C}=24.7 Hz), 150.33 (s), 151.68 (s+Pt-satellites, J_{Pt-C}=34.9 Hz), 189.6-191.5 (br, m, py-2-C-B).
ESI$^-$ of a THF solution of **4.6**: 626.22, Calculated 626.23.
Elemental Analysis (C, H, N): Calculated ($C_{30}H_{32}BN_2NaPt\cdot1.4THF$): 56.98, 5.80, 3.73 Found: 57.38, 6.50, 3.37

4.8.6 Synthesis of LPt^{II}(cyclohexene)(H) complex, 4.7

50 mg of **4.5** (95.2 µmol) was dispersed in 5 mL of dry cyclohexane in a reaction vial and to it was added 3.5 µL (2 equivalents) H_2O with rapid stirring. Immediate vigorous evolution of methane was seen. After 20 minutes, copious amounts of precipitate and a yellow supernatant was visible. The contents of the vial were filtered through a cotton plug, washed with 2 mL of cyclohexane and the filtrate was stripped

to dryness to yield 27 mg of a dark brown powder, in 50% yield. **4.7** could not be obtained in analytically pure form, presumably due to its thermal instability. Significant broadening of signals could be seen in the ^{1}H-NMR spectrum.
^{1}H NMR (22 °C, 500 MHz, $CDCl_3$, ppm) δ: -21.96 (s+Pt-satellites, 1H, J_{Pt-H}=1251.8 Hz, PtH), 1.1-2.1 (m, 15H, CH_2(9-BBN)+CH_2(cyclohexene)), 2.35 (br, 4H, C=CC*H*$_2$), 2.6-2.9 (br, m+m, 2H, CH_2(9-BBN)), 3.67 (br, 1H, BC*H*), 4.60 (br+unresolved Pt-satellites, 1H, CH=C*H*), 5.14 (s+Pt-satellites, J_{Pt-H}=~91 Hz, 1H, C*H*=CH), 6.71 (br, 1H), 6.83 (br, 1H), 7.41 (vt, *J*=7.4 Hz, 2H), 7.68 (br, 2H), 7.90 (br, 1H), 8.71 (br+Pt-satellites, *J*=~56 Hz, 1H, Py-6-CH, trans to Pt(CH=CH)).
^{13}C NMR (22 °C, 500 MHz, $CDCl_3$, ppm) δ: 21.7 (CH_2), 22.2 (br, BCH), 22.8 (CH_2), 25.3 (CH_2), 25.4 (CH_2), 27.1 (CH_2), 28.2 (CH_2), 31.1 (CH_2), 32.3 (CH_2), 32.8 (CH_2), 37.7 (br, BCH), 73.6 (J_{Pt-C}=165 Hz, (*C*H=CH)), 80.3 (J_{Pt-C}=211 Hz, Pt(CH=*C*H)), 119.1, 119.4, 127.4, 130.9, 131.3, 134.5, 135.1, 145.3, 154.2, 188 (br, py-2C), 190 (br, py-2C).
Elemental Analysis (C, H, N): Calculated ($C_{24}H_{33}BN_2Pt$): 51.90, 5.99, 5.04 Found: 52.99, 6.35, 4.92

4.8.7 Synthesis of $LPt^{II}(Me)(SMe_2)$ complex, 4.8

To a 200 mg sample of **4.5** (381 µmol) in a reaction vial equipped with a stir-bar, was added 3 mL of dimethylsulfide. The entirety of the complex dissolved, after which was added 13.5 µL of H_2O (2 eqv.) with rapid stirring. Immediate effervescence was observed followed by formation of precipitate. The mixture was let to stir for a period of 20 minutes following which a brilliant-yellow supernatant was obtained. The precipitate was filtered off by passing the mixture through an anhyd. Na_2SO_4 packed pipette, and washed with an additional 2 mL of dimethylsulfide. The solution obtained was stripped to dryness to yield a light yellow powder. The powder was washed with 1 mL of methanol to obtain analytically pure **4.8**, 195 mg as a cream colored powder, in 93% yield. **4.8** is insoluble in ether or methanol, poorly soluble in toluene but highly soluble in dichloromethane, acetone, and THF. Crystals suitable for X-ray diffraction were grown by slow evaporation of a 3mL dichloromethane solution containing 100 mg of **4.8**.
^{1}H-NMR (22 °C, 500 MHz, CD_2Cl_2, ppm) δ: 0.69 (s+d, 3H, $^{2}J_{Pt-H}$=75.0 Hz, PtMe), 1.33-2.04 (6m, 13H, 6CH_2+1B-CH), 2.3-2.5 (br, 2m, 6H, SMe_2), 4.02 (br, 1H, B-CH), 6.78 (td, 1H, *J*=6.6, 1.7 Hz, py-5-CH), 6.83 (td, 1H, *J*=6.4, 1.5 Hz, py'-5-CH), 7.41 (2t, 2H, *J*=7.6, 7.5 Hz, py-4-CH, py'-4-CH), 7.62 (unresolved-t, 2H, py-3-CH, py'-3-CH), 8.35 (d+Pt-satellites, 1H, J_{HH}=5.5, J_{Pt-H}=55.8 Hz, py-6-CH, trans to SMe_2), 8.52 (d+Pt-satellites, 1H, J_{HH}=5.7, J_{Pt-H}=19 Hz, py'-6-CH, trans to PtMe)
^{13}C-NMR (22 °C, 500 MHz, CD_2Cl_2, ppm) δ: -16.92 (s+d, $^{1}J_{Pt-C}$=721.7 Hz, PtMe), 20.5 (br, s, SMe), 22.0-23.6 (q, J_{C-B}=53 Hz, B-CH), 25.0 (br, s, SMe), 25.68 (s, CH_2), 25.7 (s, CH_2), 32.79 (s, CH_2), 32.8 (s, CH_2), 33.0 (s, CH_2), 33.4-34 (q, unresolved J_{C-B}, B-CH), 34.5 (s, CH_2), 119.7 (s, py-5-C), 119.93 (s+d, J_{Pt-C}=56 Hz), 131.0 (s+d, J_{Pt-C}=42 Hz), 131.2 (s+d, unresolved J_{Pt-C}), 134.3, 134.4, 149.7, 150.8 (s+d, J_{Pt-C}=39.7 Hz), 188.3-190.7 (q+q, br)
Elemental Analysis (C, H, N): Calculated ($C_{21}H_{31}BN_2PtS$): 45.91, 5.69, 5.10 Found: 45.74, 5.35, 4.89

4.8.8 Synthesis of $LPt^{IV}Me_3$, 4.9

100 mg of **4.5** was dissolved in 7 mL of ether in a reaction vial and 25 µL of methyl iodide (2 eqv.) was added to it. After 5 minutes of stirring, fine white precipitate could be seen. After a period of 20 minutes of stirring, the contents of the vial were filtered through a PTFE-Acrodisc filter and washed with an additional 2mL of ether. The filtrate was stripped to dryness to obtain 102 mg of a pale yellow flaky solid, **4.9**, in quantitative yield. **4.9** is stable in CD_3OD and under air at room temperatures. Prolonged heating in CD_3OD showed no signs of decomposition at temperatures up to 100 °C. X-ray quality crystals were obtained vapor diffusion of pentanes into a solution of 100 mg of **4.9** in 2 mL of dichloromethane at 40 °C.

^{1}H NMR (22 °C, 500 MHz, CD_2Cl_2, ppm) δ: -3.36 (br, s+d, 1H, J_{Pt-H}=207.7 Hz, B-CH, agostic), 0.96 (s+d, 6H, $^2J_{Pt-C}$=65.0 Hz, $PtMe_2$, equatorial), 1.4 (s+d, 3H, $^2J_{Pt-C}$=81.2 Hz, PtMe, axial), 1.39-1.52 (m, 4H, CH_2), 1.62 (br, ^{1}H, B-CH), 1.73-1.87 (br, m, 2H, CH_2), 1.89-1.97 (m, 2H, CH_2), 2.22-2.30 (m, 2H, CH_2), 7.0 (td, 2H, *J*=6.4, 1.8 Hz, py-5-CH), 7.55 (td, 2H, *J*=7.6, 1.7 Hz, py-4-CH), 7.59 (d, 2H, *J*=7.3 Hz, py-3-CH), 8.19 (d+Pt-satellites, 2H, J_{Pt-H}=18.1 Hz, *J*=5.9 Hz, py-6-CH)

^{13}C NMR (22 °C, 500 MHz, CD_2Cl_2, ppm) δ: -10.4 (s+d, $^1J_{Pt-C}$=631.0 Hz, PtMe2, equatorial), 2.0 (s+d, $^1J_{Pt-C}$=783.2 Hz, PtMe, axial), 22.0 (q, J_{C-B}=43.7 Hz, B-CH), 25.7 (s, CH_2), 31.5 (s, CH_2), 33.0 (s, CH_2, J_{Pt-C}=7.5 Hz), 56.0 (q, J_{C-B}=39 Hz, B-CH), 120.86 (s+d, J_{Pt-C}=19.5 Hz), 130.54 (br), 135.53, 145.57 (s+d, J_{Pt-C}=19.6 Hz), 189.6 (q, J_{C-B}=49 Hz, py-2-C)

Elemental Analysis (C, H, N): Calculated: 48.75, 6.04, 5.41, Found: 49.14, 5.92, 5.25

4.8.9 Synthesis of LPt^{II}(Me)(OMe), 4.10

50 mg of **4.5** was taken in a stir-bar equipped reaction vial and 3 mL of methanol was added to it. Vigorous evolution of gas was seen. The entirety of the solid dissolved after 5 minutes, and stirring was continued for a period of 20 minutes. The contents of the vial were stripped to dryness, and a brown powder was obtained. The powder was washed with 1:1 v/v ether hexane mixture and exposed to high vacuum to obtain a yellow colored powder, **4.10**. The compound is stable in CD_3OD for at least 12 hours at RT and over long periods of time in CD_3CN in the absence of air or moisture. **4.10** could not be isolated in analytically pure form even upon repeated crystallization from methanol or THF and was characterized in solution by NMR and ESI-MS. The ^{1}H and ^{13}C NMR spectra show a satisfactory purity of the sample used in our experiments.

^{1}H NMR (22 °C, 500 MHz, THF-D_8, ppm) δ: 0.76 (s+Pt-satellites, 3H, J_{Pt-H}=70.9 Hz, PtMe), 1.28-2.00 (m, 11H, BCH(1H)+CH_2(10H)), 2.36-2.56 (m+m, 2H, CH_2), 3.33 (s, 1H, residual MeOH), 3.50 (s+d, 3H, J_{Pt-H}=38 Hz, $PtOCH_3$), 4.67 (br, 1H, B-CH), 6.43 (vt, 1H, *J*=6 Hz, py-5-CH), 6.71 (vt, 1H, *J*=5.9 Hz, py'-5-CH), 7.23 (vt, 1H, *J*=7.2 Hz, py-4-CH), 7.30 (vt, 1H, *J*=6.8 Hz, py'-4-CH), 7.39 (d, 1H, *J*=7.5 Hz, py-3-CH), 7.51 (d, 1H, *J*=7.8 Hz, py'-3-CH), 8.47 (d+Pt-satellites, 1H, J_{Pt-H}=50.9, *J*=7.8 Hz, py-6-CH), 8.83 (d+unresolved Pt-satellites, 1H, *J*=5.1 Hz, py'-6-CH).

^{13}C NMR (22 °C, 500 MHz, THF-D_8, ppm) δ: -19.2 (s+d, J_{Pt-C}=848.3 Hz, $PtCH_3$), 23.0-24.6 (br, BCH), 26.4 (CH_2), 26.43 (CH_2), 31.0-32.4 (br, BCH), 33.5 (CH_2), 33.6 (CH_2), 33.9 (CH_2), 34.4 (CH_2), 60.23 (s+unresolved Pt-satellites, $PtOCH_3$), 118.3, 119.3 (s+unresolved Pt-satellites), 130.1, 130.3, 131.7, 132.8, 148.5, 152.5

(s+unresolved Pt-satellites), 187.8-189.6 (br, BC), 190.2-192.1 (br, BC). Peak Assignments were made by correlation with DEPT-45, 90 and 135 NMR spectra.
ESI^- MS of a methanolic solution basified with sodium methoxide: 518.18, Calculated 518.19.

4.8.10 Synthesis of $LPt^{II}(OMe)_2$, 4.11

40 mg of **4.5** was dissolved in 5 mL of methanol in a reaction vial equipped with a stir-bar and left stirring inside the glove box for 24h. After this period, some precipitate and darkening of the solution could be seen. The contents were filtered through a cotton plug, and stripped to dryness. The residue was washed with 2 ml of 1:1 v/v ether hexane mixture to yield a brown colored powder, 33.5 mg of **4.11** (79% yield). Complex **4.11** is only moderately soluble in methanol, hence it is necessary to have a huge amount of solvent during the synthesis of **4.11**; otherwise yields are very poor as most of **4.11** is lost in the filtration step. No exchange of Pt-bound methoxy groups was observed when dissolved in CD_3OD at RT even after 24h. Repeated recrystallization attempts progressively made the sample dirtier and **4.11** was characterized by ^{1}H-NMR spectroscopy and ESI-MS. We presume this is due to dimerization/oligomerization expected for anionic Pt^{II} complexes bearing labile anionic methoxy ligands on the Pt^{II} center.
^{1}H-NMR (22 °C, 400 MHz, CD_3CN, ppm) δ: 1.33-1.49 (br, m, 4H, CH), 1.52-1.63 (br, m, 3H, CH), 1.65-1.83 (br, m, 4H, CH), 2.36-2.51 (br, sept, 2H, CH), 3.41 (s+unresolved Pt-satellites, 6H, $Pt(OCH_3)_2$), 5.0 (br, 1H, B-CH), 6.66 (vt, *J*=6.6 Hz, 2H, py-5-CH), 7.36 (vt, *J*=8.1 Hz, 2H, py-4-CH), 7.46 (d, *J*=7.7 Hz, 2H, py-3-CH), 8.88 (d+unresolved Pt-satellites, 2H, py-6-CH).
ESI^- of a methanolic solution basified with $NaOCH_3$: 534.19, Calculated 534.20
ESI^+ of a methanolic solution with $NaBAr^F$ additive: 536.22 (**4.11**·H_2^+), Calculated 536.20

4.8.11 Synthesis of $LPt^{II}(Ph)(OMe)$, 4.14

200 mg of **4.6** (266 µmol) was dissolved in 3 mL of methanol in a reaction vial equipped with a stir-bar. In another vial, 34.0 µL (1 eqv.) of trimethylchlorosilane was dissolved in 1 mL of methanol and quantitatively transferred to the first vial containing **4.6** with rapid stirring. An additional 1 mL of methanol was used to complete the transfer. The solution was let to stir for a period of 5 minutes and rapidly stripped to dryness. During the process of evacuation, fine white precipitate of NaCl could be seen. Evacuation was completed in approx. 1h to obtain a tan colored powder. At this point, the entire solid was re-dispersed in 5 mL THF, cooled to -20 °C and 15 mg of sodium hydride was carefully added to the suspension with rapid stirring. Vigorous evolution of gas was observed and the mixture was let to stir for 10 minutes after which the contents were filtered through a PTFE–Syringe filter with an additional 1 mL of THF to aid in quantitative separation. The combined filtrates were stripped to dryness, and a light-tan colored powder was obtained. Recrystallization of the entire solid from a THF solution by addition of hexanes and precipitation by cooling to -20 °C produced 125 mg **4.14,** in 78% yield. 1.0 mole of Na-bound THF could not be removed even upon extended exposure to high-vacuum.
^{1}H NMR (22 °C, 500 MHz, THF-D_8, ppm) δ: 1.38-1.52 (br, m, 3H, CH_2(2H)+B-CH(1H)), 1.56-1.87(m, 10H, CH_2(6H)+THF(4H)), 1.88-2.03 (m, 2H, CH_2), 2.39-2.61

(m+m, 2H, CH_2), 3.43 (s+unresolved Pt-satellites, 3H, $PtOCH_3$), 5.05 (br, 1H, B-CH), 6.26 (td, *J*=5.8, 1.8 Hz, py-5-CH), 6.69-6.78 (m, 2H, py'-5-CH+Ph-p-CH), 6.87 (t, 2H, *J*=7.4 Hz, Ph-m-CH), 7.17 (td, 1H, *J*=7.6, 1.7 Hz, py-4-CH), 7.31 (td, 1H, *J*=7.5, 1.7 Hz, py'-4-CH), 7.40 (d, 1H, *J*=7.8 Hz, py-3-CH), 7.49 (d, 2H, *J*=7.1 Hz, Ph-o-CH), 7.55 (d, 1H, *J*=7.7 Hz, py'-3-CH), 8.31 (d+Pt-satellites, 1H, J_{Pt-H}=44, *J*=6.1 Hz, py-6-CH, trans to PtPh), 8.80 (d+unresolved Pt-satellites, *J*=4.9 Hz, py'-6-CH, trans to $PtOCH_3$).

^{1}H NMR (22 °C, 400 MHz, CD_3OD, ppm) δ: 1.35-1.55 (br, m, 3H, CH_2(2H)+B-CH(1H)), 1.58-1.71 (br, m, 2H, CH_2), 1.71-2.03 (br, m+m+m, THF(1.9H)+CH_2(6H)), 2.37-2.60 (br, m+m, 2H, CH_2), 3.2-3.4 (s+unresolved Pt-satellites, overlapping with CD_3OD signal), 3.72 (m, 1.9H, THF), 5.03(br, 1H, BCH), 6.30 (td, 1H, *J*=5.6, 2.2 Hz, py-5-CH), 6.75 (vt, 1H, *J*=7.4 Hz, p-Ph), 6.8-6.9 (m, 3H, m-Ph(2H)+py(1H)), 7.23 (vt, 1H, *J*=8.1 Hz, py-CH), 7.30-7.50(m, 4H, o-Ph(2H)+Py(2H)), 7.55 (d, 1H, *J*=7.7 Hz, py-3-CH), 8.11 (d+Pt-satellites, *J*=6.8, J_{Pt-H}=49 Hz, py-6-CH, trans to OCH_3), 8.86 (d+unresolved Pt-satellites, *J*=5.4 Hz, py-6-CH, trans to PtPh).

^{13}C NMR (22 °C, 500 MHz, THF-D_8, ppm) δ: 23.1-24.6 (br, BCH), 26.4 (br, m, CH_2+CH_2+THF*), 31.6-32.9 (br, BCH), 33.7 (CH_2), 33.8 (CH_2), 34.53 (CH_2), 34.57 (CH_2), 60.1 (s+unresolved Pt-satellites, $PtOCH_3$), 68.3 (THF), 118.3, 119.1, 122.1, 127.0 (J_{Pt-C}=51.7 Hz), 130, 130.2, 132.3, 133.4, 139.2, 147.2 (J_{Pt-C}=1092 Hz, Pt-ipsoPh(C)), 149.2, 153.7, 188.2-190.0 (br, BC), 190.1-191.7 (br, BC) *Complex peak at 26.4 was cross checked for correct assignment by subtracting the integral corresponding to CH_2O- (of THF at 68.3 ppm) from the integral at 26.43 ppm. Such computation results in 68.29 (set to 1 C), 26.43 (3 C).

Elemental Analysis (C, H, N): Calculated ($C_{25}H_{30}BN_2NaOPt$·1.0THF): 51.56, 5.67, 4.15 Found: 51.31, 5.73, 4.07.

4.8.12 Synthesis of 4.15 by oxidation of LPt^{II}(Me)(OMe), 4.10 or LPt^{II}(Ph)(OMe), 4.14 in methanol with O_2

200 mg of **4.10** was dissolved in 4 mL methanol in a stir-bar equipped reaction vial in the glove box. The vial was taken out from the box and was exposed to O_2 with vigorous stirring. Stirring was continued for 10 minutes following which the mixture was stripped to dryness to yield a light yellow powder. The entirety of this solid was recrystallized from a 1 mL of THF solution by precipitation with hexanes to yield 200 mg of analytically pure **4.15** in 90 % yield. Crystals suitable for XRD were grown by layering a 100 mg sample of **4.15** dissolved in 3mL of THF with 2 mL of hexanes at -20 °C. 0.4 mole of THF co-crystallized with **4.15** was visible by ^{1}H-NMR. ^{13}C NMR resonance corresponding to the 4 °C-B of the [3.3.0]bicyclooctyl fragment of **4.15** could not be located even when the possibility of overlap of this signal with those of THF in the sample was excluded by recording ^{13}C-NMR spectra after completely exchanging THF present in the sample with THF-d_8. ^{13}C-NMR peak assignments were made by correlation with DEPT 45, 90 and 135 spectra. **4.15** is unstable in the presence of even traces of acid or water but stable in the presence of excess base ($NaOCH_3$).

Oxidation of 100 mg of **4.14** was performed in a manner identical to that of **4.10** mentioned above to yield 91 mg of **4.10** in 93% yield.

^{1}H NMR (22 °C, 400 MHz, CD_3CN, ppm) δ: 0.80-0.94 (br, 3H, CH), 0.98-1.09 (br, m, 3H, CH), 1.20-1.35 (br, m, 4H, CH), 1.79 (m, 1.2H, THF), 2.56-2.78 (s+m, 3H+2H, B-OCH_3+CH), 3.25 (s unresolved Pt-satellites, 6H, Pt(OCH_3)$_2$), 3.63 (1.2H, THF), 4.22 (br, sept, 1H, 3 °C-H), 6.85 (td, 2H, *J*=6.7, 1.7 Hz, py-5-CH), 7.51 (td, 2H, *J*=7.9, 1.8 Hz, py-4-CH), 7.62 (d, 2H, *J*=7.7Hz, py-3-CH), 9.1 (d+unresolved Pt-satellites, 2H, *J*=5.7 Hz, py-6-CH).
^{13}C NMR (22 °C, 500 MHz, DMSO-*d*$_6$, ppm) δ: 25.7 (CH_2), 35.3 (CH_2), 39.1 (CH_2), 44.4 (CH), 51.6 ($BOCH_3$), 58.7 (Pt(OCH_3)$_2$), 119.8, 129.8, 132.1, 148.7, 179.0-181.1 (br, BC).
ESI$^-$ MS of a methanolic solution basified with $NaOCH_3$: 564.18, Calculated 564.20.
Elemental Analysis (C, H, N): Calculated ($C_{21}H_{30}BN_2NaO_3Pt$·0.4THF): 44.05, 5.43, 4.55 Found: 44.05, 5.58, 4.48.

4.8.13 Synthesis of 4.16 by rapid oxidation of $LPt^{II}Me_2$, 4.5 in methanol at -60 °C with O_2

200 mg of **4.5** was dissolved in 1 mL of THF inside the glove-box. In a Schlenk tube equipped with a stir-bar, 4 mL of methanol was taken, cooled to -60 °C (dry-ice/Acetone) and O_2 was bubbled through it for 5 minutes. While continuing bubbling O_2, the 1 mL THF solution of **4.5** was added to it via a syringe. The dry-ice bath was removed and the solution was allowed to warm to room temperature over a period of 10 minutes, while continuing bubbling O_2. During this time a faint odor resembling 'alkenes' was found emanating from the reaction mixture. The solution in the Schlenk tube was stripped to dryness to yield a tan-colored powder. The contents were re-dispersed in 3 mL THF, 0.1 mL water was added to it, and the contents were stirred for 10 minutes. Fine white precipitate appeared along with the formation of a light-yellow solution. The contents were filtered through a PTFE-syringe filter and stripped to dryness to yield a powder. This powder was dissolved in 2 mL $CHCl_3$ and recrystallization was attempted by precipitation with hexanes to yield 158 mg of **16** (approx. 88% yield). Trace amounts of impurities, presumably due to unavoidable methanolysis and subsequent oxidation of those byproducts could be seen in the NMR spectra.
^{1}H NMR (22 °C, 400 MHz, $CDCl_3$, ppm) δ: 1.31 (br, PtOH), 1.33 (s+Pt-satellites, 6H, J_{Pt-H}=69.4 Hz, $PtMe_2$), 3.0 (s+Pt-satellites, 3H, J_{Pt-H}=27.5 Hz, B-μ(OCH_3)-Pt), 3.57 (s, 3H, B-exo(OCH_3)), 7.11-7.16 (m, 2H, py-5-CH), 7.56-7.66 (overlapping-m, 4H, py-4-CH, py-3-CH), 8.57 (dt+Pt-satellites, 2H, *J*=5.3, 1.4 Hz, J_{Pt-H}≈16 Hz, py-6-CH)

4.8.14 Synthesis of 4.17 by oxidation of $LPt^{II}Ph_2$, 4.6 in methanol with O_2

200 mg of **4.6** was dissolved in 5 mL methanol in a reaction vial equipped with a stir-bar inside the glove box and taken out. O_2 was bubbled through the solution for a period of 10 minutes. A characteristic 'alkene' smell was noticed. The solution changed from colorless to a faint yellow gradually. The solution was stripped to dryness, during the course of which fine precipitate started to appear. The sample was further dried to obtain a solid. Part of the solid was soluble in chloroform and part insoluble. The solid contents were re-dispersed in 3 mL $CHCl_3$, 0.2 mL water was added to the mixture and stirred for 10 minutes. As before, fine white precipitate and

a light-yellow supernatant appeared. The supernatant was extracted with 2 mL chloroform in two more fractions, filtered through a PTFE-syringe filter and stripped to dryness to yield 142.6 mg of **4.17**, in 95% yield. **4.17** was recrystallized from a mixture of THF and hexanes at -20 °C, and fine colorless crystals suitable for X-ray diffraction were obtained. The same sample was used for elemental analysis.
^{1}H NMR (22 °C, 500 MHz, $CDCl_3$, ppm) δ: 0.39 (br, 1H, PtOH), 1.86 (1.2H, residual THF) 3.33 (s+Pt-satellites, 3H, J_{Pt-H}=22.5 Hz, Pt-μ(OCH_3)B), 3.69-3.78 (s+m, 4H, B-OCH_3(3H), THF (1H)), 6.99-7.22 (m+m+td, 12H, $PtPh_2$+py-5-CH), 7.67 (td, 2H, *J*=7.34, 1.3 Hz, py-4-CH), 7.73 (d, 2H, *J*=7.45, py-3-CH), 8.68 (d+unresolved Pt-satellites, 2H, *J*=5.43, py-6-CH).
^{13}C NMR (22 °C, 500 MHz, $CDCl_3$, ppm) δ: 25.8 (THF), 51.9 (s+unresolved Pt-satellites, Pt-μ-(OCH_3)B), 55.4 (s, B-OCH_3), 68.2 (THF), 122.9 (s), 125.1 (s), 127.5 (s+unresolved Pt-satellites), 127.5 (s), 129.6 (s), 133.4 (s), 137.0 (s), 146 (s), 171.1 (br, BC).
Elemental Analysis (C, H, N): Calculated ($C_{24}H_{25}BN_2O_3Pt$·0.3THF): 49.06, 4.48, 4.54 Found: 49.10, 4.84, 4.28

4.8.15 Characterization of bicyclo[3.3.0]octene, 4.18:

In a separate experiment, 50 mg of **4.6** was oxidized in a manner similar to above, the methanolic solution was cooled to 0 °C and extracted with 0.8 mL of cyclohexane-d_{12}. The cyclohexane extract was passed through a pipette packed with silica, and further filtered through a PTFE-syringe filter. The colorless solution was analyzed by ^{1}H and ^{13}C NMR, as well as GC-MS and found to match the mass of 108, corresponding to that of bicyclo[3.3.0]oct-1(5)-ene.
^{1}H-NMR (22 °C, 500 MHz, C_6D_{12}, ppm) δ: 2.10-2.16 (m, set to 8H, (C=C)C***H***), 2.18-2.25 (m, 4H, (C=C)CH_2C***H***).
^{13}C-NMR (22 °C, 500 MHz, C_6D_{12}, ppm) δ: 29.33 (C=C-CH_2-***C***H_2), 29.95 (C=C-***C***H_2-CH_2), 146.51 (C=***C***-CH_2-CH_2).
GC-MS (EI): 108

4.8.16 In-situ preparation of $LPt^{II}(CD_3)(OCD_3)$, 4.10-*d*$_6$

10 mg of **4.5** was dissolved in CD_3OD in an NMR tube and a ^{1}H-NMR spectrum was recorded immediately. According to the NMR spectrum, complete conversion of **4.5** to **4.10-*d*$_6$** had occurred. **4.10-*d*$_6$** was not isolated from solution, but characterized by ^{1}H and ^{13}C NMR spectroscopy and ESI-MS.
^{1}H NMR (22 °C, 500 MHz, CD_3OD, ppm) δ: 1.27-1.44 (br, m, 3H, CH), 1.45-1.61 (br, m, 4H, CH), 1.66-1.82 (br, m, 4H*, CH, overlapping with THF), 2.32-2.53 (m=sept+sept, 2H, CH), 4.64 (br, 1H, B-CH), 6.53 (td, *J*=6.6, 1.6 Hz, 1H, py-5-CH), 6.80 (td, *J*=6.7, 1.5 Hz, 1H, py'-5-CH), 7.27 (td, *J*=7.8, 1.5 Hz, 1H, py-4-CH), 7.34 (td, *J*=7.6, 1.6 Hz, 1H, py'-4-CH), 7.38 (d, *J*=7.9 Hz, 1H, py-3-CH), 7.50 (d, *J*=7.6 Hz, 1H, py'-3-CH), 8.48 (d, J_{Pt-H}=33, *J*=6.1 Hz, 1H, py-6-CH), 8.76 (br, d, *J*=5.0 Hz, unresolved Pt-satellites, 1H, py'-6-CH). *Peak overlapping with THF was integrated by including THF signal and then subtracting from it the integral corresponding to the non-overlapping downfield THF signal.
^{13}C NMR (22 °C, 500 MHz, CD_3OD, ppm) δ: 24.1 (br, B-CH), 26.50 (CH_2), 26.58 (CH_2, overlapping with THF), 32.6 (br, B-CH), 33.7 (CH_2), 33.8 (CH_2), 34.1 (CH_2),

34.7 (CH_2), 119.2, 120, 130.6, 130.6, 132.6, 133.6, 150.5, 153.3, 188-193 (br+br, ipso-py-C).
ESI^- of the NMR-solution basified with $NaOCD_3$: 524.22, Calculated 524.23

4.8.17 Oxidation of $LPt^{II}(Me)(OMe)$, 4.10 and $LPt^{II}(CD_3)(OCD_3)$, 4.10-*d_6* with O_2 in CD_3OD: Detection of CH_4 and CD_3H and 4.15-*d_6* or 4.15-*d_9*

Oxidation of $LPt^{II}(Me)(OMe)$. 10 mg of **4.10** was dissolved in 0.5 mL of CD_3OD and a ^1H NMR was recorded. According to NMR, no deuteration of either Pt-bound CH_3 or OCH_3 groups had occurred. 1.1 eqv. of THF present in the sample was used as an internal standard to monitor product yields. 1.0 mL of CD_3OD was saturated with O_2 and the NMR-tube was completely filled with it, and shaken. A ^1H-NMR was recorded. On comparison of the two spectra, before and after oxidation, and calibrating the integrals with previously set value for THF, oxidation was found to have occurred cleanly to form **4.15-*d_6***, in 96% yield by NMR. A very strong singlet at 0.21 ppm was visible, and assigned to methane. The Pt-bound OCH_3 did not exchange with OCD_3 of the solvent in the course of the reaction.

Oxidation of $LPt^{II}(CD_3)(OCD_3)$. The contents of the NMR-tube obtained after dissolution of **4.5** in CD_3OD were frozen with liq. N_2 and the headspace of the NMR-tube was evacuated. O_2 was then admitted into the headspace at 30 psi pressure, the NMR-tube was sealed and the contents were thawed and shaken for homogeneity. An NMR was recorded quickly within 10 minutes of thawing. According to NMR, **4.10-*d_6*** underwent complete oxidation to form **4.15-*d_9***.

Observation of CD_3H upon oxidation of 4.10-*d_6* in CD_3OD: In another similar experiment, to a 0.2mL solution of **4.10-*d_6*** in CD_3OD was added O_2-saturated CD_3OD, taking care to fill the entire headspace of the NMR tube. The NMR tube was sealed and a ^1H-NMR spectra was recorded. A septet at 0.15 ppm, corresponding to CHD_3 was observed, in addition to signals corresponding to **4.15-*d_9***.

4.15-*d_9*:

^1H NMR (22 °C, 500 MHz, CD_3OD, ppm) δ: 0.85-0.94 (br, sept, 2H, CH), 1.03-1.11 (br, sept, 2H, CH), 1.17-1.25 (br, quint, 2H, CH), 1.26-1.44 (br, m+m, 4H, CH), 2.42-2.53 (br, m, 2H, CH), 4.73 (br, sept, 1H, 3 °CH), 6.94 (td, *J*=6.7, 1.6 Hz, 2H, py-5-CH), 7.56 (vt, *J*=7.5 Hz, 2H, py-4-CH), 7.64 (d, *J*=7.9 Hz, 2H, py-3-CH), 8.82 (d, *J*=6.0 Hz, 2H, unresolved Pt-satellites, py-6-CH). Residual THF signals not reported.

^{13}C NMR (22 °C, 500 MHz, CD_3OD, ppm) δ: 27.1 (CH_2), 36.8 (CH_2), 40.4 (CH_2), 46.8 (3°-CH), 47.1 (br, B4 °C), 121.44, 133.94, 131.77, 151.59, 181.20 (br, ipso-py-C). Residual THF signals not reported.

ESI^- of the NMR solution basified with $NaOCD_3$: 573.23, Calculated 573.26.

4.8.18 In-situ preparation of $LPt^{II}(C_6D_5)_2$, 4.6-*d_{10}* : H/D exchange between $CD_3OD/LPt^{II}Ph_2$ and $CD_3OH/LPt^{II}(C_6D_5)_2$

35 mg of **4.6** was dissolved in 0.6 mL CD_3OD and a ^1H NMR was recorded immediately. The spectrum was consistent with the presence of two Pt-bound phenyl groups and a C_s symmetrical structure. The solution was monitored by ^1H NMR periodically every hour. The signals corresponding to the protons of the $PtPh_2$ moiety were found to gradually decrease in intensity and after 8h, complete deuteration of the $PtPh_2$ moiety was observed. The solution was then transferred to a vial equipped with

a stir-bar and the solvent was stripped off under vacuum. An off-white solid similar in appearance to the starting material was observed. The solid was dissolved in 0.6 mL CD_3OH and periodically monitored by ^{1}H-NMR (with suppression of the OH signal) for reappearance of the aforesaid signals. The sample underwent complete H/D exchange after a period of 4h.

4.6, immediately after dissolution in CD_3OD:

^{1}H NMR (22 °C, 500 MHz, CD_3OD, immediately after dissolution, ppm) δ: 1.42-1.56 (m, 3H, CH_2+CH), 1.73-1.90 (m+m, 11H, THF=5H, CH_2=6H), 1.93-2.06 (m, 2H, CH_2), 2.44-2.57 (m, 2H, CH_2), 3.71 (m, 5H, THF), 4.73-4.80 (br, 1H, CH), 6.48 (vt, 2H, *J*=5.5, 1.5 Hz, py-5-CH), 6.64 (vt, 2H, *J*=7.2 Hz, Ph-p-CH), 6.78 (vt, 4H, *J*=7.6 Hz, Ph-m-CH), 7.26 (td, 2H, *J*=7.6, 1.7 Hz, py-4-CH), 7.51 (d, 2H, *J*=8.0Hz, py-3-CH), 7.63 (d+Pt-satellites, 4H, J_{Pt-H}=62.0 Hz, *J*=7.1 Hz, Ph-o-CH), 8.24 (d+unresolved Pt-satellites, 2H, *J*=5.6 Hz, py-6-CH).

4.6-d_{10}, 8h after dissolution in CD_3OD:

^{1}H NMR (22 °C, 500 MHz, CD_3OD, 8h after dissolution, ppm) δ: 1.42-1.56 (m, 3H, CH_2+CH), 1.73-1.90 (m+m, 11H, THF=5H, CH_2=6H), 1.93-2.06 (m, 2H, CH_2), 2.44-2.57 (m, 2H, CH_2), 3.71 (m, 5H, THF), 4.73-4.80 (br, 1H, CH), 6.48 (vt, 2H, *J*=5.5, 1.5 Hz, py-5-CH), 7.26 (td, 2H, *J*=7.6, 1.7 Hz, py-4-CH), 7.51 (d, 2H, *J*=8.0Hz, py-3-CH), 8.24 (d+unresolved Pt-satellites, 2H, *J*=5.6 Hz, py-6-CH). Peaks corresponding to $PtPh_2$ moiety silent.

^{13}C NMR (22 °C, 500 MHz, CD_3OD, 8h after dissolution, ppm) δ: 23.7-25.0 (br, m, B-CH), 26.6 (s, THF), 26.8 (s, CH_2), 33.5-34.7 (overlapping, br, B-CH), 34.0 (s, CH_2), 35.0 (s, CH_2), 69 (s, THF), 118.9 (s+Pt-satellites, J_{Pt-C}=22.3 Hz, py-CH), 130.2 (s+unresolved Pt-satellites, py-CH), 133.3 (py-4-CH), 152.4 (s+Pt-satellites, J_{Pt-C}=34.7 Hz, py-6-CH), 190.7-192.2 (br, py-ipso-C).

ESI$^-$ MS of a methanolic solution of **4.6-d_{10}**: 636.28, Calculated 636.29.

4.8.19 In-situ preparation of $LPt^{II}(C_6D_5)(OCD_3)$, 4.14-d_8

A 0.5 mL CD_3OD solution containing 50 mg of **4.6** in a vial was let stir for 10h to convert it to **4.6-d_{10}** via complete deuteration of the $PtPh_2$ fragments, as mentioned above. Following a procedure identical to that mentioned for the synthesis of **4.14**, 9 µL (1 eqv.) of trimethylchlorosilane in 0.5 mL CD_3OD was added and immediate formation of precipitate was observed. After 10 minutes of further stirring, the mixture was stripped to dryness. To this mixture was added 2 mL THF followed by addition of 5 mg NaH. The suspension was filtered quickly and stripped to dryness to obtain a brown solid. Although trace impurities were visible in the ^{1}H-NMR spectrum in CD_3OD, the major species was identified as **4.14-d_8** by comparison with the ^{1}H-NMR spectrum of analytically pure **4.14**, in CD_3OD. Yields were not determined owing to multi-step conversions/filtrations involving minute quantities.

^{1}H NMR (22 °C, 400 MHz, CD_3OD, ppm) δ: 1.35-1.55 (br, m, 3H, CH_2(2H)+B-CH(1H)), 1.55-2.04 (17H, CH_2(8H)+THF(9H)), 2.37-2.60 (br, m+m, 2H, CH_2), 3.72 (m, 9H, THF), 5.03(br, 1H, BCH), 6.30 (td, 1H, *J*=5.6, 2.2 Hz, py-5-CH), 6.84 (vt, 1H, py-CH), 7.23 (vt, 1H, *J*=7.9 Hz, py-CH), 7.36 (vt, 1H, *J*=7.7 Hz, py-CH), 7.55 (d, 1H, *J*=7.8 Hz, py-3-CH), 8.11 (d+Pt-satellites, *J*=6.8, J_{Pt-H}=49 Hz, py-6-CH, trans to OCH_3), 8.86 (d+unresolved Pt-satellites, *J*=5.4 Hz, py-6-CH, trans to PtPh). Some

trace impurities could be seen in the ^{1}H-NMR spectrum. Peak assignments were made with respect to ^{1}H-NMR spectrum of **4.14** in CD_3OD.

4.8.20 Oxidation of $LPt^{II}(Ph)(OMe)$, 4.14 and $LPt^{II}(C_6D_5)(OCD_3)$, 4.14-*d*$_8$ with O_2 in CD_3OD: Detection of C_6H_5 and C_6D_5H

Oxidation of 4.14: 25 mg of **4.14** was dissolved in 0.6 mL CD_3OD in a sealable NMR-tube inside the glove box and a ^{1}H NMR was recorded. According to NMR, no deuteration of either Pt-bound C_6H_5 or OCH_3 fragments had occurred. The contents of the NMR-tube were then frozen, the headspace was evacuated and refilled with 30 psi O_2 and the NMR tube was sealed. The contents were thawed, the NMR tube was shaken for homogeneity and a ^{1}H NMR was recorded within 10 minutes of thawing. According to NMR, complete oxidation of **4.14** was observed along with the formation of 1 equivalent of benzene. The amount of benzene produced was quantified using signals of the THF present in **4.14** as an internal standard.

Oxidation of 4.14-*d*$_8$: A partially deuterated complex **4.14-*d*$_8$** was oxidized similarly in a NMR tube in CD_3OD and a ^{1}H NMR was recorded. One singlet at 7.16 ppm integrating to 1H (with THF as an internal standard) in the ^{1}H NMR spectrum confirmed the formation of C_6D_5H. Some unassigned decomposition was also seen.

4.8.21 In-situ synthesis of 4.16-*d*$_7$ by fast oxidation of $LPt^{II}Me_2$, 4.5 with O_2-saturated CD_3OD at -60 °C

Oxidation of 4.5: 5 mg of solid **4.5** containing 2.5 moles THF/mole complex was charged in an NMR-tube and placed at -60 °C in a dry-ice/acetone bath. 0.8 mL of CD_3OD was cooled to -60 °C in a vial and O_2 was bubbled through it for a period of 10 minutes and quickly transferred to the NMR-tube. The NMR-tube was sealed, shaken and a ^{1}H-NMR was recorded within 5 minutes. According to NMR, based on THF-internal standard, the yields of **4.16-*d*$_7$** and bicyclo[3.3.0]oct-1-ene were 92% and 94% respectively (c.f. NMR spectra). Yield for **4.16-*d*$_7$** was computed by averaging the integrations of the aromatic signals over 8 units (theoretical maximum). Partial D-incorporation into the $PtMe_2$ fragment could not be avoided. The identity of **4.16-*d*$_7$** was additionally confirmed by ESI-MS of the NMR-solution.

^{1}H NMR (22 °C, 400 MHz, CD_3OD, ppm) δ: 1.44 (s+multiplets+Pt-satellites, 4.7H, $J_{Pt\text{-}H}$=68.4 Hz, $Pt(CH_{(3-n)}D_n)_2$), 1.87 (m, THF, internal-std, 10H), 2.08-2.29 (m+m, 11.36 H, bicycloocetene), 3.73 (m, THF, internal-std, 10H), 7.32 (ddd, 1.84H, *J*=5.4, 1.5 Hz, py-5-CH), 7.70 (d, 1.72H, *J*=7.5 Hz, py-3-CH), 7.80 (td, 1.89H, *J*=7.6 Hz, py-4-CH), 8.65 (d+unresolved Pt-satellites, 1.91H, *J*=5.5 Hz, py-6-CH).

ESI^+-MS of CD_3OD solution, **4.16-*d*$_7$**·H: 485.23, Calculated: 485.21

4.8.22 Step-wise oxidation of $LPt^{II}Ph2$, 4.6 in CD_3OD under controlled supply of O_2: Detection of 4.29-*d*$_3$, and completion of oxidation to form 4.17-*d7*:

15 mg of **4.6** was dissolved in 0.6 mL of CD_3OD in a sealable NMR tube and 0.25 mL of O_2 (~0.5eqv. at RTP) taken in a syringe was slowly bubbled through the solution from the bottom of the NMR tube with a long needle. The tube was quickly sealed and shaken for 10 minutes. A ^{1}H NMR spectrum was recorded after this time. According to NMR, According to NMR, and based on THF as internal standard, **4.29-*d*$_3$** was formed in 94% yield, along with the formation of 6.5% of bicyclooctene,

4.18, and 6.5% of **4.17-*d*$_7$**. The characteristic signature of the B-bound bicyclo[3.3.0]octyl fragment, similar to that of previously characterized **4.15**, is clearly seen in the ^{1}H-NMR spectrum. An aliquot was analyzed by ESI-MS and a peak at 659.26 confirmed the identity of **4.29-*d*$_3$**. **4.29-*d*$_3$** was characterized by ^{1}H-NMR and ESI-MS only for mechanistic proof-of-concept and no attempts were made towards isolating it. The oxidation of **4.29-*d*$_3$** was completed by bubbling about 1.0 mL O_2 through the remaining solution in the NMR-tube and it was found to convert to **4.17-*d*$_7$** and **4.18** in 91% yield.

4.29-*d*$_3$:

^{1}H NMR (22 °C, 400 MHz, CD_3OD, ppm) δ: 0.93-1.02 (m, 2H, CH_2), 1.09-1.18 (m, 2H, CH_2), 1.21-1.31 (m, 2H, CH_2), 1.32-1.50 (m+m, 4H, CH_2), 2.45-2.57 (m, 2H, CH_2), 4.74 (complex-septet, 1H, BCC***H***), 6.53-6.64 (m, 4H, py-5-CH(2H)+Ph(2H)), 6.67-6.79 (m, 4H, py-4-CH(2H)+Ph(2H)), 7.34-7.54 (m, 6H, Ph), 7.79 (d, 2H, *J*=8.2 Hz, py-3-CH), 8.37 (d+unresolved Pt-satellites, 2H, py-6-CH).

ESI^- MS of CD_3OD solution basified with $NaOCD_3$: 659.27, Calculated: 659.26.

4.8.23 Oxidation of $LPt^{II}Ph_2$, 4.6 in CD_3OD by H_2O_2:

14 mg of **4.6** was dissolved in a mixture of 0.3 mL of CD_3OD and 0.3 mL THF-*d*$_8$ in a NMR tube and a ^{1}H-NMR spectrum was recorded. The THF signal was used as internal standard. 6 µL of 30% aq. H_2O_2 was added to the NMR tube and shaken, and a ^{1}H-NMR NMR spectrum was recorded immediately. According to the NMR, based on THF integration, **4.6** was completely oxidized to **4.17-*d*$_7$** (90% yield) and **4.18** (90% yield).

4.8.24 Oxidation of $LPt^{II}Ph_2$, 4.6 and LPt^{II}(Me)(OMe), 4.10 in CD_3OD with O_2 in the presence of TEMPO radical:

Oxidation of 4.6. 15 mg of solid **4.6** (20.0 µmol) was added to a vial with 6 mg (2 eqv.) solid TEMPO radical. To this vial was added 0.6 mL of CD_3OD and stirred for 2 minutes to obtain an orange colored solution. A ^{1}H-NMR was recorded and found to be a match to that of **4.6**, i.e. no reaction between **4.6** and TEMPO was observed. The peaks were broadened significantly, however, no difference in chemical shifts was observed. This solution was oxidized by bubbling O_2 through the tube for a period of 10 minutes. After this period, according to ^{1}H NMR, all starting material had converted to **4.17-*d*$_7$** and **4.18**.

ESI^+-MS of the CD_3OD solution: 603.18, Calculated: 603.16, 157.2 ($TEMPOH^+$)

Oxidation of 4.10. 15 mg of **4.10** (27.7 µmol) in the presence of 6 mg (2 eqv.) TEMPO radical in CD_3OD, O_2 was directly bubbled after dissolution for a period of 2 minutes. According to ^{1}H-NMR, oxidation was found to have occurred cleanly, and spectral match confirmed the identity of **4.15-*d*$_6$**. Signals were significantly broadened due to the presence of TEMPO.

4.8.25 Oxidation of $LPt^{II}Ph_2$, 4.6 and LPt^{II}(Me)(OMe), 4.10 in methanol with $^{18}O_2$:

A sample of 10 mg of **4.6** was oxidized under 1 atm of $^{18}O_2$ and the methanolic solution was analyzed by ESI-MS (positive mode).

ESI^+ of methanolic solution of **4.17-^{18}O** acidified with 10% HBF_4: **4.17-^{18}O·H$^+$**: 598.16, Calculated: 598.17.

Similarly, a sample of **4.10** was oxidized under 1 atom of $^{18}O_2$ in methanol, and an ESI-MS (negative mode) was recorded.
ESI^- of methanolic solution of **4.15** basified with NaOMe: 518.18, Calculated 518.19.
Thus, according to ESI-MS one ^{18}O atom was incorporated in **4.17** but none in **4.15**.

4.8.26 Oxidation of (MeO)(BCO)BPy$_2$-Pt^{II}(OMe)$_2$, 4.15 in with H_2O_2 to form (MeO)$_2$BPy$_2$-Pt^{IV}(OMe)$_2$(OH), 4.34

100 mg (170 µmol) of **4.15** was dissolved in 5 mL methanol in a reaction vial equipped with a stir-bar and 52 µL of 30% H_2O_2 (3 equivalents) was added to it with rapid stirring. After 20 minutes, the contents were stripped to dryness and the solid was extracted with 5 mL chloroform. The yellow colored solution was dried with anhyd. Na_2SO_4 and filtered through a cotton plug. 76 mg of **4.34** in 89% yield was obtained by recrystallization from this chloroform solution by precipitation with hexanes. Crystals suitable for X-ray structure determination were grown from a chloroform solution by vapor diffusion of pentanes at 25 °C.
^1H NMR (22 °C, 500 MHz, CD_2Cl_2, ppm) δ: 1.26 (br+unresolved Pt-satellites, 1H, PtOH), 3.05 (s+Pt-satellites, 6H, J_{Pt-H}=20.0 Hz, Pt(OMe)$_2$, equatorial), 3.06 (s+Pt-satellites, 3H, J_{Pt-H}=15.4 Hz, B(µ-OCH$_3$)Pt^{IV}), 3.6 (s, 3H, exo-BOCH$_3$), 7.28 (td, 2H, *J*=6.0, 1.8 Hz, py-5-CH), 7.61 (d, 2H, J+7.6 Hz, py-3-CH), 7.75 (td, 2H, *J*=7.6, 1.4 Hz, py-4-CH), 8.64 (d+Pt-satellites, 2H, *J*=5.8 Hz, J_{Pt-H}=20.9 Hz, py-6-CH).
^1H NMR (22 °C, 500 MHz, CD_2Cl_2, ppm) δ: 51.5 (s, exo-BOCH$_3$), 52.2 (s+Pt-satellites, J_{Pt-C}=6 Hz, B(µ-OCH$_3$)Pt^{IV}), 57.0 (s+Pt-satellites, J_{Pt-C}=13 Hz, Pt(OCH3)$_2$, equatorial), 124 (s+Pt-satellites, J_{Pt-C}=25 Hz), 128.2 (s+Pt-satellites, J_{Pt-C}=22 Hz), 138.6, 146.5, 169-172 (br, B-py-2-C)
ESI^+-MS: 504.14, Calculated: 504.12

4.8.27 Oxidation of LPt^{II}(OMe)$_2$, 4.11 with H_2O_2 in methanol to form (MeO)$_2$BPy$_2$Pt^{IV}(OMe)$_2$(OH), 4.34 and bicyclooctene, 4.18

25 mg of a crude sample of **4.11** was dissolved in methanol in a reaction vial and 4 equivalents of H_2O_2 was added to it with rapid stirring. After 20 minutes, white precipitate and a yellow supernatant formed. The mixture was stripped to dryness, and a part of the crude solid was extracted with C_6D_{12}. A ^1H-NMR spectra was recorded and compared to that of **4.18** and found to be a match. The rest of the solid was dissolved in $CDCl_3$ and the identity of the solid was confirmed by comparison of the concurrent ^1H-NMR spectra with that of **4.34**. Trace undetermined impurities could be seen, presumably because **4.11** was not pure. Yields were not determined.

4.8.28 Oxidation of 4.15-d_9 in CD_3OD with H_2O_2

10 mg of LPt^{II}Me$_2$, **4.5**, was dissolved in CD_3OD in an NMR tube in the glove-box and a ^1H-NMR spectra was recorded to confirm the complete conversion to LPt^{II}(CD$_3$)(OCD$_3$), **4.10-*d*$_6$**. Afterwards, O_2 was bubbled through the solution and a ^1H-NMR spectra was recorded. According to NMR, based on THF present in the sample, complete conversion of **4.10-*d*$_6$** to **4.15-*d*$_9$** had occurred as before. 6 µL of 30% H_2O_2 (3 equivalents) was added and the solution was shaken. According to a ^1H-NMR recorded after this time, quantitative formation of **4.34-*d*$_{13}$** and **4.18** had occurred.

Chapter 5: Catalytic applications of di(2-pyridyl)-dimethoxyborato-$Pt^{II/IV}$ complexes: aerobic oxidation of borohydrides and isopropanol

5.1Proposal

In our search for an anionic borate di(2-pyridyl)borate ligand that would retain the borate center in Pt^{II}-mediated oxidation chemistry, we found that replacement of one methyl in the dpdmb ligand by a methoxy was not sufficient (Chapter-III), as oxidation products corresponding to both '*methyl migration*' and '*ligand retention*' were observed. In another pursued direction involving tethered hydrocarbyls on the borate center, as in the 1,5-cyclooctanediyl derivative, unprecedented C-C and C=C coupling occurred, also leading to destruction of the borate center (Chapter-IV). Thus, without significantly modifying the di(2-pyridyl)-backbone, di(2-pyridyl)dialkoxyborato-Pt^{II} complexes were the only imminently remaining metal-ligand platform worth exploring. As mentioned before, repeated bottom-up approaches to synthesize di(2-pyridyl)dialkoxyborates were intractable. Gratifyingly, the oxidation of di(2-pyridyl)-1,5-cyclooctanediylborato-$Pt^{II}R_2$ complexes (where R=Me, **4.5** and R=Ph, **4.6**) in methanol led to the formation of the much anticipated dimethoxyborato-Pt^{IV} complexes, in excellent yields. According to the mechanism proposed for the complete oxidation of **4.5** and **4.6,** the di(2-pyridyl)dimethoxyborate ligand retains its configuration while enabling aerobic oxidation of derived

dihydrocarbyl-Pt^{II} complexes. Pending availability of a suitable reducing agent [R], a reaction $[R] + 0.5\ O_2 \xrightarrow{cat.} R - O$ involving either **4.35** or **4.17** as catalyst, as shown in Scheme 5.1, could be envisioned:

Scheme 5.1: Redox chemistry of di(2-pyridyl)dimethoxyborato-$Pt^{II\,/\,IV}Ph_2$ complexes

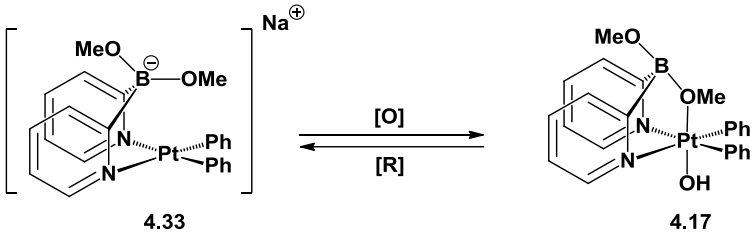

4.33 4.17

Furthermore, based on the proposed mechanism of sequential hydride abstraction from the bridgehead (B)C*H* (1,5-bicycloocatendiyl) fragment upon oxidation of **4.5** and **4.6** and from the bridge head (BC)-C*H* (3.3.0-bicyclooctyl) fragment upon oxidation of **4.28** and **4.29**, we envisioned that derivatives of **4.17** with B-bound secondary alkoxy groups, such as **5.1** might allow for a hydride transfer from the 2° C-H fragment of an alkoxy group, as shown in Scheme 5.2, leading to the formation of a Pt^{IV}(H) complex, **5.2**. Scheme 5.2 shows a direct analogy of **4.30**, **4.31 and 4.33** to **5.2**, **5.3**, and **5.4**, respectively.

Scheme 5.2: Comparison of Pt^{IV}-assisted ^{sec}C-H cleavage of B-bound proximal [3.3.0]bicyclooctyl and ispropyl fragments

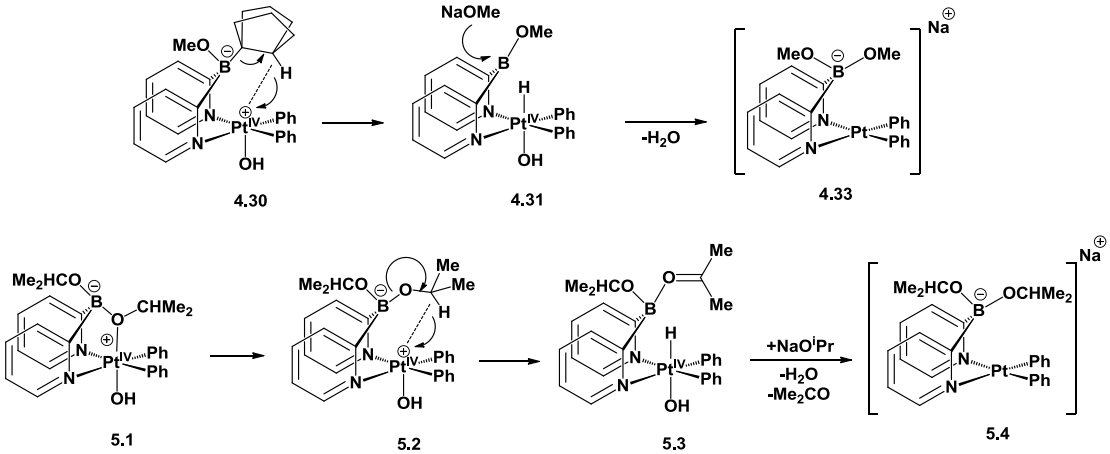

4.30 4.31 4.33

5.1 5.2 5.3 5.4

However, in order for such transformation to occur, **5.1** must isomerize to **5.2**, featuring an agostic (C-H)-Pt^{IV} bond, corresponding to a calculated gas-phase activation energy of 21.2 kcal/mole [2]. The activation energy for the C-H cleavage in **5.2** leading to **5.3**, involving a transition-state, **5.5**, shown in Figure 5.1, was found to be 13.8 kcal/mole in the gas-phase and 6.5 kcal/mole in MeOH.

Figure 5.1: DFT calculated transition-state (**5.5**) for the conversion of **5.2** to **5.3**

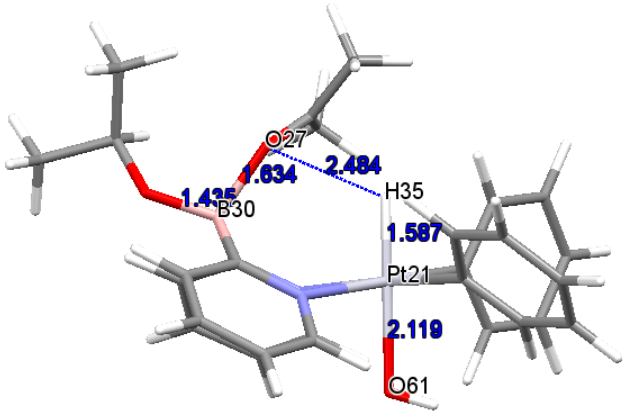

Thus, provided isomerization of **5.1** to **5.2** is possible, intramolecular C-H cleavage in **5.2** by the Pt^{IV} center might be possible. Deprotonation of the Pt^{IV}(H) fragment would then lead to a di(2-pyridyl)diisopropoxyborato-Pt^{II} complex, **5.4**, possibly allowing for a catalytic aerobic conversion of a isopropanol to acetone.

5.2 Implementation

5.2.1 Reduction of di(2-pyridyl)dimethoxyborato-$Pt^{IV}(Ph_2)(OH)$ complex with $NaBH_4$

Scheme 5.3: Reduction of di(2-pyridyl)dimethoxyborato-$Pt^{IV}Ph_2$ complex

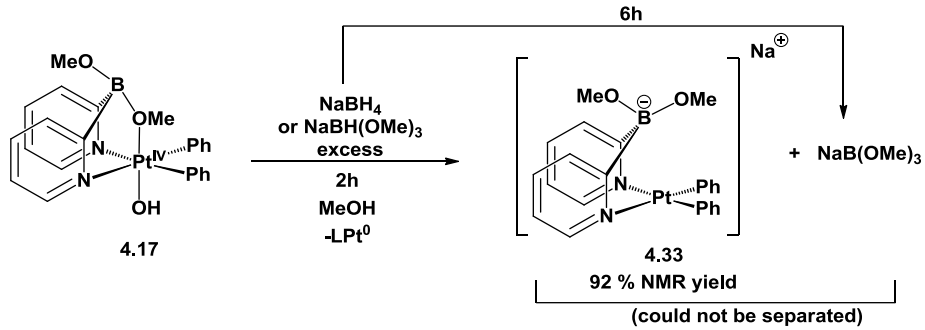

In order to access to the putative Pt^{II} complex, **4.33**, featuring the new ligand, di(2-pyridyl)dimethoxyborate, the $Pt^{IV}(Ph_2)(OH)$ complex, **4.17**, had to be reduced. Synthesis of the dimethyl-analogue of **4.32** was not attempted from a difficultly synthesized **4.16** as the hypothetical $Pt^{II}Me_2$ complex is expected to undergo methanolysis of one of the $Pt^{II}Me$ fragments in the course of the reaction.

We found that **4.17** in methanolic solutions could be reduced in 90 min by an excess of 2 equivalents of $NaBH_4$ or 5 equivalents of $NaBH(OMe)_3$ as shown in Scheme 5.3. An excess of borohydride was found to be necessary, presumably, to account for the background reaction of $NaBH_4$ with methanol. Although small amounts of colloidal material, presumed to be Pt^0 [82] formed, similar to reported reduction of Pt^{II} complexes with $NaBH_4$ leading to colloidal Pt^0, the Pt^0 was easily separated by centrifugation and/or filtration through a 0.2 µm PTFE syringe-filter. The identity of the Pt^{II} product was established by ^{1}H-NMR and ESI^--MS. Owing to the presence of a large amount of $NaB(OMe)_4$, which could not be removed completely even after

repeated recrystallization attempts, **4.33** could not be obtained in analytically pure form. It is, however, as evident from a clean aromatic region ^{1}H-NMR spectrum, the only Pt-complex is solution.

Figure 5.2: Aromatic region of the ^{1}H NMR spectrum of **4.33** (with admixed $NaB(OMe)_4$) in acetone-d_6 (22 °C, 500.132 MHz)

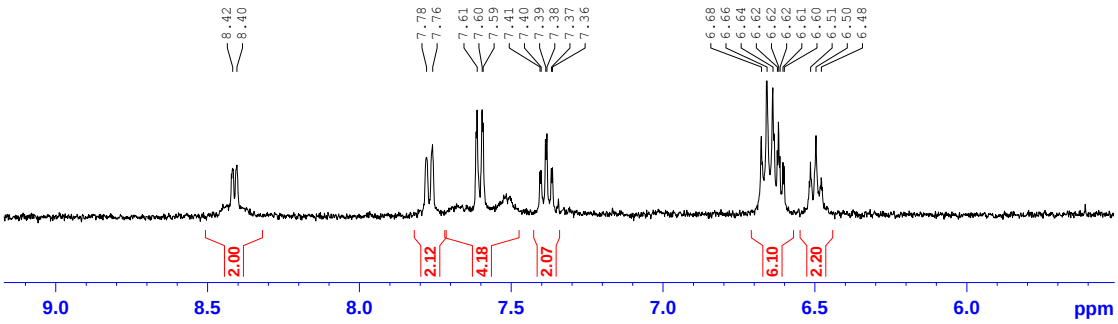

When the reduction of **4.17** with $NaBH_4$ was repeated in CD_3OD in an NMR-tube with THF as internal standard, **4.33-*d*$_{16}$** corresponding to complete deuteration at the $PtPh_2$ and $B(OCH_3)_2$ fragments was obtained in 92% NMR-yield. Although the reduction of **4.17** was complete within 90 min, the methanolysis and H/D exchange of the excess $NaBH_4$ added was complete within 6h as evident by the disappearance of the ^{1}H-NMR signals corresponding to the BH-fragment. An equivalent increase in the signal of $CD_3O\mathit{H}$ after completion of reaction and a small amount of benzene, were observed in the ^{1}H-NMR spectrum. The origin of benzene presumably stems from the same decomposition that results in Pt^{0}-black.

5.2.2 *In-situ* Oxidation of di(2-pyridyl)dimethoxyborato-$Pt^{II}Ph_2$-*d*$_{16}$ complex in CD_3OD

After completion of reduction and after complete disappearance of the ^{1}H-NMR peaks corresponding to $NaBH_4$, the CD_3OD solution containing **4.33-*d*$_{16}$** and $NaB(OMe)_4$ was exposed to O_2. Within 10 minutes of exposure to O_2, a ^{1}H-NMR

spectra was recorded. According to the NMR, complete conversion of **4.33-*d*$_{16}$** to **4.17-*d*$_{17}$** had occurred, as shown in Scheme 5.4(a).

Scheme 5.4: *In-situ* oxidation of di(2-pyridyl)dimethoxyborato-Pt^{II}Ph$_2$ complex: comparison to direct oxidation of di(2-pyridyl)-1,5-cycloocatendiylborato-Pt^{II}Ph$_2$ complex

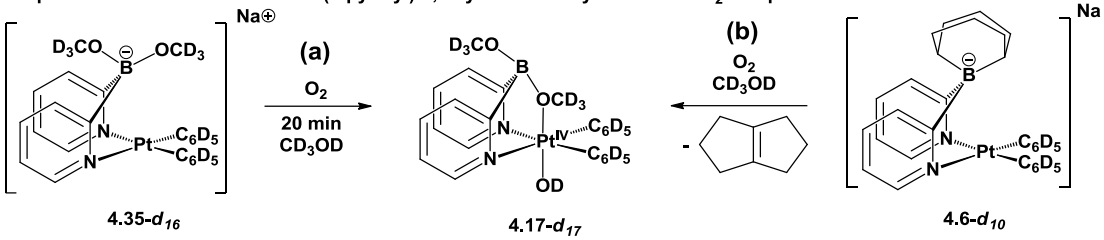

4.35-*d*$_{16}$ **4.17-*d*$_{17}$** **4.6-*d*$_{10}$**

To prove the identity of **4.17-*d*$_{17}$**, the ^{1}H-NMR spectrum of the oxidation product of the *d*$_{10}$-derivative of di(2-pyridyl)-1,5-cyclooctanediylborato-Pt^{II}Ph$_2$ complex, **4.6-*d*$_{10}$**, viz. **4.17-*d*$_{17}$** was compared and found to be a match. The ESI$^+$-MS of both solutions showed a mass of 612.1, consistent with **4.17-*d*$_{17}$**, as shown in Scheme 5.4(b). The oxidation of **4.33-*d*$_{16}$** was also performed in CD_3OD solutions with $NaB(OMe)_4$ additive and no depreciation in rates of oxidation or change in products were found, out ruling the involvement of the latter in the oxidation reactions.

Figure 5.3: ^{1}H NMR comparisons of **4.33-*d*$_{16}$** and **4.17-*d*$_{17}$** (obtained from **4.33-*d*$_{16}$** and **4.6-*d*$_{10}$**) in CD_3OD (22 °C, 400.131 MHz)
(**4.33-*d*$_{16}$,** 6h after adding $NaBH_4$, note the small amount of benzene appeared)

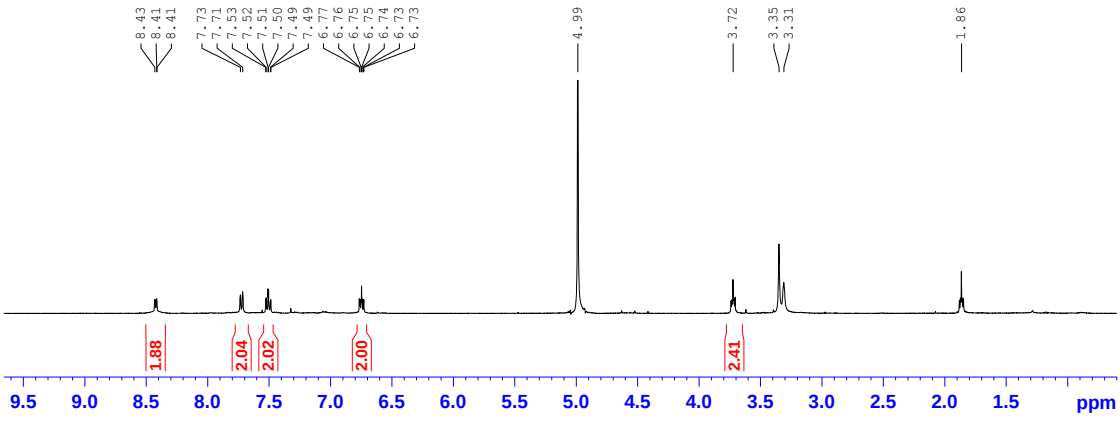

(After admitting O_2 to the solution above showing formation of **4.17-*d*$_{17}$**)

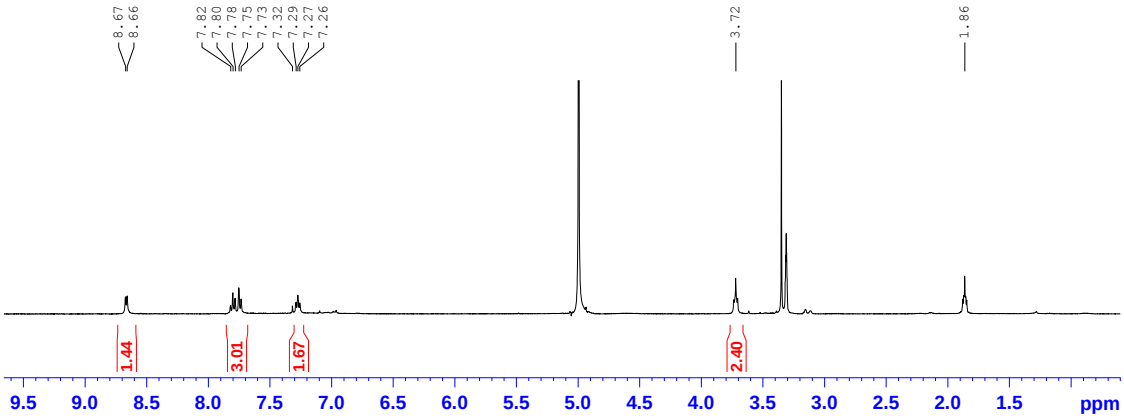

(Direct oxidation of **4.6-d$_{10}$** to **4.17-*d*$_{17}$** and **4.18**)

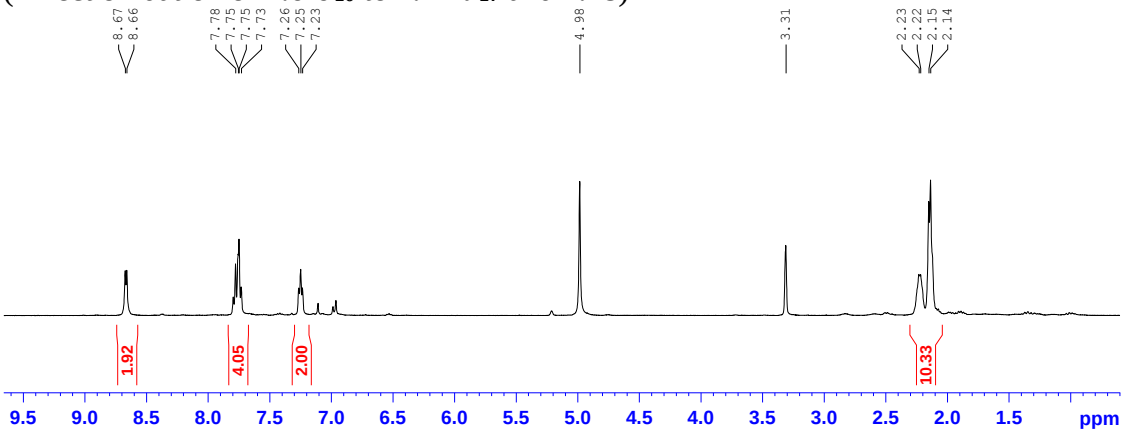

5.2.3 Mechanisms of reduction of LPt^{IV}(Ph$_2$)(OH) complexes with borohydrides

Scheme 5.5: Proposed mechanisms of reduction of di(2-pyridyl)dimethoxyborato-Pt^{IV}Ph$_2$ complex by NaBHR$_3$ (R=H, OMe)

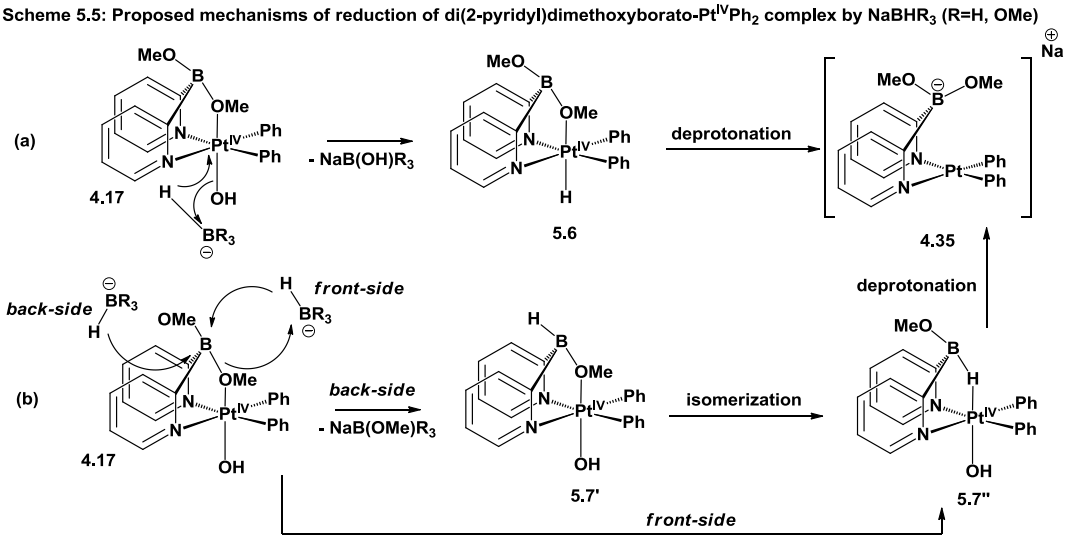

Two mechanisms for the reduction of the Pt^{IV} complex, **4.17**, by $NaBH_4$ or $NaBH(OMe)_3$ are shown in Scheme 5.5, where R = H, OMe. Based on literature precedence of concerted mechanisms of hydride delivery from borohydrides to metals [83] and organic substrates [84], two mechanisms, differing in how the borohydride source delivers a '*hydride*' fragment to the Pt^{IV} center, were proposed:

(a) Involves concerted transfer of H^- directly to the Pt^{IV} center via σ-bond metathesis with the Pt^{IV}-bound axial OH ligand to form **5.6** which can then undergo 'usual' deprotonation by methanol to generate the Pt^{II} complex, **5.5**. Although $LPt^{IV}(H)$ complexes similar to **5.6** have been synthesized by Puddephatt et al [85] by direct reaction of a $LPt^{IV}(Me_3)(OTf)$ complex with $NaBH_4$, it did not undergo reductive elimination to form any Pt^{II} product, the stability of the latter being ascribed to the presence of a Pt-Me fragment trans to the Pt-H. Thus, in the presence of a weakly trans-influencing ligand such as the B-μ-OCH_3-Pt fragment in **5.6**, deprotonation may be viable. Alternatively, **(b)** involves a sequential B-to-B and B-to-Pt *hydride* delivery. Although examples of metathetic comproportionation involving B-to-B hydride scrambling have been reported in literature [86], they involve association of tetracoordinate R_3BH^- with tricoordinate alkylboranes to produce alkylhydridoborates. Based on our experimental findings of the difficulty in breaking B-OMe bonds in non-acidic solutions, disfavoring the formation of a di(2-pyridyl)-B-methoxyborane moiety ligated to the Pt^{IV} center under current alkaline conditions, both front-side and back-side attack of the *hydride*, leading to **5.7''** or **5.7** might be extremely endergonic. An empirical test of substitution of a B-bound OCH_3 fragment by a B-H fragment was performed. The di(2-pyridyl)(methoxo)(methyl) borate

ligand, **3.1** (c.f. Chapter-III), was dissolved in CD_3OD and 2 equivalents of $NaBH_4$ and THF as internal standard was added to it. Based on the ^{1}H-NMR spectra recorded after 1 hour, no new B-H signals indicative of new product was observed. On the other hand, dihydrocarbylborohydrides are more reactive towards protonolysis [87], so the absence of new B-H signals does not necessarily rule out installation of a *hydride* on the ligated $Py_2B(OMe)_2$ to form **5.7'** or **5.7''**, i.e. mechanism (a). Closely related, stable bis(pyrazolyl)dihydridoborato-Pt^{IV} complexes have been reported in literature [88], however, only those featuring a Pt-Me trans to the B-μ-H-Pt could be isolated. In our case, with an axial OMe (in **5.6**) or OMe (in **5.7''**) ligand trans to the Pt^{IV}-H fragment, deprotonation might be viable, leading to the Pt^{II}-complex, **4.35**. It is interesting to note at this point that attempts to reduce **4.17** with even 1 equivalent of $NaBH_4$ in THF-d_8 led to complete destruction of the complex within 10 minutes, formation of >1 equivalent amounts of benzene and copious amounts of Pt^0. Regardless of the mechanism of *hydride* delivery, the different outcomes of the reaction performed in THF-d_8 and CD_3OD suggests that the putative Pt^{IV}-H complex, in the absence of methanol, reductively eliminates benzene to form an unstable three-coordinate Pt^{II}Ph complex, leading to decomposition. Similar observations have been reported by Bennett et al for Pt^{II}(Ph)(H) complexes [89].

5.2.4 Attempted preparation of diisopropoxy derivatives of di(2-pyridyl)dimethoxoborate-supported $Pt^{II}Ph_2$, 4.35, and $Pt^{IV}(Ph_2)(OH)$, 4.17 complexes

Scheme 5.6: Susbtitution of B-bound methoxy fragments in di(2-pyridyl)dimethoxyborato-Pt complexes

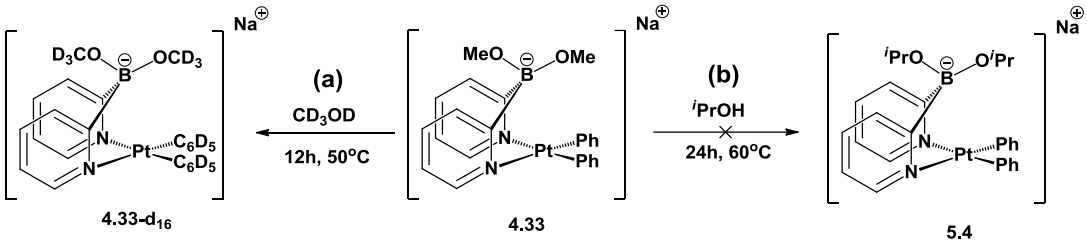

As discussed before, substitution of either B-bound OCH_3 fragments in **4.17** with OCD_3 was slow in CD_3OD even at elevated temperatures of 80 °C. On the other hand similar exchange for the Pt^{II}Ph2 complex, **4.33**, was more facile, as shown in Scheme 5.6(a), with complete conversion to **4.33-*d_{16}*** in CD_3OD in 12h at 50 °C. Therefore in order to observe a diisopropylborate variant **5.4**, it was imperative to attempt reaction of **4.33** with isopropanol, as shown in Scheme 5.6(b). To our disappointment, **4.33** (with admixed $NaB(OMe)_4$) dissolved in isopropanol showed no exchange of the B-bound OCH_3 for O^iPr even after heating at 60 °C for 24h. When the solution was warmed further to 80 °C, black precipitate formed, indicating decomposition. An ESI^--MS on an aliquot of the reaction mixture did not show signals at 606.2 or 634.2 which would suggest replacement of one or two B-bound OCH_3 fragments with O^iPr fragments.

Scheme 5.7: Attempted synthesis of di(2-pyridyl)diisopropoxyborato-$Pt^{IV}(Ph_2)(OH)$ complex

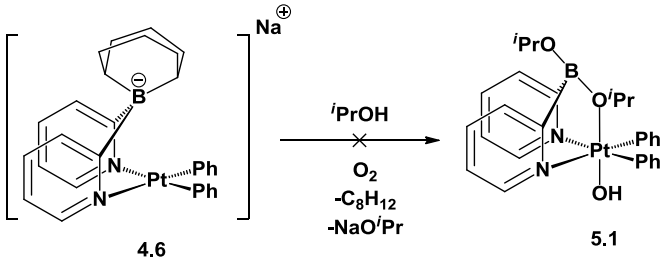

We then attempted to synthesize the diisopropylborate variant of the $Pt^{IV}(Ph_2)(OH)$ complex, i.e. **5.1**, via aerobic oxidation of the di(2-pyridyl)-1,5-cyclooctanediylborato-$Pt^{II}Ph_2$ complex, **4.6** in isopropanol, as shown in Scheme 5.7. As opposed to the rapid aerobic oxidation of **4.6** in methanol which yields clean formation of di(2-pyridyl)dimethoxyborato-$Pt^{IV}(Ph_2)(OH)$, the oxidation of **4.6** performed in isopropanol with O_2 produced an intractable mixture of products and further attempts to isolate diisopropoxoborate Pt^{II}/Pt^{IV} variants were discarded. We presumed that the higher steric bulk imposed by two isopropoxy fragments severely hindered the formation of **5.1**. Owing to the higher thermal stability of the $Pt^{IV}(Ph_2)(OH)$complex, **4.17**, catalytic oxidation of isopropanol was attempted directly, with di(2-pyridyl)-dimethoxyborato-$Pt^{IV}(Ph_2)(OH)$, **4.17**, as pre-catalyst, in the hope that the aforementioned substitution would happen in-situ to generate the active catalyst, by substitution of one or more methoxy for isopropoxy fragments on the boron center.

5.3 Results and Discussion

5.3.1 Catalytic aerobic oxidation of $NaBH(OMe)_3$ and $NaBH_4$

Based on the success of reducing the $Pt^{IV}Ph_2$ complex, **4.17** and re-oxidizing **4.35-*d_{16}*** in the same pot, we decided to investigate the possibility to use **4.17** as a catalyst in the conversion of a '*hydride*' source into '*proton*' source. To the best of our knowledge, *homogenous*, *aerobic* and *catalytic* conversion of $NaBH_4$ or $NaBH(OMe)_3$ to $NaB(OMe)_4$ is hitherto unreported. As such, catalytic conversion of borohydrides to '*inorganic*' borates, which have great potential in fuel cell

applications [90] are typically carried out by mixed-metal oxides [91] or by electro-catalysis [92] in protic solvents. A limiting factor for such applications is uncontrolled protonolysis of the B-H fragment leading to unwanted H_2 gas evolution [93], the extent of which could be reduced by establishing a faster oxidation process [94]. Since the oxidation of the di(2-pyridyl)dimethoxyborate-supported $Pt^{II}Ph_2$ complex, **4.35**, was rapid, we felt it pertinent to explore the viability of using our $Pt^{IV}(Ph_2)(OH)$ complex, **4.17**, as a catalyst in the aerobic oxidation of $NaBH_4$ or any other borohydride reagent. If the least reactive $NaBH(OMe)_3$ could also be catalytically converted to $NaB(OMe)_4$, there is no doubt that similar catalysis would also work for $NaBH_4$, given the fact that attempts to reduce **4.17** in methanol by both were successful. In order to suppress decomposition of **4.17** immediately after addition of $NaBH_4$, catalytic oxidations of $NaBH_4$ were performed with two-fold excess of NaOMe added, based on the known effect of alkalinity on the protolytic stability of $NaBH_4$ [95].

100 mg of $NaBH(OMe)_3$ (0.78 mmol in $[H^-]$) or 5 mg of $NaBH_4$ (0.54 mmol in $[H^-]$), with 2 equivalents of NaOMe in the latter case, were dissolved in CD_3OD in an NMR tube, and appropriate amounts of **4.17** were added with THF as internal standard. The NMR-tube was quickly exposed to 16 psi of O_2, and reaction progress was monitored at intervals of 1h. TONs/h were calculated by integrating residual 'B-H' resonances (q+sept., -0.18 ppm) with respect to THF signal intensity. The decrease in integral intensity corresponding to the B-H resonance was correlated to the increase in the $CD_3O\mathit{H}$ signal intensity. A similar experiment was performed in the absence of O_2 to correct for the slow background methanolysis and H/D exchange of the BH fragment.

The TOF of at about 178/hour was observed for $Na[BH(OMe)_3]$ with 0.5 mole % catalyst loading and 216/hour for $NaBH_4$ with 1.66 mole % catalyst loading. Note that catalyst mole % was calculated based on the number of oxidizable BH fragments in the substrate. Consistent with the presence of continuous supply of excess O_2 and fast oxidation of the $Pt^{II}Ph_2$ complex **5.5**, when $NaBH(OMe)_3$ or $NaBH_4$ was completely oxidized after 1 hour, the only Pt-containing species observed in solution by ^{1}H-NMR spectroscopy was **4.17-*d_{17}***.

Table 5.1. The catalytic performance of complex **4.17** in the oxidation of $Na[BH(OMe)_3]$ with O_2 (1 atm) in 0.8 mL CD_3OD at 22 ^oC; reaction time is 1.0 hour.

#	$Na[BH(OMe)_3]$, mg	Catalyst **4.17**, mole %	Conversion of $Na[BH(OMe)_3]$, %	TON
1	50.0	-	3.2	-
2	100.0	0.5	92.2	178[a]
3	50.0	1.0	100	97[a]
4	50.0	2.15	100	45[a]

[a] The value is corrected for the contribution of the background reaction.

Table 5.2. The catalytic performance of complex **4.17** in the oxidation of $NaBH_4$ with O_2 (1 atm) in 0.6 mL CD_3OD at 22 ^oC; reaction time is 1.0 hour.

#	$NaBH_4$, mg	Catalyst **4.17**, mole %	NaOMe added	Conversion of $NaBH_4$, %	TON
1	5	-	14.2	10.1	-
2	5	1.66	14.2	100	216[b]
4	5	5	14.2	100	71.9[b]

[b] The value is corrected for the contribution of the background reaction, TONs reported are based on 4 oxidizable Hydrides in $NaBH_4$.

5.3.2 Catalytic oxidation of isopropanol by di(2-pyridyl)dimethoxyborato-$Pt^{IV}(Ph_2)(OH)$

Selective oxidation of alcohols is extremely important for the synthesis of commodity chemicals and intermediates [96]. Typically, oxidation of alcohols involve use of halogenated solvents [97], as well as use of waste-producing stoichiometric oxidants [98]. An ideal system could involve water or even the alcohol being oxidized as solvent and O_2 as oxidant. Although there have been reports involving both [99], the role of O_2 is not fully understood. Very few examples of aerobic oxidation of alcohols without the need of sacrificial H_2 acceptors exists [100]. With our new ligand at hand, and DFT predicted appreciable activation energy barrier (of agostic C-H deprotonation) calculated, we decided to explore aerobic oxidation of isopropanol with **4.17** as a catalyst. As **4.17** was not appreciably soluble in isopropanol, a solution of it in 1:1 THF : isopropanol v/v mixture in a Schlenk flask was exposed to 30 psi O_2 and the solution was immersed in an oil bath at 80 °C (t=0). The reaction was monitored by recording ^{1}H-NMR spectra of aliquots every 2h initially. Since no acetone was found to have formed in 8h, the reaction was hence forth monitored every 24h, as shown in Figure 5.4. According to NMR, at t=32h, a singlet resonance at 2.1 ppm was visible. At t=56h, by integrating the signal w.r.t to THF, a TON of 3.8 was calculated. An ESI^+-MS recorded on an aliquot taken from the reaction vessel after this time period showed, in addition to a major signal at 596.1 corresponding to **4.17**H^+, a small peak at 624.1 corresponding to substitution of *one* B-bound OCH_3 fragment by a O^iPr fragment, i.e **5.8** (c.f. Scheme 5.8, Figure 5.2). Owing to significant decomposition evident in the aromatic region of the NMR spectrum

suggestive of catalyst decomposition, consistent with trace amounts of benzene at t=56h, the reaction was not monitored further. The presence of acetone was confirmed by comparing NMR spectra before and after adding an external authentic sample of acetone. Acetone was detected as a peak at 59.1 corresponding to an H^+-adduct by DART-ESI^+-MS of an aliquot of the reaction mixture, as shown in Figure 5.5. No acetone was detected by ^{1}H-NMR in a control experiment with a 1:1 THF-d_8 : isopropanol v/v mixture heated at 80 °C for 4 days under 30 psi pressure of O_2. A plot of moles of acetone formed versus time is depicted in Figure 5.4

Figure 5.4: ESI^+-MS spectrum of an aliquot of the reaction mixture showing in addition to a signal at 596.1 corresponding to **4.17**H^+, another small signal at 624.1 corresponding to **5.8**H^+:

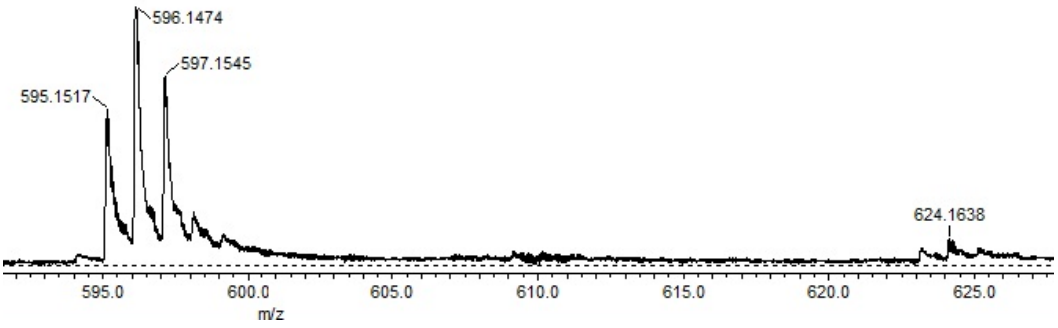

Figure 5.5: DART-ESI^+-MS spectrum of an aliquot of the reaction mixture:

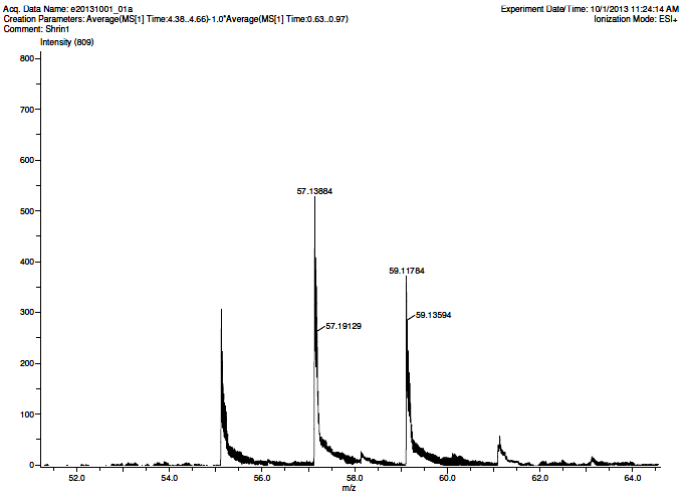

Figure 5.6: Plot of TONs of acetone and benzene over time:

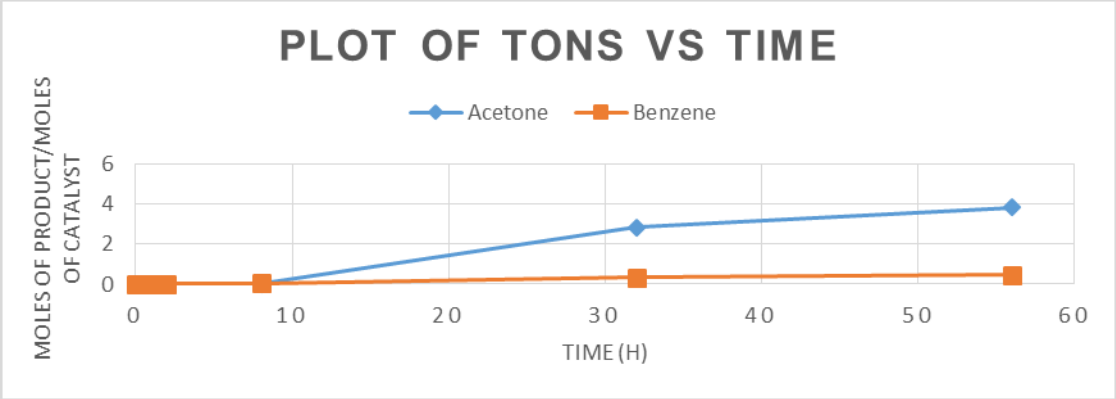

5.3.3 Mechanism of aerobic oxidation of isopropanol

Scheme 5.8: Proposed mechanism for the catalytic oxidation of isopropanol: $Me_2CHOH + 0.5\ O_2 \rightarrow Me_2CO + H_2O$

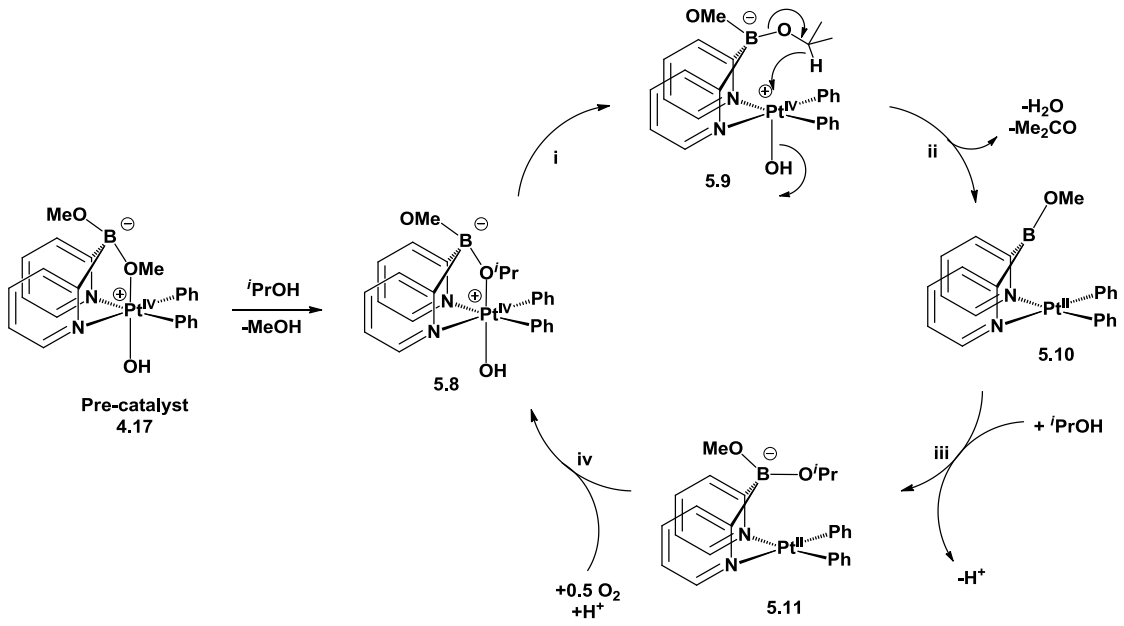

According to the proposed mechanism, shown in Scheme 5.8, **5.8** undergoes cleavage of the Pt^{IV}-O^{i}Pr bond, in step (i) to form a transient 2 °CH-agostic complex, **5.9**. Based on the preference for *O*-atom ligation over agostic C-H bonds towards sufficing as the sixth axial coordination site on octahedral Pt^{IV} centers (c.f. Scheme

3.4), we presume this step to be the most endergonic and hence the rate-liming step in the catalytic cycle. A C-H to Pt^{IV} *hydride migration* similar to that discussed in Scheme 5.2, via elimination of water (step (ii)) leads to the formation of acetone and the neutral Pt^{II} complex, **5.10**. In order for aerobic oxidation to take place, the anionic borate center is replenished by iPrOH to generate **5.11** and one mole of proton (step (iii)). The proton can be shuttled back to aid in the oxidation, step (iv), to regenerate the active catalyst species, **5.8**, thus completing the cycle.

Based on the observation of an induction period of 8h, and failure to synthesize complexes **5.1** or **5.3**, we presumed that the initiation of the catalytic reaction includes the formation of the catalytically active species, **5.8**, via the initial displacement of the B-bound OMe fragment in **4.17**. Thus in order to achieve higher TONs, the Pt^{IV} center has to be modified appropriately to facilitate Pt^{IV}-O^{i}Pr bond cleavage, which may be achieved by replacing the Pt^{IV}-bound phenyl groups by bulkier aryls.

5.4 Conclusions

The di(2-pyridyl)dimethoxyborate ligand is the first borate ligand capable of resisting degradation while enabling aerobic oxidation of derived organo-Pt^{II} complexes. We found that supported $Pt^{IV}(Ph_2)(OH)$ complexes are able catalysts in the aerobic oxidation of both $NaBH_4$ and $NaBH(OMe)_3$ in high TOFs of ~200. To the best of our knowledge, *homogenous, aerobic* and *catalytic* conversion of $NaBH_4$ or $NaBH(OMe)_3$ to $NaB(OMe)_4$ is hitherto unreported. As opposed to a direct borohydride fuel cell, which operates at high temperaures of >70 °C, the catalysis reported herein operates at ambient temperatures at pressures of O_2 slightly more than

atmospheric. No adverse effects of alkalinity, which was maintained to retard background protonolysis of borohydrides, was observed.

Furthermore, the di(2-pyridyl)dimethoxoborato-$Pt^{IV}(Ph_2)(OH)$ complex was found to be involved in the catalytic aerobic oxidation of isopropanol. Although TONs achieved were low and TOFs lower, appropriate Pt-centered modifications might allow for a more efficient alcohol oxidation catalyst.

5.5 Experimental Section

5.5.1 Preparation of di(2-pyridyl)dimethoxyborato-$Pt^{II}Ph_2$ complex, 4.33:

25 mg of **4.17** (42 µmol) was dispersed in 2 mL of methanol. To this suspension was added 5mg $NaBH_4$. After stirring for 1h, the mixture was filtered through a PTFE syringe filter and the filtrate was stripped to dryness to obtain 30 mg of a tan colored solid. A ^{1}H-NMR and ESI-MS of the crude product confirmed the identity of **4.33**. **4.33** could not be obtained in analytically pure form owing to a large amount of $NaB(OCH_3)_4$ which could not be removed from the sample even after attempted recrystallization from THF: heptanes mixture or attempts to selectively extract **4.33** with various solvents.

^{1}H NMR (22 °C, 400 MHz, acetone-d_6, ppm) δ:
6.49 (vt, 2H, *J*=7.5 Hz, Ph-p-CH), 6.57-6.71 (m, 6H, Ph-m-CH (4H), py-5-CH (2H)), 7.38 (td, 2H, *J*=7.7, 1.7 Hz, py-4-CH), 7.6 (d+Pt-satellites, 4H, *J*=7.7 Hz, J_{Pt-H}=~63 Hz, Ph-o-CH), 7.76 (d, 2H, *J*=8.4 Hz, py-3-CH), 8.41 (d+unresolved Pt-satellites, 2H, *J*=5.9 Hz, py-6-CH)

^{1}H NMR (22 °C, 400 MHz, CD_3OD, ppm) δ: 3.35 (br, $B(OMe)_2$+$NaB(OMe)_4$), 6.6 (vt, *J*=7.2 Hz, 2H, p-Ph), 6.75 (m, 6H, m-Ph(4H)+py-4-CH(2H)), 7.48-7.58(m, 6H, o-Ph+py-4-CH), 7.73 (d, 2H, *J*=8.6 Hz, py-3-CH), 8.43 (d+unresolved-Pt-satellites, 2H, py-6-CH).

ESI- (of methanolic solution): 578.18, Calculated: 578.16

5.5.2 Preparation of di(2-pyridyl)dimethoxyborato-$Pt^{II}(C_6D_5)_2$ complex, 4.33-d_{16} by reduction of 4.17

A sealable NMR-tube was charged with 15mg of **4.17** (25.2 µmol) and 3.0 mg $NaBH_4$ (79.3 µmol). To this was added 0.7 mL of CD_3OD cooled to -20 °C and the NMR-tube was shaken. Slow bubbling and formation of trace amounts of Pt-black was seen. The reaction mixture was monitored by ^{1}H-NMR using THF present in the sample as internal standard and reaction was found to be complete in 90 minutes. According to NMR, 83% of all starting material was converted to **4.33-d_{16}**. The mixture was then filtered through a PTFE-syringe filter to obtain a clear light-yellow

filtrate. An ESI-MS (negative mode) was recorded using 0.1 mL aliquot of the filtrate. The rest of the filtrate was saved in an NMR tube for the purpose of oxidation.

4.33-d_{16} ^{1}H NMR (22 °C, 400 MHz, CD_3OD, ppm): δ: 6.74 (td, 2H, *J*=5.8, 1.8 Hz, py-5-CH), 7.50 (td, 2H, *J*=7.2, 1.8 Hz, py-4-CH), 7.7 (d, *J*=7.8 Hz, py-3-CH), 8.4 (d+unresolved Pt-satellites, 2H, py-6-CH)

ESI^- (of CD_3OD solution): 594.19, Calculated: 594.16

5.5.3. In-situ oxidation of 4.33-*d_{16}* to 4.17-*d_{17}*. O_2 was bubbled through the NMR solution obtained from (A) for a period of 10 minutes and an NMR was recorded. According to NMR, **4.17-*d_{17}*** was formed in 83% yield. Some benzene, presumably from decomposition, was seen in the NMR spectrum. ESI-MS was recorded of the filtrate.

ESI^+ (of CD_3OD solution): **4.17-*d_{17}*·**H: 612.19, Calculated: 612.17

5.5.4. Direct oxidation of 4.6-*d_{10}* to 4.17-*d_{17}* and 4.18. 15 mg of **4.6** was dissolved in CD_3OD and stored in a sealed NMR-tube for 8h as mentioned before. After 8h a ^{1}H-NMR was recorded to confirm complete deuteration of the $PtPh_2$ fragment. At this point, O_2 was bubbled through the solution for a period of 10 minutes and a ^{1}H-NMR was recorded. According to NMR, complete conversion of **4.6-*d_{10}*** to **4.17-*d_{17}*** had occurred and the spectra was found to be a match with the product of oxidation of **4.33-*d_{16}*** viz. **4.17-*d_{17}***. Signals corresponding to bicyclo[3.3.0]oct-1-ene were found to match to those observed in the experiment where **4.6** was oxidized prior to deuteration of the $PtPh_2$ fragment.

5.5.5 Catalytic oxidation of $NaBH_4$ and $NaBH(OMe)_3$:

Oxidation of $Na[BH(OMe)_3]$

(50.0 mg; 0.391 mmol) was performed with 0.5, 1.0, and 2.0 mole % catalyst 12 loading in 0.8 mL CD_3OD with THF as internal standard. Catalyst was weighed out, dissolved in 0.3 mL CD_3OD and appropriate amount of $NaBH(OMe)_3$ (see Table below) as a solution in 0.3 mL CD_3OD were combined under argon atmosphere. Oxygen gas was admitted into the reaction mixture which was stirred vigorously in a 5 mL Schlenk flask. An ^{1}H NMR spectrum was recorded before introducing O_2 and after 1h of the reaction. The decrease in the integral intensity corresponding to the BH fragment of $[BH(OMe)_3]^-$ (q+sept., -0.18 ppm) matched the increase in the $CD_3O\mathit{H}$ signal intensity. A similar experiment was performed in the absence of O_2 to correct for the slow background methanolysis and the H/D exchange of the BH fragment.

Oxidation of $NaBH_4$ was similarly performed. A stock solution of 76 mg catalyst in 3 mL CD_3OD containing THF as internal standard was prepared, appropriate amounts of this solution was added to a 5 mL Schlenk flask containing 5mg (0.132 mmol $NaBH_4$), with added 14.2 mg of NaOMe in each run to suppress protonolysis of $NaBH_4$.

A similar experiment was performed in the absence of O_2 to correct for the slow background methanolysis and the H/D exchange of the BH fragment.

The TOF of at about 178/hour was observed for $Na[BH(OMe)_3]$ with 0.5 mole % catalyst loading and 216/hour for $NaBH_4$ with 1.66 mole % catalyst loading.

Figure 5.7: Representative ^{1}H-NMR spectra for the monitoring of aerobic oxidation of $NaBH_4$:

(a) immediately after combining catalyst **4.17** (1.66 mole%) and $NaBH_4$, showing B-H signals:

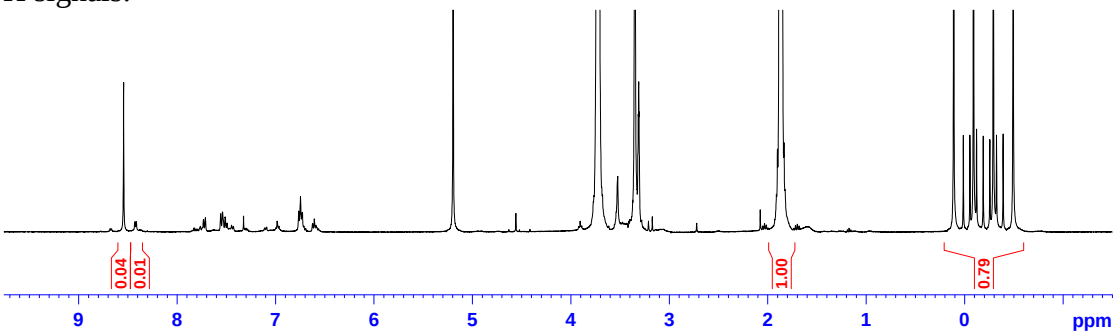

(b) 1h after admitting O_2 to (a), showing complete depletion of B-H signals

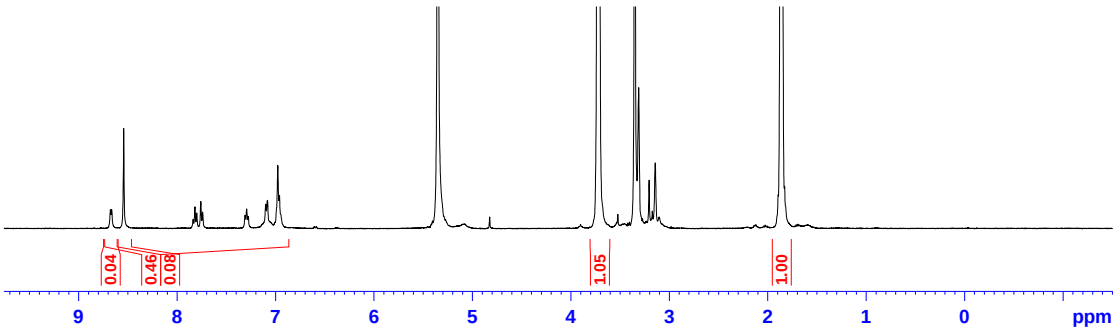

(c) immediately after combining catalyst **4.17** (2 mole%) and $NaBH(OMe)_3$, showing B-H signals:

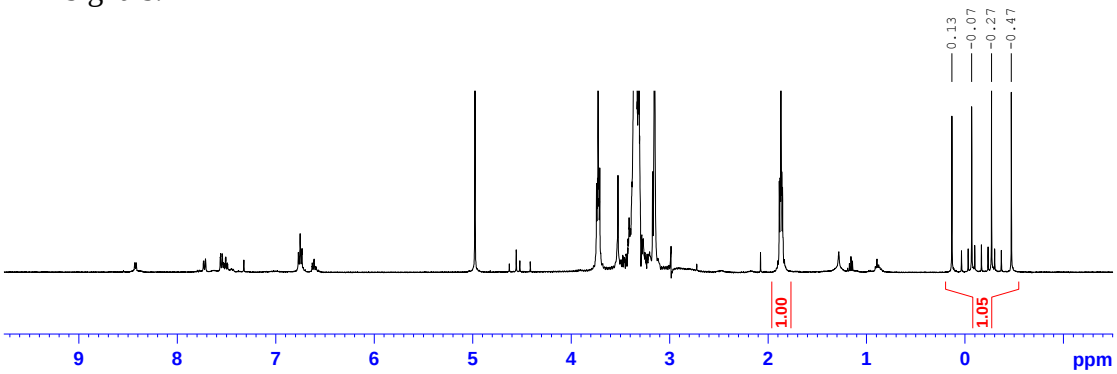

(d) 1h after admitting O_2 to (c), showing complete depletion of B-H signals

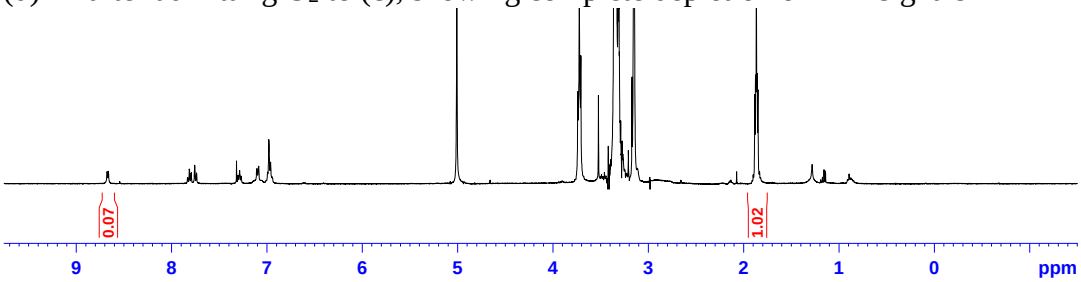

5.5.6: Catalytic aerobic oxidation of isopropanol:

78 mg of **4.17** (131 µmol) was charged into a 25 mL Schlenk flask in the glove-box. To this was added a 2mL equimolar solution of THF:^{i}PrOH. A 25 µL aliquot was taken out, and the Schenk flask was freeze pumped to remove Argon, following which it was filled with O_2 at 30 psi pressure and Teflon sealed. The iimediate aliquot was dissolved in $CDCl_3$, and a ^{1}H-NMR spectra was recorded, and referenced at t=0. The mixture was immersed in an oil-bath maintained at 80 °C. 25 µL aliquots were taken out at 1, 2, 8, 32, and 56 h with similar periodic monitoring. Acetone in moles was calculated based on THF signals corresponding to the sample. At t=8 h, when the first traces of acetone were seen, the NMR solution in $CDCl_3$ was analyzed by ESI-MS. At t=56 h, based on THF integral intensity, 8% catalyst survived. TON was calculated to be 3.8 with a corresponding TOF of 0.06/h. At this point the sample was analyzed by DART-MS. ^{1}H-NMR signals could not be reliably integrated due to dilution.

^{1}H NMR (22 °C, 400 MHz, $CDCl_3$, ppm) δ:

<u>Before oxidation:</u>

6.68 (vt), 6.74 (overlapping multiplet), 6.78 (t), 6.95 (m), 7.40 (m), 7.55 (m), 7.75 (d), 8.45 (d)

<u>After Oxidation (80 °C, t=56h):</u>

Major species: 6.98 (m), 7.25-7.29 (overlapping with $CDCl_3$), 7.33 (C_6H_6), 7.42 (t), 7.57 (m), 8.58 (m)

Minor species: 7.08(m), 7.46, 7.74, 7.96(t), 8.41, 8.66 (d)

Appendix

^{13}C NMR (22 °C, 500 MHz, CD_3CN, ppm) spectrum of (dpdmb)Pt^{II}(Me)(SMe_2), 2.9

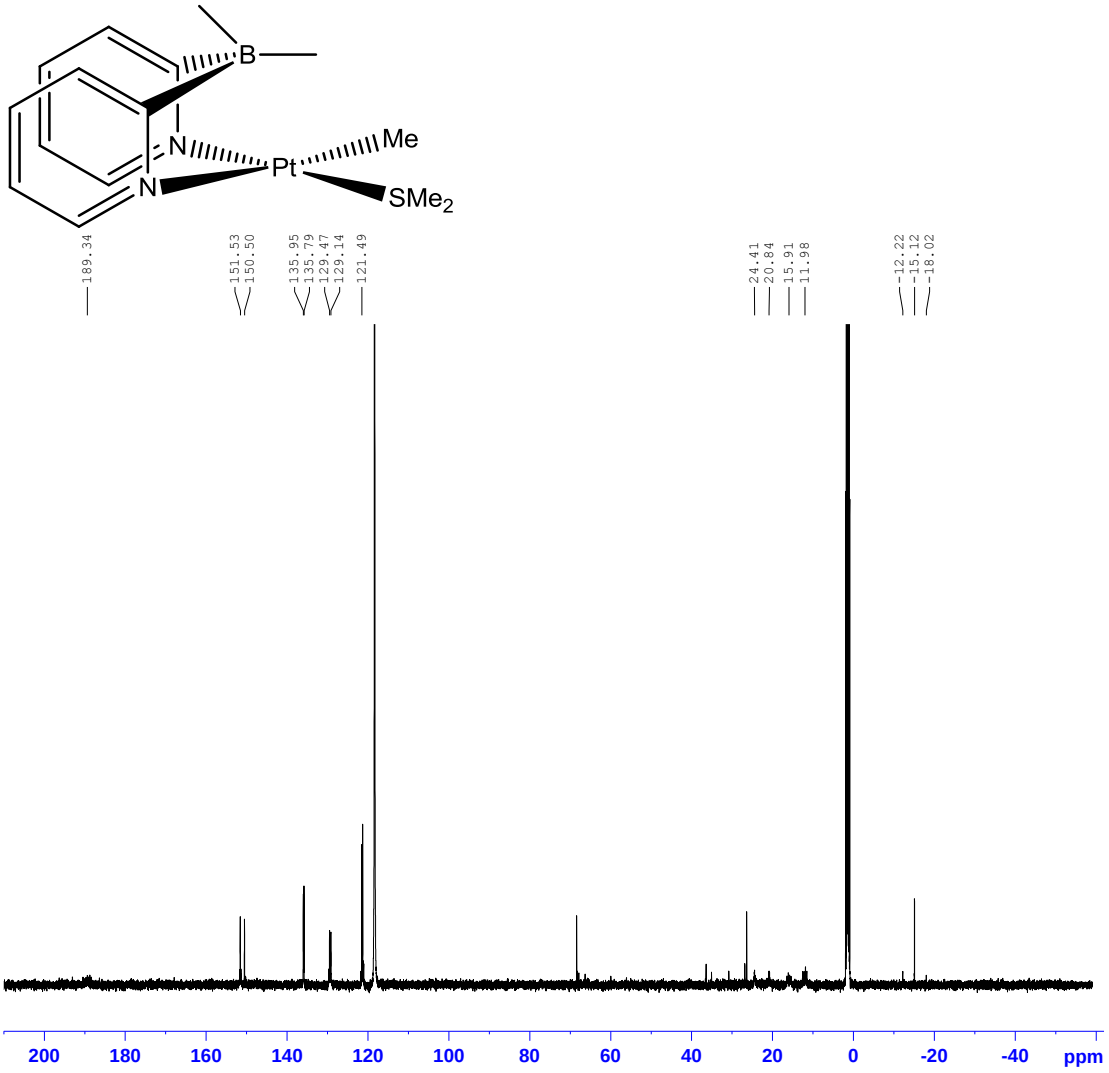

^{13}C NMR (22 °C, 500 MHz, acetone-d_6, ppm) spectrum of [(dpdmb)Pt^{II}(SMe$_2$)(NCMe)](BF$_4$) complex, 2.11

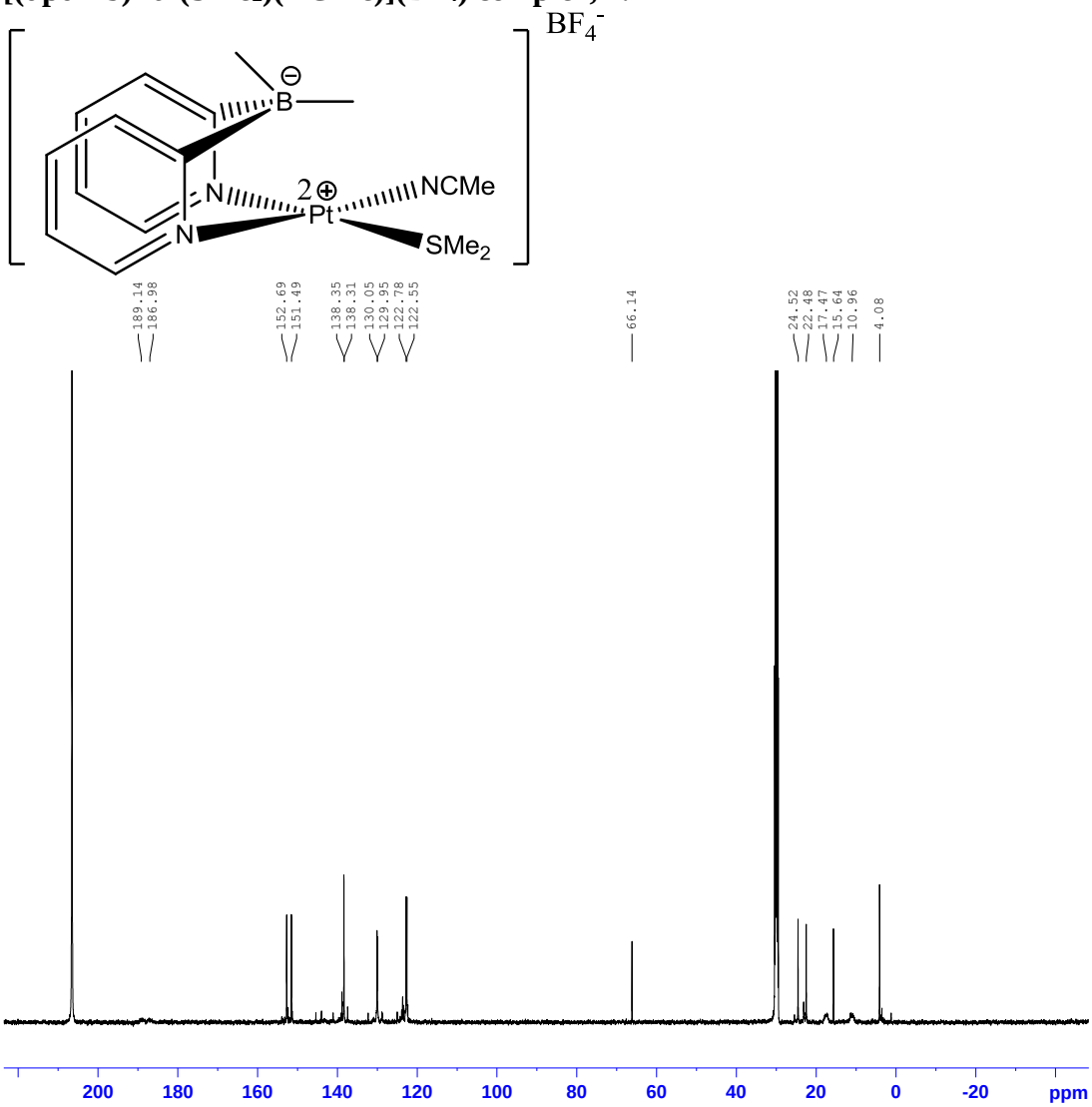

^{13}C NMR (22 °C, 500 MHz, acetone-d_6, ppm) spectrum of [(MeO-mdpb)Pt^{IV}Me$_2$(SMe$_2$)]OAc, 2.14

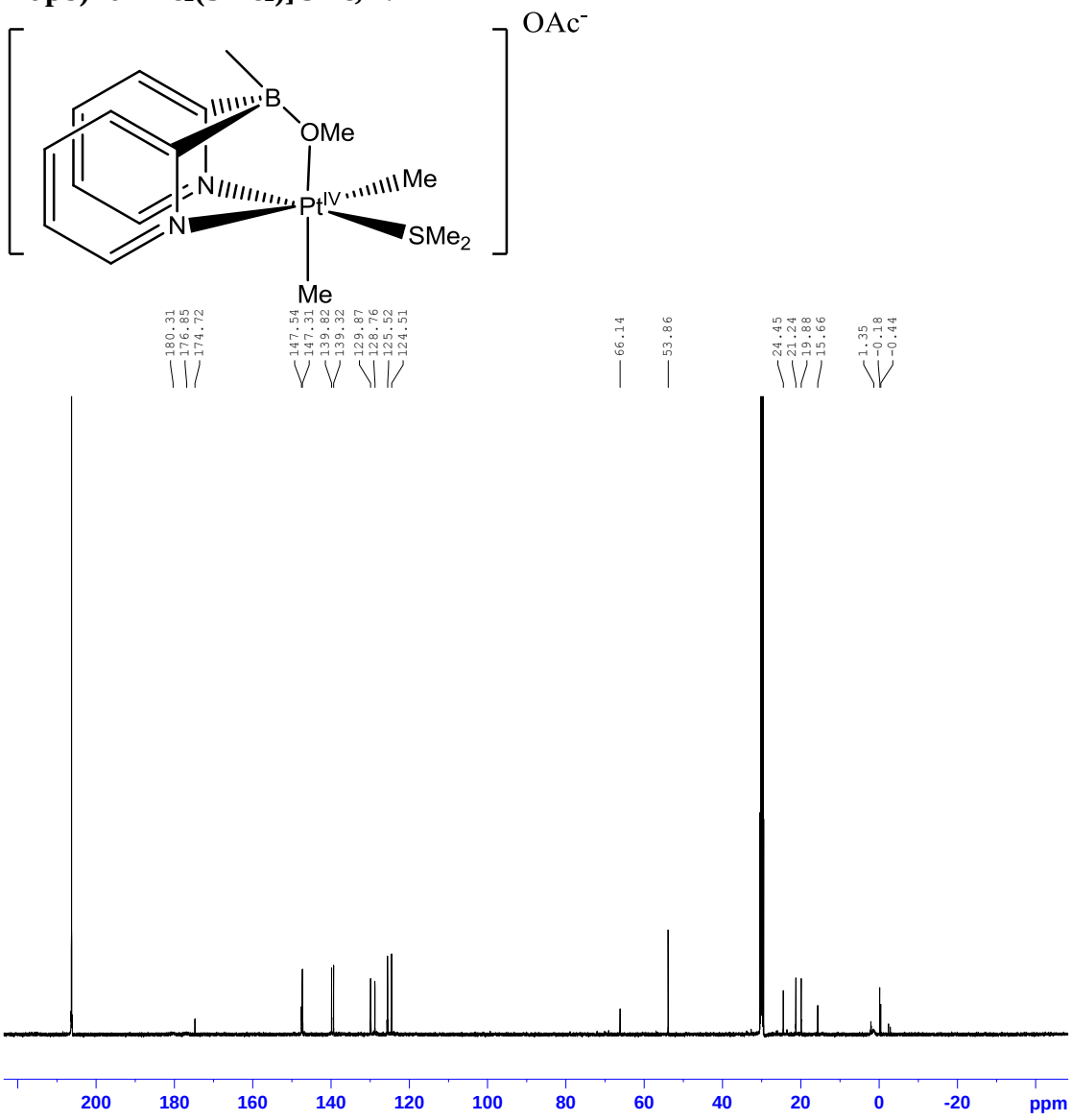

^{1}H-NMR (22 °C, 500 MHz, DMSO-D$_6$, ppm) spectrum of sodium (Me)(MeO)BPy$_2$, 3.1

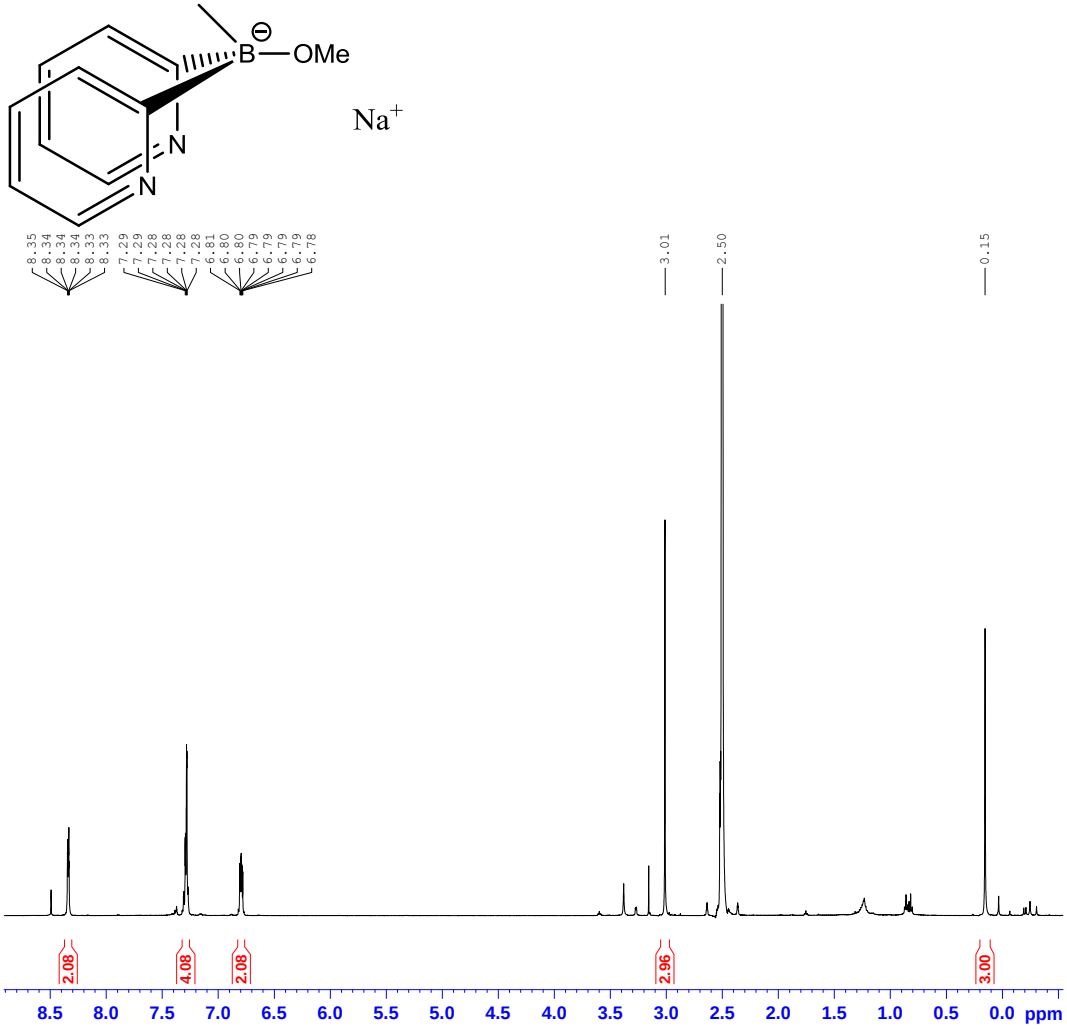

^{13}C-NMR (22 °C, 500 MHz, DMSO-D$_6$, ppm) spectrum of sodium (Me)(MeO)BPy$_2$, 3.1

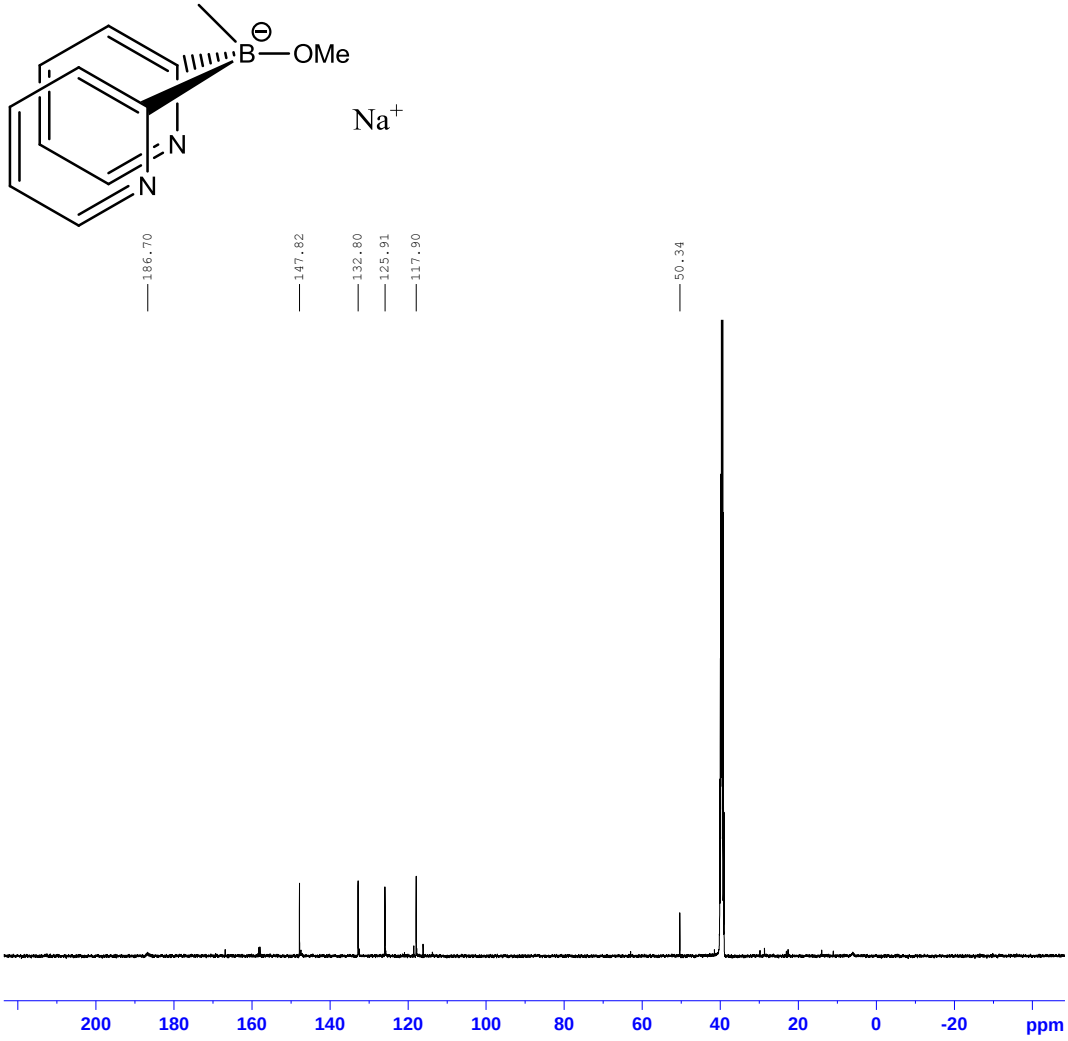

^{13}C-NMR (22 °C, 500 MHz, CD_3CN, ppm) spectrum of sodium (methoxy)(methyl)di(2-pyridyl)borato-$Pt^{II}Me_2$ complex, 3.5

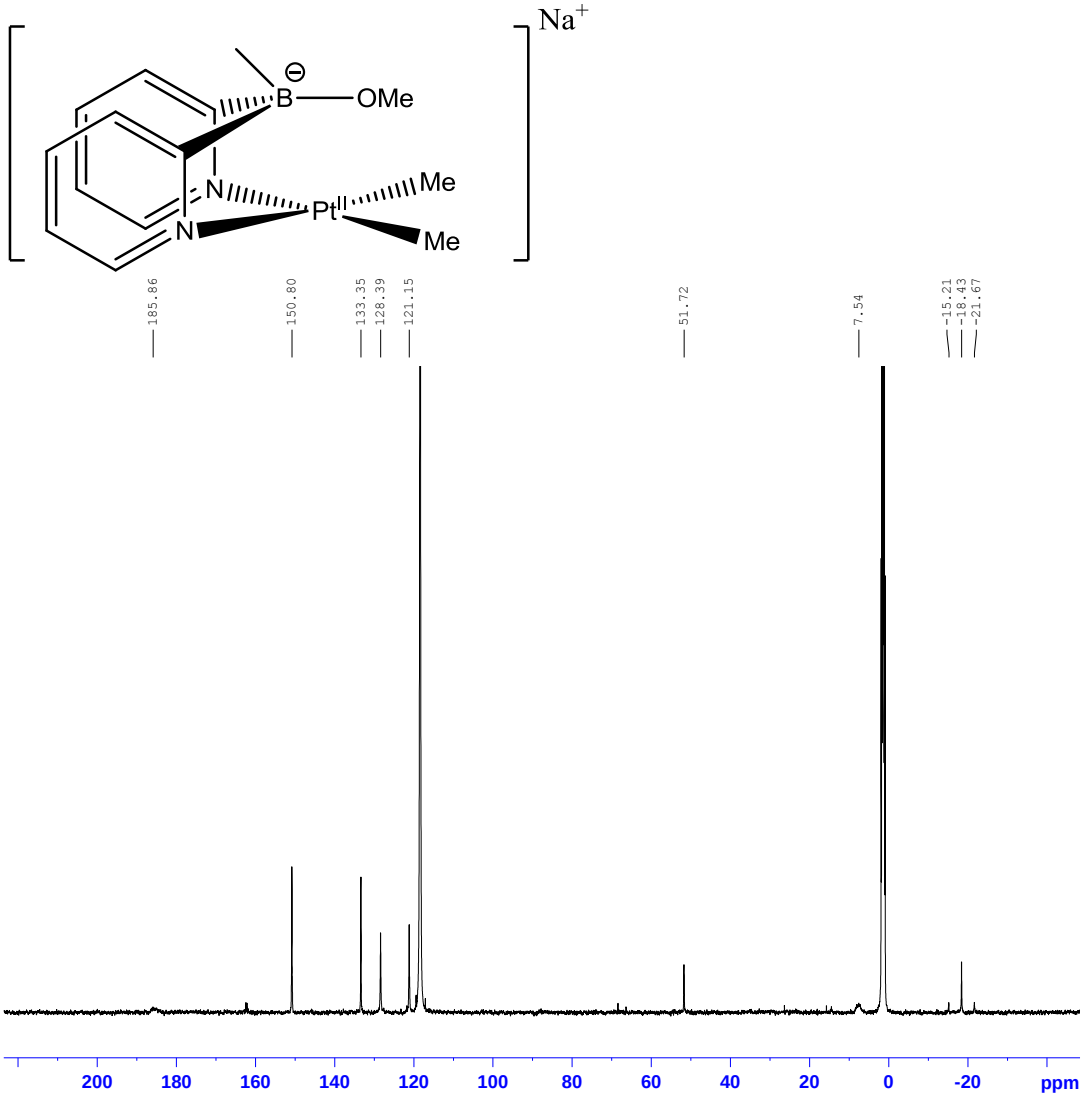

^{1}H-NMR (22 °C, 500 MHz, $CDCl_3$, ppm) spectrum of (methoxy)(methyl)di(2-pyridyl)borato-Pt^{IV}Me$_3$ complex, 3.7

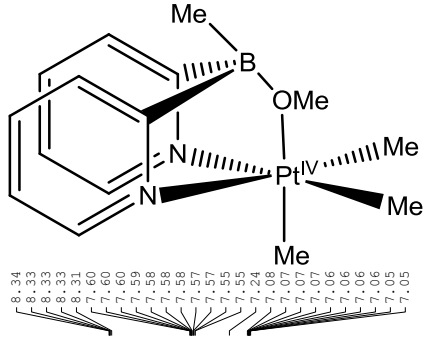

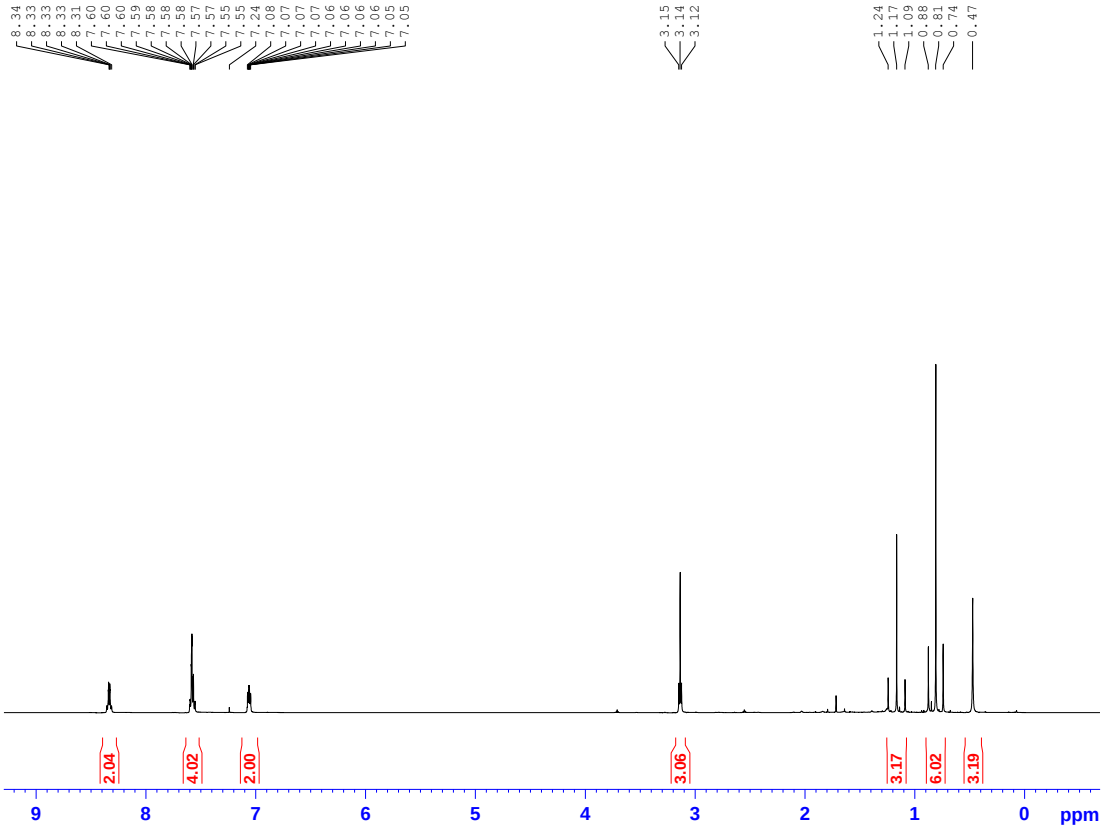

^{13}C-NMR (22 °C, 500 MHz, $CDCl_3$, ppm) spectrum of (methoxy)(methyl)di(2-pyridyl)borato-$Pt^{IV}Me_3$ complex, 3.7

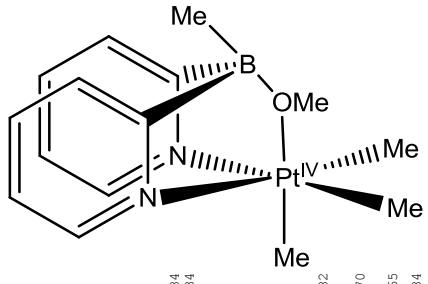

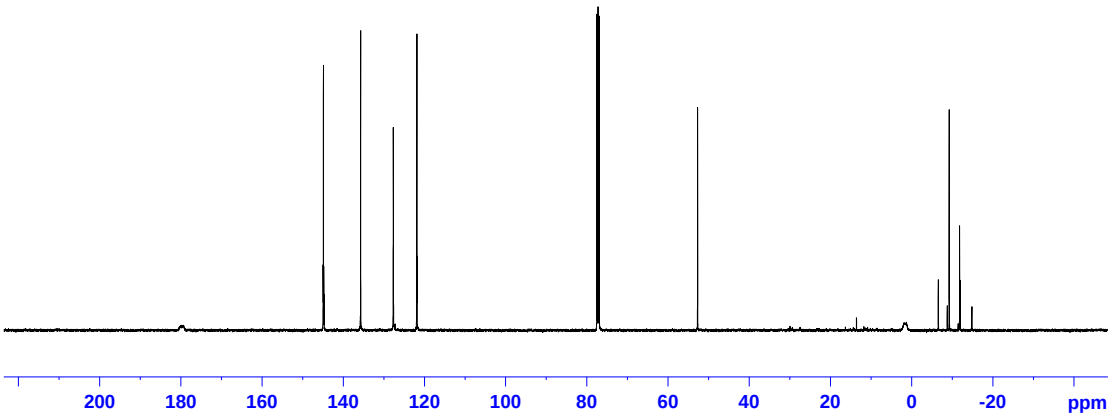

^{1}H NMR (22 °C, 500 MHz, DMSO-D$_6$, ppm) spectrum of hydrogen-di(2-pyridyl)-1,5-cyclooctanediylborate(L), LH·HCl, 4.2

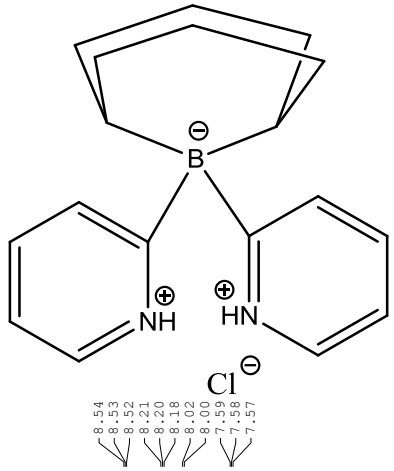

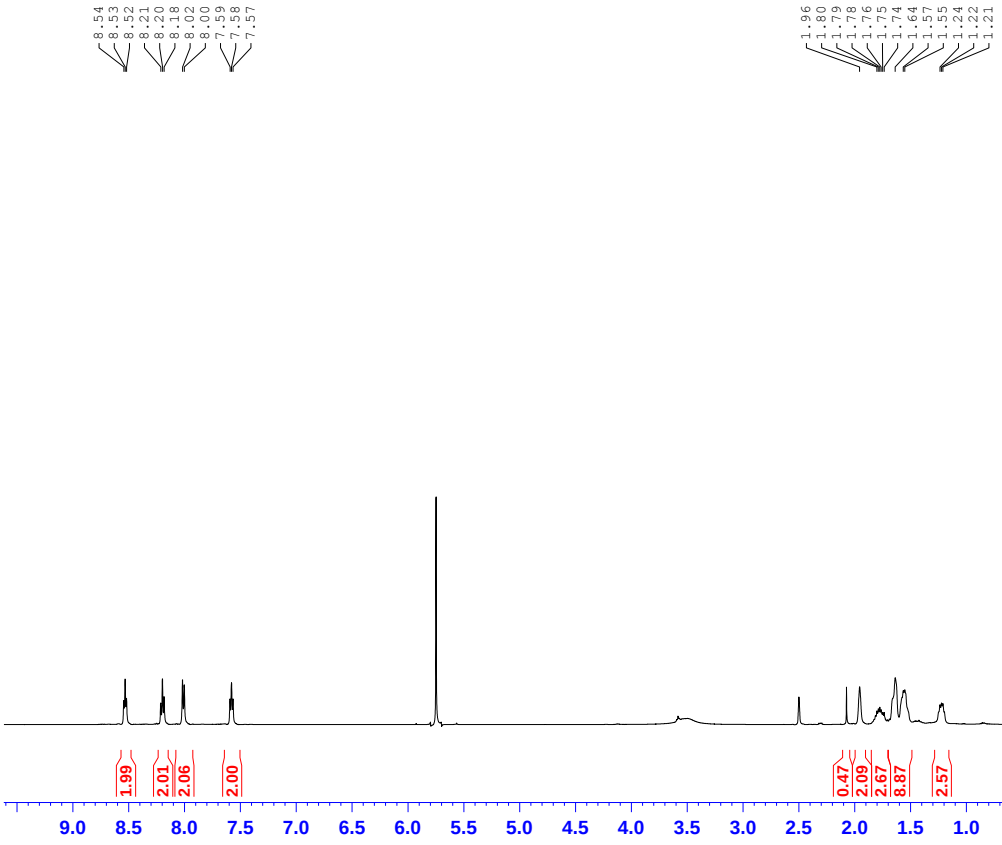

^{13}C NMR (22 °C, 500 MHz, DMSO-D$_6$, ppm) spectrum of hydrogen-di(2-pyridyl)-1,5-cyclooctanediylborate(L), LH·HCl, 4.2

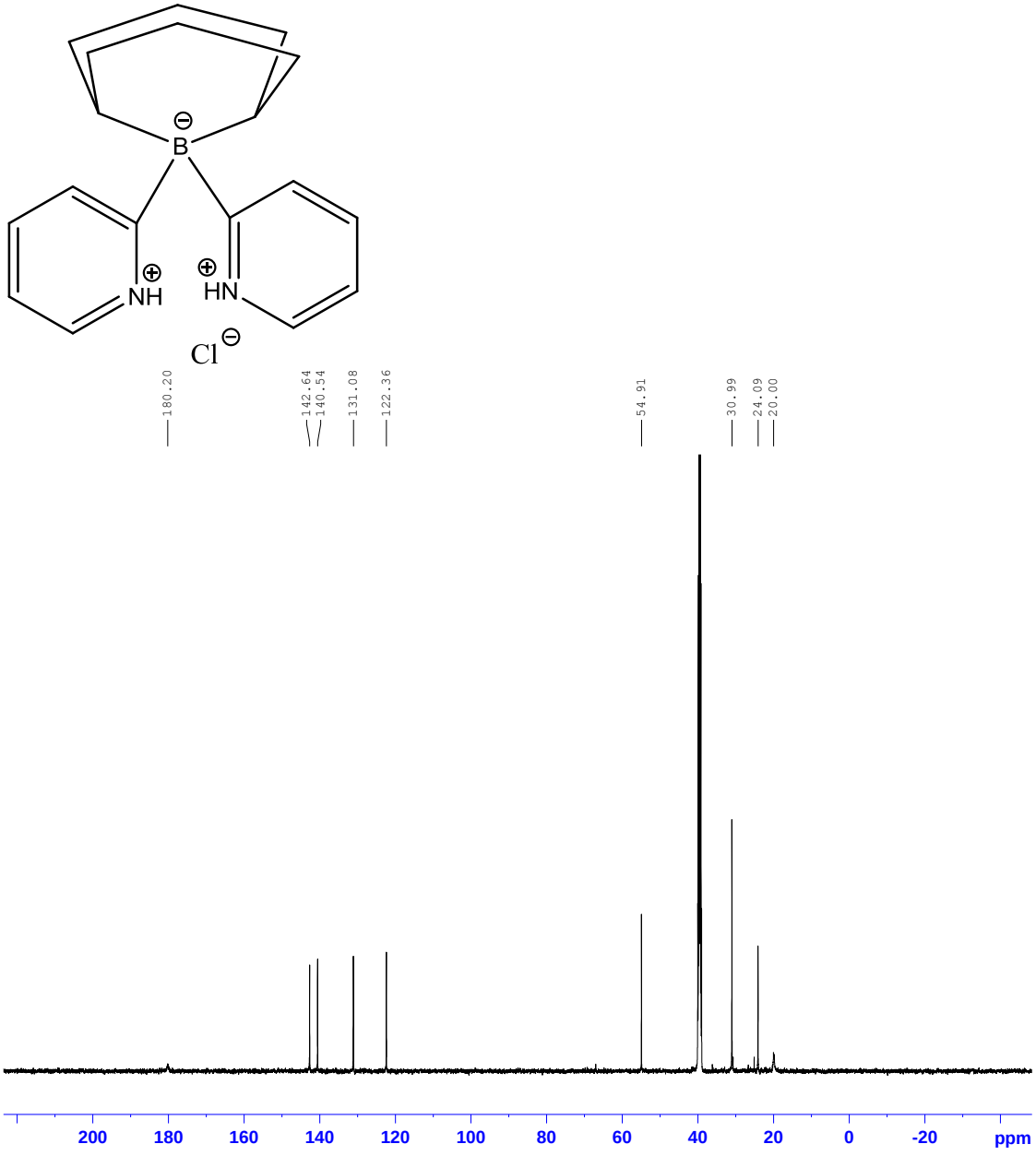

^{13}C NMR (22 °C, 500 MHz, CD_3CN, ppm) spectrum of di(2-pyridyl)-1,5-cyclooctanediylborato-$Pt^{II}Me_2$ complex, 4.5

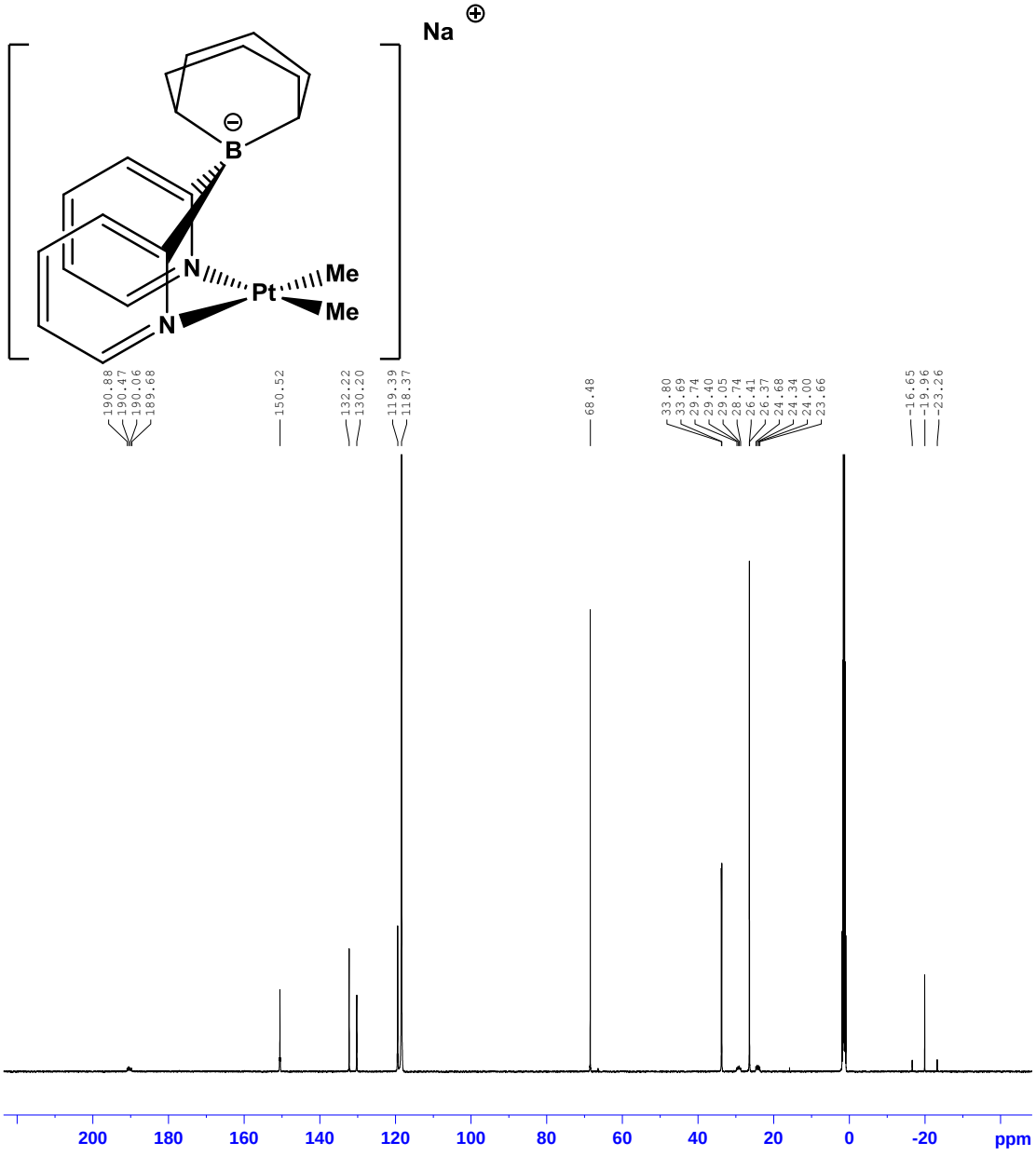

^{13}C NMR (22 °C, 500 MHz, CD_3CN, ppm) spectrum of di(2-pyridyl)-1,5-cyclooctanediylborato-$Pt^{II}Ph_2$ complex, 4.6

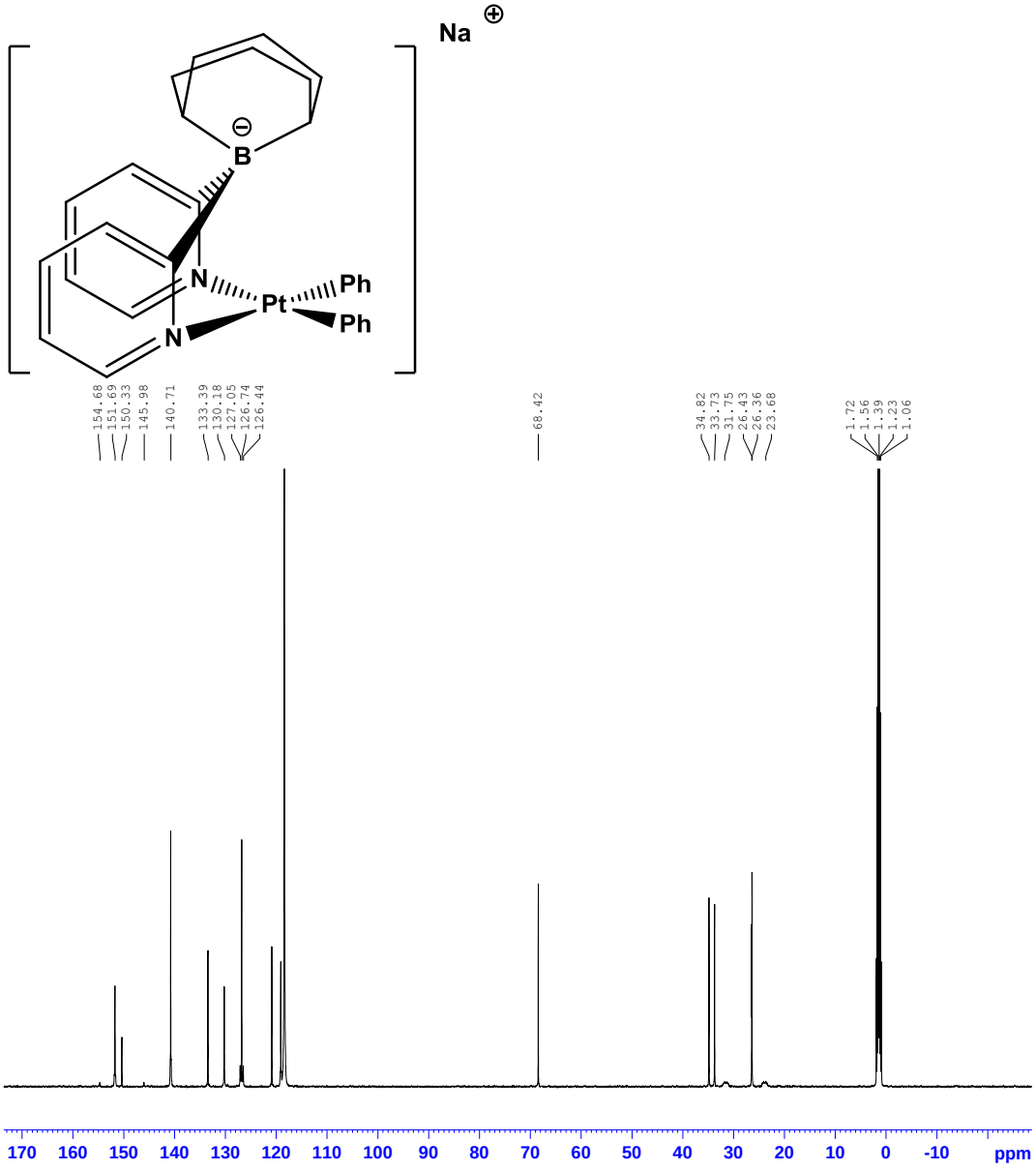

^{1}H NMR (22 °C, 500 MHz, $CDCl_3$, ppm) spectrum of di(2-pyridyl)-1,5-cyclooctanediylborato-Pt^{II}(cyclohexene)(H) complex, 4.7

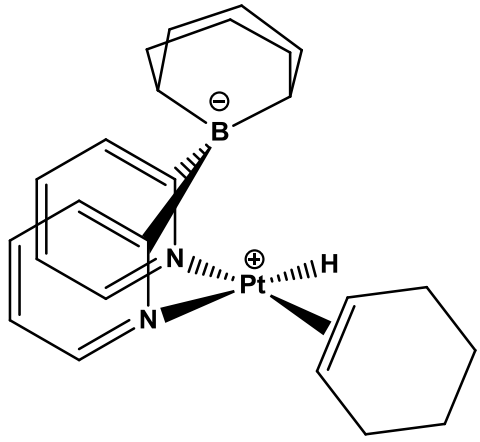

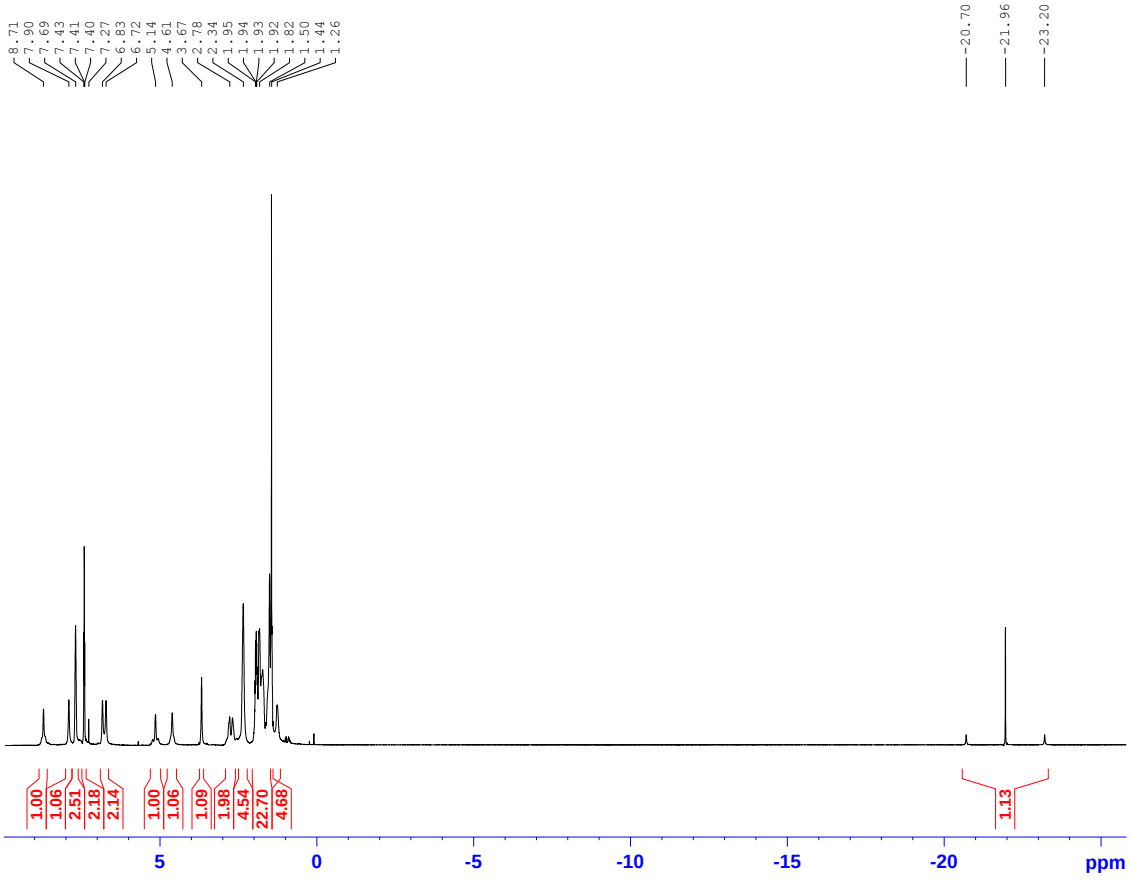

^{13}C NMR (22 °C, 500 MHz, $CDCl_3$, ppm) spectrum of di(2-pyridyl)-1,5-cyclooctanediylborato-Pt^{II}(cyclohexene)(H) complex, 4.7

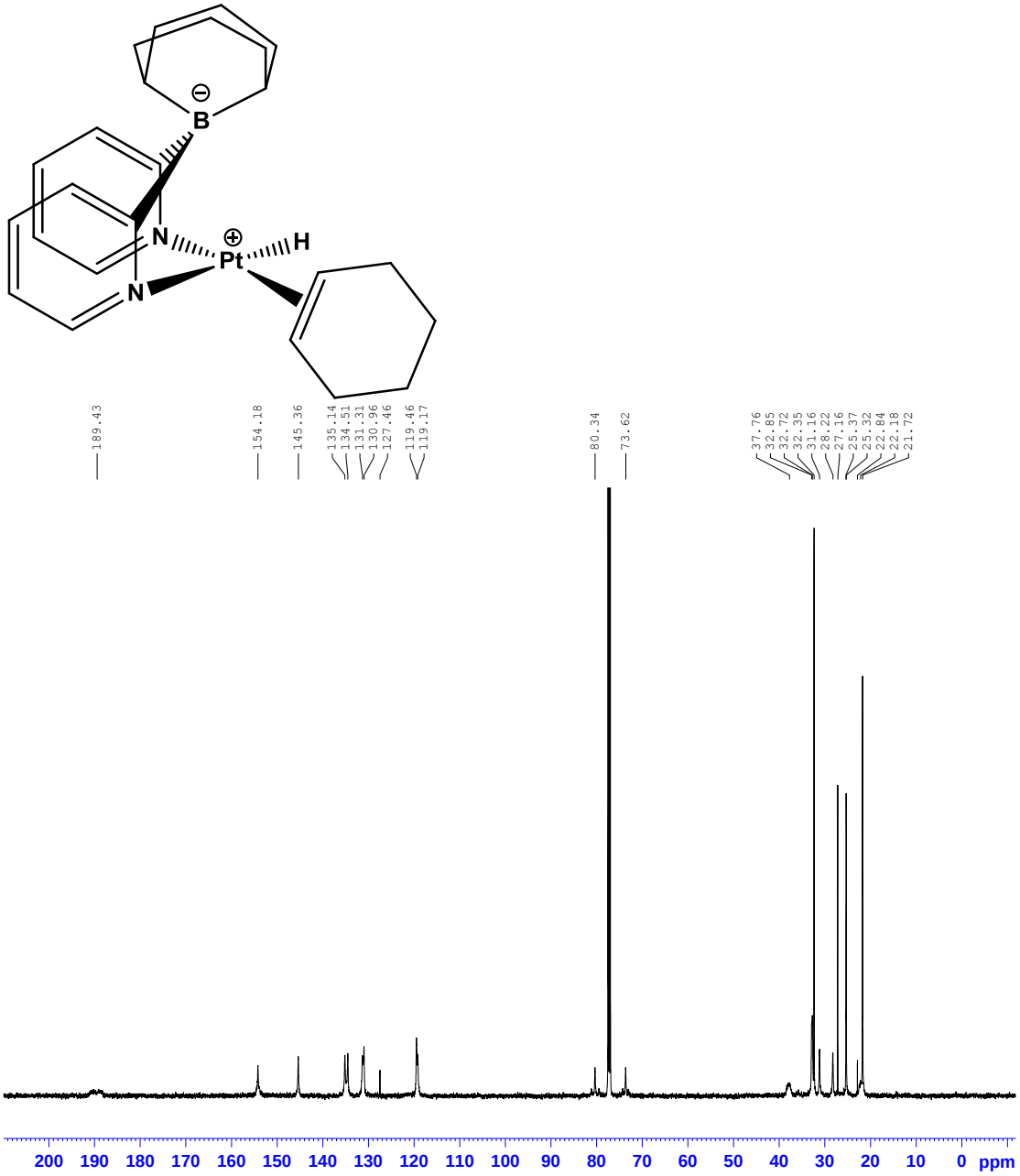

^{1}H-NMR (22 °C, 500 MHz, CD_2Cl_2, ppm) spectrum of di(2-pyridyl)-1,5-cyclooctanediylborato-Pt^{II}(Me)(SMe_2) complex, 4.8

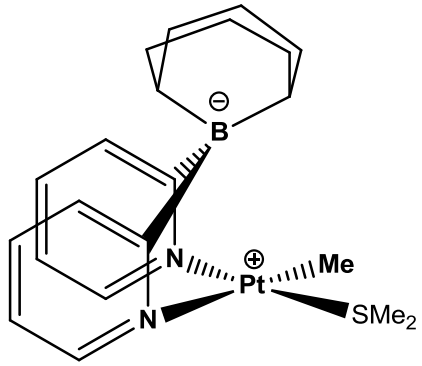

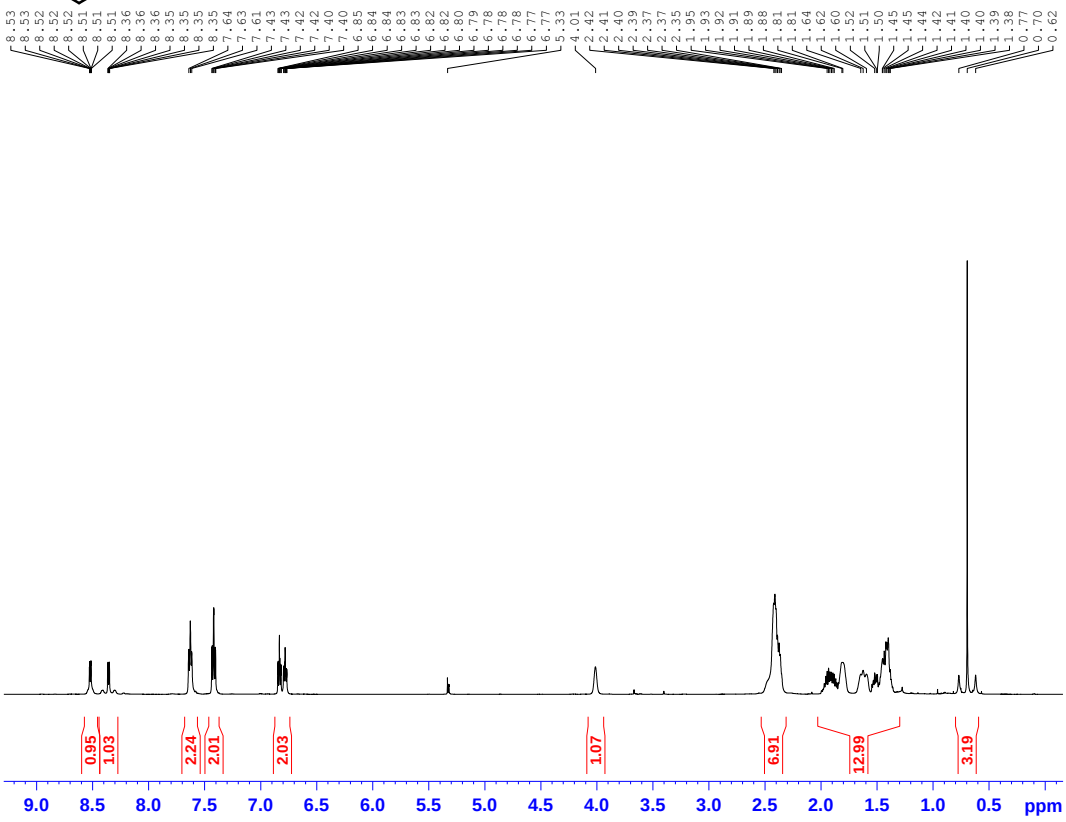

^{13}C-NMR (22 °C, 500 MHz, CD_2Cl_2, ppm) spectrum of di(2-pyridyl)-1,5-cyclooctanediylborato-Pt^{II}(Me)(SMe_2) complex, 4.8

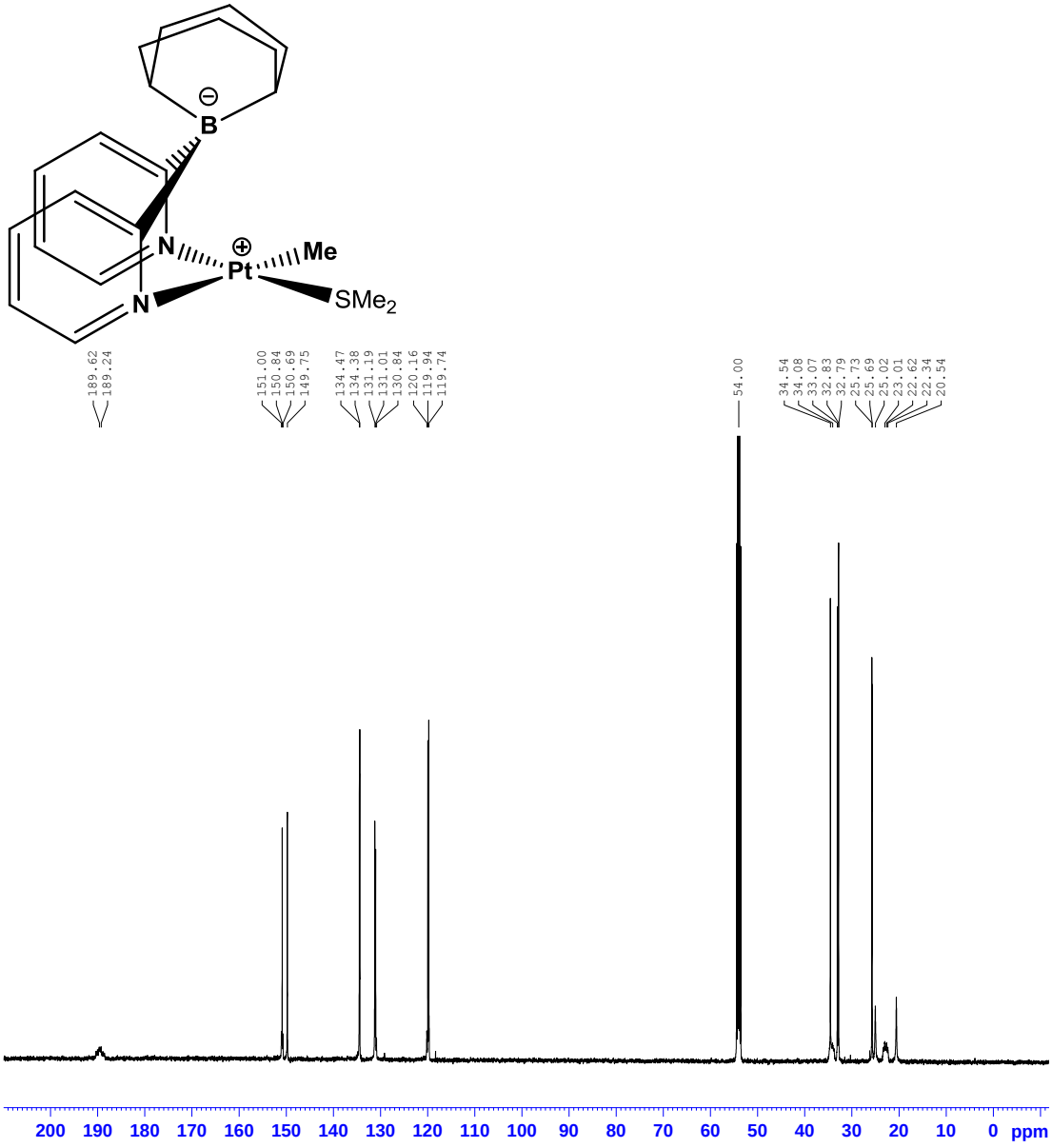

^{13}C NMR (22 °C, 500 MHz, CD_2Cl_2, ppm) spectrum of di(2-pyridyl)-1,5-cyclooctanediylborato-Pt^{IV}Me$_3$, 4.9

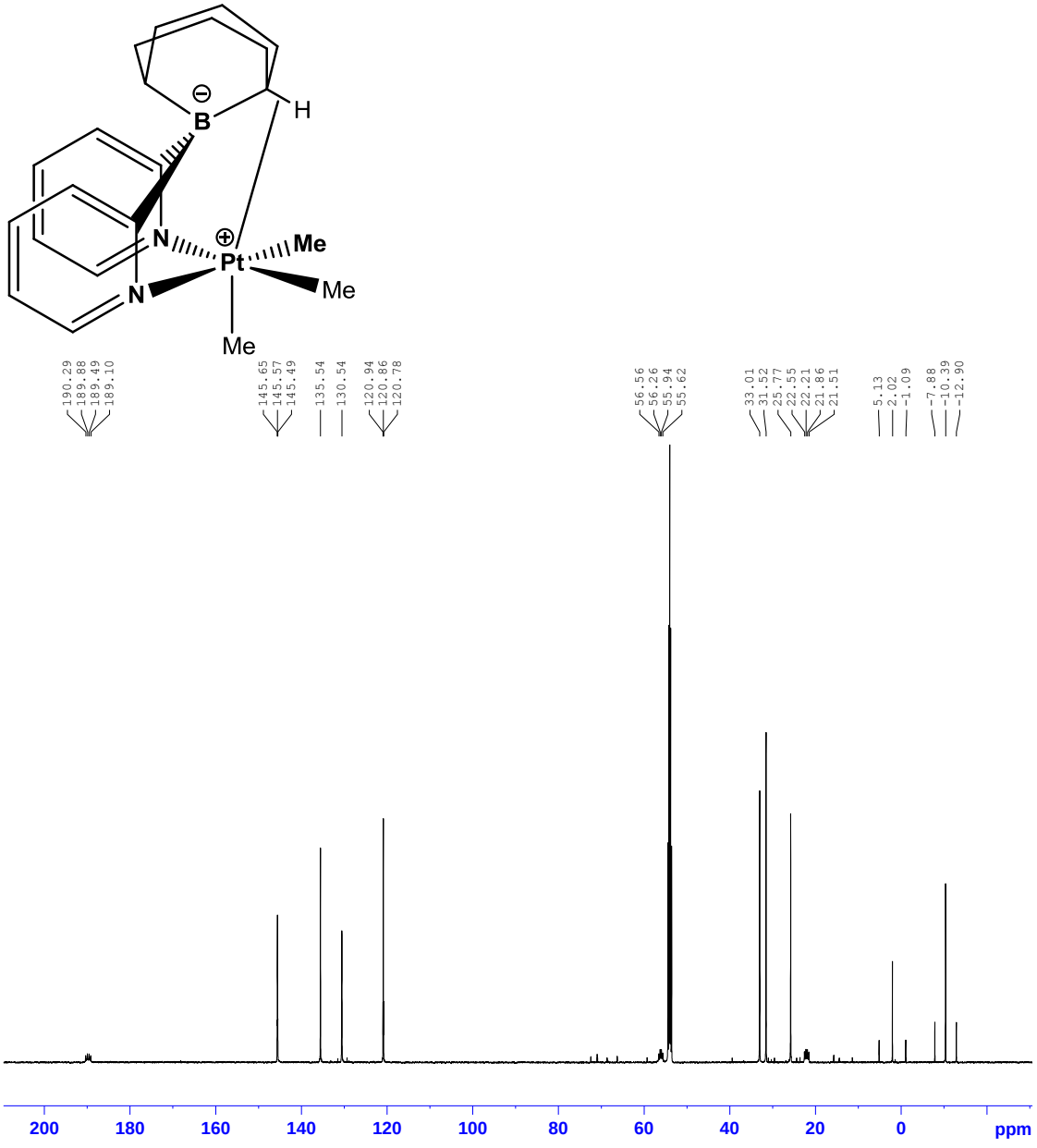

^{13}C NMR (22 °C, 500 MHz, THF-D_8, ppm) spectrum of di(2-pyridyl)-1,5-cyclooctanediylborato-Pt^{II}(Me)(OMe)

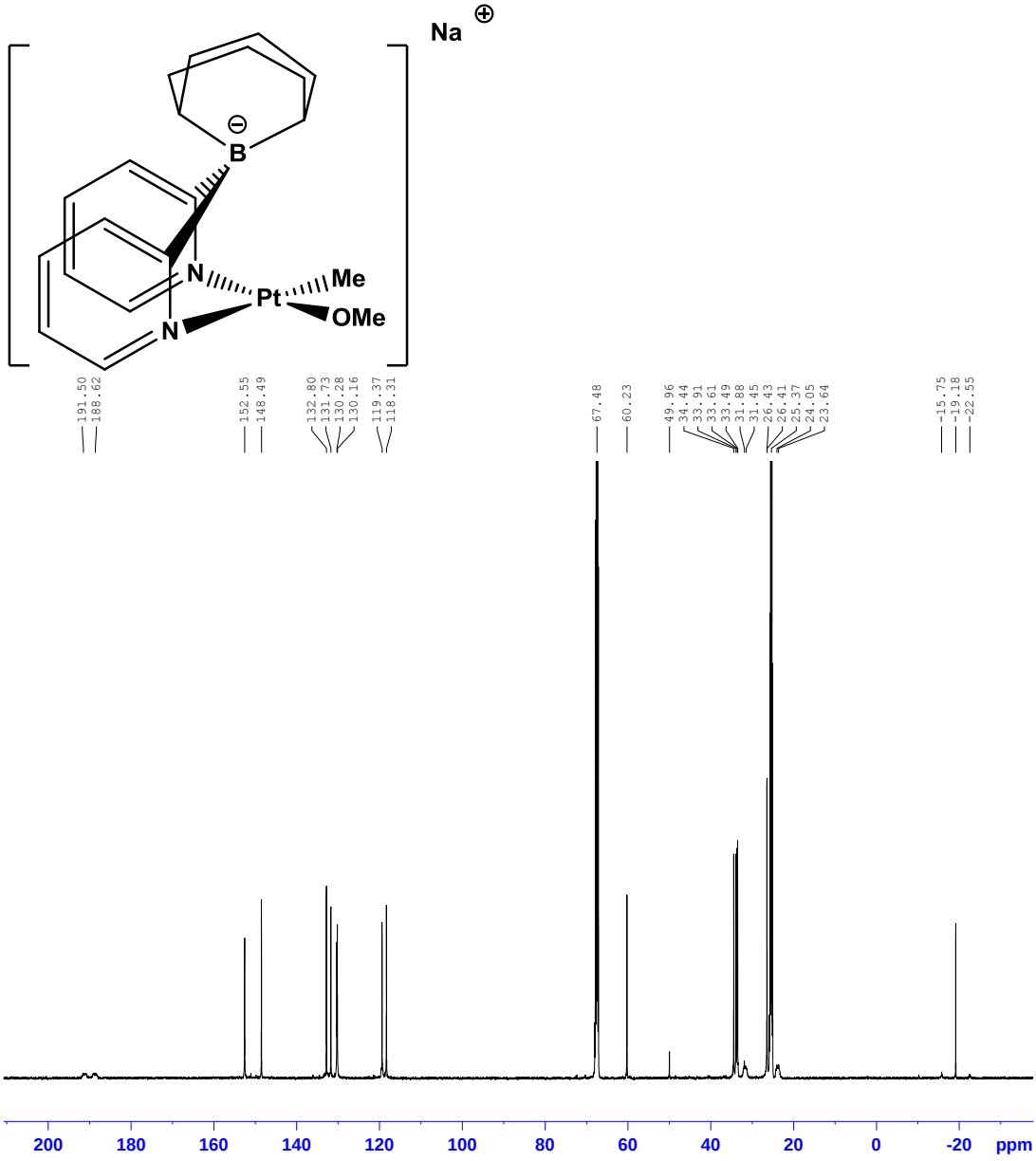

^{1}H NMR (22 °C, 500 MHz, THF-D_8, ppm) spectrum of di(2-pyridyl)-1,5-cyclooctanediylborato-Pt^{II}(Ph)(OMe), 4.14

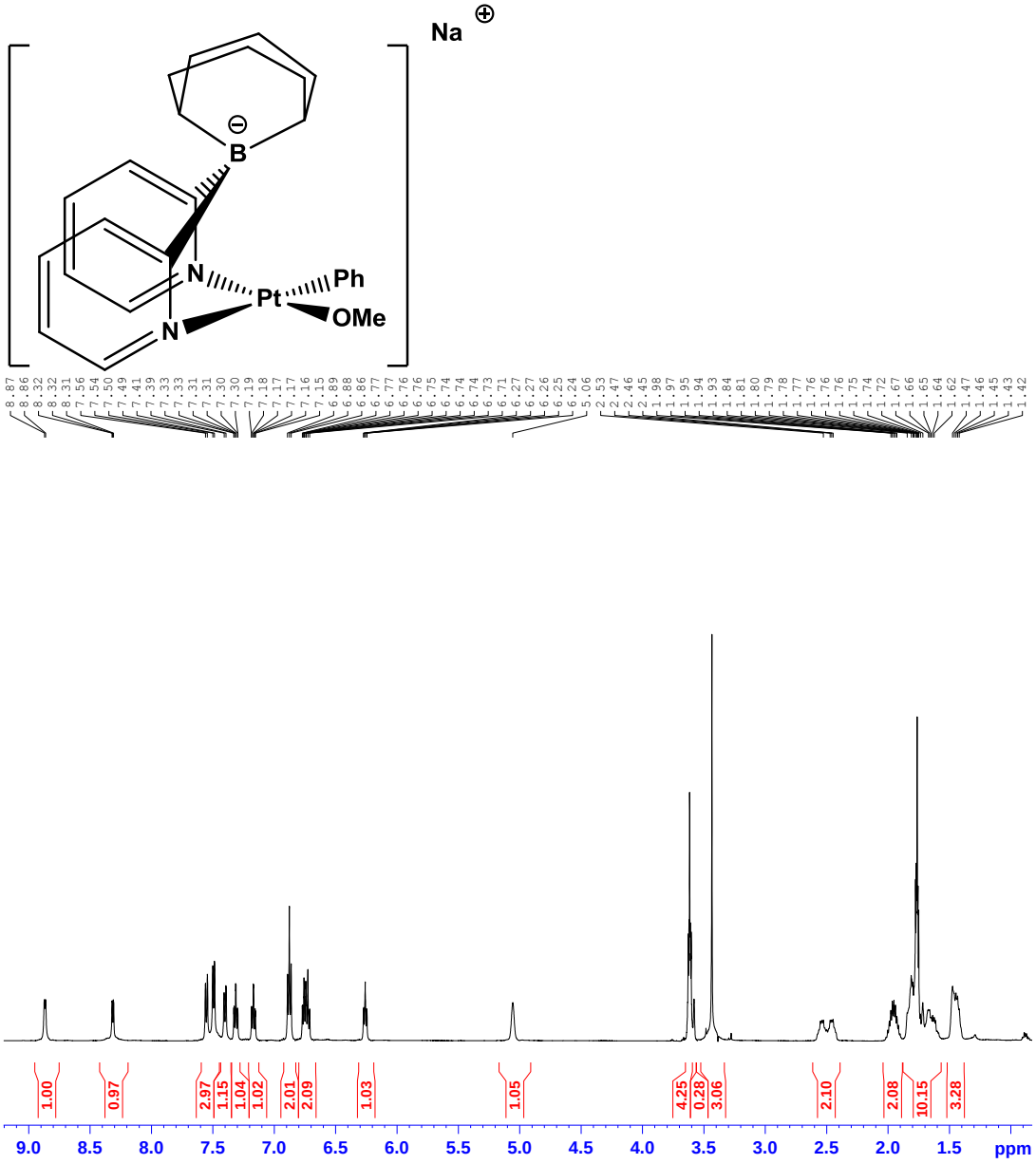

^{13}C NMR (22 °C, 500 MHz, THF-D_8, ppm) spectrum of di(2-pyridyl)-1,5-cyclooctanediylborato-Pt^{II}(Ph)(OMe), 4.14

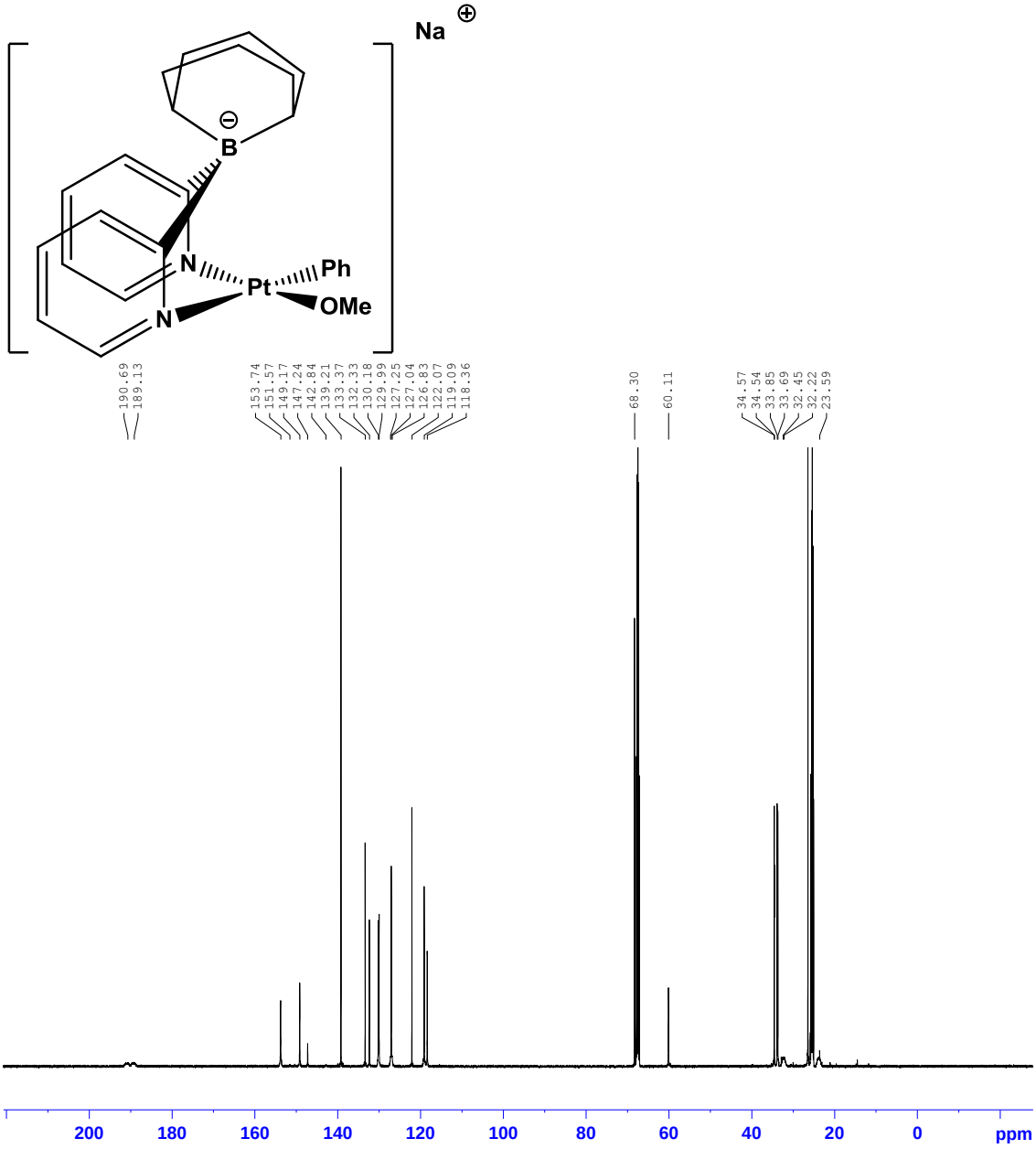

^{13}C NMR (22 °C, 500 MHz, DMSO-d_6, ppm) spectrum of di(2-pyridyl)(methoxy)(3.3.0bicyclooctyl)borato-Pt^{II}(OMe)$_2$, 4.15

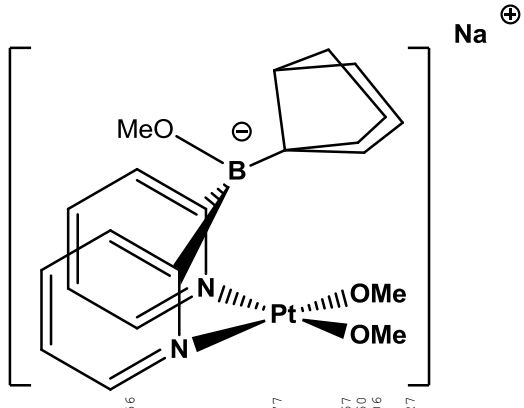

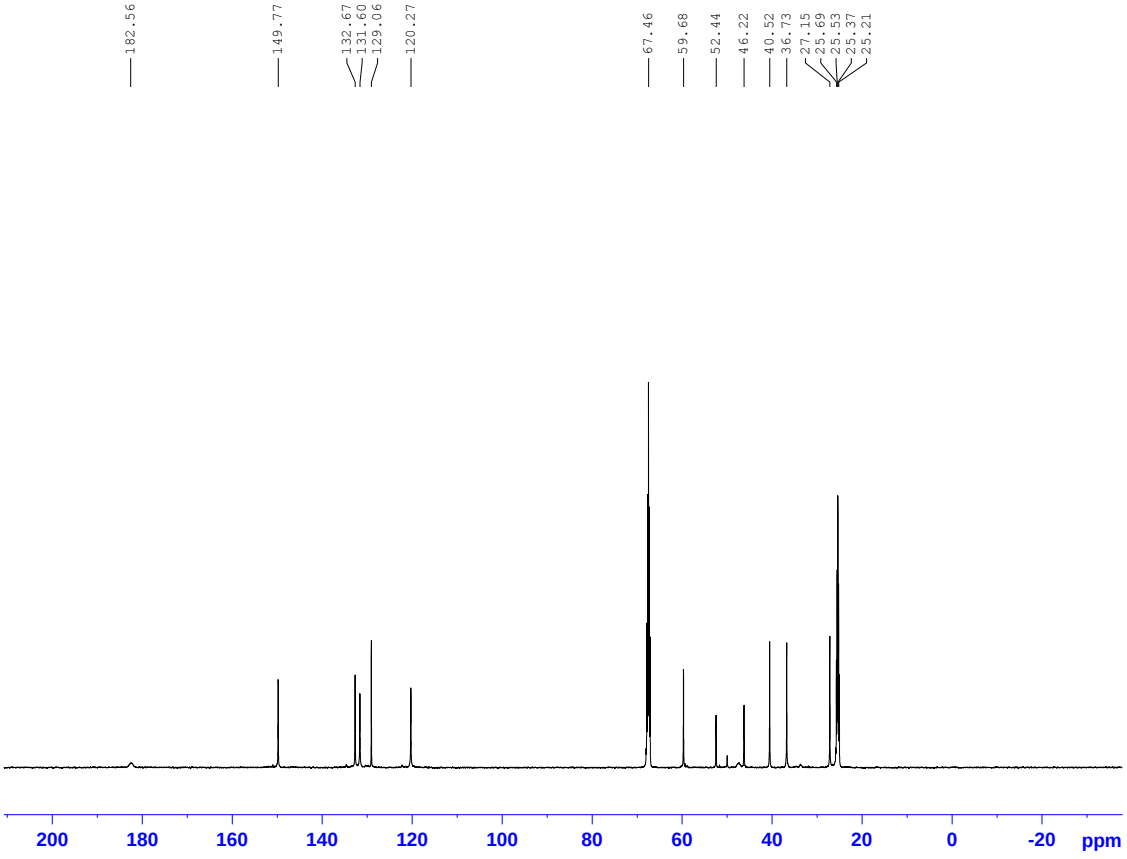

^{1}H NMR (22 °C, 500 MHz, $CDCl_3$, ppm) spectrum of di(2-pyridyl)dimethoxyborate-$Pt^{IV}(Ph_2)(OH)$ complex, 4.17

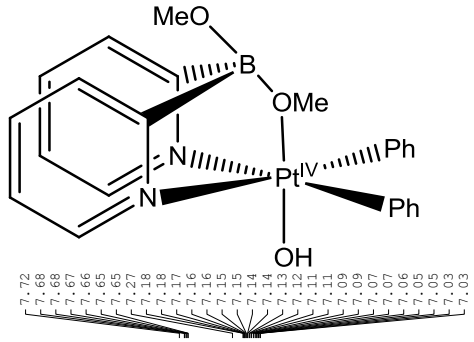

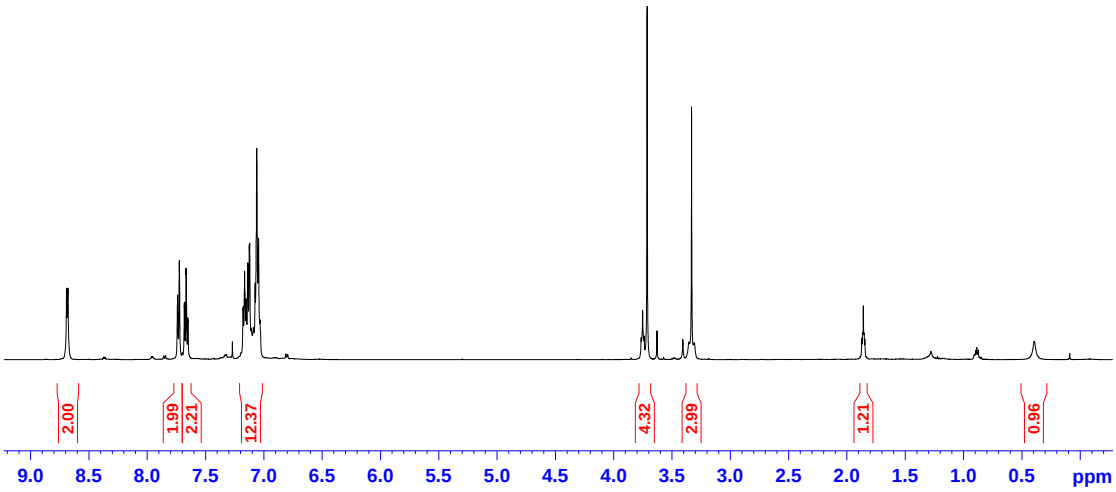

^{13}C NMR (22 °C, 500 MHz, $CDCl_3$, ppm) spectrum of di(2-pyridyl)dimethoxyborate-$Pt^{IV}(Ph_2)(OH)$ complex, 4.17

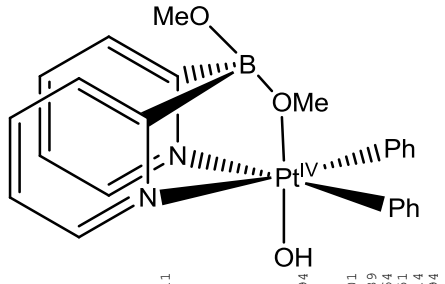

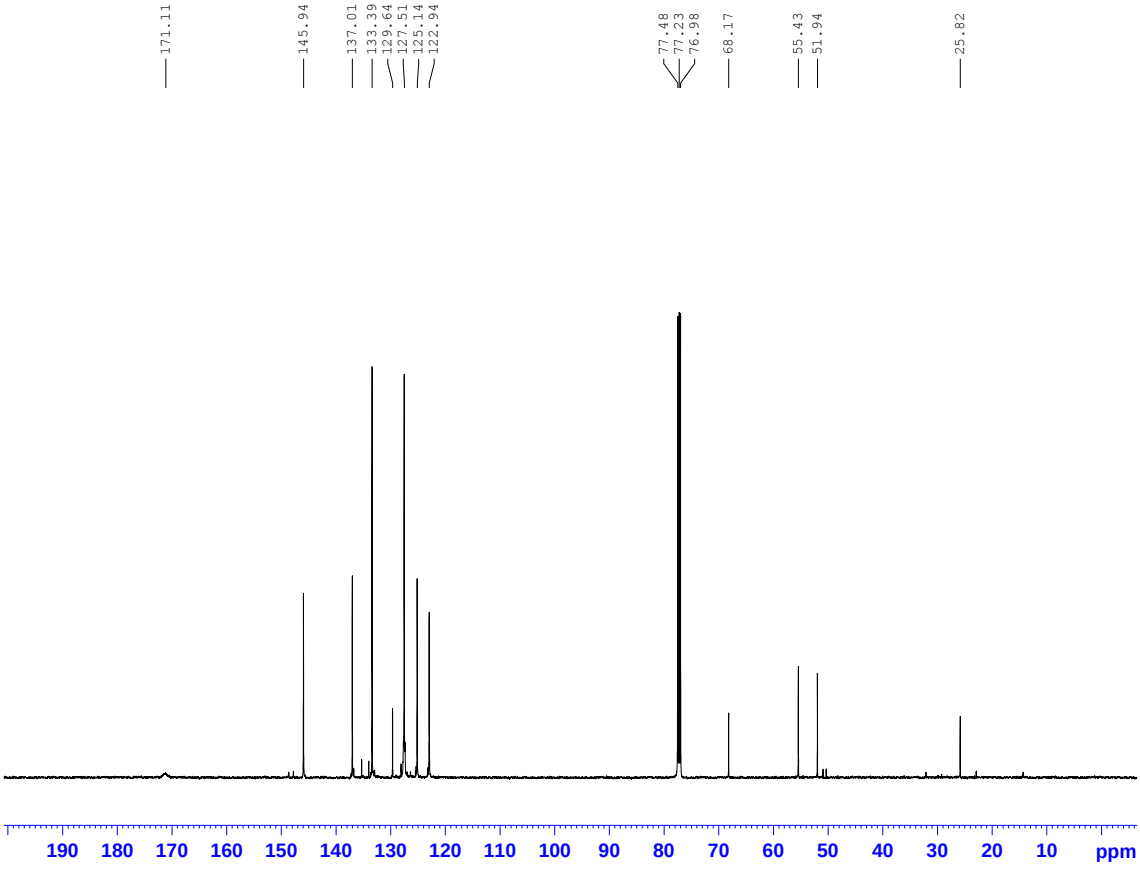

^{1}H NMR (22 °C, 500 MHz, CD_2Cl_2, ppm) spectrum of di(2-pyridyldimethoxyborato-$Pt^{IV}(OMe)_2(OH)$, 4.34

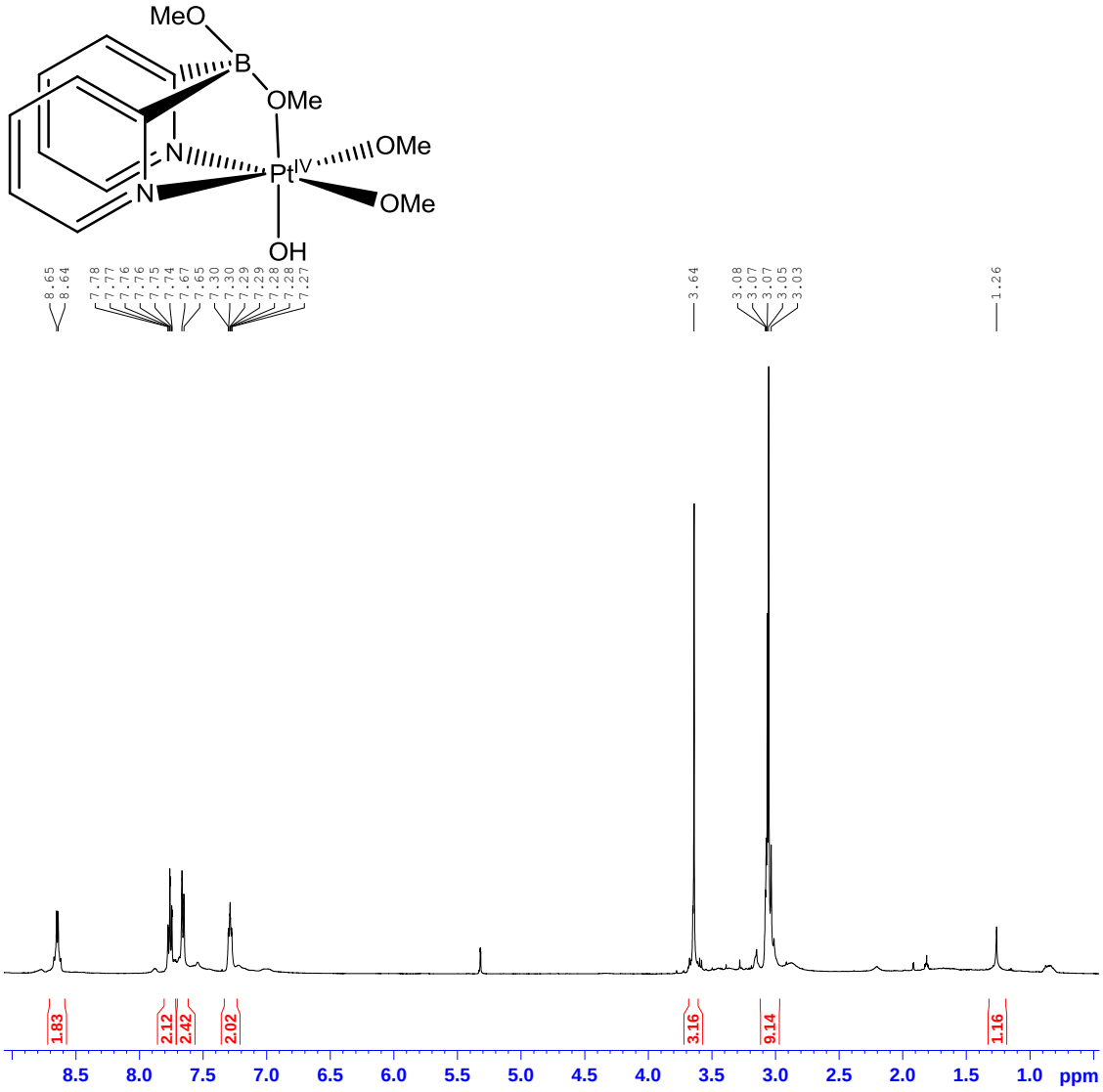

^{13}C NMR (22 °C, 500 MHz, CD_2Cl_2, ppm) spectrum of di(2-pyridyldimethoxyborato -$Pt^{IV}(OMe)_2(OH)$, 4.34

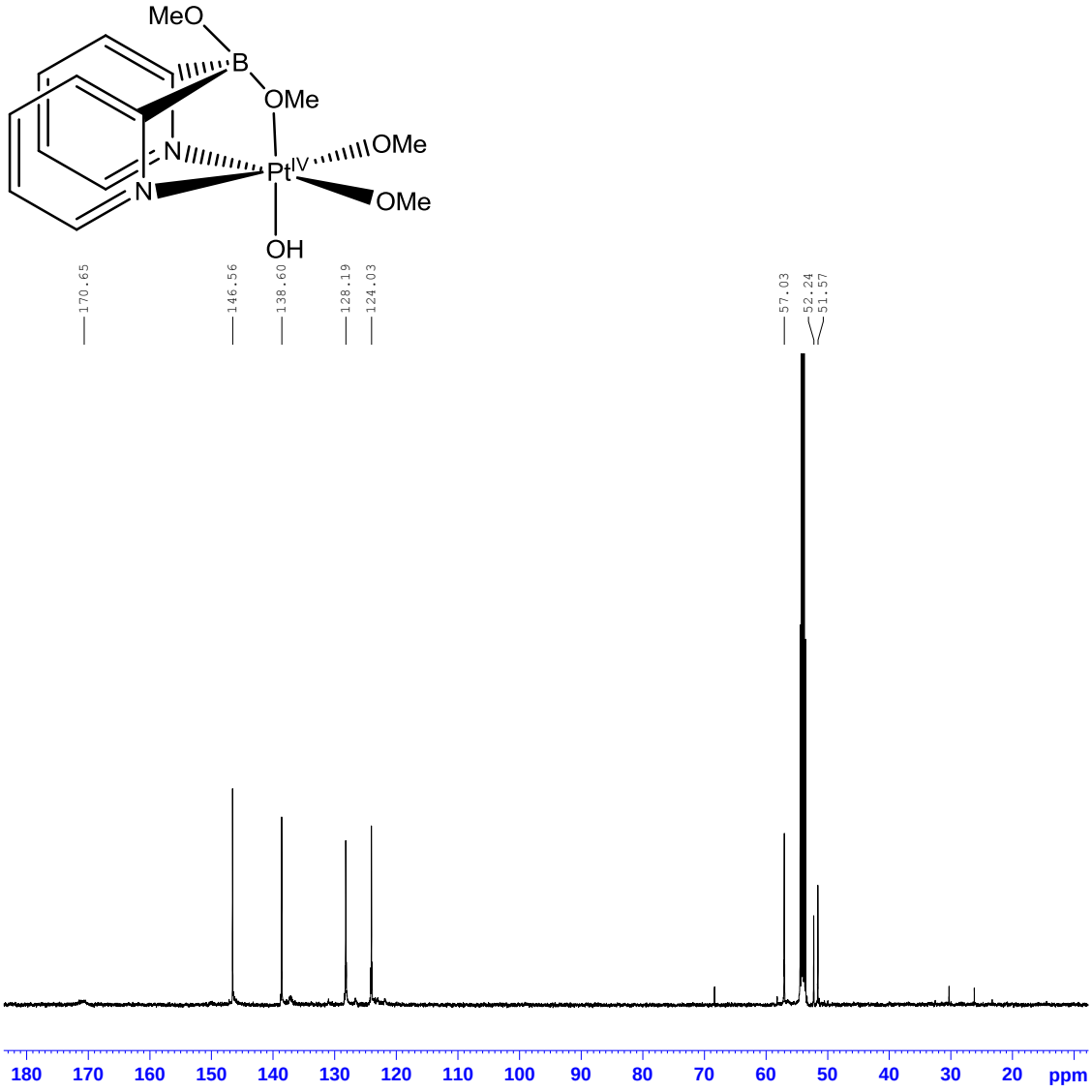

References

[1] Puddephatt et al., *J. Chem. Soc.,Chem.Comm.*, **1981**, 15, 805

[2] DFT Calculations were performed by Prof. Andrei N. Vedernikov using the Priroda Package with additional solvent correction implemented in the Jaguar package.

Laikov, D. N. *Chemical Physics Letters.* **1997**, *281*, 151

Parr, R. G.; Yang, W. *Density-functional Theory of Atoms and Molecules*; Oxford University Press: Oxford, 1989. Perdew, J. P.; Burke, K.; Ernzerhof, M. *Phys. Rev. Lett.* **1996**, *77*, 3865 Jaguar, version 7.9, Schrödinger, LLC, New York, NY, 2012.

[3] Periana, R.; Bhalla, G.; Tenn, W. *J. Mol. Catal. A:* **2004**, *220*, 7

[4] Stahl, S.; Labinger, J.; Bercaw, J. *Angew. Chem. Int. Ed.* **1998**, *37*, 2180

[5] Crabtree, R. H. *Chem. Rev.* **2010**, *110*, 575

[6] Hashiguchi, B. G.; Bischof, S. M.; Konnick, M. M.; Periana, R. A. *Acc. Chem. Res.* **2012**, *45*, 885

[7] Labinger, J.; Bercaw, J. *Nature* **417**, 507

[8] Davies, H.M.L. *Angew. Chem. Int. Ed.*, **2006**, *45*, 6422. Godula, K.; Sames, D., *Science*, **2006**, *312*, 67. *Handbook of CH Transformations* (Ed. G. Dyker), Wiley-VCH, Weinheim, **2005**.

[9] Wendlandt, A. E.; Suess, A. M.; Stahl, S. S. *Angew. Chemie Int. Ed.* **2011**, *50*, 11062

[10] Sakaki, S. *Theoretical Aspects of Transition Metal Catalysis SE - 2*; Frenking, G., Ed.; Springer Berlin Heidelberg, **2005**, 12, 31

[11] Lersch, M.; Tilset, M. *Chem. Rev*. **2005,** *105*, 2471

[12] Goldman, A. S.; Goldberg, K. I. In *Activation and Functionalization of C-H Bonds*; American Chemical Society, 2004; 885, 1

[13] Garnett, J. L.; Hodges, R. J. *J. Am. Chem. Soc.* **1967**, *89*, 4546

[14] Hay, A.S. *J. Org. Chem*. **1962**, *27*, 3320

[15] Geletii, Y.V.; Shilov, A.E. *Kinetics and Catalysis* **1983**, *24*, 413

[16] Shilov, A.; Shul'pin, G. *Chem. Rev* **1997**, *97*, 2879

[17] Periana, R.; Taube, D.; Gamble, S.; Taube, H.; Satoh, T.; Fujii, H. *Science* **1998**, *280*, 560

[18] Vedernikov, A. N. *Curr. Org. Chem.* **2007**, *11*, 1401

[19] Lin, M.; Shen, C.; Garcia-Zayas, E.; Sen, A. *J. Am. Chem. Soc* **2001**, *123*, 1000

[20] Dangel, B.; Johnson, J.; Sames, D. *J. Am. Chem. Soc* **2001**, *123*, 8149

[21] Rosenthal, J.; Nocera, D. G. *Acc. Chem. Res.* **2007**, *40*, 543

[22] Arndtsen, B. A.; Bergman, R. G.; Mobley, T. A.; Peterson, T. H. *Acc. Chem. Res.* **1995**, *28*, 154

[23] Vedernikov, A. N.; Shamov, G. A.; Solomonov, B. N. *Russ. J. Gen. Chem*. **1999**, 69, 1102 Vedernikov, A. N.; Shamov, G. A.; Solomonov, B. N. *Russ. J. Gen. Chem*. **1998**, *68*, 1462 Vedernikov, A. N.; Shamov, G. A.; Solomonov, B. N. *Russ. J. Gen. Chem*. **1998,** *68*, 675 Vedernikov, A. N.; Shamov, G. A.; Solomonov, B. N. *Russ. J. Gen. Chem*. **1998**, *68*, 667

[24] Owen, J.S.; Labinger, J.A.; Bercaw, J.E., *J. Am. Chem. Soc.*, **2006**, *128*, 2005. Driver, T.G.; Day, M.W.; Labinger, J.A.; Bercaw, J.E., *Organometallics*, **2005**, *24*, 3644

[25] Monaghan, P.; Puddephatt, R. *Organometallics* **1984**, *3*, 444

[26] Rostovtsev, V.; Labinger, J.; Bercaw, J.; Lasseter, T.; Goldberg, K. *Organometallics* **1998**, *17*, 4530

[27] Grice, K.; Goldberg, K. *Organometallics* **2009**, *28*, 953

[28] Reinartz, S.; White, P. S.; Brookhart, M.; Templeton, J. L. *Organometallics* **2000**, *19*, 3854

[29] Reinartz, S.; White, P. S.; Brookhart, M.; Templeton, J. L. *J. Am. Chem. Soc.* **2001**, *123*, 6425

[30] Vedernikov, A. N.; Binfield, S. A.; Zavalij, P. Y.; Khusnutdinova, J. R. *J. Am. Chem. Soc.* **2006**, *128*, 82

[31] Khusnutdinova, J. "Ligand-enabled Platinum-carbon Bond Functionalization Utilizing Dioxygen as the Terminal Oxidant" *Doc. Diss. Res*, University of Maryland, College Park, **2009**

[32] Thomas, J.C.; Peters, J.C., *J. Am. Chem. Soc.*, **2001**, *123*, 5100

[33] Karshtedt, D.; McBee, J. L.; Bell, A. T.; Tilley, T. D., *Organometallics*, **2006**, 25, 1801

[34] Khaskin, E. "New Ligand Motifs for Platinum-based Shilov Chemistry and Detours Into Basic Organometallic Research" *Doc. Diss. Res*, University of Maryland, College Park, **2009**

[35] Hodgkins, T. G.; Powell, D. R. *Inorg. Chem.* **1996**, *35*, 2140

[36] Khaskin, E.; Zavalij, P. Y.; Vedernikov, A. N. *J. Am. Chem. Soc.* **2006**, *128*, 13054

[37] Vedernikov, A. N.; Fettinger, J. C.; Mohr, F. *J. Am. Chem. Soc.* **2004**, *126*, 11160

[38] Fekl, U.; Goldberg, K. I. *Adv. Inorg. Chem.* **2003**, *54*, 259

[39] Labinger, J. A.; Herring, A. M.; Lyon, D. K.; Luinstra, G. A.; Bercaw, J. E.; Horvath, I. T.; Eller, K. *Organometallics* **1993**, *12*, 895

[40] Khaskin, E.; Zavalij, P. Y.; Vedernikov, A. N. *J. Am. Chem. Soc.* **2008**, *130*, 10088

[41] Dyker, G. *Handbook of CH transformations: applications in organic synthesis*; Wiley-VCH, **2005**

[42] Sinigalia, R.; Michelin, R. A.; Pinna, F.; Strukul, G. *Organometallics* **1987**, *6*, 728

[43] Grubbs, R. H. *Handbook of Metathesis*; Wiley-VCH, **2003**.

[44] Helfer, D. S.; Atwood, J. D. *Organometallics* **2004**, *23*, 2412

[45] Burk, M. J.; Crabtree, R. H. *J. Am. Chem. Soc.* **1987**, *109*, 8025

[46] Choi, J.; MacArthur, A. H. R.; Brookhart, M.; Goldman, A. S. *Chem. Rev.* **2011**, *111*, 1761

[47] Kloek, S. M.; Goldberg, K. I. *J. Am. Chem. Soc.* **2007**, *129*, 3460

[48] Kostelansky, C. N.; MacDonald, M. G.; White, P. S.; Templeton, J. L. *Organometallics* **2006**, *25*, 2993

[49] Khaskin, E.; Lew, D. L.; Pal, S.; Vedernikov, A. N. *Chem. Commun.* **2009**, 6270

[50] Zhu, K.; Achord, P. D.; Zhang, X.; Krogh-Jespersen, K.; Goldman, A. S. *J. Am. Chem. Soc.* **2004**, *126*, 13044

[51] Chen, G. S.; Labinger, J. A.; Bercaw, J. E. *Proc. Natl. Acad. Sci.* **2007**, *104*, 6915

[52] Khaskin, E.; Zavalij, P. Y.; Vedernikov, A. N. *Angew. Chemie* **2007**, *119*, 6425

[53] Bryndza, H. E.; Calabrese, J. C.; Marsi, M.; Roe, D. C.; Tam, W.; Bercaw, J. E. *J. Am. Chem. Soc.* **1986**, *108*, 4805

[54] Sommerer, S. O.; Abboud, K. A. *Acta Crystallogr. Sect. C Cryst. Struct. Commun.* **1993**, *49*, 1152

[55] Canty, A. J.; Stevens, E. A. *Inorganica Chim. Acta* **1981**, *55*, L57

[56] Oyamada, J.; Kitamura, T. *Tetrahedron* **2009**, *65*, 3842

[57] Gatard, S.; Guo, C.; Foxman, B. M.; Ozerov, O. V. *Organometallics* **2007**, *26*, 6066

[58] Minniti, D.; Alibrandi, G.; Tobe, M. L.; Romeo, R. *Inorg. Chem.* **1987**, *26*, 3956

[59] Annibale, G.; Bonivento, M.; Cattalini, L.; Michelon, G. *Inorg. Chem.* **1984**, *23*, 2829

[60] Romeo, R.; Amico, G. D.; Inorganica, C.; Analitica, C.; Sperone, S.; Agata, V. S. **2006**, 3435

[61] Fiala, Z.; Navrátil, M. *Chem. Pap.* **1978**, *32*, 51

[62] Khusnutdinova, J. R.; Newman, L. L.; Zavalij, P. Y.; Lam, Y.-F.; Vedernikov, A. N. *J. Am. Chem. Soc.* **2008**, *130*, 2174

[63] Conley, B. L.; Guess, D.; Williams, T. J. *J. Am. Chem. Soc.* **2011**, *133*, 14212

[64] Tatsumi, K.; Hoffmann, R.; Yamamoto, A.; Stille, J. K. *Bull. Chem. Soc. Jpn.* **1981**, *54*, 1857

[65] Scheuermann, M. L.; Fekl, U.; Kaminsky, W.; Goldberg, K. I. *Organometallics* **2010**, *29*, 4749

[66] Muetterties, E. L. *The chemistry of boron and its compounds*; Wiley, **1967**

[67] Brown, H. C.; Kramer, G. W.; Levy, A. B.; Midland, M. M. *Organic syntheses via boranes*; Wiley New York, **1975**

[68] Fekl, U.; Kaminsky, W.; Goldberg, K. I. *J. Am. Chem. Soc.* **2001**, *123*, 6423

[69] Atkins, P.; De Paula, J. *Elements of physical chemistry*; Macmillan, **2009**

[70] Trofimenko, S.; Calabrese, J. C.; Thompson, J. S. **1992**, 914

[71] Chisholm, M. H.; Iyer, S. S.; Streib, W. E. *New J. Chem.* **2000**, *24*, 393. Bortolin, M.; Bucher, U. E.; Rueegger, H.; Venanzi, L. M.; Albinati, A.; al., et *Organometallics* **1992**, *11*, 2514

[72] Chengzhong Cui, *Doc. Diss. Res.*, Newark Rutgers- The State University of New Jersey **2010**

[73] Sikorski, J. A.; Bhat, N. G.; Cole, T. E.; Wang, K. K.; Brown, H. C. *J. Org. Chem.* **1986**, *51*, 4521

[74] Schilder, M.; Reseach, S.; Brown, H. C.; Jayaramanib, S. **1992**, *7*, 1948

[75] Krishnamurthy, S.; Brown, H. C. *J. Org. Chem.* **1975**, *40*, 1864

[76] Yamamoto, Y.; Toi, H.; Murahashi, S.-I.; Moritani, I. *J. Am. Chem. Soc.* **1975**, *97*, 2558

[77] Warner, P.; LaRose, R.; Schleis, T. *Tetrahedron Lett.* **1974**, *15*, 1409

[78] Rendina, L. M.; Puddephatt, R. J. *Chem. Rev.* **1997**, *97*, 1735

[79] Barriga, S. *Synlett* **2001**, *2001*, 563

[80] Ishii, Y.; Sakaguchi, S.; Iwahama, T. *Adv. Synth. Catal.* **2001**, *343*, 393

[81] Bartlett, K. L.; Goldberg, K. I.; Borden, W. T. *J. Am. Chem. Soc.* **2000**, *122*, 1456

[82] Brown, H. C.; Brown, C. A. *J. Am. Chem. Soc.* **1962**, *84*, 1494

[83] Osby, J. O.; Heinzman, S. W.; Ganem, B. *J. Am. Chem. Soc.* **1986**, *108*, 67

[84] Rickborn, B.; Wuesthoff, M. T. *J. Am. Chem. Soc.* **1970**, *92*, 6894

[85] Hill, G. S.; Puddephatt, R. J. **1996**, *7863*, 8745

[86] Ting, C.; Messerle, L. *J. Am. Chem. Soc.* **1989**, *111*, 3449

[87] Schlesinger, H. I.; Brown, H. C.; Finholt, A. E.; Gilbreath, J. R.; Hoekstra, H. R.; Hyde, E. K. *J. Am. Chem. Soc.* **1953**, *75*, 215

[88] King, R. B.; Bond, A. *J. Am. Chem. Soc.* **1974**, *96*, 1338

[89] Arnold, D. P.; Bennett, M. A. *Inorg. Chem.* **1984**, *23*, 2110

[90] De Leon, C. P.; Walsh, F. C.; Pletcher, D.; Browning, D. J.; Lakeman, J. B. *J. Power Sources* **2006**, *155*, 172

[91] Chatenet, M.; Micoud, F.; Roche, I.; Chainet, E.; Vondrák, J. *Electrochim. Acta* **2006**, *51*, 5452

[92] Geng, X.; Zhang, H.; Ye, W.; Ma, Y.; Zhong, H. *J. Power Sources* **2008**, *185*, 627

[93] Li, Z. P.; Liu, B. H.; Arai, K.; Suda, S. *J. Alloys Compd.* **2005**, *404*, 648

[94] Santos, D. M.; Condeco, J. A.; Franco, M. W.; Sequeira, C. A. *ECS Trans.* **2007**, *3*, 19

[95] Lyttle, D. A.; Jensen, E. H.; Struck, W. A. *Anal. Chem.* **1952**, *24*, 1843

[96] Ten Brink, G.-J.; Arends, I. W. C. E.; Sheldon, R. A. *Science* **2000**, *287*, 1636

[97] Sheldon, R. A. *Chem. Soc. Rev.* **2012**, *41*, 1437

[98] Ley, S. V; Madin, A. *Compr. Org. Synth. Sel. Strateg. Effic. Mod. Org. Chem. Oxid.* **1991**, *7*, 251

[99] Zope, B. N.; Hibbitts, D. D.; Neurock, M.; Davis, R. J. *Science* **2010**, *330*, 74

[100] Zweifel, T.; Naubron, J.; Grützmacher, H. *Angew. Chemie Int. Ed.* **2009**, *48*, 55